The geology and the ore mineralization in the Keban area, east Turkey

M. Tuncay Kines

THE GEOLOGY AND THE ORE MINERALIZATION IN THE KEBAN AREA, EAST TURKEY

A THESIS SUBMITTED FOR THE DEGREE OF DOCTOR OF PHILOSOPHY IN THE UNIVERSITY OF DURHAM

by

M. TUNCAY KINES (Dipl. Geol. Istanbul)

GREY COLLEGE

JANUARY 1969

ABSTRACT

The Keban mine is one of the most important lead and zinc producers in Turkey. It is located 54 km NW of Elazig county, eastern Turkey.

The Keban metamorphic massif consists of calc-schists, dolomite marble, phyllite and marble. It forms part of the eastern Taurid belt, a prolongation of the Alpine orogenic belt.

The principal structural feature of the area is the northern extension of the Malatya-Keban anticline, a major recumbent fold with a NE-SW axis. Later movements acting in different directions gave rise to N-S, E-W, NW-SE and NE-SW directed folding and faulting over the previous anticline. Small bodies of quartz-syenite porphyry, of Paleocene age, intrude the metasediments.

Detailed study by chemistry, petrography and X-ray techniques on sanidine accounts for a composition range between $Or_{65}\ Ab_{35}$ and $Or_{99}\ Ab_{1}$. The ratio of Or to Ab tends to increase outwards from the central parts of the igneous body.

Skarn zones have developed in association with the intrusion of quartz-syenite porphyry. These are located mainly within the metasediments. The magnetite deposit of Zereyandere, the scheelite deposit of Kebandere and the main sulphide deposit were formed as part of the process of skarn formation. Minor amounts of some manganese minerals, and the minerals vanadinite and descloizite derived from the main sulphide deposit, are also found in the

district.

The main sulphide deposit of economic importance chiefly includes sphalerite, galena, iron and copper sulphides and several sulfo-salts in subordinate amounts. Of the by-products, silver comes from galena, polybasite and tennantite. Arsenopyrite in addition to chalcopyrite contains trace concentrations of gold.

All the evidence suggests that the quartz-syenite porphyry is the source of mineralization. The location of ore minerals is controlled by certain rock types and by major and minor structural elements. Variation of vapour fugacity and temperature during mineralization are indicated by more than one stage of formation for certain ore minerals. The presence of different gangue minerals marks the fluctuating nature of the ore forming fluids whose last stage is believed to be alkaline rather than acidic.

The main sulphide deposit is accepted as a semi-metasomatic contact deposit, while the magnetite and scheelite deposits are classified as being contact metamorphic.

Using various methods, a temperature range of formation between 620° and 78°C is estimated for the ore minerals of the main sulphide deposit. For the ore minerals of the scheelite and magnetite deposits, the range is from 743°C down to 225°C.

ACKNOWLEDGEMENTS

The author wishes to thank Professor K.C. Dunham, the former Head of Department and the supervisor of this research, for his advice and encouragement, and for the research facilities in this department during the first two years of the research. I would also like to express my thanks to Professor G.M. Brown, the Head of Department, for permitting me to make free use of the laboratory and technical assistance.

In particular I should like to express my sincere appreciation to Mr. R. Phillips for his valuable advice, continued interest and for critically reading the manuscript.

Dr. C.H. Emeleus is gratefully acknowledged for his suggestions, help with the petrography and the electron-probe microanalysis, and critically reading the manuscript.

The author would like to thank Dr. J.G. Holland for his assistance with the X-ray spectrograph investigation and computering.

Personal acknowledgement is due to Dr. D.M. Hirst for help with the optical spectrograph investigation.

Grateful thanks are due to Mr. G. Wilson and the technical staff of this department.

This research was financed through a research fund from the Mineral Research and Exploration Institute of Turkey (M.T.A.)

The author is also indebted to Dr. S. Alpan, the Director General to M.T.A. for his stimulation and encouragement throughout the research.

Thanks are due to the management of the Keban mining company, a subsidiary of the National Mining Company (Etibank) for the arrangement and all possible facilities during the writer's stay at the Keban mine.

TABLE OF CONTENTS

LIST OF FIGURES

LIST OF FIGURES (Condt.)

LIST OF TABLES

LIST OF TABLES (Contd.)

LIST OF PLATES

Plate No.

CHAPTER I

INTRODUCTION

Geography

The Keban mining town and the area under investigation in Elazig County, East Turkey are located in an eastward bend of the Upper Firat river (Euphrates) which runs down across Syria and Iraq before reaching the Persian Gulf (Figs. 1 and 2). It is about 54 km NW of Elazig. A high standard road with few bends provides access to the town which is 3 km away from the Firat main adit of the working mine. The mining area covers parts of the 1:25,000 scale topographic sheets Malatya K41-a3 and K41-64, and lies mainly in the 5 km grid square 75,90. The detailed geological mapping was carried out on a topographic sheet, enlarged two and a half times by a photographic technique from the above mentioned sheets. The mapped area is about 30 km^2.

The Firat river, one of the biggest rivers in Turkey, runs roughly from N to S through the centre of the area dividing it into eastern and western sections, of which the eastern section contains the workable mineralization.

Away from the narrow river valley at an elevation of about 700 m the ground rises steeply in both directions to heights of about 1000 metres. The isolated peak of the Soğanlitepe (1295 m) is the highest point in the area (Fig.3).

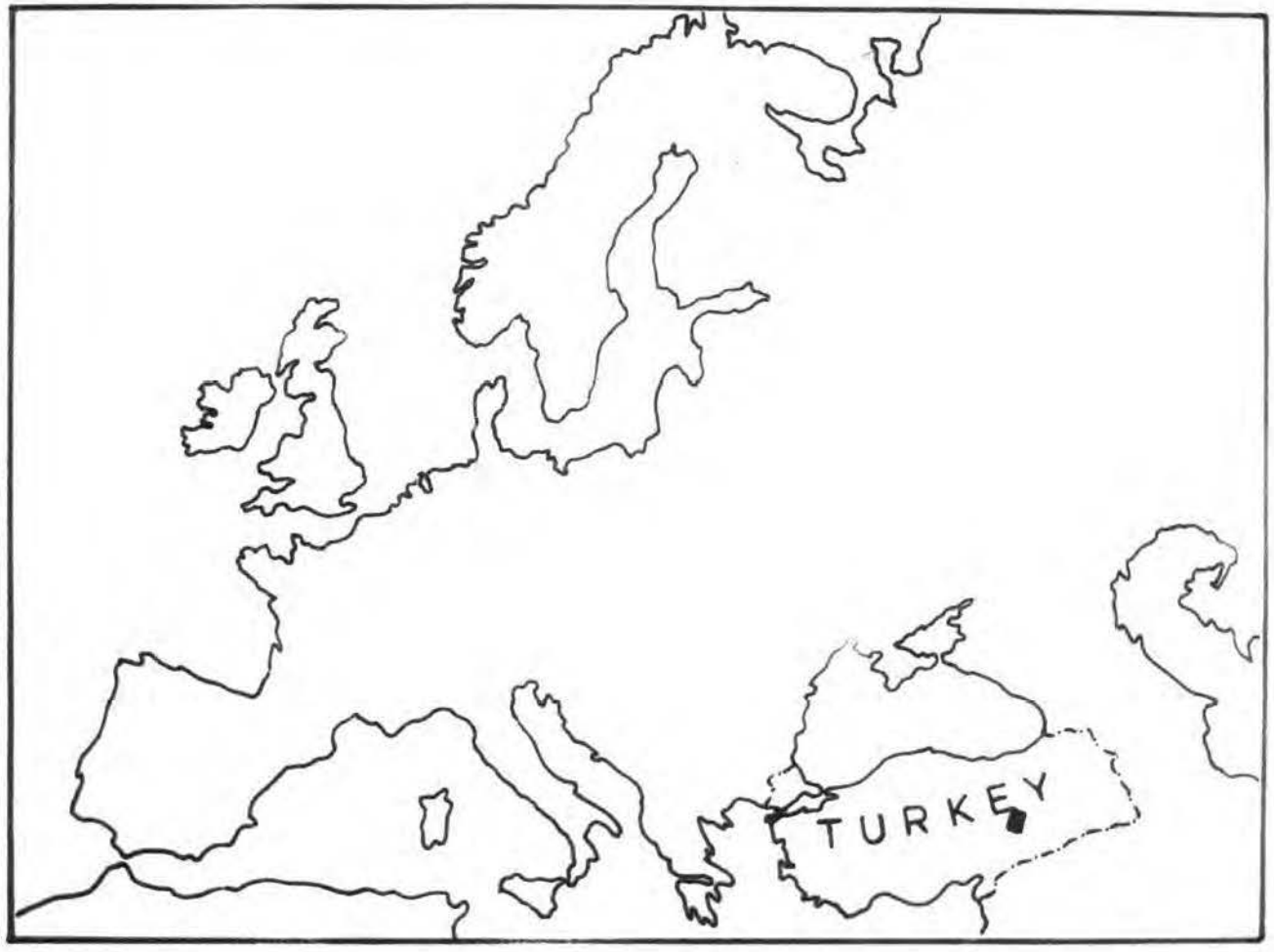

Fig. 1 INDEX MAP OF TURKEY SHOWING THE KEBAN AREA

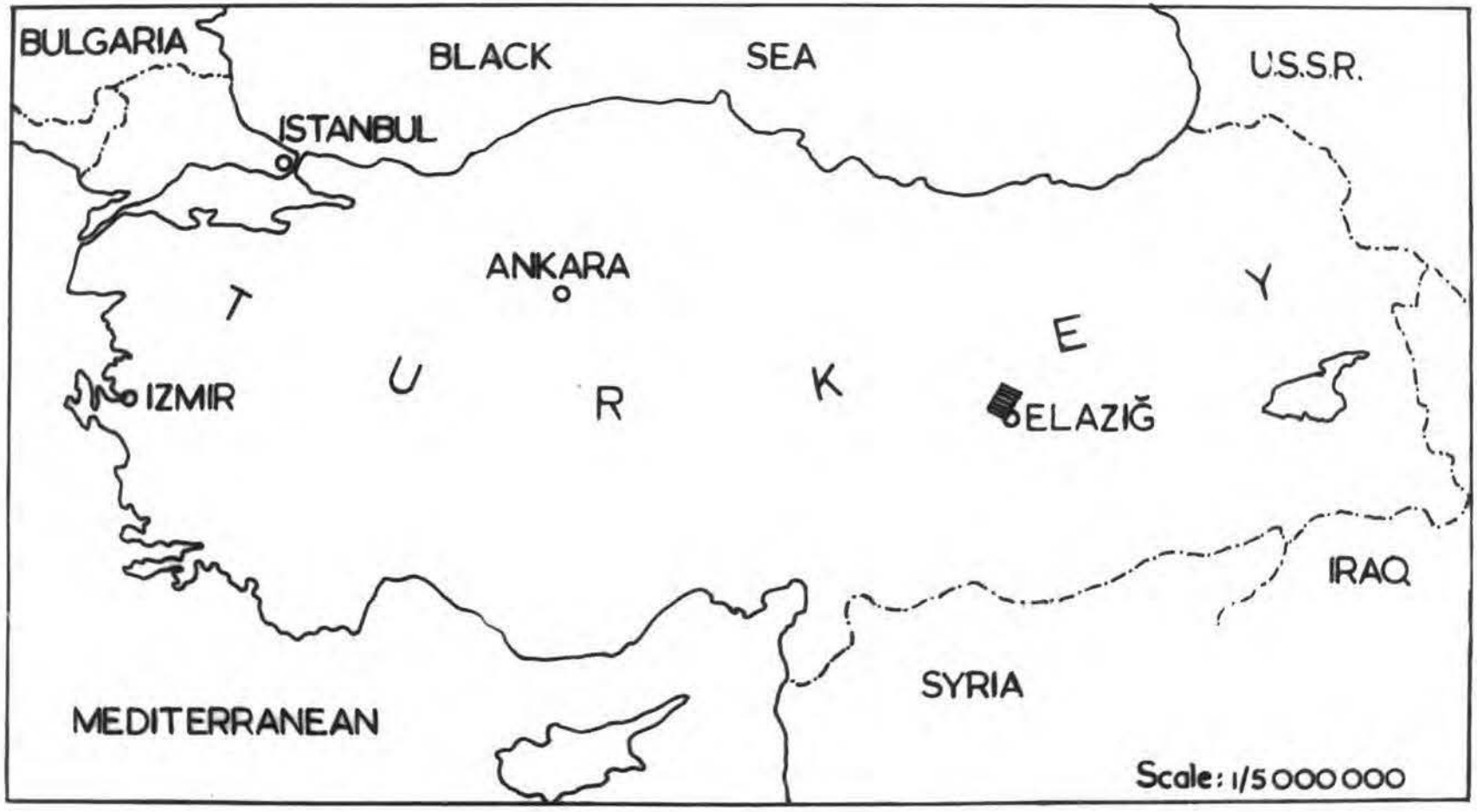

Fig. 2 Location map showing the Keban area

The climate in the province is extreme, being very hot during summer periods and very cold during winter periods. Rainy seasons occur in the autumn and the spring.

There is no vegetation cover in the broad sense but small clusters of oak and fruit trees are found restricted to the margins of the rivers and springs. The main tributaries of the Firat river flow from the eastern area. Among them, the Kebandere, the Zereyandere and the Pamukdere flow roughly parallel to each other, from east to west, and are intermittent streams. In the northwest the Karamagaradere with numberless branches flows in a N-S direction on a plain wider than that of the main river. This is a good example of insequent type drainage. Fig.4 illustrates the main tributaries and drainage patterns in the area. In rainy seasons the flow of the Firat river increases enormously.

Apart from the mining, the local economy is based on crop agriculture and to a lesser extent on sheep-farming.

Keban is one of the most crowded towns in the region, around it there are some village-like settlements locally called mezra. Where water is abundant as on a plain or in the valleys, a sort of hamlet provides summer camping for local immigrants with their sheep.

A very big dam with power plant is being constructed on the Firat river in the area, which is to control its irregular and seasonal flowage. The dam will be used to generate electricity as well as for irrigation purposes, and is to be completed in the 1970's.

History of Mining

The Keban area is one of the oldest mining districts in Eastern Anatolia. Mine workings have been in operation in the area for an unknown period of time. The earliest production record dates from 1728, which is previous to Fiscbach who was a renowned miner, and visited the district in 1877. He pointed out that extraction had been confined mainly to silver and a little lead. Although the production figures to the present are incomplete, it is unlikely that the area had produced great quantities of ore, until a big smelter came into operation in the 1900's when silver extraction reached 4-5,000 kgs per annum. The district was first famed for silver, and so had been known as "Gümüş Madeni", which means the Silver Mine, for a long time. There are some indications that mining operations were mainly open pit workings around the Zeytindag section, where galena occurrences had the greatest proportion of silver, rather than underground workings. A piece of hand picked tailing taken from a tailing stock around a stoped open pit was analysed for silver content by the present company and showed 915 gr of silver per ton of ore, by contrast the present content is 144 gr of silver per ton of concentrated galena.

In between 1934 and 1940 The Mineral Research and Exploration Institute of Turkey (M.T.A.) carried out an intense

Fig. 3 TOPOGRAPHIC MAP OF THE KEBAN AREA

exploration scheme in order to investigate the possibilities for full-scale mining. Estimations of ore reserves revealed the fact that 94,000 tons of lead/zinc with an average of 11% grade could be present. All field and exploration work came to an end in 1952 and the mine was then taken over by the State-owned mining company (Etibank). Since then mining has yielded 225,000 tons of varying grade ore up to 1964. The lead/zinc smelter was built in 1953 and has been operating up to the present. Recent production rate is just over 20,000 tons per annum.

In the 1950's M.T.A. worked on the scheelite mineralization at Kebandere in the Etibank concession, and estimated that 1830 tons of 0.85% WO_3 and 250,000 tons of 0.62% WO_3 scheelite are present. No mining operations have started, as it has been supposed that it is not workable mineralization.

Previous Work:

Much work has been done on the Keban area since the earliest reports by Fiscbach in 1877.

In 1935 H.Yener suggested that the rocks making up the area must have been subject to tectonic movements, giving rise to a synclinal structure with an axis lying in a north-east direction. He pointed out that marble underlying calc-phyllite is exposed on both sides of the syncline, and that the tectonics of the area are extremely complex as a result of movements which produced

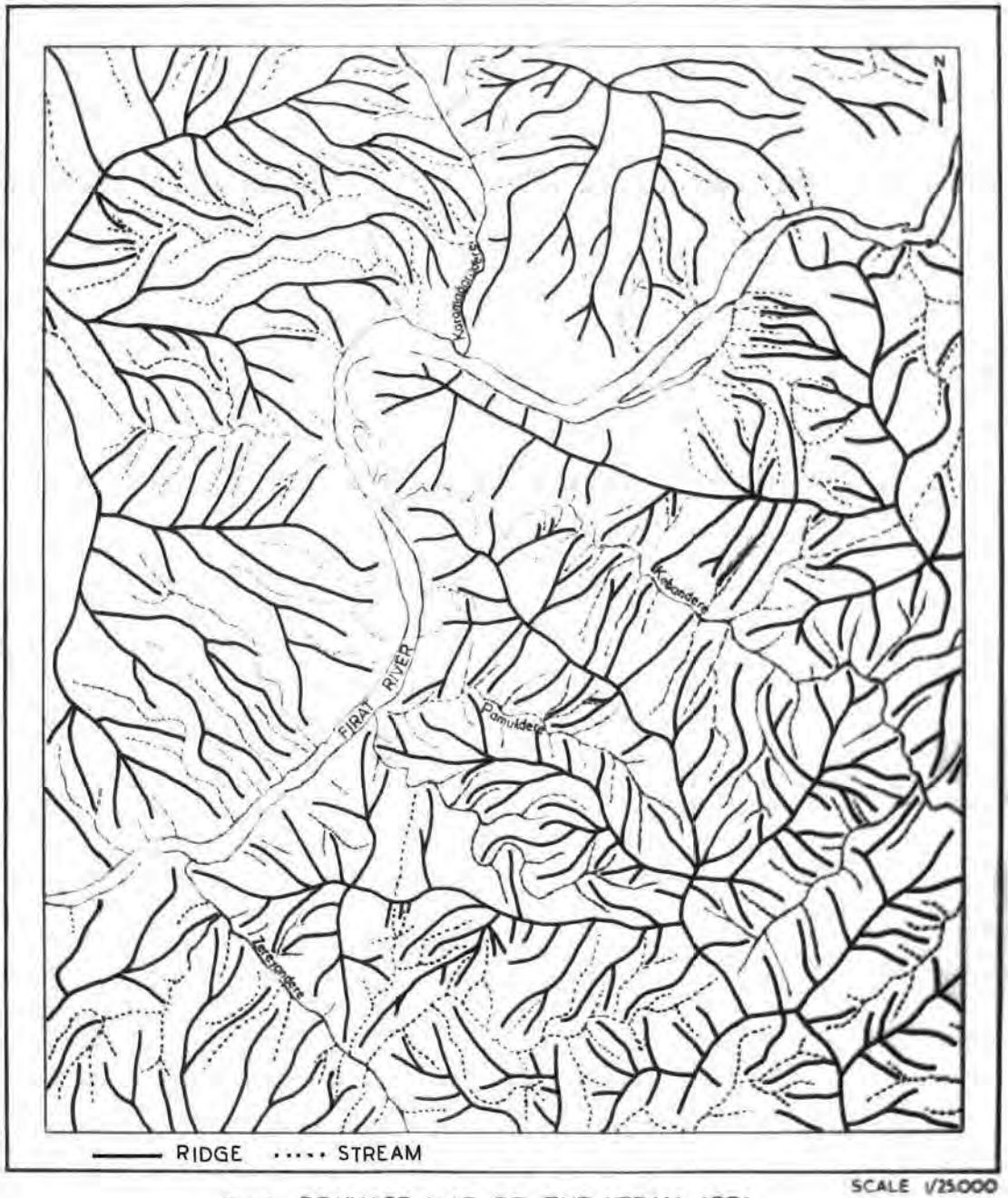

Fig 4 DRAINAGE MAP OF THE KEBAN AREA

folding, faulting etc.

P. Arni examined the area around Keban between 1937-1939 and showed the existence of argillaceous shales, micaceous shales and low-grade metamorphic limestone within a limestone flysch series. According to him the tectonic structure was thrust-faulted and complex.

In 1937 Professor Maucher paid a short visit to the area, and worked exclusively on the petrology and mineralogy of the host rocks and the syenite porphyry intrusion. His report covers a brief description of all rocks regardless of their stratigraphic settings. He also divided the mineralization into four major groups on the basis of origin: a) Galena-silver-sphalerite occurring within the Siftillitepe-Zeytindağ-Derebaca triangle; b) Copper-scheelite deposit at Kebandere; c) Magnetite deposit exposed at Zereyandere; d) Vanadinite found in the walls of a cave to the west. It is worth mentioning that for the first time he drew up a paragenetic table in which the order of mineralization is as follows: pyrite, loellingite, sphalerite, galena. This work led him to conclude that ore mineralization took place after the syenite porphyry had completed its crystallization.

In 1938 Professor Oelsner included all the rocks in the massif in two divisions; a lower marble series and an upper

schist series.

The first detailed map of the area, with a scale of 1:5,000, was completed by N. Tolun in 1950, who at first concentrated on mineralization and exploration. Afterwards he modified and enlarged the previous map on the basis of work and suggestions made by Kovenko. In addition to the surface mapping he made a partial underground map of the 745 m level, the main adit to the Firat deposit. His conception of the structure was that of an inclined syncline with a N-S axis. He also claimed that the tectonic movements producing the present major structure most probably were of Paleozoic age, and classified the rocks in the sequence in terms of stratigraphy and petrology, which is in a broad sense divided into two separate units; the upper marble and the lower schists. Tolun placed the mica-schist as a basement, overlying the calc-schist-sericite-schist and uppermost marble, and shared Kovenko's opinion that there are two different types of syenite porphyry with free quartz and with a small proportion of quartz respectively. The observation made on the relation between syenite porphyry and ore mineralization was of importance, and led him to conclude that the porphyry dykes lying in N-S directions along the marble to the west were mineralized while the igneous body capping the Siftillitepe was entirely devoid of

mineralization. He stated that the deposit is of hydrothermal-metasomatic origin.

In 1952 Professor Borchert also suggested a two-fold division based on stratigraphic settings: a) Lower calcareous schist, b) Upper phyllite marble. His suggestion was that the area gained its present structure by means of the Alpine orogenic movements prior to mineralization.

Following Borchert's work, Professor G. Sağiroğlu regarded the marble as a separate rock unit, and claimed that it was younger then the phyllite. He established two different tectonic periods which were responsible for the present major structure.

In 1961 D.J. Geoffrey determined the rocks under four major series, from the basement upwards: a) Paleozoic calco-schist and schists, b) Permo-Carboniferous marble, c) Upper Permian graphite-sericite schist, d) Eocene/Miocene conglomerates. He concluded that the igneous intrusion had taken place just after the Eocene, and ore bearing fluids in the body had formed lead/zinc deposits. The major structure is that of an assymetric syncline lying in a NE-SW direction. He was in agreement with N. Tolun on the fact that overthrusting from the southeast must have been the cause for the major fault running between the marble and the graphite phyllite and syenite porphyry dyke. Geoffrey distinguished two kinds of ore association in relation to their mode of occurrence:

a) Fine-grained galena-pyrite-sphalerite, in a contact between marble and graphite phyllite, with a calcite gangue, b) Coarse-grained galena together with small amounts of pyrite and sphalerite in marble. It was pointed out that there had been three main ore deposits in the mineralized area; a) The Ağamağara deposit, situated between surface and 800 m above sea level to the east, b) The Derebaca deposit, between 815 m and 745 m levels, c) The Firat deposit between 745 m and 688 m levels. The first two ore deposits are now stoped out and are inaccessible.

In 1964 I. Kumbasar submitted her doctoral thesis on the area, in which she reviewed all earlier investigations. Her study covered the mineralogy and metallogenesis of the rocks and ore minerals without dealing with their geological settings and mutual relations. All geological data and maps were taken from the work of N. Tolun and others. Kumbasar paid some attention to the contact auroles around the syenite porphyry, and studied the skarn minerals in some detail. In the vicinity of syenite porphyry intrusions cutting calc-phyllite at the Kebandere section, some ore minerals of contact metamorphism followed the skarn minerals. Among them magnetite, specular hematite, marcasite, pyrite, scheelite, valeriite, chalcopyrite, sphalerite and native gold are of importance. At the Zereyandere

section several magnetite lenses in association with chalcopyrite originated by means of a contact pneumatolysis process throughout nearby skarn zones. She concluded that the temperature at which ore minerals had crystallized must have been between 370° and 490°C.

The Purpose of the Present Work

Scarcity of basic data on petrology, ore mineralogy and structure have led to considerable uncertainty concerning the geology of the area. The general geological setting and ore mineralization have long been in doubt and there has been little agreement between the previous workers. Several exploration attempts in the past have been based on this unreliable and contradictory data and have consequently suffered setbacks so that full-scale mining never started.

The purpose of the present study, besides the detailed surface and underground mapping which has not been done before except at the 745 m level (the main adit), was to collect as much reliable basic data as possible in the short time available, and to establish the major structure in outline, and the relation of mineralization - particularly sulphide mineralization - to the major structure and its probable source. The new data should aid exploration in the near future, and may lead to full-scale mining operations.

Brief Geology of Turkey

Turkey is a bridge between the European continent and Asia. It is about 1700 km E-W by 520 km N-S, and is roughly rectangular in outline (see Fig.1). The country is surrounded by the Black Sea in the north, the Aegean Sea and Sea of Marmara to the west and the Mediterranean in the south. The two mountain chains making the backbone of the Anatolian peninsula run almost parallel to each other on its north and south shores. The Pontid (in the north) and Taurus (in the south) mountain systems merge towards the east where they produce an extremely rugged hinterland. The Anatolian mountain system is an eastern extension of the Alpine orogenic system.

The peninsula and east Thrace are made of sedimentary, igneous and metamorphic rocks covering in age from Precambrian up to Recent.

Turkey is broadly divided into four major successive tectonic units; from north to south as follows: The Pontid, The Anatolid, The Taurid and the Iranid (Ketin, 1966). These tectonic units lie broadly parallel to each other in an east-west direction which are well in accordance with the divisions in the neighbouring countries (see Fig.5).

The Pontid tectonic unit:

This belt is dominantly made of unmetamorphosed fossiliferous marine formations from the Silurian up to the Pliocene. In addition to these, metamorphic massifs occur in some areas mainly the western part of the belt. The Caledonian, the Hercynian and the early Alpine (Kimmerian) movements have been active in this belt. The Pyreneean and

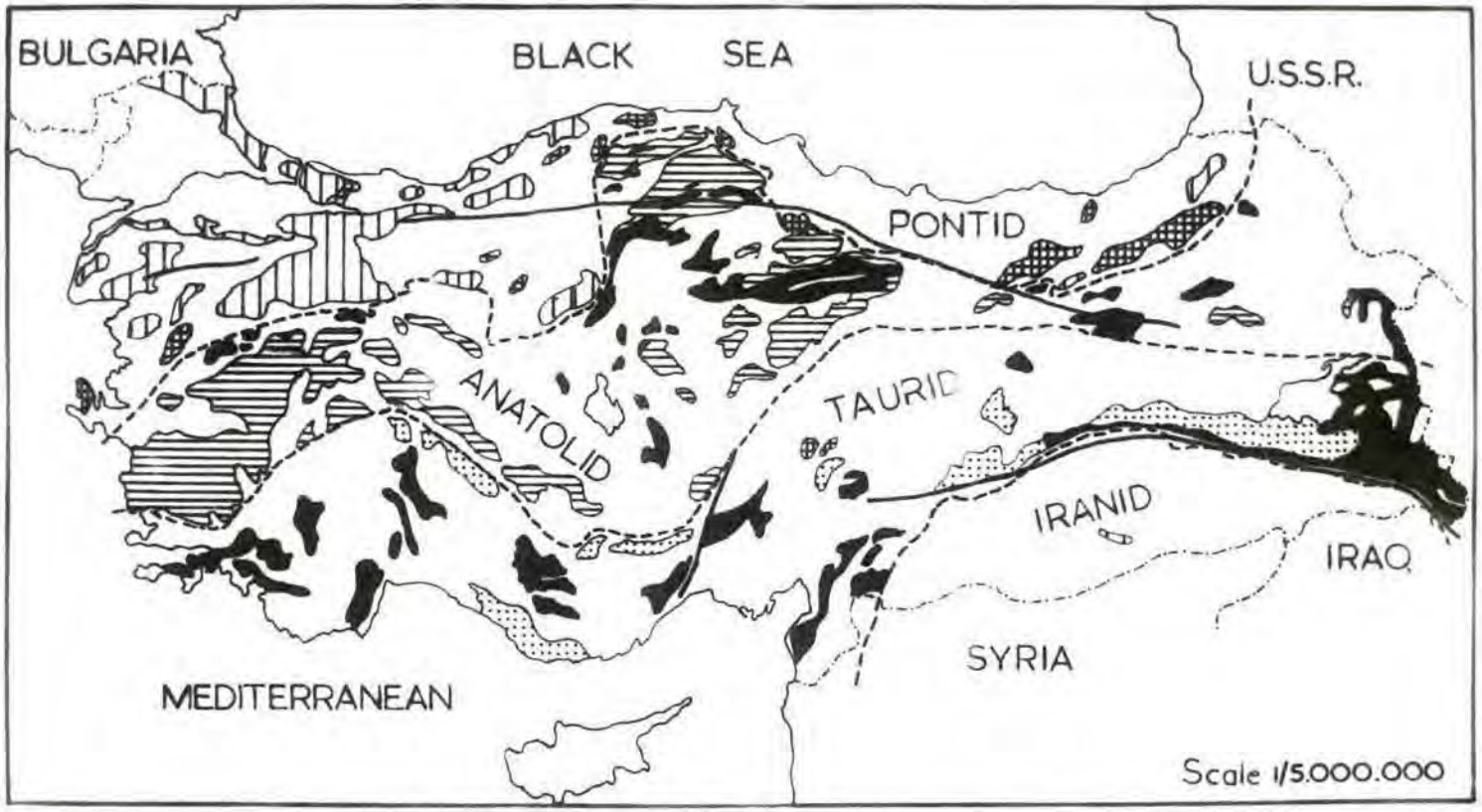

Region of early Alpine Kimmerian folding
Region of Caledonian & Hercynian orogeny
Ophiolites
Region of middle & late Alpine orogeny
Zone of middle Alpine metamorphism
Zone of early Alpine metamorphism
---- Limit of the tectonic units
—— Faults

Fig. 5 THE GENERAL GEOLOGY OF TURKEY WITH ITS TECTONIC UNITS

Helvetic phases following the previous ones are regarded as the paroxysm of the Alpine orogeneses. Important transgressions with respect to the orogenic evolution took place during the Triassic, the Jurassic, the Upper Cretaceous and the early Tertiary. In connection with the orogenic movements, predominantly ultrabasic intrusions occurred throughout the belt which are of importance from the standpoint of ore mineralization because they produced the rich copper and base metal deposits.

The Anatolid tectonic unit

The Anatolid contains the Middle and West Anatolian crystalline massifs or Alpine metamorphosed series and ophiolites of the Upper Cretaceous. These formations are over-lapped unconformably by the Tertiary formations. This belt appears much more stable than that of the Pontid belt. The former shows neither detectable orogenic unconformity between the Paleozoic and the Mesozoic nor the trace of pre-Alpine movements. The Laramian phase developed strongly during the end of Cretaceous, which was followed by the Pyreneean and the Helvetic phases. The folding was obviously completed by the Miocene. Magmatic activity particularly involving basic and acidic intrusions appears to have reached its peak during the Laramian phase.

Since the Keban metamorphic massif is located within the Taurid orogenic belt, it merits relatively more detail than the others, hence it is dealt with separately further on.

The Iranid tectonic unit

The Iranid, accepted as being the foredeep of the Alpine geosyncline of Asia Minor, is made from the Jura-type folding. The region appears to have developed in continued sedimentation from the possible infra-Cambrian up to late Pliocene. Sediments with shallow-water facies suffer neither metamorphism nor magmatic activity. The orogenic movements start with the Laramian phase reaching its peak at the end of Miocene. These movements have mainly given rise to the overturning of anticlines and regional faulting. The magmatic activity is represented by recent flow basalts which occupy large areas in south-east Turkey.

The magmatic activation shows remarkable variations in nature with respect to the defined geological times, which are closely related to ore deposits of the country. These variations are broadly outlined in the country basis as follows: acidic intrusive/extrusive rocks had exclusively come into action during the Paleozoic and to a lesser extent during the Mesozoic while ultrabasic activation was manifestly confined to the Mesozoic. The Tertiary, and following this, the Quarternary, mainly suffered ultrabasic intrusions with all kinds of transitions into extrusive varieties.

A large part of the regional metamorphism which was responsible for making the old foundations in Turkey took place in early Paleozoic and to a much lesser extent during the Mesozoic. Whole rocks, making up the sequence have been subjected to the following major orogenic movements in order of decreasing age: pre-Caledonian, Caledonian, Hercynian and Alpine which was responsible for the present major

structure in the Anatolian peninsula.

Features of the Taurid tectonic unit:

The Taurid tectonic unit is an eastern prolongation of the Alpine mountain chains in Greece and Albania. It occupies an area between the Middle Alpine Anatolid (a part of the Anatolid) in the north and the Iranid of Caledonian to Hercynian age in the south-east. This east-west running belt with a present surface varying between 65-200 km in width becomes progressively narrower towards the east, and continues beyond Turkish territory.

This belt mainly consists of thick conformable sedimentary rocks of marine facies accumulated from the Ordovician up to the end of the Miocene. However, there are also Paleozoic crystalline massifs lying east-west such as Bitlis, Malatya-Pötürge etc., and situated parallel to the trend of the orogenic belt. Those crystalline massifs are most probably Paleozoic in age, and were invaded by intrusions which were mainly acidic in nature. It has been claimed that there was only limited magmatic activity during the Cretaceous when the peridotite-harzburgite of Elasiğ/Tunceli and Ergani/Guleman, the serpentines of Aladağ and Pozanti, and the peridotite-gabbro of the Fethiye region in western Anatolia were forming.

The Alpine movements starting with the Kimmerian phase reached a peak at the end of the Cretaceous followed by paroxysmal movements during the Oligocene. The Taurus mountain range from which the belt name derives, assumed its general formation after the Miocene.

CHAPTER II

GENERAL GEOLOGY OF THE KEBAN AREA

Regional Geology:

The Keban metamorphic massif is rectangular in outline, approximately 35 km by 12.5 km in size. It is separated from the Mesozoic and Tertiary formations by a Permo-Carboniferous blanket limestone surrounding the core of metamorphic rocks (Fig.6). The stratified limestone which reaches several hundred meters in thickness, displays many karstic features, and borders core formation of marble, crystalline limestone and dolomites of uncertain age, and diorite-gabbro and serpentine in the east. Towards the south extensive Eocene formations separate the massif from the Malatya depression which is part of the Malatya-Pötüge Paleozoic massif. The western extension of the stratified limestone is surrounded by Miocene outcrops which filled in depressions of various size in the limestone. Elsewhere andesites and Neogene of continental facies came into contact with the massif. (Baykal, 1966).

The Keban massif forms the northernmost extension of the Malatya-Keban anticline over the Taurid belt, (Fig.7). The massif itself represents an axial depression over the major anticline while its southernmost part suffered a culmination in an E-W direction. The area under investigation is a small part of the massif, on which a recumbent fold trending in a NE-SW direction forms the major early structure. Following it, N-S and about E-W thrust structures together with minor folds complete the structure of the area.

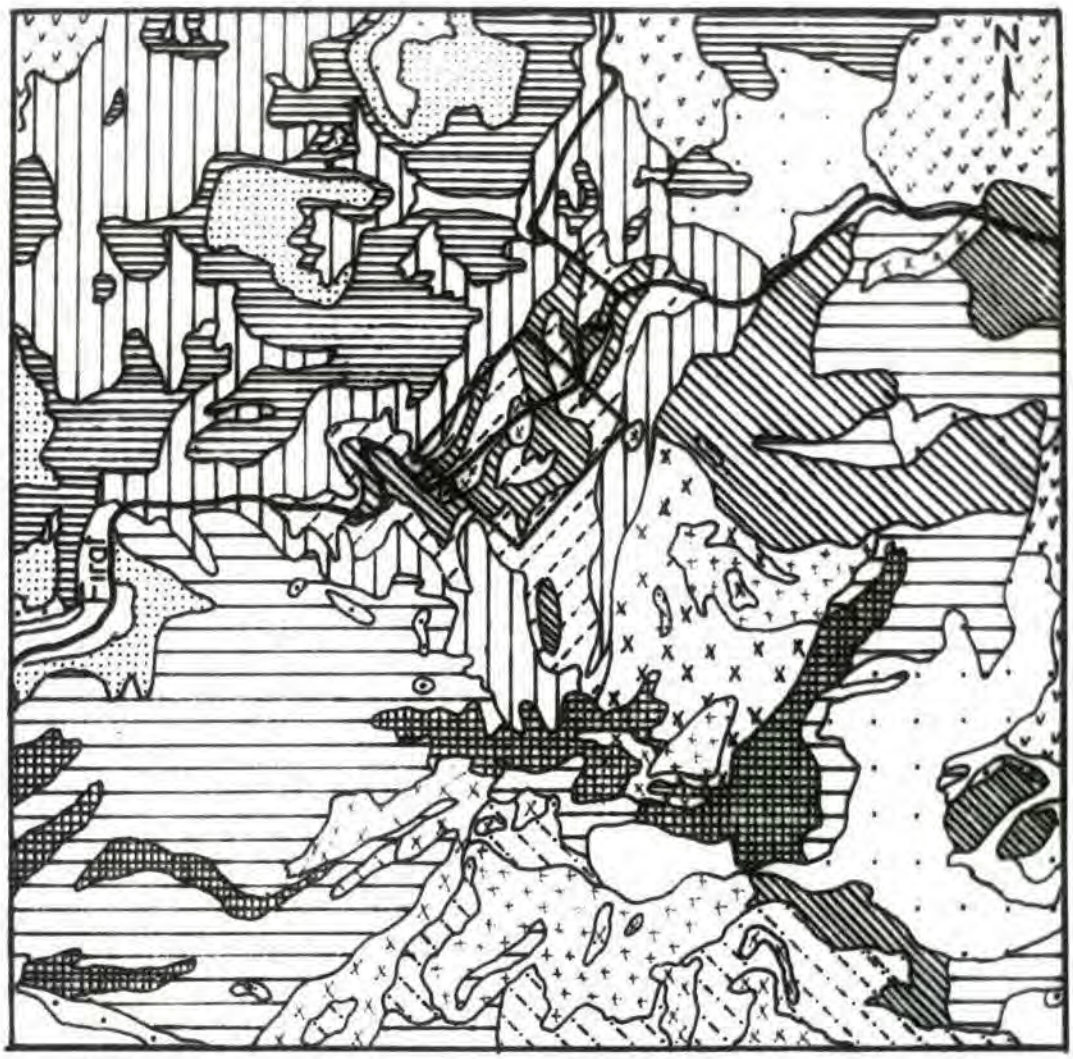

Fig.6 Geologic map of the Keban massif ı the area studied is outlined (After Türkiye Jeoloji Haritası Sivas sheet 1/500.000)

Field Geology

Detailed geological mapping at a scale of 1:10,000 has been carried out over an area of 30 km^2. In addition 4.09 km of underground workings have also been mapped at the 1:500 scale. (See Figs. 8, 9, 10 and 11 in the pocket).

An account of the field occurrences together with a brief description of petrography for each rock in the area is given in the following pages. For detail the reader is referred to the petrography chapter.

Metamorphic rocks

The metamorphic rocks of the massif have been divided into four types based on field observations and microscopic study. Of these, two are subdivided. The boundaries between the four types are as follows in stratigraphical order, youngest at the bottom.

1. Calc-Schist
   a) Chlorite-epidote calc-schist
   b) Fine-grained sericite marble-schist
   c) Sericite calc-schist
2. Fine-grained dolomite marble
3. Phyllite
   a) Calcareous graphite phyllite
   b) Calcareous quartz phyllite
4. Massive marble

1. Calc-schist

a) Chlorite-epidote calc-schist

This rock being the basement has limited outcrop distribution

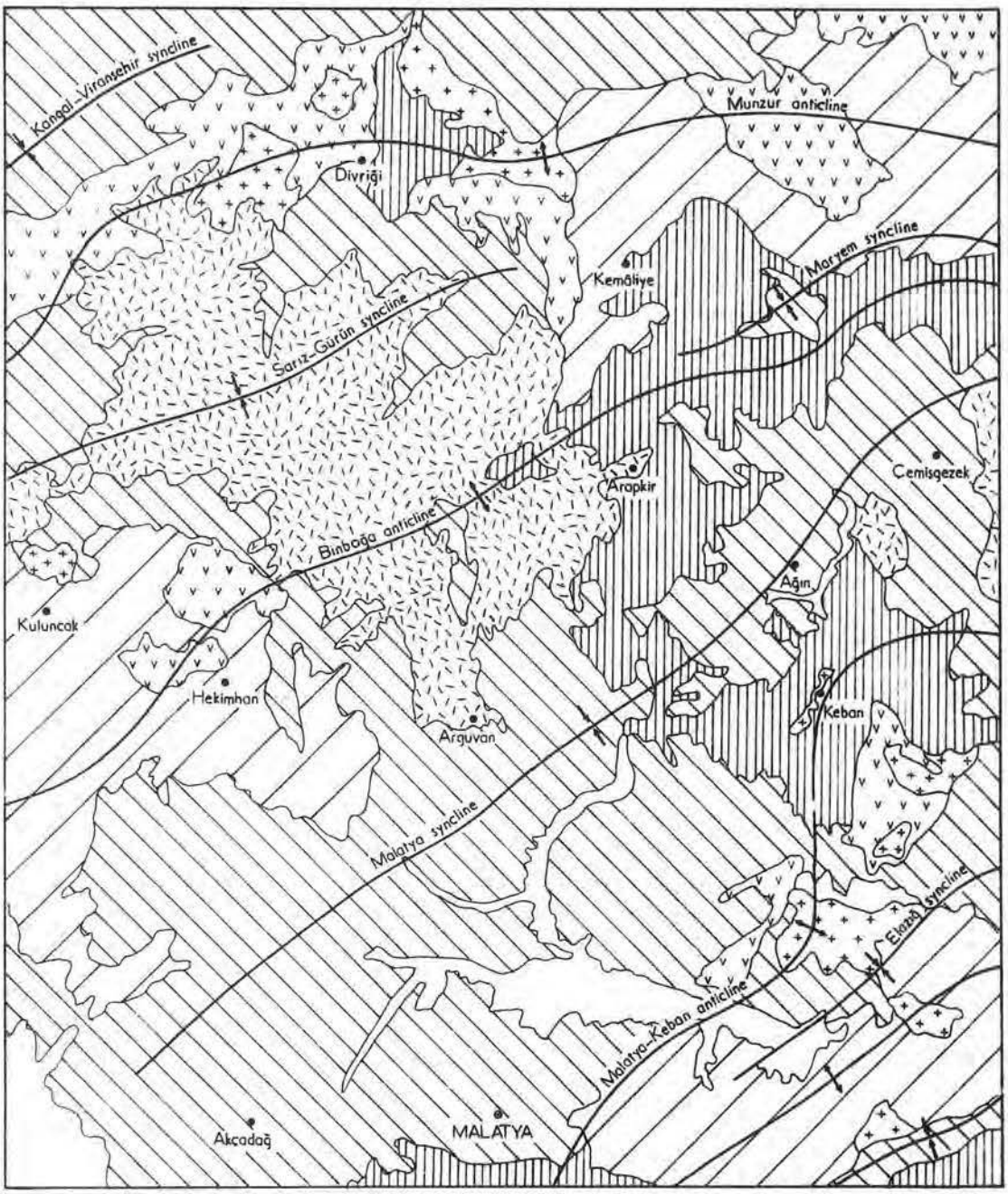

Fig. 7 STRUCTURAL MAP OF THE KEBAN REGION

After Türkiye Jeoloji Haritası Sivas Sheet 1/500.000

which is readily traceable between the Firat river where it makes a sharp curve down to the south, and the Kebandere. Further south there is a lateral transition to (b) fine-grained sericite marble-schist. Both of these lithologies appear to grade upwards into (c) sericite calc-schist, but because of the gradational boundaries between these the three subdivisions are not separately mappable. The abundance of green chlorite and epidote give the chlorite-epidote calc-schist a greenish grey colour. Because of distinct foliation, jointing and step-like formation in the rock it forms cliffs up to 10 metres high in the banks of the Firat river. In hand specimen, a well-developed foliation is revealed by the presence of chlorite-rich and epidote-rich bands and there are occasional small lenses of calcite (Plate 1).

b) Fine-grained sericite marble schist

This subdivision rests conformably on the chlorite-epidote schist, and crops out at the junction between the Kebandere and the Firat river, and stretches further to the south in a strip along the east bank, where it dips down to a 500 m long dolomite-marble exposure. The schist appears around the main adit beneath the dolomite-marble, and its outcrop then gradually becomes wider and wider down to the south, and leaves the mapping area along the

Plate 1 Outcrop patterns of Calc-Schist and Dolomite Marble on the east slope of the Firat river. The Siftillitepe, far background, is capped by Quartz Syenite porphyry (looking N).

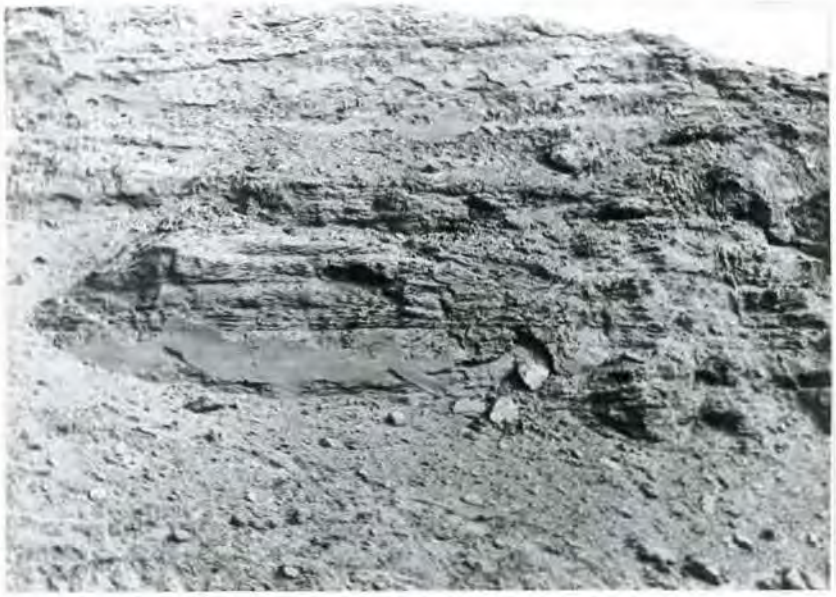

Plate 2 Outcrop pattern of Phyllite in a brook cutting (looking S).

line of the river. To the south of the main adit, there are some marked progressive transitions in vertical and horizontal directions, such as a relative abundance of sericite-marble lenses 0.30 - 2.50 m long, along a foliation plane at the bottom, which pass into marble lenses in the upper levels, reaching up to 7.00 - 10.00 m long and 0.50 - 2.00 m thick. Finally these marble lenses become so abundant that they produce alternating marble layers between schists. At the northwestern part of the mapped area the rock covers extensive areas along State Highway 69 heading northwest, and the exposure is linked with a narrow passage to the south. This creamy white and beige coloured rock with a silky sheen on the foliation planes is easily differentiated from the underlying and overlying subdivisions. Calcite layers a few mm thick alternate with very thin layers of sericite which occasionally show a little biotite. Sericite layers define the well-developed foliation, and small lenses of calcite enclosed by sericite are also present. Fine-grained calcite forms about 90% of the rock.

c) Sericite calc-schist

The sericite calc-schist overlies the fine-grained marble schist, and further south it passes into a sericite calc-schist which is seen to be free of marble lenses, and is interbedded in marble

layers. Despite weathering, its light grey-beige colour is easily recognisable. Highly laminated rock has outcrops extending in a north-south direction on the two sides of the Firat river. No stratigraphic or tectonic unconformity between the two subdivisions can be detected.

Sericite becomes much more common in the top subdivision than in the lower subdivisions. As a result of the increase in sericite, the foliation planes become much more pronounced. The highly schistose rock is brownish-beige in colour. Excess sericite in some layers gives the rock a silky appearance. An increase in both proportion and size of calcite lenses is also marked in hand specimens, as compared with the fine-grained sericite marble schist. Perfect foliation develops exclusively in micaceous layers, rather than in lenticular form.

2. Fine-grained dolomite marble:

This compact brown rock with numerous fractures is exposed all along the slopes facing the Firat river (Plate 1). A Cliff-like dolomite marble outcrop 700 m from Nalli Ziyaret to the west is cut by a syenite porphyry dyke. Afterwards the exposure dips down to a blanket of recent polymictic conglomerates, then reappears in a rather large outcrop on the south side of the Kebandere, and continues by the river as far as 350 m south

of the main adit, where a wedge of calc-schist comes between it and the river for a distance of about 500 m long. The exposure makes a sharp turn west to the Hantepe because of a NW-SE fault which lies west of the Hantepe. It continues again to the south becoming wider. There is a large disconnection between the Büyüktastepe and south of the Delilktetas (942 m) where a sheet of syenite porphyry borders the overlying marble instead of the dolomite marble. After crossing the gap, the dolomite marble wedge with its sharp point in the north gives two separate exposures with a sheet-like igneous rock between them. The dolomite marble also covers large areas in the extreme southwest corner of the mapping area.

No outcrops of the northern prolongation of the dolomite marble on the east slope between the calc-schist and the phyllite have been found. However, on the other slope, the rock appears in its right stratigraphic position, and pinches out after 1.5 km. Following the discontinuity over 2 km another wedge becomes visible. Small exposures of dolomite marble not being mappable occur in a line between the two wedges. There seems to have been an incomplete sedimentation over a local area, which also suggests lateral change between the calc-schist and the dolomite marble.

Grey and light brown dolomite marble is confined to the north, on the east slope, it is massive and extremely fractured but gradually turns into poorly to moderately-defined layers towards the south.

Graphite and carbonaceous contaminants become increasingly abundant further south. Some manganese minerals are also constituent of the common impurities. At the Pamukdere the upper part of the massive fractured rock passes into relatively well-layered dark dolomite marble with interfingered contact between two, a wedge of one being barely 5 m thick.

Further south, in the northwest to the Büyüktastepe, the rock is apparently made of two different levels; the lower light beige marble, and the upper layered dark grey dolomite marble. The former with a little proportion of sericite consists of layers of an average thickness of 0.20 m. The latter is composed of strongly pronounced layers varying between 0.30 and 1.00 m in thickness. Its southern extension alternates with calcareous graphite-phyllite, and passes upwards into the massive dolomite marble marking gradiation into the overlying calcareous graphite-phyllite. All layers containing carbonaceous impurities are cut by numerous veins of coarse, clear calcite in association with quartz and sericite flakes. The veins probably represent old channelways, the fluids passed throughout them and removed the carbonaceous impurity to a certain extent.

Still further south around the Zereyandere the rock alternates with sericite calc-schist, thin marble layers and small marble lenses, which all together exhibit gradiation down to the calc-schist. The

combined microscopic study and field evidence show that the dolomite marble tends to be less metamorphosed as it passes to the south.

The dolomite marble exposed on the other flank starts with a massive, fractured basement, and continues all the way in the mapped area, and then progressively converts into thin layers, intercalated with the calcareous graphite phyllite. No equivalent of the dark-grey upper level in the east side, has been found in the western part. The other difference is the existance of overlying comformable calcareous graphite phyllite, however it is found as small smashed, and disconnected strips along the N-S trending major fault which brought the marble into contact with the dolomite marble. A small-sized (barely 9.00 m thick) calcareous graphite phyllite outcrop is mainly restricted to the ground between 100 m north to the Derebaca main adit entrance and some distance northwest to the Büyüktastepe.

Dark brown and dark grey brittle rocks with intense fracturing are stained by iron oxides, and are cut by white clear calcite veins. The foliation can hardly be seen in hand specimens collected from the outcrops in the north, while specimens taken from the southern part maintain moderately developed foliation. The dark coloured hard and compact hand specimen is made of fine-grained dolomite, in which the foliation is recognisable by means of carbonaceous impurities. Since the rock is resistant, perfect sets of joints caused production of

cobble size fragments on weathering. Weathering together with descending water gives rise to irregular patterns on open surfaces in the rock.

3. Phyllite

The phyllite is a fine or medium-fine grained schistose rock consisting of variable amounts of quartz, calcite, muscovite/sericite, graphite with albite and accessory minerals. As a whole the rock covers an area between the two marble outcrops in the middle of the mapping area. Towards the east its outcrop is terminated by the marble trending in a N-S direction from the central phyllite. Although the exposures of phyllite in the eastern part of the mapped area are discontinuous, out of the area the rock becomes more abundant. To a lesser extent outcrops are seen to have been restricted to the west along the marble in the north where contact between the phyllite and underlying calc-schist is obscured by metasomatised syenite porphyry which is emplaced between the two rocks. In places intrusive igneous rock borders the two schists. A similar contact is traceable on the west side where the calcareous graphite-phyllite seems to be resting over the calc-schist. The majority of the west border of the area is confined to the phyllite with the exception of a marble exposure at the Halceuliği sarti. The following two subdivisions can be distinguished in the field; the calcareous-graphite phyllite at the bottom, and the calcareous-quartz phyllite at the top. (Plate 2).

a) Calcareous-graphite phyllite

As seen along the Kebandere and through the underground workings this has an abundance of graphite in comparison with the upper part. A flaky, patchy or pod-like appearance due to the high flaky mineral content is easily recognised. Disconnected tiny quartz or calcite lenses on foliation planes locally alternate with flaky layers. At the Kebandere section near to the scheelite mineralization, the lower phyllite shows a distinct alternation of graphite and calcite, in dark and light bands. In places the rock, where cut by the syenite porphyry, has a different appearance because of enrichment in the quartz content and depletion in graphite content. There are also numerous clear calcite and quartz veinlets in association with pyrite nodules through the rock. It is seen that the rock is brecciated where it has come into contact with marble producing great numbers of isolated adjacent marble blocks and pebbles.

b) Calcareous-quartz phyllite

The rock varying from light brown or beige to dark in colour and having satin finished foliation planes owing to the presence of sericite, with calcite lenses and marble layers between flaky minerals is quite distinctive except at its contact with the intrusive rock. At a horizon some 30 metres above the base, there is an abundance of boudinage structures whose competent cores are made of quartz or calcite respectively depending upon their local abundance, the surrounding rock being much richer in chlorite than in the average

rock elsewhere. Above this horizon thin bluish calcite layers alternating with graphite, sericite and chlorite pass upwards into a graphite rich variety, very dark in colour, which gradually becomes a phyllite changing from a quartz rich to a brown coloured micaceous variety. In places, what may be termed "marble rafts" (isolated marble lenses) float through the upper half of the sequence, their position in the field being well in accordance with the major structural trend. These are due to the different rigidity between marble and surrounding phyllite, and result from the mechanical contact of movements acting on them.

4. Marble

This uppermost rock type of the sequence forms the high ground trending N-S, and encloses the area to the east. Its exposure is cut transversely by the Firat river in the north (Plate 3) and the Kebandere in the south where its surface width is as much as 2.2 km. The Zeytindağ marble 0.8 km across seems to be separated on the surface from the main body, but is believed to be connected to it at depth.

The rock being fractured and massive shows no layering, stratification or any other primary features that might have been present prior to metamorphism. Outside the mapped area to the south it has a poor layering as the top is approached.

The marble is composed of fine to coarse grains of calcite in

Plate 3 Exposures of Marble cut by the Firat river (looking N).

Plate 4 Quartz-Syenite Porphyry outcrops exposed in a cutting of State Highway 69 (looking N).

association with flaky minerals, and quartz and opaque minerals in accessory amounts. White and reddish brown are the predominant colours, and are seen everywhere except the places where it has been subjected to igneous activity. Clear calcite and quartz veinlets cutting across the marble are a common feature.

As seen from the surface map in the east the marble is free from intrusions except in the extreme northern part. On the other hand, the marble in the west is associated with the syenite porphyry.

Despite its massive nature, it is a cavernous marble, due to surface and underground water percolating through the fractures and cracks. The northern extremity of the eastern part has well-developed caverns of a range of different size.

Igneous rock:

Bodies of syenite porphyry, the only igenous rock type found, outcrop in a N-S belt across the middle of the area. This is believed to be a major structural line. Both sheets and dykes are represented. The occurrences at the Zereyandere, and between the Siftillitepe and the Nalli Ziyaret, and the Karamağaradere are believed to be eroded remnants of sheets (Plate 4). The sheet syenite porphyry of the Zereyandere section is found between the calc-schist and the dolomite marble, with a rather invariable dipping of 30° to the SE, which more or less coincides with the dipping in the

vicinity. Further north and some distance west to the Büyüktastepe the rock joins the separate eastern branch cutting the dolomite marble which is in part sheet-like, although its attitude through the cutting makes frequent change between 25° and 70°SE. After the two separate have joined, the single sheet with a maximum exposure width at outset keeps the same setting towards north as far as a cross-fault, 230 m west of Hasantepe, and its northern extremity turns into a dyke barely 5.00 m thick which keeps a trending parallel to the river for 1.2 km long with a dipping of 45° to the SE.

The Siftillitepe body is enclosed by several remnants from the main body in the north and south, with a distance to the main body which seems to be equal to the surface distance. In contrast the Nalli Ziyaret body has numerous radiating branches cutting through the bordering phyllite. One of which is barely 10 m thick.

Elsewhere igneous activity is incorporated in dykes of different sizes, one of which is very remarkable being 10 m thick and about 5 km long, and follows the western marble from the south to south of the Kebandere with a dipping between 45° and 75° to the SE.

Its apparent colour changes from light speckled beige to

yellowish or reddish brown with respect to degree of alteration and size of the rock. However, in large bodies a decrease in grain size radiating towards the periphery is detectable to the naked eye. Exceptionally growth of euhedral alkali feldspar crystals as much as 5 cm long, with different orientation in the centre, reveal a kind of gradual change towards the border zones; in any case the well-defined porphyry appearance is distinctive or in extreme cases is poorly visible depending upon its degree of alteration.

Age of the intrusions:

It has long been claimed by several workers that the intrusion has taken place after the Cretaceous or during early Tertiary. Ketin (1966) suggested that "The granitic-dioritic rocks (namely the Keban syenite porphyries) from Elazig/Malatya, and the syenites of Divrik had occurred in the Cretaceous beds, and were covered by the Eocene". Kovenko (1937) pointed out that the syenite cuts the adjacent upper Mesozoic limestone. Those three igneous bodies are located relatively close to each other, and have close similarities in connection with petrology, mineralogy and metallogenesis. The present author examined the alkali syenite intrusion in Kuluncak/Malatya in the 1966 field season. This alkali syenite cuts through the fossiliferous Jurassic-Cretaceous limestone, and is overlaid by the Eocene basal

conglomerates which includes pebbles of the syenite (Plate 5). Therefore it must have been intruded during the Paleocene or most probably during the Upper Paleocene.

Volcanic breccia:

Two small outcrops of volcanic breccia barely 5.00 m thick are exposed in Highway 69 about 250 m north east of the Nalli Ziyaret syenite porphyry body (Plate 6). The breccias are close to several small-scale porphyry dykes. They dip between 65° and 80° northeast, and have sharp contacts with the enclosing phyllite. Their fragments fall into the lapilli group (4-32 mm across) of accidental origin, derived from the host rock and immediately underlying formations. The fragments include phyllite, calc-schist, marble, feldspars and opaque minerals which are cemented by a greenish grey hard looking glassy matrix. The fragments usually appear to be rounded rather than angular thus being an evidence of attrition. Disintegration of the fragments, and rounding of separated fragments are most readily accounted for as a consequence of abrasion and attrition (cf. Reynolds, 1954).

Recent sedimentary rocks:

Sedimentary rocks are entirely represented by detrital rocks derived from previously formed metamorphic or igneous rocks, and contribute in a small amount to the sequence. Relatively small

Plate 5 Syenite overlaid by the Eocene basal conglomerates in the Kuluncak region/Malatya (looking NE).

Plate 6 Volcanic breccia (looking S).

outcrops are encountered along and in the immediate vicinity of the Kebandere and the Firat river. In places where the old topographic surface was relatively flat the rock extended over a large area, contrasting with its narrow strips of the steep areas. In the north, along the Karamağaradere, the terrace-like conglomerates in narrow strips occupy an area between the 740-760 m levels, and dip gently to the SE. Two blankets of conglomerate, maximum 210 m wide in a N-S direction rest over the basement some distance east and west of the Karamağaradere. Further south ribbon-like conglomerates are seen to be between the Firat river and the Highway 69. Towards the east a large north-south directional exposure was separated by a cross-cut brook. An extensive conglomerate lying in an east-west direction occurs between the Kebandere in the south and the Firat river in the north, in a rather thick blanket, and it disappears in wedge-out along the Kebandere upriver. The southern prolongation has been cut off by the river, on which the mine road rests.

The polymictic conglomerates, making both terrace and channel deposits were unconformably accumulated over the old erosion surface of the schists (Plate 7). Their thickness attains up to 60 m, generally varying between 0.5 - 10 m. The initial surface angle was about 15° in a southerly direction. The rock, which has reached some degree of induration, is made up of some far

Plate 7 Polymictic conglomerates resting over the eroded surface of Calc-Schist, on the road to the main adit (looking E).

Plate 8 Grossularite and andradite crystals showing zoning. x50.

travelled rock fragments including ophiolitic rocks, glaucophane schists and granitic rocks transported from the surrounding or far distant massives, besides pebbles and blocks of the local rocks. The roundness varies from good to moderate. All the constituents are poorly sorted, and are cemented by a calcareous/ clayey sandy matrix.

Impure sand banks and loose pebbles to cobbles in size are found along the Firat river, and at the junction between it and its tributaries there have been accumulations on varying scales.

Regional metamorphism

The Keban metamorphic massif is one of the several old metamorphic massifs isolated from each other by younger sedimentary systems in the Taurid Belt. The massif, part of which is under investigation comprises the northern elongation of the old basement system running from the south. Within the belt there is a wide range of metamorphic facies. The Binboğa mountain range in the west consists of rocks exclusively formed in the epizone facies. As lower and lower horizons appear on the surface towards the Malatya-Pötüge massif in the east, augen gneiss mixed with granites and pyroxenites become visible, and these are characteristic rocks of the Katazone facies. Therefore there is a gradation from the epizone to the Katazone towards the east. By contrast the Keban massif is composed of rocks belonging to the epizone facies of Grubenmann (Baykal, 1966).

In the Keban massif low-grade regional metamorphic processes resulted in the alteration of magnesia rich and pure limestone rocks to the dolomite marble while the pure marble suffered almost complete recrystallization, and the carbonate rich pelitic rocks with variable amounts of organic impurities were altered to phyllite and calc-schist.

The present mineral assemblages belong to the greenschist facies. They involve its two subfacies respectively: a) Muscovite/sericite-chlorite subfacies, b) Biotite-chlorite subfacies (in both cases with excess silica and K_2O). It is, however, clear that the muscovite-chlorite sub-facies has a much wider distribution, than the biotite-chlorite subfacies. Biotite being a common critical mineral associating with the subfacies is present in decreasing abundance within the schistose rocks. Therefore, prevailing metamorphic conditions were in favour of the lowest grade metamorphism. However, there are some indications marking a tendency towards relatively higher metamorphism, which is not on a regional scale. An increase in chlorite and epidote content of the lower calc-schist implies a slight gradation into the albite-epidote-amphibolite facies. The occasional appearance of actinolite also supports the gradation. Limitation of the metamorphic facies based on the anorthite content in the plagioclases gives additional evidence for the

higher degree of metamorphism. The plagioclase mainly found in the calc-schist and the phyllite has an average An content exceeding 7% which is the upper limit for the greenschist facies. (Turner and Verhoogen, 1960). Since the plagioclase with a higher anorthite content is mainly associated with epidote, it indicates that the temperature attained during the metamorphism surpassed the temperature limit for a greenschist facies (Winkler, 1965).

The temperature at which change from one subfacies to the other took place, merits some consideration in the light of present evidence. The absence of periclase-brucite assemblage and diopside throughout the siliceous dolomite marble indicates relatively low temperature, as diopside forms at 490°C from breaking down of siliceous dolomite limestone (Bowen, 1940). On the other hand partial co-existance of the biotite-chlorite subfacies exceeds the limit so the temperature under the relatively high fluid pressure, at the beginning of this subfacies must have been around 450° to 470°C (Winkler, 1965).

The date of the regional metamorphism may be estimated by correlation of the other massifs to their surroundings within the Taurid belt. The Binboğa mountain range in the west is covered by the fossiliferous Devonian and Silurian rocks, and is enclosed by the Permo-Carboniferous rocks. The formation overlying

the Keban massif is claimed to be Permo-Carboniferous, and it has close comparison in many aspects to the Permo-Carboniferous of the Binboğa mountains. None of these rocks has undergone regional metamorphism (Baykal, 1966). Therefore, the regional metamorphism over a large area most probably must have taken place before the Silurian.

Contact metamorphism and metasomatism

The metamorphic rocks surrounding the igneous rock have all been affected by the fluids and heat generated by the intrusion. The affected areas are broadly located along the Kebandere, around the Nalli Ziyaret, the Zereyandere and to a lesser extent along the Karamağaradere. Under the thermal influence pyrometamorphic hornfels formed as xenoliths, these are found within the igneous rock. In addition normal contact hornfels or spotted schists occur in the immediate vicinity of the syenite porphyry in which graphite and flaky minerals make concentration barely 3 cm in diameter. This aureole is between 2 m and 75 m in width depending upon the size of the intrusive body. Immediately adjacent to the intrusion the influence has been so intense that the original character of the phyllite is no longer recognizable and complete recrystallization has taken place at the expense of foliation. In some places such as the Siftillitepe a marked depletion in graphite content was noted. By contrast, at the

Kebandere graphite in the phyllite is so rearranged that it alternates in black bands with pale recrystallized calcite and quartz. The twinning common in normal calcite of the white marble has partly been destroyed, and borders of the individual grains have been attacked and corroded. In addition the calcite in these recrystallized areas (next to the igneous body) is strongly fluorescent in shade of pink, whereas the normal white marble does not fluoresce under ultra-violet light. The fluorescence is apparently due to trace amounts of lead present in the recrystallized calcite but not in the normal marble (Schulman and others, 1947). An increase in quartz and calcite veinlets is observed as the syenite porphyry is approached. The dolomite marble immediately west of the Nalli Ziyaret body became a massive rock due to complete recrystallization but was subsequently made friable by the metasomatism; it can now be crushed into small pieces with gentle hammering.

Under the conditions of combined contact metamorphism and metasomatism a skarn zone of variable width was formed around the intrusive body. A close examination reveals that the skarn zone is formed mainly in the metamorphic rocks, with only a little in the quartz-syenite porphyry. There is no complete gradation from the host rocks into the skarn zone. The skarn contains grossularite in lenses barely 1 m thick in the phyllite, and sharp discontinuity across the contact suggests the skarn formed

almost as along a front. It is a striking thing that in some places there is a relative concentration of skarn silicates in rocks far from the igneous body raising the possibility that in these areas there was no great influx of elements from the igneous rock, and these changes were produced chiefly by local rearrangements.

The skarn zones vary considerably from place to place. Despite this they may be grouped on the basis of the most frequent and characteristic mineral assemblages. The grouping is as follows:

a) Wollastonite-garnet-vezuvianite-phlogopite occurrence at the Kebandere.

b) Vezuvianite-actinolite-diopside occurrence at the Nalli Ziyaret.

c) Garnet-chondrodite-scapolite-lepidolite occurrence at the Zereyandere.

a) Wollastonite-garnet-vezuvianite-phlogopite group:

The wollastonite is apparently limited to the higher temperature skarns, and is found in small amount restricted entirely to the Kebandere. Its formation along with feldspar, garnet and vezuvianite indicates excess alumina in the host rock. The garnet is exceptionally abundant in this zone; two kinds of garnet in terms of Gr-An-Al composition are identified as being grossularite and andradite. Their composition was obtained by the cell-size measurements on the diffractometer, against refraction indices.

(Sriramadas, 1957). The average value for gossularite and andradite is tabulated in table 1.

Table 1

Mineral	cell size A°	R.I.	Composition
Grossularite	11.605	1.76	$Gr_{82}\ An_{16}\ Al_{2}$
Andradite	11.980	1.87	$An_{90}\ Gr_{3}\ Al_{7}$

Both grossularite and andradite show a compositional zoning indicating disequilibrium in crystallization (Plate 8). The euhedral crystals making aggregates are coloured in a range of dark brown and pearl brown. The crystal size stays in a wide range from 0.2 mm to 1.5 cm. Apart from their massive nature they never exceed 10% of the rock by volume. Complex twinning is common. In places where iron is available grossularite displays a transition into iron bearing andradite which differs from grossularite by its distinct brownish pleochroic colour and anisotropism. The vezuvianite has a rather limited distribution, and occurs in a close association with feldspar and grossularite. Needle-like and anhedral grains of vezuvianite with a distinct parting resemble very much grossularite under the plain light. Its faint pleochroic colour varying in grey, and unzoned grains are dissimilar to grossularite.

b) Vezuvianite-actinolite-diopside group:

Actinolite with characteristic amphibole cross-section and fibrous grains are restricted to the Nalli Ziyaret section. Two

and is found with corroded outlines. Two generations of scapolite and lepidotite are present.

Besides the above mentioned minerals, fluorite, albite, epidote, quartz and calcite are common constituents of almost every skarn zone. Iron oxides and sulphide minerals along with scheelite and native gold (Kumbasar, 1964) are also sometimes found within the skarn zones.

Of these, fluorite merits a brief explanation as it carries radioactive features. Two types of fluorite have been found through the area; the wide-spread dark purple fluorite first to crystallize is associated with skarn formations while the pale green variety accompanies the lead/zinc mineralization as a gangue mineral. A few exceptions occur in places where the purple fluorite is lined by the green variety in vugs, indicating age relation and a long break in time as revealed by the contact between them. Dark purple colouring is caused by either radiation or an appreciable amount of strontium. (Dunham, 1952 and Steyn, 1954). In fact the main substitution to Ca^{+2} is Sr^{+2} which has the ionic radii of 1.27 A° being bigger than for Ca^{+} 1.06 A°. When Sr substitutes for Ca an increase in the cube-edge takes place over the fluorite crystal. According to Steyn very dark purple fluorite may include as much as 1% Sr in, which are mainly confined granite and alkali rocks. It is believed that both processes were responsible for the purple fluorite occurring in the area. In fact it has been reported that

thorium and uranium are present in the syenite porphyry. (Personal communication). This is also supported by the XRF (X-ray fluorescent) analysis which showed the presence of additional radium. The cell-size measurements were made on two types of fluorite by the powder camera method, using Ilford Ind.B slow exposure. The results together with certain trace elements in both fluorites are given in table 3.

Table 3

Sample No.	Cell-size A°	Sr	Ba	Zr	Rb	Zn	Cu	Ni	Sm	ppm
ER-12 (purple)	5.462	68	88	35	1	44	47	27	?	
ER-26 (green)	5.460	33	75	2	<1	54	32	<1	?	

From the table their strontium and barium content are well in accordance with Steyn's claim because the former element of the purple fluorite is twice that in the green variety. The green colouration may be due to the presence of bivalent samarium (Feofilov, 1956 and Bill, 1967) but the XRF analyses failed to detect its presence, it may be likely the case is that it is under the detection limit of the instrument.

As a result, following the thermal metamorphism, Li, F, Ka, Na, Cl, CO_2, S, Fe and Si emanated from the magma to produce the skarn zones. Since the occurrence of chondrodite is restricted to places where magnesium is available, this suggests little or no magnesium emanation took place.

Wall-rock alteration

The wide-spread wall-rock alteration is associated with the syenite porphyry intrusion and the subsequent ore mineralization. Although all-gradations are present, it has become evident that the wall-rock alteration occurred in three different stages. These stages differ from each other on the basis of mineral assemblage, mode of occurrence and time at which they formed. Under the influence of the combined contact metamorphism and metasomatism of the syenite porphyry, calc-silicate and the other derivatives formed particularly in the Kebandere, Nalli Ziyaret and Zereyandere sections. The extensive presence of calc-silicate, especially of grossularite and to a lesser extent andradite and quartz itself illustrates intense silicification. In the Kebandere section a marble originally having less than 1% SiO_2 bordering the igneous body produced abundant grossularite as well as quartz in accessory amounts. Under decreasing temperature conditions away from the intrusion margins the following wall-rock alteration zones are identified: a) Sericite-kaolinite, b) Fluorite-sulphide-iron ore-garnet, c) Garnet-quartz-calcite. The process from which these alteration zones formed is attributed to the first stage.

The over-all evidence suggests that the second stage alteration has possibly taken place between the first stage described and the formation of the main sulphide ore deposits.

This stage is well demonstrated by alteration of certain minerals, such as feldspar, amphibole and biotite in the syenite porphyry and the bordering rocks. In general, plagioclase is altered to sericite, calcite, clay minerals, dominantly kaolinite, and to a minor degree to epidote. Amphibole and biotite commonly alter to chlorite, but epidote, carbonate and iron oxides are frequent products.

The alteration, closely related to the lead-zinc mineralization provides the last major stage which is characterised by intense silicification, carbonation and sericitization together with some clay minerals production. In most cases the last stage is found overlapping the previously formed stages, particularly the second stage. The syenite porphyry bodies cut in the 745 and 705 m levels demonstrate the overlapping phenomena, in which a net-work of ivory coloured sericite and kaolinite veins, 1-3 cm thick cover the exposed bodies cutting the hornblende previously altered to chlorite. It is an interesting feature that alkali feldspars appear to be the least affected mineral in a completely loose matrix, however, close examination reveals tiny strings of sericite and kaolinite in the alkali feldspar crystals. Generally the intensity and width of an altered zone next to an ore shoot seems to be proportion to the size of ore shoots e.g. at the 140 observation point (see fig.11 in the pocket) an ore-shoot barely 0.50 m thick, emplaced in a contact

between the igneous rock and the phyllite has an altered zone of sericite 10 cm thick.

By contrast to the igneous rock, the marble usually suffers intense limonitization and less intense silicification, in addition to assimilation which results in irregular boundaries. On the other hand, the phyllite with calcite lenses appears to have suffered less alteration in comparison with the igneous rock. However, the appearance of sericite, clay minerals, chlorite and quartz are evidence for similar alteration.

To summarize, the alterations found in the Keban area are characteristic of the alteration products of carbonate-rich rock by acid igneous intrusions.

The alteration produces marked physical changes and leaching. The leaching is very conspicuous in most of the underground syenite porphyry where light colour rock resulted from sericite, calcite, quartz and clay minerals formation. Light coloured earthy rock with higher porosity sometimes coincides with the ivory coloured net-work of sericite and kaolinite veins in contrast to the hard compact rock found elsewhere. Further colour changes on oxidation of the products of alteration emphasise the leaching, by oxidation of pyrite to limonite and hematite which is a widespread feature in both the igneous rock and the marble through the underground workings. The presence of sericite indicates removal of CaO, K_2O and Na_2O (Wayne, 1962). Formation of gypsum near ore shoots

is evidence for CaO removal from the zones bordering ore-shoots. Marble is usually bleached adjacent to ore-shoots. An increase in porosity (Lemish, 1959) is a part resultant of wall-rock alteration, but grains in calcite and quartz in some instances, along with recrystallization reduced the porosity minimum giving rise to a hard brittle rock. Partial removal of graphite and other carbonaceous impurities in both the phyllite and dark dolomite marble are also indicated by leaching. In some cases graphite penetrates into visible size fractures in bordering marble. As a result of alteration exceptionally large calcite crystals formed (e.g. one of single crystals measures 5 cm in diameter) while unaltered calcite grains stay between fine and medium in size. However a reduction in grain size has also taken place as a consequence of the alteration of phenocrysts. Replacement of feldspars particularly plagioclase results in an extreme change in grain size. For instance feldspar crystals ranging up to 2 cm in length are partly replaced by sericite flakes averaging 0.01 mm in length. The amphibole and biotite display similar reduction in grain size on the production of chlorite.

Systematic sampling on a traverse across the ore-shoot and the marble allowed determination of the strontium and fluorine dispersion patterns with respect to ore mineralization (Chapter V)

The fluorine content shows a steady decrease away from the ore-shoot while the strontium does a sharp depletion near the ore-shoot and a concentration outside the influence area.

CHAPTER III

STRUCTURAL GEOLOGY

Introduction

The Keban area appears to have suffered severe deformation. It is formed by the northern prolongation of an anticline running from the south. The anticline involved movement from the NW towards the SE, thus producing an asymmetrical recumbent fold trending NE-SW with axial plane dipping SE (Baykal, 1966). Superimposed on the major structure, there are open symmetrical folds with axes trending to NNW-SSE. Subsequently tectonic movement produced an approximately N-S trending upthrust in association with, or immediately following, the syenite porphyry intrusion. Afterwards there was approximately E-W intense faulting, involving some wrench faults, and folding. The most recent tectonic movements have given rise to approximately E-W faulting affecting the recent river deposits (see fig.12 in pocket).

In the following pages the account of the structural elements found in the area will be given in some detail.

Bedding

This is regarded as the primary structural element. Bedding is often obscure, but may have been obliterated by the extensive thermal metamorphism associated with the syenite porphyry. Although bedding often cannot be directly seen, its presence and direction can generally be inferred from the positions of the boundaries

between major lithological units; these boundaries are accepted as being original bedding planes. Poorly-developed original bedding in marble, where present, is marked by ill-defined graded grains and alternating black layers and laminae due to impurities in the pure white horizons. In the south of the area, the primary bedding becomes much more conspicuous as the massive marble passes into moderately-well bedded rock with limonitized laminae prior to metamorphism and micaceous schist; a metasediment derivative of impurities in limestone. The primary bedding of dolomite marble generally coincides with the S_1 foliation planes (see page 47). Both the calc-schist and the phyllite have a primary bedding, usually marked by differences in compositional and colour banding.

Lineation

The lineations in the area are defined by features such as the preferred orientation of inequant mineral grains, minor fold axes, long axes of stretched calcite and quartz lenses; on S_1 foliation planes, intersection of a cleavage with the foliation plane, intersection of two cleavages, boudinage structures, intersections of primary bedding with cleavage and striations. The striations, which are well developed on the S_1 foliation plane of the calc-schist and the phyllite, resemble slickensides in which minerals readjust themselves in a direction parallel to each

other. Slickensides together with striation are invariably α-lineations while the other linear elements are regarded as β-lineations. As many β-lineation measurements as possible were taken throughout the area, and then all readings were plotted on an equal area net. The distribution of the poles on the lower hemisphere of the figure 13 illustrates that the three dominant lineations are directed to the NE, SE, and E respecitvely, which is well in accordance with the directions of the folds, joint and fault patterns. This suggests that β-lineations have been produced by the movements which have formed the other structural elements.

Foliation

The term foliation is used here in a sense similar to that of schistosity (Turner and Verhoogen, 1960), which has a non-genetic meaning to include all parallel fabrics which tend to impart a certain degree of fissility parallel to their planes in rocks. The foliation structures in the area, include: a) Preferred orientation of flaky and platy minerals, particularly muscovite/sericite, graphite and epidote, b) Compositional banding, c) Flattened and stretched lensoid calcite and quartz, d) the presence of minor folds.

The foliation is generally parallel to the lithological

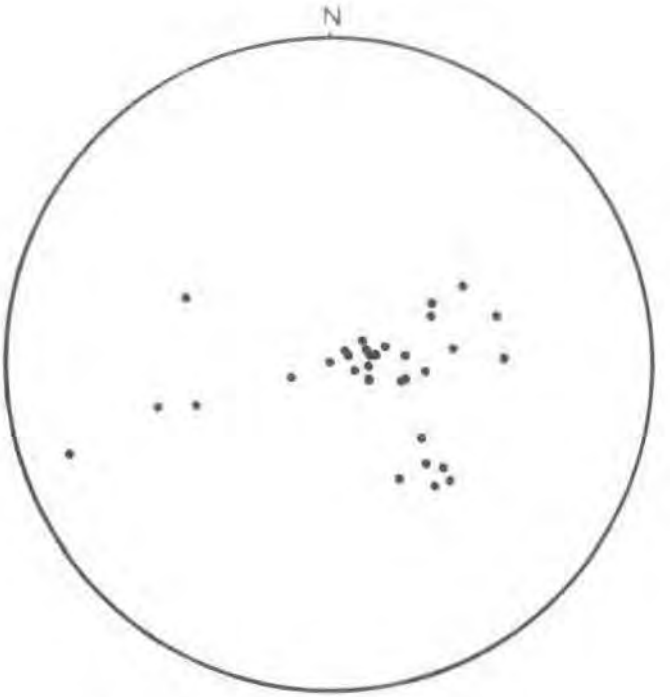

Fig. 13 Orientation of linear structures in metasediments (32 readings)

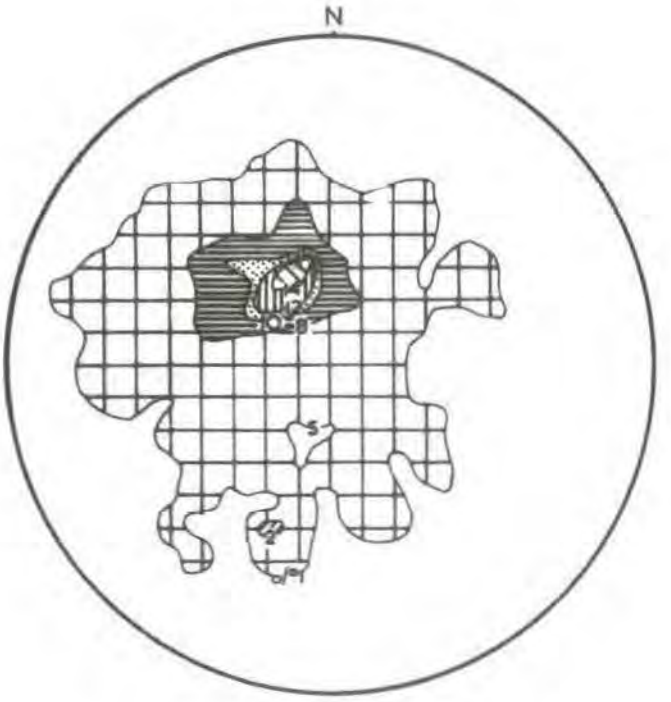

Fig. 14 Orientation of foliation structure in metasediments (280 readings)

boundaries on either a local or a regional scale, which suggests that the primary foliation (here after referred to as S_1), essentially coincides with the original depositional layering in the rocks of the sequence. Field observation and microscopic study reveal that as many as three sets of foliations developed in these rocks. Where two foliations are visible, the well developed and striking foliation is regarded as the S_1 foliation. The later, less dominant foliation being S_2 makes an angle between 30° and 90° with the earlier S_1 foliation. Although the S_3 foliation often cannot be seen in the field, its presence and mutual relations can be inferred by microscopic study; often micaceous layers in the calc-schist and the phyllite define a distinct S_3 foliation between S_1 and S_2 which are mainly marked by cleavage planes in contrast to the S_1 foliation planes. From the study of thin sections, the S_3 foliation seems to have a close relation with the S_1 foliation; wherever present S_3 is accompanied by S_1 foliation. Its formation is closely related to shear movements acting along the S_1 foliation planes. A few minor exceptions occur in some highly schistose samples where the S_3 foliation plane owes its origin to shearing movements acting parallel to the S_2 planes.

The stereogram for S_1 and S_2 foliation planes shows a dominant foliation in the NW quadrant corresponding with a

foliation plane which trends NE-SW and dips SE (fig.14). Although the foliations invariably dip SE, the angle varies between 10° and 80°. The average dip on the stereogram is 26°. The second less dominant foliation is represented by a plane striking 125° and dipping 18° to the NE, which is a foliation of S_2. Both foliations are related to foldings; the S_1 foliation planes lie parallel to the axial plane of recumbent folds which dip SE, while the other coincides with NW-SE folds whose axial planes trend towards the NE.

Cleavage

A pronounced axial plane cleavage develops with the overturned and open symmetric folds in the phyllite and calc-schist. It trends N-S and usually dips between 35° and 42° to the E. It is often found that these cleavage planes have been expanded up to 1 cm by clear calcite and quartz veinlets. At the Zereyandere section near the river mouth one of the best examples of axial plane cleavage in a calc-schist interlayered with thin marble layers develops in such a way that the cleavage is restricted to the marble layers and it progressively dies out in the immediate vicinity of the flaky layers. (Plate 9). As a result of axial plane cleavage, gliding lamellae were formed in the competent marble layers.

Fracture cleavage of interbed-shear origin is dominantly present in the calc-schist interbedded with thin marble layers

Plate 9 Axial plane cleavage developed in a marble layer of Calc-Schist. The cleavage dies out towards the bordering micaceous layers on both sides and shows slight rotation along the shear planes vertical to the axial plane cleavage (looking N).

Plate 10 A part of the major recumbent fold with folds developed later on, in the bed of Zereyandere (looking N).

mainly exposed in the southeast of the area. This type of cleavage mainly develops perpendicular to the primary bedding of calc-schist, and less commonly these fractures show a little rotation where a thin layer of incompetent calc-schist lies between two competent layers of marble. This rotated fracture cleavage suggests that it originated from a shear-couple (Badgley, 1965). Fracture cleavage is generally present in the massive marble which shows intense fracturing close to shear zones. By contrast in the dolomite marble it generally appears to coincide with the S_1 foliation planes. Four sets of fracture cleavages were identified in the light of combined field and microscopic examinations; one set develops parallel to the regional S_1 foliation planes while the other set is perpendicular. The remaining two sets make an angle of approximately 45° with this foliation.

The sharp refolding of the S_1 foliation planes tends to produce a shear fracture, which is termed here 'crenulation cleavage', in which flexuring of the S_1 foliation planes rotates the platy minerals of the rock towards parallelism with the new fracture planes. This type of cleavage invariably occurs in the tightly folded micaceous phyllite, and is always associated with the S_2 and S_3 foliation planes. Turner and Weiss (1963) describe

these new fracture surfaces: "The surfaces of slip are not discrete fractures but rather laminar domains of intense strain". Lack of apparent discrete planes in the Keban phyllite may suggest that these domains were converted into a foliation schistosity by syntectonic or post-tectonic recrystallization of micas. (White, 1949, Turner and Weiss, 1963).

Slaty cleavage mainly developed in micaceous layers of schistose rocks where it is generally found that this type of cleavage coincides with the S_1 foliation planes; in other words, it is coincident with the bedding. Badgley (1965) reports similar occurrences from the Mount Isa group. In addition, another variety of slaty cleavage was produced in places where the phyllite suffered severe deformation, which seems to lie approximately parallel to the fold axis, and this cleavage is assumed to postdate the widespread cleavage coinciding with the primary bedding.

In the syenite porphyry, closely spaced parallel cracks, surrounding phenocrysts in a fine matrix, appear to have originated during cooling of the intrusive body. Hence these cracks may be regarded as a tension cleavage.

Boudinage

The boudinage structures usually occur within the phyllite and calc-schist. However, well developed boudinage structures are exclusively confined to a horizon in the uppermost part of the

calcareous quartz phyllite. Since quartz rich layers are locally interstratified with readily deformed micaceous layers, they develop more proper boudins in comparison with the calc-schist. In general boudin segments are made of calcite, which have been found in some cases enclosing a limonitized quartz core, less commonly they have a quartz core. The pinched intersections between the segments almost invariably show recrystallization of rock material, namely calcite and quartz. Segments have a variable range size from 0.05 to 1.00 m long. Four types of boudin structures are distinguishable in terms of segment size and their mode of occurrence; a) Continuous-truncated segment type, b) Pinched-out disconnected segment type, c) Disintegrated segment type, d) Beaded segment type (see Fig.15). The first type is the most common, followed by the pinched-out disconnected type. The disintegrated segment type incorporates boudin made entirely of quartz segments which having been much more rigid, this reflects the fact that the rock has been under the pressure of acting forces for a relatively long time. This relationship has been noted at the 91 sampling point (see fig.16 in pocket). Finally, the last type is restricted in occurrence to calc-schist interbedded with marble layers at the southern extremity of the area mapped.

The places where boudinage was subjected to post-formation

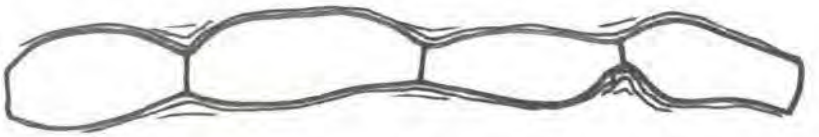

Continous truncated segment type

Pinched out disconnected segment type

Disintegrated segment type

Beaded segment type

Fig. 15 TYPES OF BOUDIN STRUCTURES

deformation which created faulting and folding in two directions at about right angles to each other, are limited to the upper part of the calcareous quartz phyllite in the central area. The plane of contact between two segments is always normal to the foliation plane in which they rest. In general, the long axis of boudins on foliation planes trends between 105° and 130° to the SE with a dipping angle of 10° to 35° SE, which coincides with the regional trend and dip in the area.

The origin of boudin structure, it is believed, arises by extension of limbs during folding. (Coe, 1959).

Folding

Major folds: The major anticline which followed the regional metamorphism (Baykal, 1966) was pushed towards the SE by forces generated from the NW, thus forming a recumbent fold whose axial plane strikes NE-SW, and dips 52° to the SE. Since its northern extremity in the thesis area was obliterated by the syenite porphyry intrusion and subsequent tectonic events, no detailed study could be made. Nevertheless, minor folds formed in this manner were taken into consideration in order to establish the relations with the other major folds. The attitudes of axial plane measurements on the recumbent fold make a second degree maximum on an equal area lower hemisphere projection (fig.17). The weak maximum reflects directly the limited outcrop on which reliable measurements could be taken. The maximum trends about

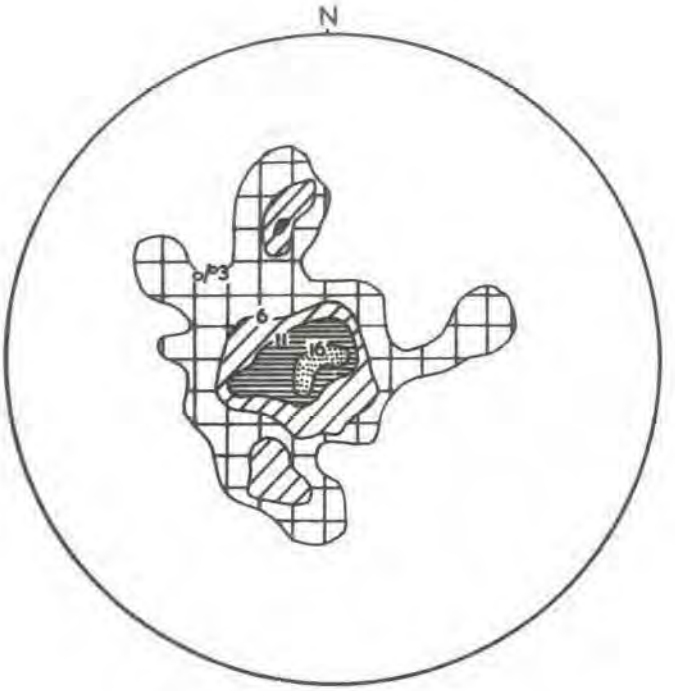

Fig. 17 Fold axis variations in metasediments the Keban area (37 readings)

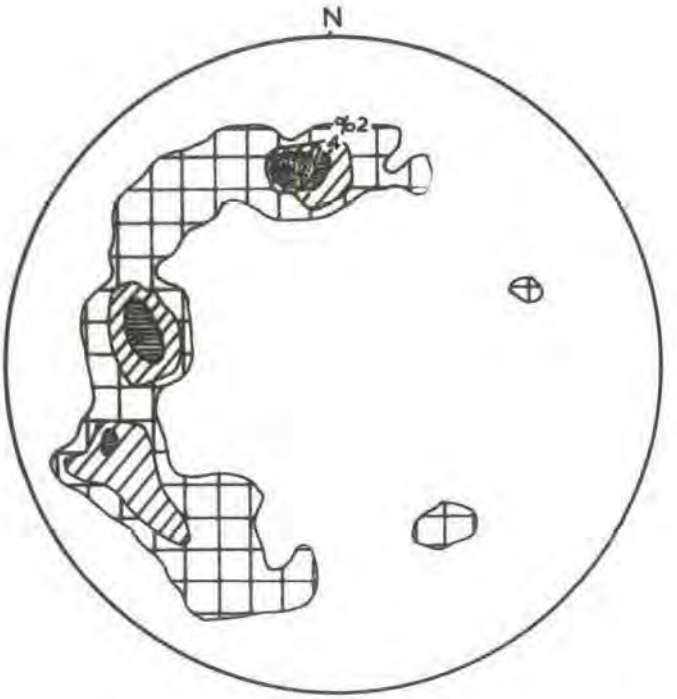

Fig. 18 Distribution of poles to fault planes measured at surface outcrops the Keban area (18 readings)

30°, and dips 38° to the SE. The difference between the average dip and the dip on the major recumbent fold in the south suggests that the recumbent fold progressively turns into a gentle dipping fold towards the north, this change may have resulted from uplift by the syenite porphyry intrusion.

The third maximum representing the NW-SE trend fold pattern originated on the recumbent fold, dips with an angle of 32° to the NE, which may be tied with that of a fold system covering large areas in the Taurid Orogenic Belt.

The youngest, best developed subhorizontal fold sets with a N-S trend give the strongest concentration among the folds.

An E-W directional fold system is missing on the stereogram, instead there is a dominant fault phase. In a few places small-size anticlines and synclines are developed, mainly in the phyllite, representing the E-W directional fold system.

In considering the age relation of the orogenic phases, it is, with some certainty possible to delimit the major structural events. Metamorphic massifs within the Taurid Belt have come under the influence of an orogenic phase prior to the Silurian. (Baykal, 1966). Some workers made their conclusions by correlating them to large massifs with their surroundings, over large areas. If this suggestion was true then the second folding striking NW-SE most probably would suffer the Caledonian phase. As has already been stated the intrusion of the syenite porphyry had evidently taken

place during the Upper Paleocene, either early movements of the Pyreneean phases or late movements of the Laramide orogeny must have been responsible for the magmatic intrusion and contemporaneous or subsequent thrusting. Lack of an obvious correlation for the intense E-W faulting has made dating uncertain. As the late Alpine phases were intensive throughout the belt, it is however, possible that this faulting has been formed by one of the phases of the Alpine orogeny, which could most probably be the Pyreneean phase.(Plate 10).

Minor folds: Minor folds are related to movements along the foliation planes of the rocks, and were mainly accentuated in the phyllite and calc-schist due to their flexibility. In the massive marble and to a lesser extent in the dolomite marble minor folding is negligible in the area studies. The term minor folds includes folds both microscopic and small scale structures observed in the field.

Recumbent and overturned folds are mainly found in or close to the core of the major recumbent fold (Plate 11). From the widespread occurrence of drag folds it is possible to deduce the direction in which mass transport must have taken place; the direction of overturn of drag folds involved indicates that mass transport took place towards the SE. In addition to the drag folds in a few localities both the phyllite and the calc-schist have moderately-developed parasitic folds which differ from drag folds by having other minute folds

Plate 11 Minor folds developed over a recumbent fold, a part of the major recumbent fold (looking N).

Plate 12 A plagioclase metacryst consisting of graphite streaks in a micaceous layer of Phyllite shows rotational movements. x80.

developed on their crests.

The cleavage/slip folding, encountered both in the field and on a microscopic scale, resulted from shear movements. It is created by preference in rocks which have closely spaced banding, and its fold axis generally coincides with the S_1 foliation planes. It is commonly the case that some minor folds provide evidence of several movements in accordance with the major structures. The presence of two or more sets of open symmetric folds in the same rock, and the occurrence of refolded S_1 foliation planes are notable examples. The ribs developed on the open symmetric folds lie parallel about N-S and E-W directions and bear a subvertical axial plane. Synsedimentary quartz veins (mainly in the phyllite) appear to have suffered the early stage deformation producing folds with a thickness crest attaining up to 0.3 m thick. Although disharmonic folding is widely distributed everywhere, it only develops on a small-scale. The asymmetric or subsymmetric inclined limbs of a disharmonic folding die out in a space of at least 1.75 m thick.

The majority of the sodic plagioclase in the phyllite or calc-schist appears to have some connection with the minor structures. For example some coarse grains of euhedral plagioclase which is of pre-kinematic origin enclose streaks of graphite, and they were rotated around clockwise. This

rotation amounts up to 50° to the S_1 foliation plane. Shear movements acting parallel to S_1 foliation planes are responsible in forming these structures (Plate 12). In contrast some plagioclase crystals having folded graphite streaks did not suffer rotation. Moreover, quite a high proportion of the pre-kinematic albite is completely surrounded by micaceous material. Post-kinematic plagioclase has no response with flaky layers.

Faults

After the movements in which the two major directional foldings formed, the rocks seem to fail to produce large major folding and instead they readjusted by producing large faults. As a result the upthrusting took place in an approximately N-S direction (Plate 13). Large scale upthrusting is related to the magmatic intrusions which acted similarly to uplifting, and which is in part combined with approximately E-W directional movements. This was followed by two sets of faults making an acute angle which is intersected by the E-W directional set. They appear to involve some wrench faults. Owing to the difference in rigidity a mechanical contact developed between the phyllite and the marble. The well formed mechanical contact is mainly located in the eastern part of the field area.

The most striking fault-pattern trends approximately N-S

Plate 13 N-S directional upthrust between the footwall dolomite marble and the hanging wall massive marble. The adit to the main sulphide deposit is seen on the left side (looking N).

Plate 14 A mechanical contact of Phyllite and Marble is invaded by Quartz-Syenite Porphyry (looking NE).

This upthrust brought the marble into contact with the dolomite marble for a distance of 4 km on the east slope of the Firat river. The brecciated fault zone separating the two rocks is barely 1 m thick. It is clearly visible along the strike, and mainly rests on the foot-wall side of the dolomite marble. There are some exceptions where a smashed outcrop of the phyllite not more than 10 m thick takes its correct stratigraphic position over the dolomite marble. The fault zone has a steep dip to the E at the surface, but in depth it gradually becomes gentle dipping, and in the underground workings in the 745 m level, it was found to be flat-lying. The breccia zone is composed of fragments as much as 15 cm across. These are of calc-schist, dolomite marble, phyllite, and quartz syenite porphyry, all of which are cemented by a limonitized matrix. Another N-S directional fault zone running roughly parallel to the western fault described above separates the marble from the phyllite. The crush zone seems to involve only phyllite and marble fragments which are embedded in a limonitized matrix, and varies in thickness over a short distance. A group of approximately N-S trending faults is present on both slopes of the Firat river. These dip eastwards at a steep angle. The conclusion of this study is that these faults are gravity faults. Fault movement shows variations, and the direction of the displacement on one fault

is not necessarily the same as that on a gravity fault on the west slope. A study of the displacement over the major upthrust did not give a realistic figure, but it must have been several times the figure for that on the gravity fault. It is believed that the present course of the Firat river keeps to the two fault zones in the area under consideration, especially in its approximately N-S course which is defined by several syn-thetic gravity faults. All the gravity faults so far depicted have no effect on the syenite porphyry intrusion therefore they were formed before the intrusion. By contrast, the presence of a considerable proportion of the igneous rock fragments within the breccia zones of the upthrust is evident for post-intrusion movement on that fracture. Two sets of NE-SW and NW-SE trend faults are accepted as being dominant events in addition to the upthrust. The mutual relation between them suggests that the set of NE-SW trending faults is younger than the other set. Since they are gravity faults, their combined displacement is more clearly measureable. However, the displacement varies from several decimeters up to several tens of meters. Over the area studied the gravity faults exhibit some similarities of length, dip and thickness of their fault zones. The traceable distance of slip throw, which in some instances makes a gentle turn on the strike, varies between 40 m and 12 m. Individual

faults often dip at a steep angle towards the SE, but less commonly to the NW. The fault plane or zones are frequently found to be sharp, and filled mainly by breccia. A set of NW-SE striking faults transected by the NE-SW fault pattern seems to concentrate on slopes of the Firat river because of the strip-like forms they are clearly seen. This set shows a rather gentle turn on one end along the strike, and involves faults of 10 m to 1.5 km long. Because of relatively poor exposures, the phyllite areas give little clue to their existance, for a long distance. Although most of the faults are regarded as being of gravity type with dips of between 45° and 72° to the NE, a few faults showing characteristics of wrench faults have been observed. The movement is such that both sinistral and dextral varieties were produced, suggesting that approximately NW-SE directional compression was in action at the time of faulting. A complimentary fault pattern running nearly E-W is believed to synchronous with or just after the NW-SE set, and is accepted as being a gravity fault.

All the contact zones between the marble and the phyllite exposures show that both the rocks have been strongly disturbed and that they are often separated by a wide fault breccia. The latter consists of intermingled and strongly pulverised phyllite. Along the line of contact, the marble rises in steep cliffs

containing abundant slickensided surfaces. Since different directional slickensides are prevalent it is, however, concluded that the contact suffered several times from movements. The presence of quartz and calcite balls, a few cm across, in the phyllite of the eastern part bordering on the marble, which were originally in lenses, gives additional evidence of these movements. At least one of these is attributed to a movement prior to the syenite porphyry intrusion, which appears to have intruded a mechanical contact zone between the marble and the phyllite. (Plate 14). It is remarkable that the fragments within the igneous rock are only of phyllite, which is a common feature along the mechanical contact where marble participates very little in brecciation. The contact with a general tendency in a N-S direction ranges from 0.2 to 3.5 m in thickness, and the dip varies from 50° and 70° mainly to the E.

In general faulting synchronous with or later than the intrusion has close relation with the igneous body which acted in some extent as uplifting agents. The evidence is that a faulted roof was formed by a slight doming of upward magma pressure which presumably assisted in the faulting e.g. as seen in the "Dilimli" ore shoot (fig.11). The uplifting also gave rise to block faulting which turned the massif into a

tectonic complex. The faults around the margins of the igneous rock are considered to be closely connected with the emplacement of the igneous body.

Lastly, two very recent faults in alluvium have been found in a road cutting 1.3 km N from the town center of Keban. These gravity faults strike NEN-SWS and dip with an angle of 70° to the northwestern.

As many measurements as possible were taken from the faults visible in surface outcrops (fig.18). There are the three dominant directions, they are followed by one less dominant direction. The best developed fault plane is a E-W trending and dipping to the S with an angle of 56°. The second dominant fault plane strikes N 10 E and dips 50° SE, and lastly the third dominant fault is a N 15 W trending and dipping 60° to the NE. Those of three fault planes are in good agreement with faults of different phases described above.

Fig.19 illustrates the measurements taken from the faults exposed through the underground workings. Although very small shifting of the maximum areas on the stereogram is evident, the underground fault patterns coincide with those found at the surface.

Joints

Joints are well developed throughout the mapped area.

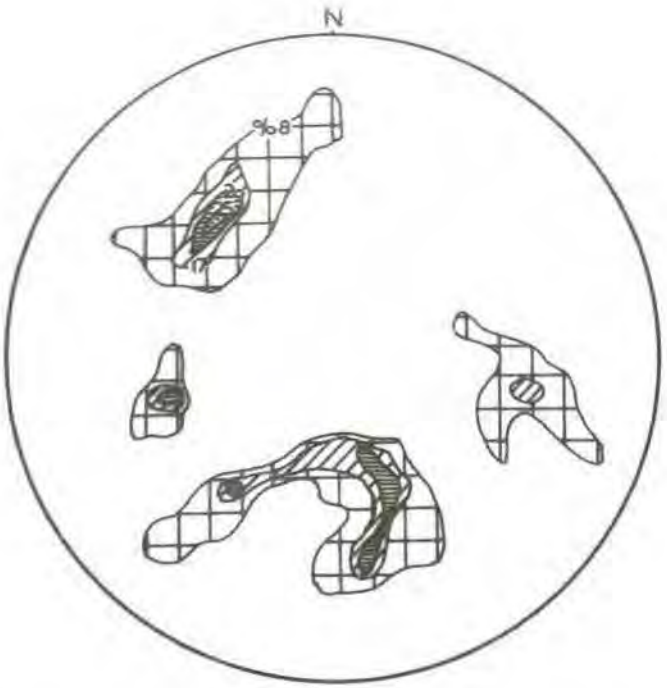

Fig. 19 Distribution of poles to fault planes measured underground outcrops the Keban area (124 readings)

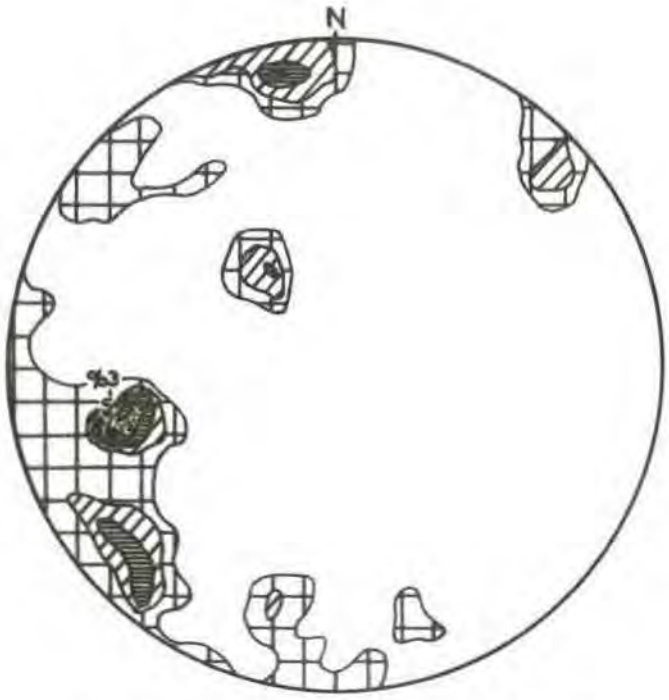

Fig. 20 Distribution of joints in metasediments (198 readings)

NE-SW and SES-NWN trending and nearly vertical joints are predominant in the wall rocks. The joint patterns of the metamorphic rocks and the syenite porphyry have been considered separately.

In the contoured stereogram of fig.20 drawn on an equal area net, all measurements from the metamorphic rocks are combined. This figure displays 178 joint readings plotted on a lower hemisphere. The 52 readings from the igneous rock are represented in fig.21.

Fig.20 shows that within the metamorphic rocks as a whole, there are four dominant directions which are followed by three less dominant directions. The best-developed is a NWN-SES trending which is a group of 64° dipping joints. Almost vertical joints with a strike ENE-WSW make up the next strongest concentration, followed by joints which trend about 135° and dip to the SW. Finally, a set of joints trends about 15°, and dips at an angle of 70° to the NW.

Although joint patterns from the syenite porphyry seem to have four dominant directions, only two of these in a broad sense coincide with those in the metamorphic rocks, but one of them appears to be rather steeper dipping. The best-developed set of joints trends SE-NW and dips S at 75° to the NE. The next maximum has a similar trend to that of the strongest maximum, and has a general tendency towards a SW dip.

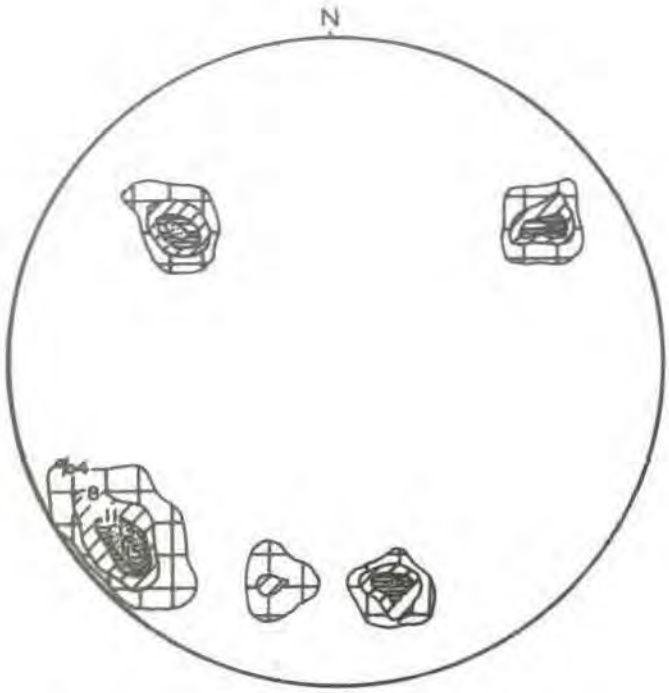

Fig. 21 Joint pattern variations in the quartz syenite porphyry (52 readings)

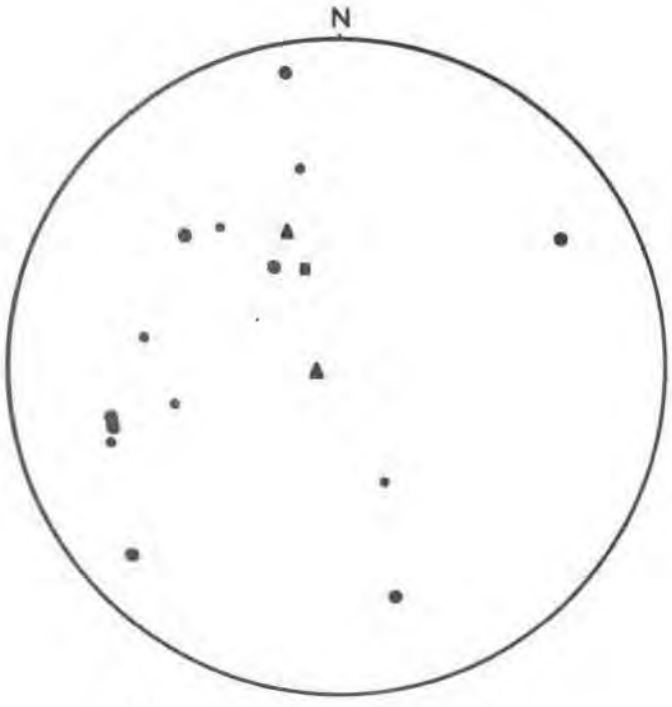

Fig. 22 Summary of structural data contained in Figures 14, 17, 18, 19, 20, 21. (Foli. ■, fold ▲, fault •, joint ●.)

A set of dissimilar pattern consists of joints trending ENE-WSW and dipping NW with an angle of 62°. The last joint set trends NE-SW and dips at steep angles SE. From the comparison of the joint patterns it is concluded that some of the joints were produced during cooling of the igneous body. Therefore the joints originated under this process may be interpreted as tension joints. Apart from the joint patterns incorporated on the stereogram the present author observed a few clear examples of tension joints in different directions. As the measurements from these tension joints are few, they failed to produce any maximum on the stereogram. The set of NW-SE directional joints in the area must have been formed after the syenite porphyry intrusion.

In the area studied the general foliation strikes NE-SW and dips 18° towards the SE, a strong joint set is closely parallel to this direction.

The joint patterns for the area as a whole may be summarized as follows:

a) A set of subvertical joints trending NWN-SES

b) A set of joints trending ENE-WSW which are vertical

c) A set of nearly vertical joints with a dipping tendency towards the SW

d) A set of joints trending 15°, and dipping with an angle of 70° to the NW.

As the remainder of them were small concentrations they

were negligible, and therefore were not taken into consideration in the summary of joint patterns.

The relation between joint patterns and fold axis may be established by studying two corresponding stereograms. Only one set of joints is developed more or less parallel to the fold axis, while the other two sets consist of joints nearly at right angles to the fold axis. This relation suggests that the origin of the joints is synchronous with or later than that of the folds.

Fig.22 summarizes the maximum concentrations for most of the structural elements described in the chapter, on an equal area lower hemisphere net.

CHAPTER IV

PETROGRAPHY

Petrography of the metamorphic rocks

The petrography of the metamorphic rocks with their subdivision in the area are described in some detail in this Chapter. These rocks show some similarities in many aspects; among them recrystallization becomes predominant. Highly granulose samples studied display a strong recrystallization accentuated by grains of calcite and quartz. In addition to common granoblastic texture, mutual relations of grains provide further proof for the recrystallization; grains with well developed annealed fabric meet each other in triple junctions at about 120° which is called the contact angle. This angle originates under the force of interfacial tension of the corresponding grains. Voll, (1960) claims that the interfacial tension acts in such a way that the triangle of forces determines the angle between three interfaces at a given contact. In contrast a larger grain meets with two smaller ones at a triple junction making an angle more than 120°. An interfacial angle over 120° is attributed to a higher interfacial tension. Therefore grains with a high interfacial angle are thought to expand at the expense of next grain or grains. Similarly grains with equally

developed angles are evident for a complete recrystallization (opt. cita).

Almost every specimen examined suffers some degree of tectonic deformation which may be in a certain grain or on the thin section scale. The presence of pressure shadow, Boehmn and gliding lamellae, bent flaky minerals, granulation and formation of mylonite indicate a large range of disturbances from mild to extreme stages (Plate 15,16). Some calcite grains with bent gliding lamellae, and some quartz grains with undulose extinction and rotated slickensides provide evidence of deformation at several periods (Plate 17). Shear movements acting parallel to the S_1 foliation planes caused some rotations (Plate 12). This type of deformation is present in plagioclase of micaceous rocks. In addition to several types of common cleavage structures developed, the crenulation cleavage is dominantly produced in the phyllite, which infers an earlier deformation history, and is almost always associated with secondary or superimposed folding (Rickard, 1961). Although of minor amounts, the development of kink-bands is confined to rocks which have suffered severe deformation, and this structure occurs by replacement of planes with a planar anisotropy (Hoeppener, 1955).

The well developed S_1 foliation planes are defined by the parallelism of flaky minerals in schistose rocks. Grains of

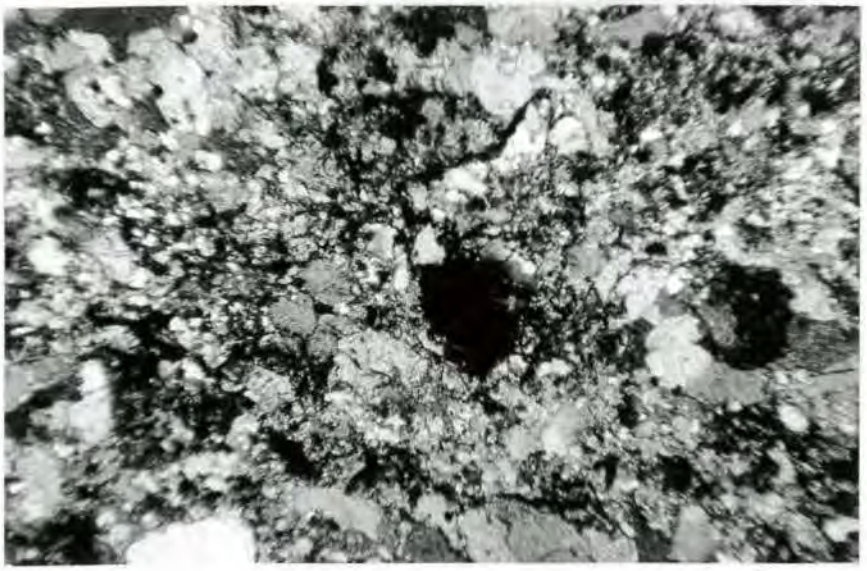

Plate 15 A quartz phenocryst at the extinction position shows Boehmn lamellae. x80.

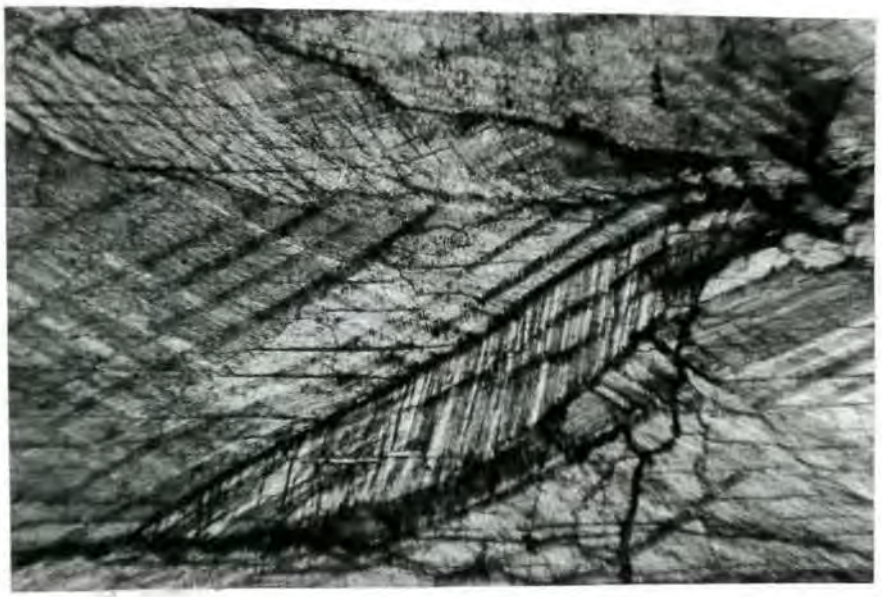

Plate 16 Calcite grains with bent gliding lamellae are evident for multi-phase deformation. x80.

calcite and quartz, alternating with mica rich layers, accentuate the foliation planes. The majority of long dimension of calcite grains and long dimension of lenses made from calcite or quartz grains lie parallel to the flaky mineral bands. Frequent alternations of mineralogical banding occur particularly in the phyllite, and define a strong foliation.

1/Calc-schist

1/a - Chlorite-epidote calc-schist:

The chlorite-epidote calc-schist is the lowest rock in the Keban metamorphic sequence. A marked alteration of green and beige colours distinguishes this rock from the overlying subdivision. Green bands approximately 0.5 mm thick consist mainly clinochlore, epidote and plagioclase. The intervening bands, which are at least 3 mm thick, are composed almost entirely of calcite grains. Chloritoid, graphite, sericite, brown and green biotite, apatite and zircon are ever-present accessory minerals, listed in order of abundance. Pyrite, hematite and probably magnetite with their alteration products of geothite and limonite comprise the opaque minerals. The texture is invariably lepidoblastic.

Calcite: This mineral has a widespread distribution through the rock. Calcite grains are consistently anhedral, and rarely exceed 1 mm in diameter. A uniform grain size of 0.1 mm is dominant. Though clear grains are in a majority, in

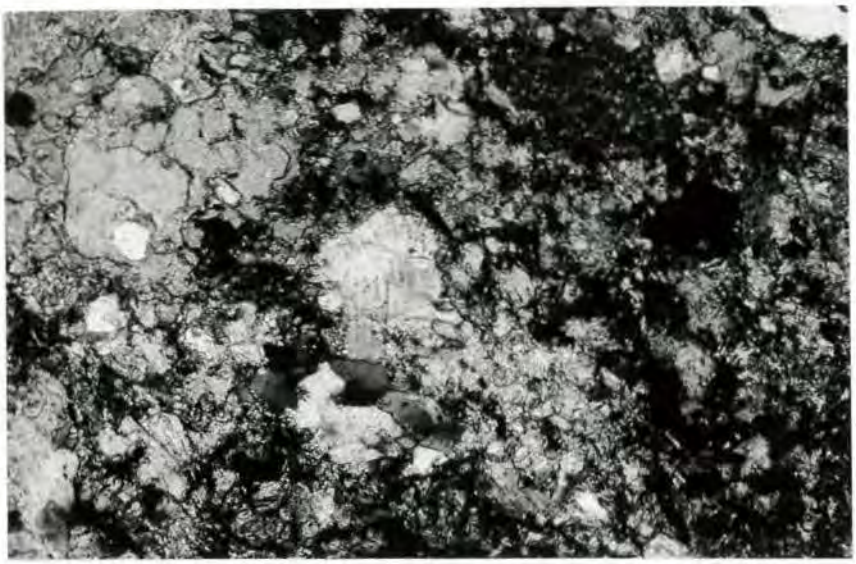

Plate 17 Bent slickenside developed on a quartz metacryst. x80.

Plate 18 Sanidine phenocryst showing oscillatory zoning is embedded in a granular matrix of Quartz Syenite Porphyry. x80.

many places stained and dusty calcite is in excess over the former ones where opaque minerals are more abundant. An earthy iron oxide usually stains grain boundaries. Locally calcite shows twin lamellae.

Clinochlore: Clinochlore being a variety of chlorite is found as aggregates and lath-like in form. Sometimes green bands 0.2 mm thick are made up entirely of clinochlore. The mineral occasionally wraps around a lenticular-shaped epidotic core, and attains a length of 0.2 mm. The clinochlore, with polysynthetic twinning, displays low birefringence and some degree of absorbtion together with pleochroism, the absorbtion scheme being $X>Z$. The average extinction angle lies about 9° to the (001) cleavage crystals which have a slight difference in their optical characteristics and settings are regarded as second generation. Truly discrete, lath-shaped grains show comparatively less absorbtion and birefringence, and are orientated independently of the general foliations. Interstitial and overgrowth crystals of chlinochlore have inclusions of calcite along cleavage traces. The mineral mainly appears to replace the plagioclase grains.

Despite its limited distribution another chlorite variety identified as chloritoid forms in metacryst and lath-shaped crystals measuring up to 0.3 mm. This mineral mainly occurs as overgrowths on calcite with numerous calciate inclusions,

along cleavage traces. Chloritoid shows pleochroism in greenish tint, and twinning formed according to mica law. Lack of preferred orientation, and this development of overgrowth suggest the chloritoid to be of thermal metamorphic origin.

Epidote: As a primary constituent the epidote is variable in content from one specimen to another. The greenish bands are composed mainly of interlocking birefringent epidote ranging from 0.1 to 0.4 mm in diameter. Yellowish green pleochroic anhedral and subhedral grains with preferred orientation are mixingly found in aggregates or discrete. Fine-grained anhedral epidote grains rest by preference in thin crescent-like streaks enclosed by brown biotite or clinochlore. There are also epidote grains interlocking with calcite or biotite. Although not often seen, plagioclase appears to rim the subhedral epidote, which in turn replaces and pseudomorphs the plagioclase.

Plagioclase: Anhedral and euhedral plagioclase seem to have formed in equal proportions. Plagioclase occurs as individual crystals rather than in aggregate form, and its grain size stays in a range barely 0.5 mm in diameter. Two types of plagioclase in terms of formation have been identified; anhedral grains particularly confined to mica rich layers which envelope the plagioclase instead of cutting across, are believed

to have formed first; that is, they are contemporaneous with the other minerals derived from the regional metamorphism. The early plagioclase grains appear to keep a steady course parallel to the general preferred orientation in a given sample, exception occurs where some grains suffer a little rotation. The plagioclase crystals with no preferred orientation form both metacrysts and aggregates of grains, and are restricted in occurrence at areas where the igneous rock is present, which suggests that the late plagioclase was the product of this invading rock. The compositions of both plagioclases have been estimated by the extinction method on albite twins cut across 010 plane. According to results the early plagioclase shows reversed compositional zoning; that is the core composition lies in the range An_{6-9} giving an average of An_{7}. Although no accurate measurements were obtained to estimate the marginal composition, it is probable that the anorthite content in margins approaches a value similar to that for the late plagioclase, which ranges from 20 to 26% An. Plagioclase with higher anorthite content is full of inclusions particularly calcite varying greatly in size, and exhibits corroded margins possibly by post-formation fluids. Dominant albite twinning with two broad individual twin lamellae resembles Carlsbad twinning; the difference between two is that an albite twinning 001 cleavage traces on a 100 face intersect each other about 8° on the composition line dominates the polysynthetic

twinning in both plagioclase varieties. Occasionally Baveno twinning develops.

Alteration of the plagioclase seems to be closely related to the mineral composition; as a whole, plagioclase with high anorthite content suffers comparatively more intense alteration than the early plagioclases which have mainly alteration-free clear cores while the margins are altered in these reverse-zoned crystals.

Biotite: Brown and green biotite are present, but brown mica is dominant. Lath-like brown biotite rarely exceeds 0.3 mm in length. Laths with ragged edges are associated with both mica-rich layers and granular bands where they are mainly found interstitial towards the calcite grains. Strongly absorbant and pleochroic brown biotite suffers marginal alteration to limonite, or complete alteration to chlorite. Olive green biotite, mainly in discrete lath-like crystals occurs in streaks more or less parallel to the preferred orientation. It is barely 0.2 mm long. Complete and incomplete alteration to chlorite is striking. Occasionally chlorite after biotite tends to form metacryst. Thus green chlorite with high birefringence appears to be an intermediate stage between some biotite and chlorite (Moorhouse, 1964).

Graphite: A very small quantity of graphite is sometimes associated with flaky minerals giving the rock an earthy appearance. The graphite is distributed intermittently.

Sericite: The few flakes of sericite present seem to depend on the biotite content; whenever a little biotite is present, limited sericite occurs, otherwise no sericite was detectable.

Euhedral and fine-grain zircon and apatite are consistently found as individual grains, and are common accessory minerals.

In some sections (e.g. 312) a lath-like, sometimes radiating, dusty looking and brown coloured mineral of 0.4 mm long occurs. The mineral is usually as an overgrowth on calcite and is independent of the general foliation. This mineral has yellowish-brown pleochroism and high birefringence, it may be vesuvianite.

Opaque minerals: Pyrite is the dominant opaque mineral, occuring in euhedral crystals up to 1 mm in diameter. From its relation with other minerals, the pyrite obviously formed at a late stage. Some pyrite crystals are mantled by quartz and lesser amounts of chlorite which have crystallized in the pressure shadows around pyrite crystals. Fibrous chlorite normal to the pyrite margins shows no visible rotation, in contrast to the pyrite, hematite is mainly anhedral, and was subjected to some degree of alteration producing limonite and goethite.

1/b - Fine-grained sericite marble schist

This beige coloured rock is very similar to the lower subdivision except the relative abundance of mineral

constituents. The rock is composed mainly of calcite bands alternating with irregular intervals from 0.5 to 1.5 mm thick. These calcite bands usually merge into each other. Sericite rich layers alternate with the calcite bands. The fine-grained anhedral calcite makes up to 90% of the rock. Sericite is the second constituent next to calcite. Plagioclase, quartz, clinochlore, epidote, biotite, graphite zircon and opaque minerals are found in accessory amounts. The rock is seamed by calcite veins, approximately 0.2 mm thick, and these fractures are either parallel or oblique to the S_1 foliation planes. When the veins parallel the S_1 planes, they are of irregular width, but never leave vugs between the adjacent veins.

1/c - Sericite calc-schist

The sericite calc-schist is marked by an increase in sericite, plagioclase, quartz and graphite content at the expense of calcite. Just before the top, intergradation into the dolomite marble takes place in a microscopic scale. The principal constituents are calcite and sericite. Accessory minerals consist of plagioclase, quartz, clinochlore, prochlorite, graphite, siderite and opaque minerals in order of abundance. Lepidoblastic texture is very common. Quartz grains with corroded margins have developed in several of the specimens studied, the corrosion is due to the action of thermal fluids.

2/Dolomite marble:

This rock is comprised almost entirely of fine-grained

dolomite and calcite. After staining (see appendix), an attempt was made to estimate the dolomite content; however, as the rock is very fine-grained it was difficult to make an accurate estimation. The accessory minerals, present in amounts less than 5%, are quartz, opal and various micas. A few samples taken from the dark dolomite marble contain carbonaceous, clay and manganese impurities. From XRD powder camera study it was found that the manganese impurity is in the form of bementite and rhodonite; and the presence of montmorillonite and illite were also proved. Equigranular grains of anhedral dolomite consistently form granoblastic texture. Grains of dolomite tend to be much smaller than calcite grains (Harker, 1964), and all the specimens examined have a grain size of 0.01 mm for dolomite compared to calcite grains of 0.10 mm in diameter in the same specimen. The dolomite marble is frequently cut by numerous veinlets of clear calcite and quartz associated with sericite and opaque minerals. Some microscopic scale veinlets show good examples of crustification, in which the order of crystallization inwards from the vein wall is as follows: calcite, quartz and sericite which usually occurs in vugs with different orientation.

Rhomb-shaped dolomite metacrysts have numerous minute inclusions of a mineral which is probably calcite. The inclusions

are generally restricted to core zones rather than margins. Streaks of predominantly rhomb casts after dolomite, maintain approximate parallel direction to each other. Afterwards these casts were converted into a drusy mosaic whose walls are lined by vertical fibrous sericite and less commonly by chlorite. The vugs contain large euhedral crystals of calcite which have suffered replacement by opal. The order of replacement was calcite → dolomite → quartz/opal. Because of incomplete dolomitization, the dolomite marble has the appearance of a breccia with fine grain matrix of dolomite. These breccias belong to casts attacked by dolomitization, prior to metamorphism. (For further explanation see page 105).

In a few specimens collected near the magnetite deposit of the Zereyandere section well-crystallized dolomite crystals occur as a fracture filling material in association with iron oxide. Well-preserved rhombs of dolomite measuring up to 1 mm long show zoning marked by iron staining. This may be a hydrothermal dolomite connected to ore mineralization (Robertson, 1951).

3/Phyllite

The phyllite consists principally of ~~generally more than 5%~~ calcite, quartz and sericite respectively. In some cases plagioclase, chlorite and graphite exceed 5%, if present, biotite, zircon,

apatite and opaque minerals are present in very small amounts. For the nomenclature of phyllite 20 samples collected from different spots along the section I and II covering the subdivisions have been counted on a basis of 1000 points in each thin section (Fig.16 in pocket). They were named on the two major mineral constituents being calcite and quartz regardless of their accessory composition except graphite, and then the nomenclature was established according to excess calcite and quartz. Where the calcite content in the corresponding rock is dominant, the rock is referred to as calcareous phyllite, with excess of quartz it is regarded as quartz phyllite. Local concentrations of certain minerals was not taken into account. The samples taken from the lower subdivision are calcite-rich while in the upper subdivision quartz is dominant. In some cases layers made entirely of quartz with a lesser proportion of flaky minerals are interstratified with the quartz phyllite. The modal analyses are tabulated in table 4, and the variation in the modal composition is illustrated as a histogram in fig.23. According to modal analysis, the lower and upper subdivisions are named as the calcareous graphite phyllite and the calcareous quartz phyllite respectively.

Although the prevailing texture is invariably lepidoblastic, wherever quartz and calcite layers reach their maximum thickness, a granoblastic texture as an intertexture occurs along with the

Table 4 Modal analyses of the Phyllite

Section I

	Sample No.	300	301	302	303	304	305	306	117	307	308	13
	Nomenclature	C.G.P.	C.G.P.	C.G.P.	C.G.P.	C.G.P.	C.G.P.	C.G.P.	C.G.P.	C.G.P.	C.G.P.	C.G.P.
	Calcite	43.0	36.4	27.4	57.2	45.0	56.6	74.2	49.0	67.4	36.6	64.6
Vol	Quartz	27.0	35.4	26.2	33.2	35.0	9.0	14.4	28.8	14.8	24.4	12.6
%	Sericite	11.2	12.4	25.2	0.4	6.6	17.8	2.2	10.4	6.0	11.4	3.0
	Feldspar	6.0	3.6	10.4	5.2	4.0	10.4	3.4	4.0	2.8	14.0	9.4
	Chlorite	6.0	1.8	1.2	-	0.8	2.0	-	2.6	0.4	4.2	0.6
	Graphite	4.6	7.8	7.4	4.2	4.0	3.6	5.1	4.0	4.4	5.4	4.4
	Opaques	2.0	2.6	1.8	3.0	18.0	0.6	0.2	3.6	3.2	4.0	5.4

Section II

	Sample No.	110	94	95	96	17	18	19	20	22
	Nomenclature	C.Q.P.	Ch.Q.P.	C.Q.P.	C.Q.P.	C.Q.P.	C.Q.P.	C.Q.P.	C.Q.P.	C.Q.P.
	Calcite	24.2	-	37.6	35.6	45.6	33.6	31.0	40.4	20.6
Vol	Quartz	44.8	55.0	40.2	38.8	27.0	40.4	38.4	43.8	48.4
%	Sericite	21.2	21.6	11.2	9.2	11.0	14.0	20.6	7.6	9.6
	Feldspar	2.0	-	1.8	9.0	12.0	3.8	3.2	1.4	6.6
	Chlorite	3.6	22.6	3.2	0.8	2.2	2.2	1.0	0.8	2.2
	Graphite	2.2	0.2	2.0	1.8	0.8	3.2	0.2	1.0	6.0
	Opaques	2.0	0.6	4.0	4.8	1.4	3.8	5.6	5.0	6.6

C.G.P: Calcareous graphite phyllite, C.Q.P: Calcareous quartz phyllite,
Ch.Q.P. Chlorite quartz phyllite

lepidoblastic texture.

3/a - Calcareous graphite phyllite

This lower subdivision is characterised by an excess of calcite over quartz, and ~~dominant~~ important graphite. The other mineral constituents are plagioclase, sericite, chlorite and opaque minerals.

Calcite: The rock is generally composed of fine-grained (< 0.1 mm) anhedral calcite, but coarse grains with a tendency towards lenticular form may be up to 1 mm in diameter. The calcite grains are generally found in layers associated with quartz and plagioclase, being lenses and discrete in form. The lenticular areas, which are barely 7 mm long are devoid of any other minerals, occasionally fine-grained calcite may form the core. Flaky minerals in layers envelope the lenticular forms with a sharp contact between two different mineral assemblages. In thin section (LP-1) graphite-rich layers are seen enclosing the lensoid areas, and they pinch out at the extremities of the lenses. Calcite-rich layers consisting almost entirely of uniform grains are up to 1 mm thick. Frequent alternation of flaky minerals at irregular intervals may disturb this layout, reducing the thickness 0.2 mm.

Quartz: Fine-grained anhedral quartz of uniform size is mainly set in between calcite grains. Usually discrete quartz grains are found interlocked with calcite grains, but sometimes

Table 6 Composition of alkali feldspars

Sample No.	hkl	2θ	Structural state	Composition	Int.Std	2θ Int.Std.
199	$\bar{2}01$	20.91		Or_{99} Ab_{1}	CaF_2	28.30
	002	27.72				
	060	41.65	High sanidine			
	$\bar{2}04$	50.95				
177	$\bar{2}01$	20.96		Or_{94} Ab_{6}	"	"
	002	28.36				
	060	41.74	High sanidine			
	$\bar{2}04$	50.94				
303/A	$\bar{2}01$	21.03		$Or_{87.8}$ $Ab_{12.2}$	"	"
	002	27.70				
	060	41.73	High sanidine			
	$\bar{2}04$	50.98				
131	$\bar{2}01$	21.04		$Or_{85.5}$ $Ab_{14.5}$	"	"
	002	27.64				
	060	40.68	P50-56 Orthoclase			
	$\bar{2}04$	50.80				
163	$\bar{2}01$	21.05		$Or_{85.9}$ $Ab_{14.1}$	"	"
	002	27.65				
	060	41.75	High sanidine			
	$\bar{2}04$	50.94				
104*	$\bar{2}01$	21.13		$Or_{79.5}$ $Ab_{20.5}$	"	"
	002	28.00				
	060	41.95	High sanidine			
	$\bar{2}04$	51.17				
66	$\bar{2}01$	21.14		$Or_{78.5}$ $Ab_{21.5}$	"	"
	002	27.92				
	060	41.92	High sanidine			
	$\bar{2}04$	51.12				
153*	$\bar{2}01$	21.15		$Or_{76.5}$ $Ab_{23.5}$	"	"
	002	27.86				
	060	41.88	High sanidine			
	$\bar{2}04$	51.05				
K-1	$\bar{2}01$	21.20		$Or_{73.8}$ $Ab_{26.2}$	"	"
	002	27.93				
	060	41.83	High sanidine			
	$\bar{2}04$	51.05				
132	$\bar{2}01$	21.20		$Or_{73.8}$ $Ab_{26.2}$	"	"
	002	27.90				
	060	41.90	Between P50-56			
	$\bar{2}04$	51.15	and high sanidine			
276	$\bar{2}01$	21.20		$Or_{73.8}$ $Ab_{26.2}$	"	"
	002	27.70				
	060	41.75	P50-56 Orthoclase			
	$\bar{2}04$	50.83				
TK-151	$\bar{2}01$	21.30		Or_{65} Ab_{35}	"	"
	002	28.05				
	060	42.03	High sanidine			
	$\bar{2}04$	51.25				
TK-150	$\bar{2}01$	21.25		Or_{69} Ab_{31}	"	"
	002	27.60				
	060	41.65	Between P50-56			
	$\bar{2}04$	50.85	and high sanidine			

*Underground samples.

Fig. 23 Modal distribution of the minerals in the phyllite along the section I and II

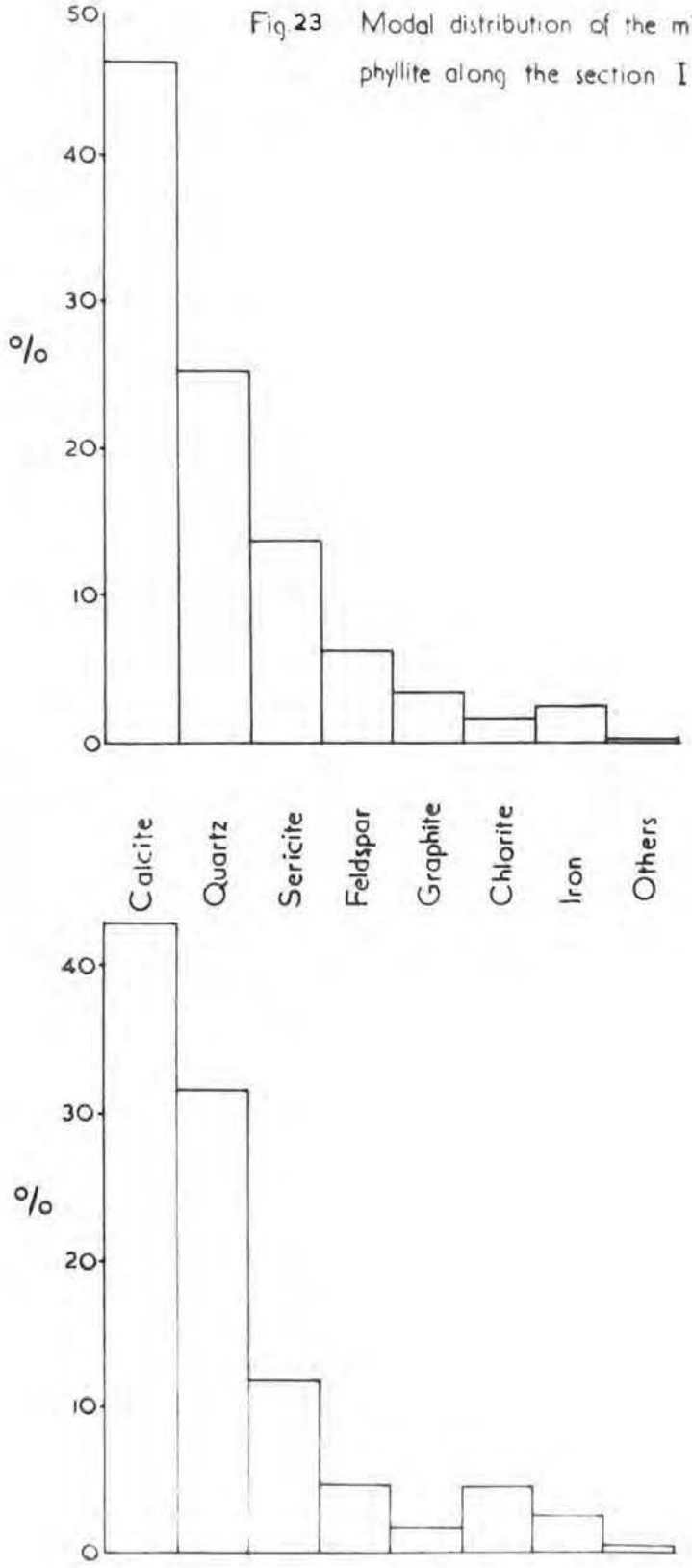

several grains form aggregates of varying size. In a few thin sections from relatively intensely sheared rocks, shear quartz is found to have developed. Numerous minute inclusions (calcite?) in quartz lie along the streaks parallel to each other, giving rise to production of boehemn lamellae. The quartz crystals are corroded to a certain extent, the space being later filled by calcite.

Plagioclase: Plagioclase of the lower subdivision is very similar to those found in the calc-schist. The primary plagioclase has a compositional range between 7 and 10 % An, being generally 8% An while those derivative of the metasomatism give a composition of An_{23}. Albitization is a common event in samples collected near the igneous rock where the margins of the original plagioclase involve as much as 12% An. Inclusions, particularly graphite streaks, are restricted to cores while the margins are devoid of streaks inferring that albitization is younger than that of the tectonic movement causing the minor folds. Three types of plagioclase in terms of deformation were recognised; pre- deformation, paracrystalline and post deformation. The pre-deformation plagioclase coincides with the general preferred orientation with its long dimension. The crystals are enclosed by micaceous layers instead of cutting across, while the post-deformation type with helicitic texture includes folded streaks mainly of graphite. But the paracrystalline

plagioclase implies a rotation beside the folded streaks.

Graphite: Graphite commonly accompanies sericite, and it appears in layers and disrupted aggregates rather than discrete grains. The graphite-rich layers of maximum 0.2 mm thick include a sericite clot in a central position.

Sericite: Sericite is the second principal flaky mineral after graphite. It occurs in lath-shaped anhedral crystals. In addition to sericite metacrysts up to 0.2 mm long the mineral is found as minute interstitial crystals and aggregates. The majority of lath-shaped fine grains are incorporated in layers which are accentuated by graphite outlines. This type of sericite forms continuous layers except where shearing was in action. Metacrysts and minute interstitial grains are set in a matrix of calcite and quartz.

Chlorite: Among the chlorite varieties, prochlorite and clinochlore were identified optically. Their modal distribution indicates great variations from one specimen to another. Local concentrations up to 6% are present.

Although of minor amounts, biotite, epidote, zircon and apatite are the accessory constituents of the lower subdivision. Of them anhedral, green and buff coloured, discrete biotite grains suffer various degree of alteration into chlorite in cores and limonite in margins.

Pyrite, magnetite and ilmenite with a skeleton form are the

opaque minerals, found mainly in euhedral forms.

3/b - Calcareous quartz phyllite

The quartz content in the calcareous quartz phyllite increases upward in comparison with that in the lower subdivision, in the succession, and is in excess of calcite. Alternating layers made entirely of quartz with a lesser amount of flaky minerals enter into the rock. The proportions of sericite and chlorite increases at the expense of graphite. Locally sericite seems to be greatly concentrated so as to produce highly schistose interlayers. Higher in the subdivision calcite again tends to be dominant in locally developed bluish layers and marble "islands". These lime-rich formations comprise pure granular calcite with quartz, sericite and opaque minerals in accessory amounts. Large quartz crystals may occur in boudinage structures where they are in the form of lenses exceeding 10 mm in diameter. All granular minerals display cataclastic texture.

4/Marble

The marble has calcite as its principal mineral. The majority of sections examined from various localities, except from the areas which suffered ore mineralization and contact metamorphism, are found to consist entirely of calcite (>90%) generally in grains < 0.1 mm diameter, thus forming pure marble. When accessory minerals are present, they never exceed 8% of the total rock volume.

Quartz, plagioclase, sericite, chlorite, epidote, biotite, siderite, dolomite, zircon and opaque minerals (mainly pyrite) listed in order of abundance are among the accessory constituents. The texture is always granoblastic. In a rare case calcite associating with micaceous mineral yields lepidoblastic texture.

Calcite: The great majority of calcite grains tend to be anhedral, while the others have a tendency towards being subhedral. In the fine-grained variety calcite is of uniform grain size, and is never found as discrete grains, by contrast to the relatively large grains of the lenticular form. Grain boundaries may display slight difference in form; two main types of boundary are recognisable depending upon the degree of deformation. The rocks subjected to intense dislocation produce sutured-type boundaries, while rocks which suffered little or considerably less deformation have curved crystal boundaries. Because of the iron oxide penetration, margins of grains become distinct with earthy appearance. Another effect is reflected by microstylolites which are less important in the marble of the Keban area since microstylolites are not represented in large proportions. Occasional examples are found to be coated by iron oxide and a little insoluble material, probably some clay variety. Calcite veins of both pre- and post-deformation are largely present. Although drusy mosaic is very uncommon, an

example was encountered, which has two large vugs of rhombs in outline and several small-size ones.

Replacement of calcite is a widespread phenomenon among grains; by eliminating some exceptions, it is however, possible to establish a general trend, that is, relatively fine grains are more susceptible to replacement than the larger grains. The replacement is defined as pre- and post-deformation since some large grains having inclusions are enclosed by a set of twin lamellae while the other twin lamella is cut by a younger inclusion, and gliding lamellae are no longer present beyond the inclusion.

Quartz: Uniformly sorted, euhedral and anhedral quartz grains rarely exceed 1 mm in diameter. Grains smaller than 0.1 mm make up the majority. Quartz disseminated between calcite grains tends to become larger, interstitial quartz is especially found to have this tendency. As well as occurring as disseminated grains, aggregates of several quartz grains are formed. It is more likely that two generations of quartz are determinable by reference to their mode of occurrence; a) Primary sedimentary, b) Post-sedimentary. The former with dimensional orientation lies parallel to the crude foliation of the rock while the latter is independent of the orientation.

Plagioclase: Euhedral and anhedral crystals of plagioclase

appear to occur in equal proportions. Fine-grained plagioclase crystals have a comminuted nature when they are associated with micaceous minerals, otherwise the mineral tends to be separated. Although of minor amounts two types of plagioclase similar to those found in calc-schist and phyllite are present in marble.

Sericite: The minute sericite crystals tend to become euhedral, as well as forming minute shreds. Sericite with a maximum length of 0.2 mm is a common constituent of the flaky mineral assemblage in the marble. Less common individual grains take the place between calcite grains. The majority are faintly pleochroic in greenish-brownish colours with a high birefringence attaining up to the yellow of the second order. Crystals always seem to keep the prevailing preferred orientation. In the sericite-plagioclase rich layers, up to 0.2 mm thick, the plagioclase is charged with streaks of sericite in zones parallel to its length.

Chlorite: Chlorite is one of the common constituents of the sericite-plagioclase assemblage in the marble. The mineral occurs as minutely shredded, non-pleochroic grains between sericite. Because of the fine grains it was not possible to establish the variety by its optical properties. Since prochlorite is widespread in the schistose rocks in the area, the chlorite in the marble is probably the same variety.

Epidote: A small amount of epidote is always present with

the other accessory minerals. Euhedral and anhedral grains with a maximum length of 0.2 mm maintain an individual distribution. The mineral is pleochroic in dull brown and has a colourful strong birefringence up to lower third-order, hence it is regarded as an epidote with high iron content.

Biotite: A very few examples of biotite were encountered in the phyllosilicate layers. The very small grains were only identifiable by their strong absorbtion.

Dolomite: A limited number of dolomite grains have been found in several thin sections. Despite its scarcity well-formed dolomite crystals are present. Euhedral grains (measuring 0.4 mm) appear as overgrowths on calcite.

Zircon: Euhedral grains of zircon up to 0.2 mm in diameter are found as individual grains scattered through the rock. Their long axes mainly lie parallel to the general trend within the rock. In addition occasional siderite and apatite crystals are also present.

Opaque minerals: Fine-grained, mainly euhedral pyrite and magnetite are the principal opaque minerals. The pyrite is in greater amount than the magnetite. Pyrite as a late stage formation sets in veins, fractures and foliation planes.

Petrography of the quartz syenite porphyry

The quartz syenite porphyry is mainly composed of sanidine, orthoclase and plagioclase with accessory proportions of hornblende, biotite, quartz, sphene, epidote, zircon, apatite and opaque minerals (pyrite, magnetite, hematite etc.). Because of alteration and late stage metasomatism secondary calcite, quartz/chalcedony, sericite and some clay minerals tend to replace the original mineral assemblage. Where the skarn zones are created, their products such as scheelite, grossularite, andradite, fluorite, vesuvianite, wollastonite and sulphide minerals are present in various amounts (Table 5). All minerals are set in a fine-grained matrix.

The feldspar content plays a major part in naming the alkali rich intermediate rocks. In the Keban area, from consideration of the ratio of alkali feldspar to plagioclase, it is seen that both alkali syenite porphyry and orthosyenite porphyry are present. On the other hand, the rock shows some similarities to an adamellite and monzonite in its ratios of alkali feldspar to plagioclase, and of biotite to hornblende. As the alkali feldspar/plagioclase ratio varies greatly from place to place this criterion is inadequate to cover all the examples of igneous rocks studied; it has only local importance. Sharp compositional variations over small distances make it difficult to divide the rock into mappable

Table 5 Modal analyses of the Quartz Syenite Porphyry

	Sample No.	171	178	W-3	223	137	66	132	153	276	200
Vol. %	K-feldspar	25.8	36.8	40.6	24.2	28.8	23.8	17.0	21.8	63.8	29.0
	Plagioclase	4.8	12.2	-	10.8	13.2	11.8	8.0	16.8	18.0	13.0
	Matrix	61.0	38.2	49.8	51.4	51.8	56.2	66.8	45.8	-	52.0
	Quartz	2.4	6.2	1.8	1.0	1.2	1.8	2.2	6.4	8.6	1.3
	Hornblende	0.6	1.0	5.8	0.2	1.2	1.6	1.0	1.4	5.4	1.0
	Calcite	-	3.2	-	0.8	0.4	4.2	3.8	6.4	0.6	1.8
	Biotite	0.2	-	0.4	-	1.4	-	-	0.2	-	1.4
	Zircon	0.2	-	0.4	-	-	-	-	-	0.6	-
	Sphene	-	0.2	-	-	-	-	-	-	1.8	-
	Opaques	-	-	1.0	4.4	2.0	0.6	1.4	1.2	0.8	0.2

units, for example the samples having no plagioclase at the Zereyandere and Kebandere sections are very close to the samples in which plagioclase is present. For these reasons no attempt has been made to divide the syenite porphyry into lithological units. One thing common to all types is that the SiO_2 content is consistently over 60% in every chemical analysis from the area, and there is always a high alkali content. Thus, despite local variations, the whole of the igneous bodies, considering its hypabyssal nature will be referred to as Quartz Syenite Porphyry.

The modal composition of 10 quartz syenite porphyry specimens from the Keban area plotted on a Q-A-P triangular diagram after Streckeisen (1967) is compared with the similar rocks from various areas in fig.24. The majority of the samples and the arithmetic mean for 10 specimens fall inside the syenite area. On the other hand comparison of the modal composition with monzonite on a Q-A-P triangular diagram for monzonite gives negative slope, because the majority of the samples and the arithmetic mean for 10 samples are not located inside the monzonite area (fig.25). On the basis of chemical analysis (see Chapter V) the Keban igneous rock is closely comparable to some of the quartz syenites of Kûngnât Fjeld and Gardar Igneous Province (Watt, 1966).

Despite the local irregularities in the alkali feldspar to plagioclase ratio, the plagioclase appears ina broad sense, to decrease towards the margins in the central area in the Siftillitepe.

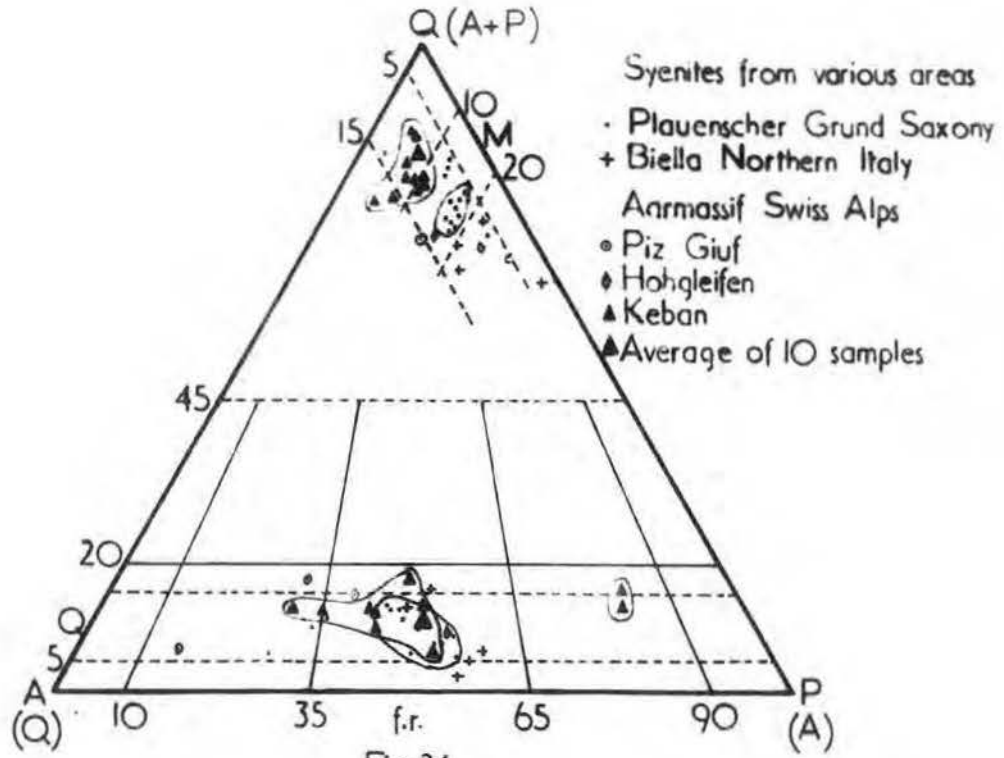
Q (A+P)
5
10
15
M
20
45
20
Q
5
A
(Q)
10
35
f.r.
65
90
P
(A)
Syenites from various areas
· Plauenscher Grund Saxony
+ Biella Northern Italy
Aarmassif Swiss Alps
◦ Piz Giuf
♦ Hohgleifen
▲ Keban
▲ Average of 10 samples

Fig. 24

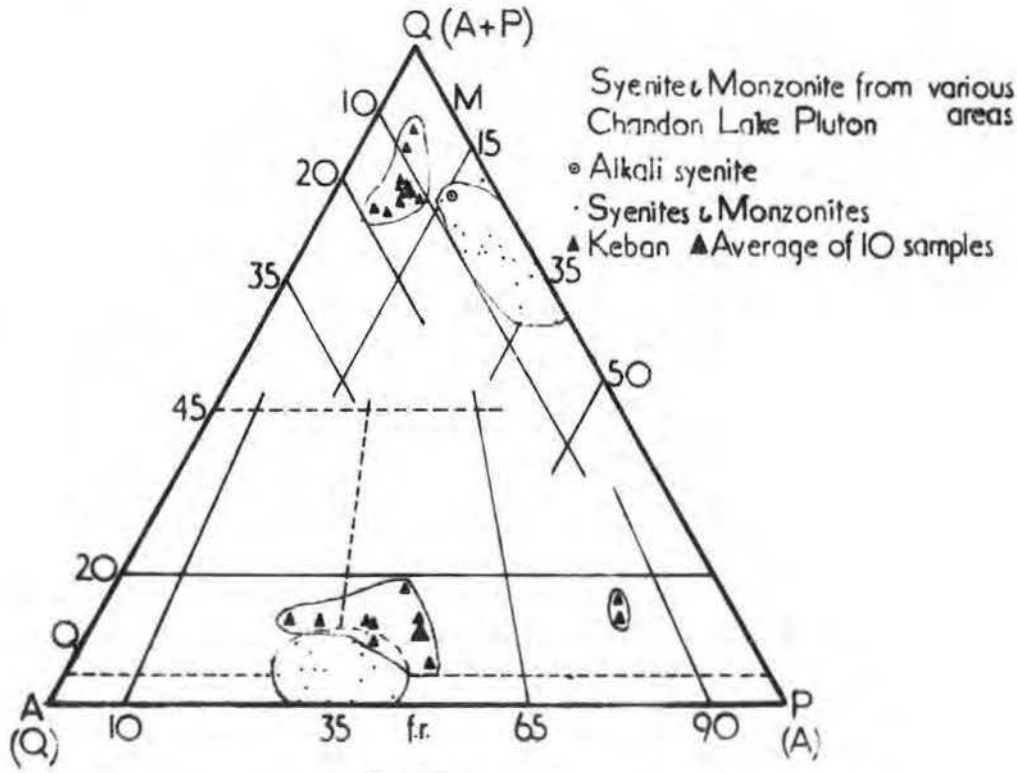
Q (A+P)
10
M
15
20
35
35
50
45
20
Q
A
(Q)
10
35
f.r.
65
90
P
(A)
Syenite & Monzonite from various areas
Chandon Lake Pluton
◦ Alkali syenite
· Syenites & Monzonites
▲ Keban ▲ Average of 10 samples

Fig. 25

Alkali feldspars are in excess of plagioclase in dykes. Outwards decrease in grain size, as a result of cooling, is accompanied by an increase in the proportion of groundmass, which in extreme cases attains up to 66% of the rock (Table 5). However, the reverse may occur in marginal parts or dykes subjected to metasomatism, where there may be exceptionally coarse crystallization of secondary origin.

Primary minerals

Sanidine: Beautifully developed euhedral and subhedral sanidine crystals are present in a wide size range from 0.2 mm to 5 mm in length. They are mainly found as individual phenocrysts and in the groundmass. The groundmass sanidine is lath-shaped or anhedral giving a felsitic texture; the crystals are up to 0.1 mm in diameter. Whenever present several sanidine grains with or without plagioclase are clustered together. When they are in aggregates, they meet each other with sutured boundaries. Although of distinctive appearance dimensional alignment is uncommon though occasionally trachytic texture is found. Sanidine shows disequilibrium in crystallization as evidenced by the pronounced oscillatory and normal zoning. (Plate 18). The sanidine composition was estimated on the basis of the extinction angle on a 010 face (Tuttle, 1952), and the three peak method (Wright, 1968). The composition corresponding to the extinction angle, was read from this curve. For this purpose, extinction measurements on at least

6 suitable grains in each thin section were taken. Afterwards the readings were made on the average extinction angle for every specimen. Thus obtained extinction angles lie between 5° and 9° corresponding with a composition Or_{80} Ab+An_{20} and Or_{36} Ab+An_{64} respectively. Although there is no sharp relationship in their distribution, sanidines with high extinction angle, namely more sodic varieties, are more common towards the interior of the igneous rock, while margins and dykes include sanidine of low sodic content. An estimate for the alkali feldspar composition for 12 rock samples has been done by the X-ray diffraction process described by Wright (fig.26). To the results tabulated in table 6 the composition ranges from $Or_{99.0}$ $Ab_{1.0}$ to $Or_{65.0}$ $Ab_{35.0}$. Although the figures obtained from the two methods are not quite in agreement, the composition with highest albite content ($Or_{65}Ab_{35}$) is in good agreement with the composition of a single sanidine crystal in the samples taken from the central area in the igneous body. The compositions found by XRD method and chemical analysis of single crystal for each sample are given in table 7. (see Chapter V).

Table 7

Sample No.	XRD	Chemical Analysis
TK - 151	Or_{65} Ab_{35}	$Or_{64.6}$ $Ab_{30.4}$ $An_{5.0}$
TK - 150	Or_{69} Ab_{31}	$Or_{66.5}$ $Ab_{30.6}$ $An_{2.9}$

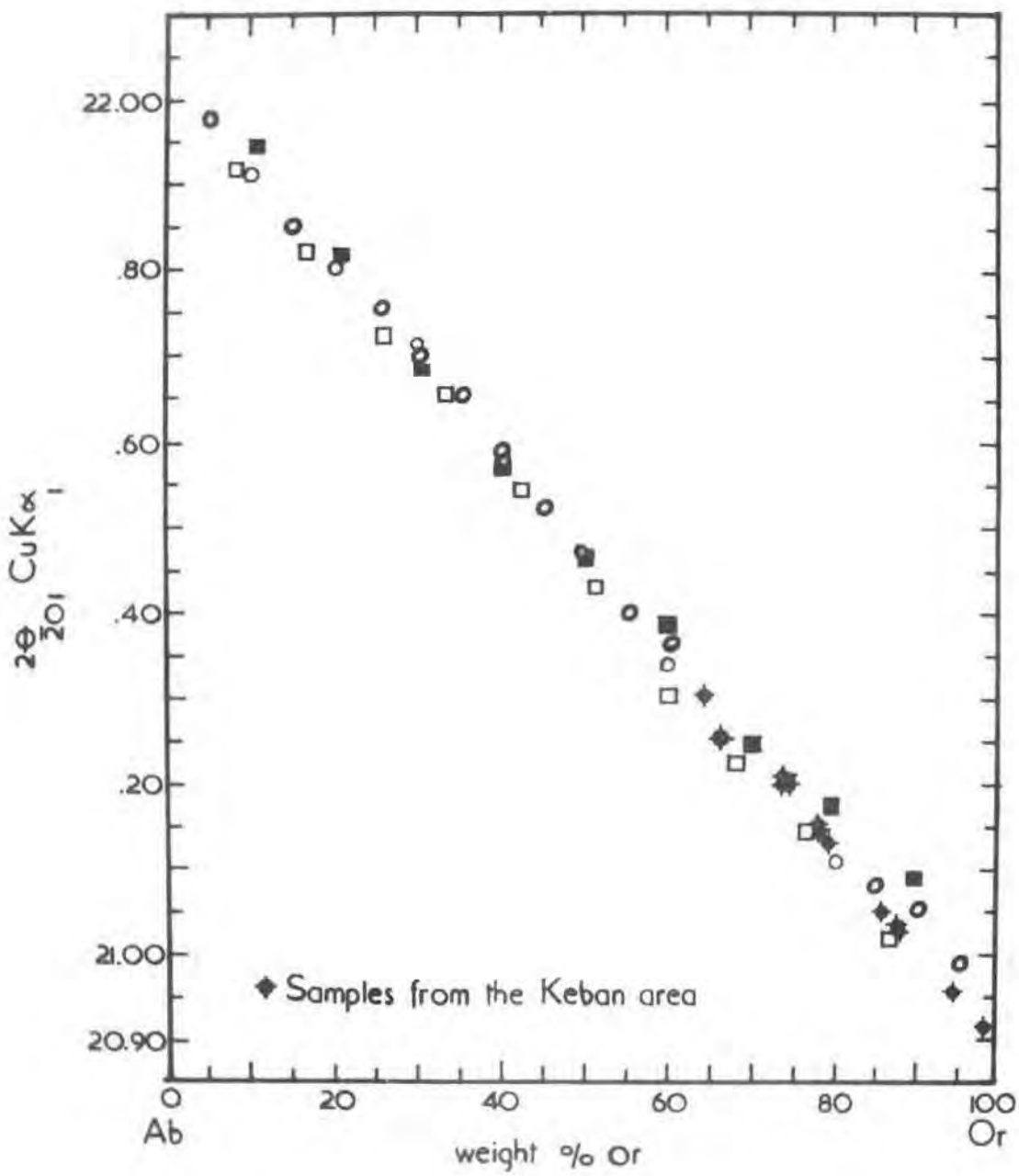

Fig. 26 Compositional variations of alkali feldspar with $2\theta_{\bar{2}01}$ reflection

(After Wright, 1968)

From fig.27 it is obvious that the relative content of plagioclase displays an outward decrease from the central area in the igneous rock. Wherever possible core and margin compositions were estimated by the extinction angle of crystals. From the limited number of readings, it appears that there is a more sodic composition in the margins. Usually the core composition is around Or_{80} $Ab+An_{20}$. Because of the very narrow margins no ~~realistic~~ precise estimation was obtained of the marginal composition.

$2V_{\alpha}$ angle in the sanidine varies between 0° and 12°. Crystals having a 2V of 0° or so give uniaxial figure on rotation. The twinning formed according to the Carlsbad law is very common.

The most striking feature of the sanidine is that the majority of the crystals show inclusions of fairly well formed plagioclase crystals, and less commonly alkali feldspar, sphene and hornblende. Where abundant, the included minerals are oriented in zones coinciding with the growth faces of the crystal. (Plate 19). With a few exceptions, the parallel alignment of the enclosed grains is most likely the result of grain growth which took place in a medium which had not reached complete solidification; as the crystal grows it captures the adjacent crystals, forcing them to lie approximately parallel to the growing boundaries. At the end numerous enclosed crystals occur in geometric concentric streaks which lie parallel to each other with various distance. (Fig.28).

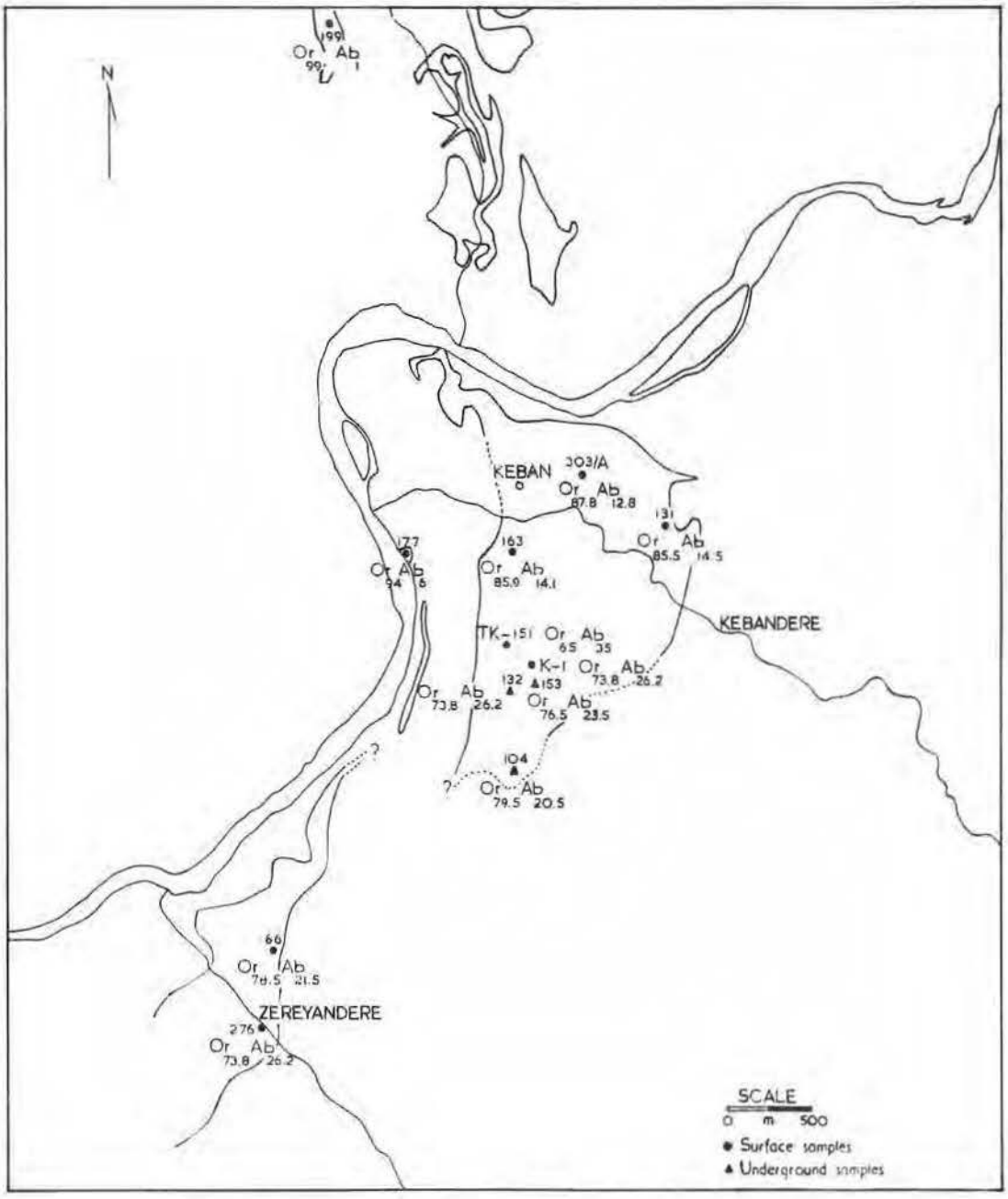

Fig.27 COMPOSITIONAL DISTRIBUTION OF ALKALI FELDSPAR IN THE QUARTZ SYENITE PORPHYRY

As a consequence of albitization, originally descrete crystals so developed that a hypidiomorphic texture replaced the felsitic texture (Plate 20). In this way interstitial and overgrowth feldspars developed. Albitization is also supported by the fact that it is commonly accompanied by the introduction of quartz into interstices. (Wahlstrom, 1950).

A few sanidines appear to have suffered corrosion, most probably relating to the ore mineralization. Veinlets of quartz and calcite cut across some sanidine phenocrysts. Apart from the selective alteration of zoned sanidine, as a whole alteration is very limited on sanidine. When alteration is present, it occurs along cleavage and cracks or grain boundaries producing sericite, and kaolin developed mainly in dendrite-like patterns over crystals.

Orthoclase: Euhedral and subhedral orthoclase in phenocrysts and aggregates, ranging between 0.3 and 2.5 mm grain size comes next to sanidine in abundance. The orthoclase has both oscillatory and normal zoning. Its composition lies between Or_{98} $Ab+An_2$ and Or_{58} $Ab+An_{42}$. The estimations were made on the basis of maximum extinction method on a 010 face for each grain. No relationship in a realistic sense with respect to mineral composition to distribution was established. $2V_\alpha$ measurements show erratic variations which can be broadly grouped on two headings; angles between 50° and 57°, and angles between 68° and 72°. Rare examples

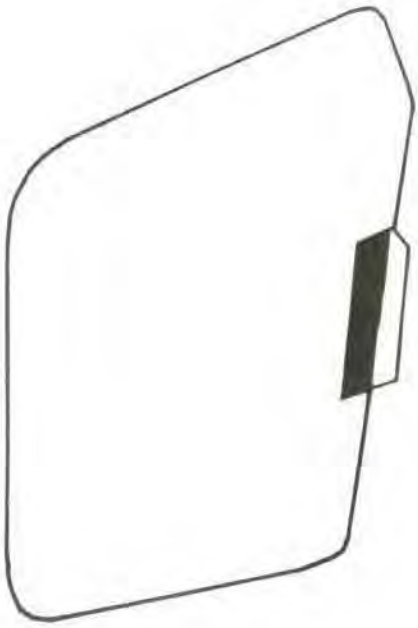

PHASE I

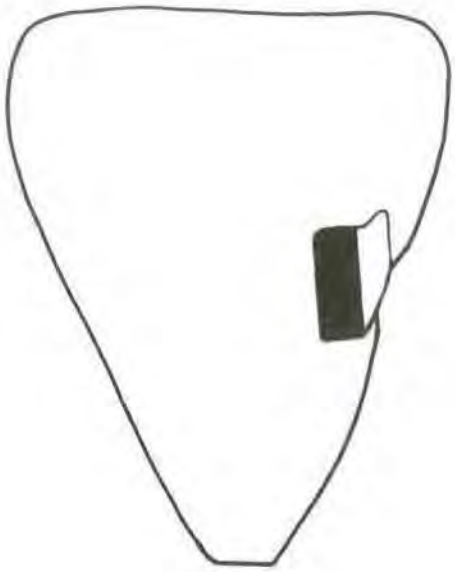

PHASE II

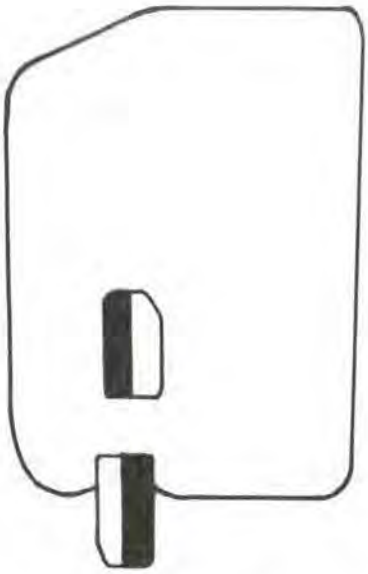

PHASE III

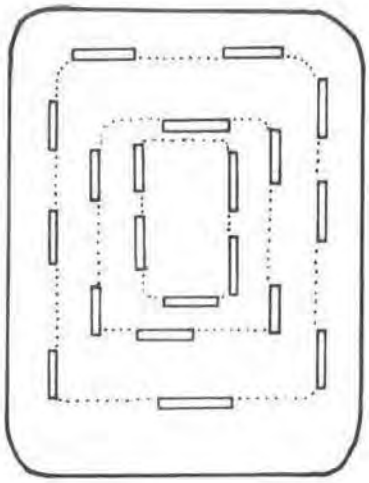

PHASE IV

Fig. 28 STAGES OF GRAIN GROWTH IN ALKALI FELDSPARS

of perthite in microstrings are present. A few orthoclase crystals together with sanidine produce micrographic texture. Alteration is very similar to that in sanidine.

Plagioclase: Euhedral plagioclase crystals ranging from 0.2 to 7 mm are found as phenocrysts, as aggregates and as inclusions in the alkali feldspars. By contrast to the alkali feldspars, plagioclase exhibits less zoning. When zoning is present, the normal zoning is commoner than the oscillatory type, but the majority of plagioclase crystals are devoid of visible zoning (Plate 21). The original plagioclase appears to have both alkali feldspar and plagioclase inclusions along with the other early stage minerals and it is the case that plagioclase occasionally surrounds an alkali feldspar (Plate 22). From their mutual relations and mode of occurrence it is, however, possible to conclude that there must have been two generations of plagioclase. Polysynthetic albite and combined albite-carlsbad twinning are the most common ones, occasionally pericline twinning also incorporates with the common twinning. Uncommonly plagioclase with a chess-board texture is present.

The plagioclase content indicates a composition ranging from An_{26} to An_{32} mainly in cores. This composition gradually changes down to An_{12} towards the margins.

Locally mineralized quartz-syenite porphyry has plagioclase

Plate 19 A large sanidine phenocryst consists of numerous plagioclase inclusions aligned in streaks parallel to the growing faces of the crystal. x10.

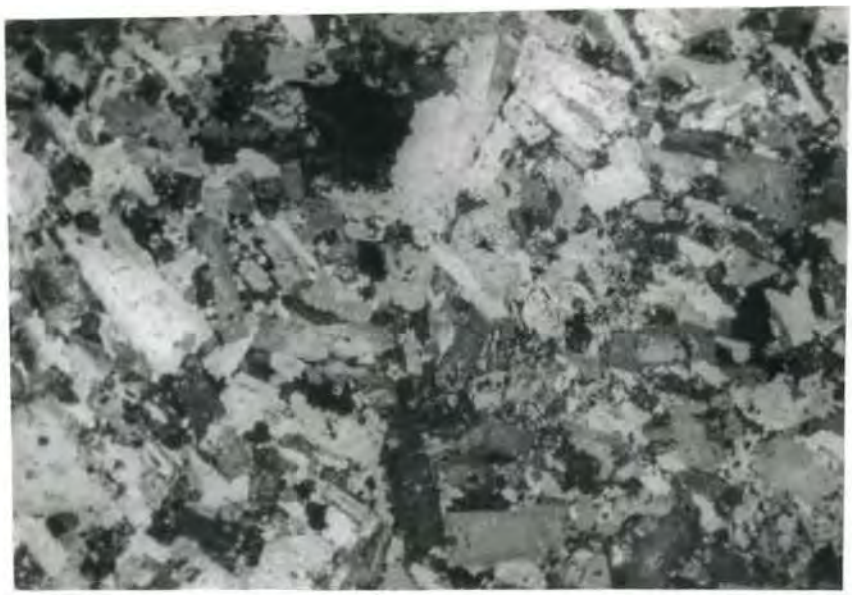

Plate 20 Quartz-Syenite Porphyry with hipidiomorphic texture made of alkali feldspar and plagioclase grains. x10.

crystals that suffered corrosion producing crescent-like shapes in margins, which in turn were occupied either by calcite or quartz. The matrix replaced by plagioclase is located in narrow margins. Where the contact metamorphism was in action calc-silicate minerals generally seem to develop at the expense of plagioclase. The plate 23 pictures a good example of this kind of development in which the grossularite replaces the plagioclase so that in its outlines even the albite twinning is distinctly visible under crossed nichols.

Because of the zoning present, selective alteration of plagioclase occurs; the great majority of plagioclases have cores either completely removed or filled up by calcite, quartz or sericite (Plate 21). This alteration appears to depend entirely on the An-content. The majority of plagioclase inclusions in alkali feldspars have been attacked by deep alteration of this type. Where ore minerals occur, complete alteration and removal of plagioclase is evidenced by the presence of euhedral casts which still preserve very thin rims of alkali feldspar. Calcite, quartz, opal, sericite and kaolin have been observed as alteration products after plagioclase.

Hornblende: The hornblende content of the rock varies locally. Although hornblende is a common constituent, a few thin sections appear to be free from it. The mineral mainly occurs in euhedral and subhedral, individual grains. Lath-like or typical amphibole

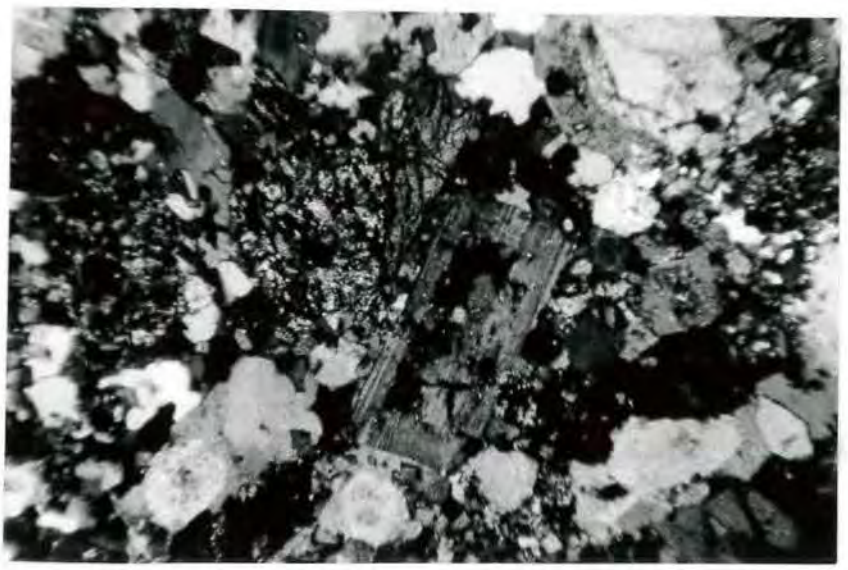

Plate 21 Euhedral plagioclase crystal showing normal zoning and selective alteration. x80.

Plate 22 Zoned sanidine with several plagioclase inclusions lying parallel to its growing faces is enclosed by plagioclase phenocrysts. x80.

cross sections are common. Grain size ranges between 0.3 and 4 mm in a long dimension. The hornblende is always found to be pleochroic with the following two pleochroic schemes; α = pale green, γ = green, β = olive green, and α = greenish brown, γ = dark green, β = dirty green. The difference in pleochroism may be due to different alterations. The hornblende rarely has twinning formed on a 100 face, and includes inclusions of early stage apatite, zircon and sphene. The refractive indice measurements for nZ have only been carried out on limited grains owing to the alteration. Thus it gives nZ = 1.66. The average $2V_{\alpha}$ angle for the several grains have been found as 79°. The combined refractive indice and $2V_{\alpha}$ angle correspond to a composition of 80Mg: $(Mg+Fe^{+2}+Fe^{+3}+Mn)$ on the diagram after Tröger (1959).

In relation to ore mineralization, relatively large calcite and quartz crystals line the hornblende casts forming crustification. An iron ore, possibly geothite, is also found to cover the cast walls. The alteration of hornblende appears to have covered all stages; in the early stage, biotite with a little chlorite develops in marginal zones, as the alteration advances a pseudomorph after hornblende is found to have filled by calcite, quartz, chlorite, epidote and iron oxides. At an intermediate stage, relatively fresh core is rimmed either by calcite or quartz (Plate 24).

Sphene: Sphene is a common accessory in all the specimens although its modal analysis never exceeds 1.8% of the rock volume.

Plate 23 Grossularite replacing plagioclase. Note polysynthetic twinning in plagioclase is still visible. x50.

Plate 24 Marginally altered hornblende.

Euhedral grains barely 1 mm long occur in slender prisms and typical cross sections of individual crystals. The mineral looks to be slightly pleochroic, giving a pleochroic scheme as follows: α = pale brown, γ = yellow brown. The sphene very frequently forms twins involving two narrow twin lamellae on the 100 plane, and suffers very little alteration along cracks and grain boundaries (Plate 25).

Biotite: This flaky mineral occurs in various proportions in all the specimens examined. Lath-like biotite is set in a fine-grained matrix. Grains with a discrete habit attain as much as 1 mm in length, but the great majority never exceed a length of 0.5 mm. Biotite with two rugged ends is dark brown in colour. Pleochroism is extreme, with α = dull brown, γ = dark brown, β = yellowish brown; therefore the absorbtion scheme is as follows: $\alpha < \beta < \gamma$. Biotite crystals are usually bent, and altered to chlorite, sericite and limonite. Unusually a secondary sphene forms as an alteration product in biotite. Very rarely a red coloured goethite takes its place in a biotite. The formation of goethite suggests that the biotite has been subjected to heating (Kumbasar, 1964).

Zircon: Euhedral zircon is an ever-present accessory mineral. Individual grains up to 0.2 mm in diameter tend to be unzoned, and rest in a fine matrix or in phenocrysts as an inclusion.

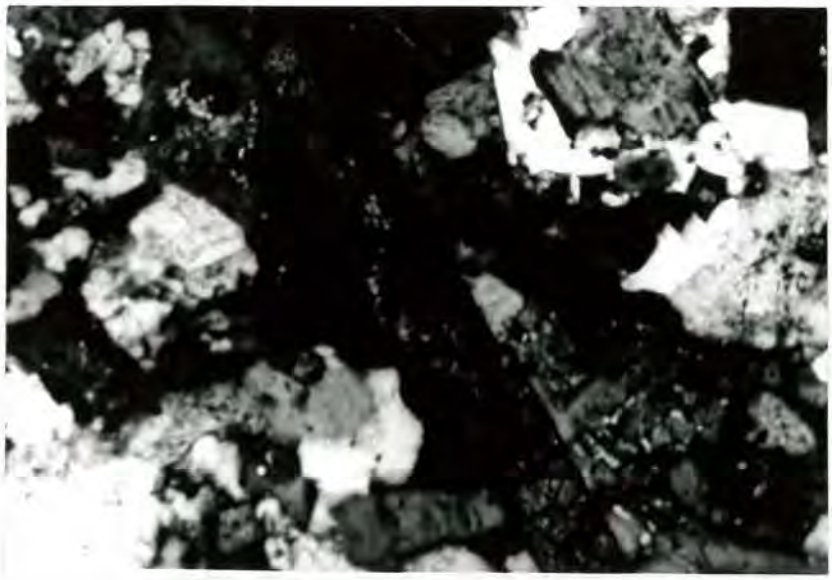

Plate 25 Slender prism of sphene shows twinning formed on 100 face as twin-plane. x80.

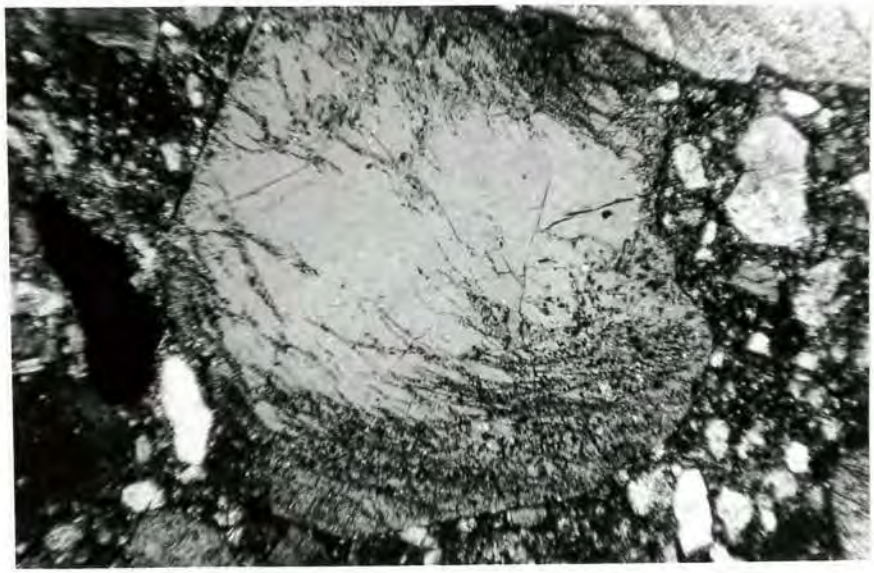

Plate 26 Alkali feldspar fragment including S-like streaks due to rotational movements in a fluid medium. x80.

Apatite: This early stage mineral is as common as zircon, and is invariably euhedral in form. Fine-grained apatite with a maximum length of 0.3 mm has similarities in distribution to zircon.

Quartz: The primary quartz is present as interstitial wedges in almost all the marginal quartz syenite porphyry. Its modal proportion varies between 1.8% and 6.4% of the rock. There is a general tendency for the quartz content to show a steady increase outwards from the central part of the igneous rock, in which quartz is absent.

Epidote: Epidote occurs as minute grains up to 0.1 mm in diameter, and is invariably in small amounts. The primary epidote differs from the secondary epidote by a distinct colour of brownish-green, and mode of occurrence.

Secondary minerals

The secondary minerals of the quartz syenite porphyry originate by two processes, namely as alteration products of primary igneous minerals, and as hydrothermal emanations from a magmatic source. Some secondary minerals are formed by both processes, others only by alteration.

Quartz: Of secondary minerals quartz is a good example of one formed by the former process. Its distribution shows similarity to the primary quartz; an increase outwards from the central areas in the igneous body. When quartz is set in the matrix,

the mineral incorporates in irregular form, either as interstitial between two granular grains or clots disseminated in the matrix. Euhedral quartz is relatively larger than the matrix-filling quartz, and occurs after plagioclase or hornblende. In some cases cast-filling quartz makes crustifications, leaving vugs in the centre. This type of quartz displays tectonic effects with pressure-shadows and grid-like fracture patterns. Quartz originating as a result of alteration mainly coexists with calcite and sericite. Beside quartz, opal also occurs in the matrix and decomposed grains.

Calcite: Anhedral fine-grained calcite forms irregular dispersion patterns in the igneous rock. The calcite distribution is controlled by hydrothermal activity and the mineral variety which it replaces, it may show sharp local variations e.g. calcite content increases relatively in the igneous body bordering an ore shoot because of calcification.

Sericite: Minute lath-like sericite is generally set in a feldspar matrix where it occupies cleavage traces, cracks and margins in the host.

Kaolin: This clay mineral, identifiable from its earthy appearance, forms as the result of advanced alteration.

Opaque minerals: Iron oxides of magnetite and hematite together with the other sulphides are present. Their amounts are very variable from place to place. Goethite and less commonly lepidocrocite are formed as alteration products.

Matrix

Although some thin sections examined are devoid of the matrix, the great majority of the rock proved to have a fine-grain matrix. By using a staining technique (see appendix) the matrix and phenocrysts proportion respectively were estimated by a point-counter. According to results on the ten thin sections, the matrix share varies from 45.8% to 66.8% (Table 5). The matrix is made up mainly of alkali feldspar and less commonly plagioclase, glass, quartz, calcite and opaque minerals. The majority of the alkali feldspar is sanidine which occurs in microliths and less commonly as felsitic aggregates ranging between 0.08 and 0.20 mm long. In the groundmass is a dominant textural element is felsitic together with microliths (e.g. is the crudely oriented plexus of alkali feldspar laths). Between the laths are set phenocrysts with very fine-grained or glassy material in the intersertal region.

The matrix textures found in the rock have been identified as hyalofelsitic, felsitic, trachytic, hypidiomorphic, pilotaxic and vitrophyric in order of abundance (Williams, 1965). An estimate for their distribution on 30 specimens is shown in table 8.

Table 8

Matrix	%
Hyalofelsitic	28
Felsitic	24
Trachytic	24
Hypidiomorphic	12
Pilotaxic	8
Vitrophyric	4

In general the groundmass suffers a little alteration and staining by iron oxides, and is seamed by calcite, less commonly quartz veinlets. In places where alteration reaches an advance stage in connection with the ore mineralization, the dusty and deeply stained groundmass becomes dominant.

In the light of thin section examination a paragenetic table for the primary minerals in the quartz syenite porphyry have been established (Table 9).

Table 9

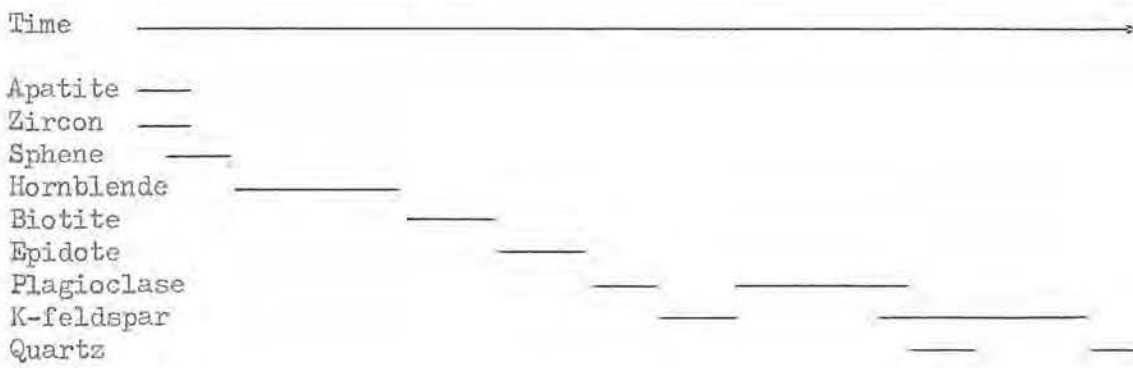

Structural state of feldspars

In the last decade the determination of structural state of feldspars in igneous rocks by means of advance X-ray techniques has received much attention. The X-ray technique modified by Smith and Gay (1958) has been widely used for plagioclase in igneous rocks formed in various stages. But this method requires knowledge of the normative plagioclase content calculated from the whole rock analysis. Most recently a new

X-ray technique for the structural state of alkali feldspars was developed by Wright (1968), which only requires certain 2θ values corresponding to the reflections which were claimed to be function of the structural state of the alkali feldspar. These two methods were applied to plagioclase and alkali feldspar in quartz-syenite porphyry from the Keban area respectively.

Structural state of alkali feldspar

The study of the structural state of alkali feldspar in the quartz syenite porphyry were carried out for 13 specimens on a Philips XRD (PW1051), following the procedure described by Wright (1968). The two 2θ values obtained from the relative separation of the peaks 060 and $\bar{2}04$ were plotted on a diagram shown by fig.29. 10 out of 13 specimens are located inside the area where high sanidine - high albite series form, but the two specimens fall into the P50-56 orthoclase region. In table 6 the specimens examined and their structural state are tabulated individually.

Structural state of plagioclase

The structural state of plagioclase was determined from the relative separations of the peaks $2\bar{2}0$, $1\bar{3}1$ and 131 on X-ray diffractometer patterns from the whole rocks. These measurements give values of the function (F) $2\theta_{131} + 2\theta_{2\bar{2}0} - 4\theta_{1\bar{3}1}$, and these

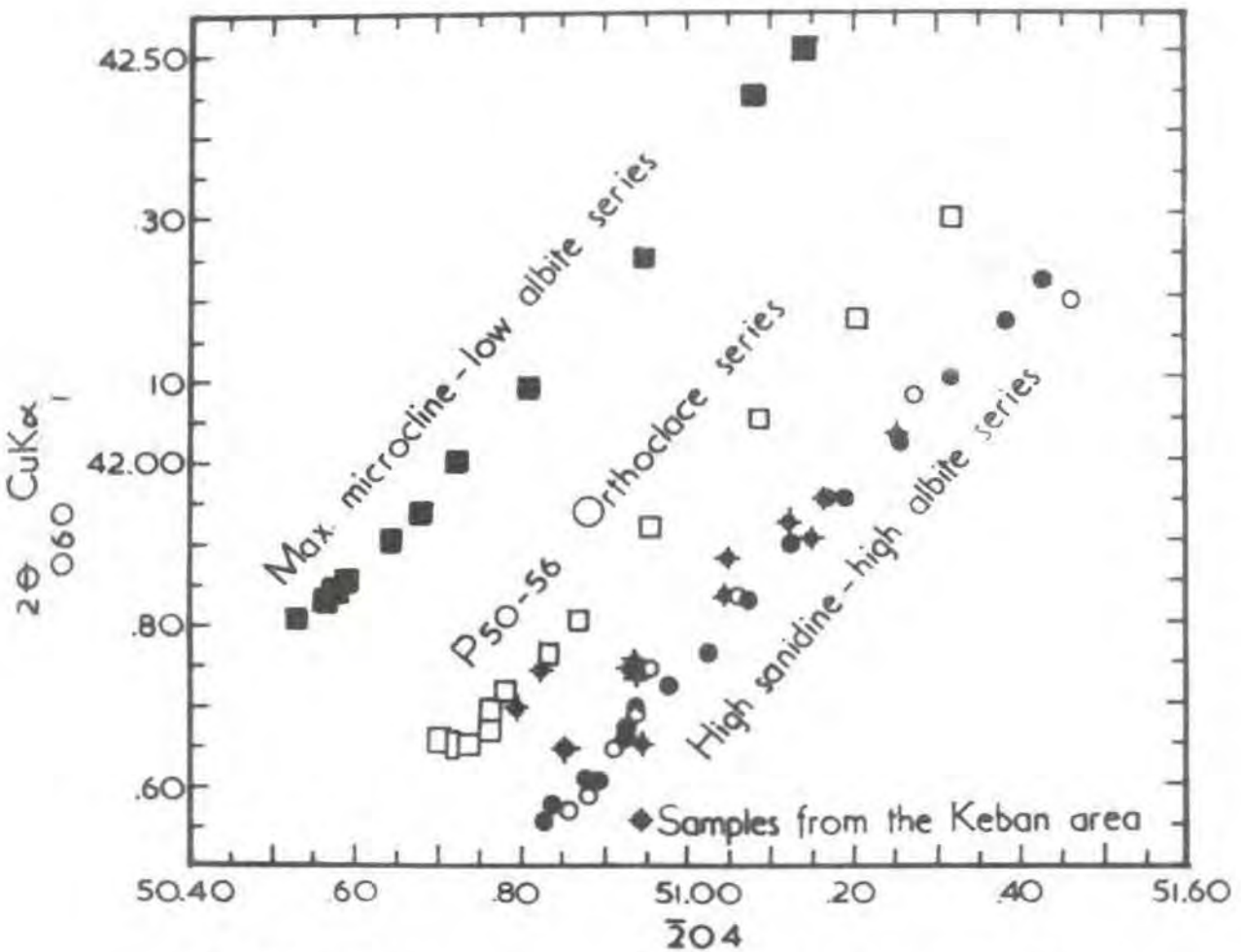

Fig. 29 Variation in structural state of alkali feldspars
(After, Wright 1968)

functions were plotted against their weight % An defined by their normative compositions. In spite of the uncertainty in composition, due mainly to the zoning seven specimens on which determinations have been carried out, give a function value ranging from -0.50 to -0.64 (Table 10). Thus the seven specimens are closely located inside the triangle lying within the area defined for the intermediate structural state (hypabyssal) (Fig.30). On the other hand plotting their An composition obtained from the microscopic study, gives a reverse result, being low temperature structural state. The difference between the bulk and phenocryst composition is a resultant of plagioclase with low An content which participates in the matrix, and reduces the bulk composition as a whole.

Table 10

Sample No.	$2\theta_{\bar{2}20}$	$2\theta_{1\bar{3}1}$	$2\theta_{131}$	F	Bulk composition wt.% An	Phenocryst composition %An
TK-151	28.32	29.87	30.90	-0.52	10	29
G-125	28.36	29.90	30.88	-0.56	4	28
262	28.42	29.97	30.88	-0.64	4	28
TK-141	28.42	29.97	30.92	-0.60	7	27
82	28.41	29.88	30.85	-0.50	12	26
263	28.37	29.87	30.87	-0.50	5	28
TK-150	28.37	29.86	30.86	-0.51	10	27

Petrography of the volcanic breccia

The volcanic breccia is composed of mineral derivatives of the igenous rocks and of accidental fragments from the phyllite, marble, calc-schist and probably the dolomite marble. Actinolite,

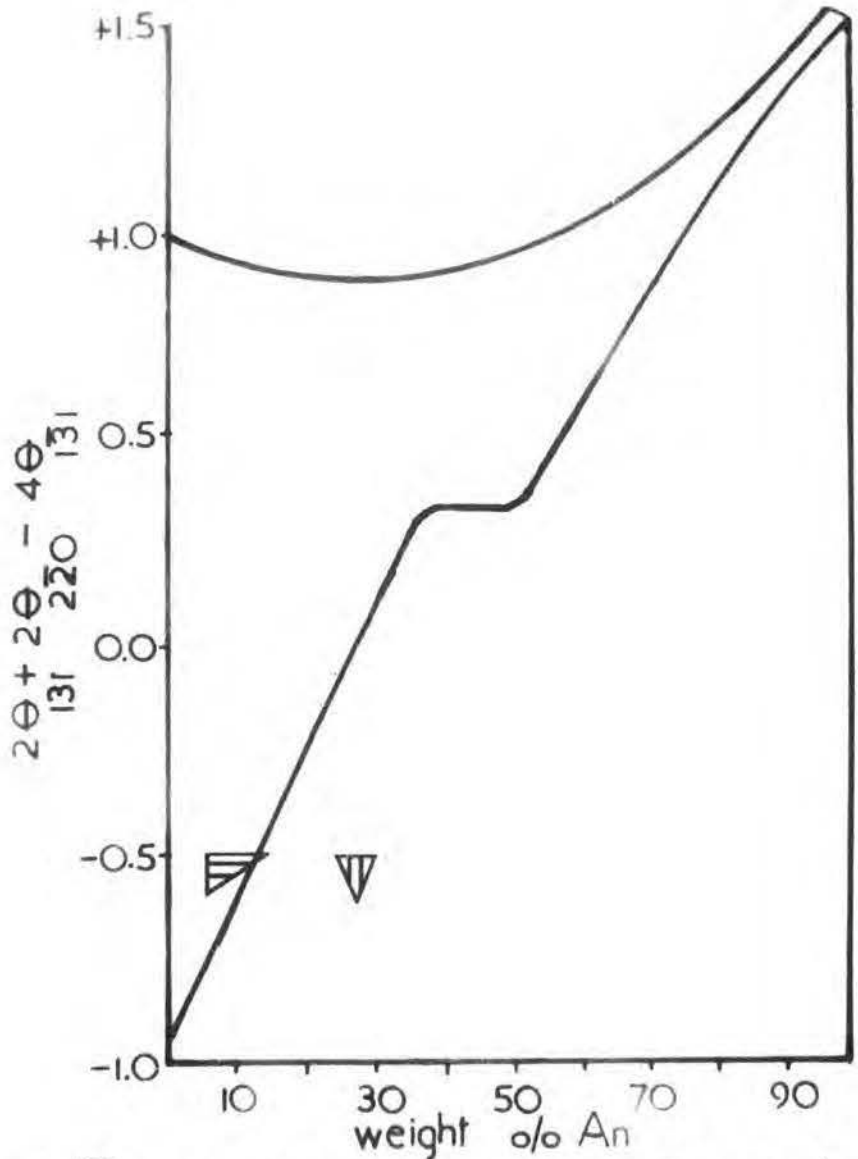

Fig. 30 The structural state of plagioclase in the Keban quartz syenite porphyry

(After Smith & Gay 1958)

chloritoid, calcite, quartz and the ore minerals of hematite and specular hematite are additional minerals formed by the igneous process. Biotite, hornblende, zircon and apatite are found in accessory amounts. All grains show to a certain degree roundness ranging from subrounded to rounded. The fragments are consistently found to be isolated in the groundmass. Disintegration and rounding of fragments and of mineral grains are most readily accounted for as a consequence of abrasion and attrition. (Reynolds, 1954). Corrosion and pebble-like forms are clearly the result of attrition of originally angular fragments in a moving medium. (Pitcher & Read, 1952).

The fragments fall into the lapilli group (4-32 mm), they are of accidental origin derived from the host rock and the immediately underlying rocks. The accidental fragments make up 11% of the rock by volume, while the accessory fragments form 17% . In two sections (332 & 335) detailed measurements were made of the fragment sizes (Fig.31). (332) belongs to the surface sample, (335) comes from a spot 60 m below the former point. From the comparison of two histograms (fig.32), it is seen that there is an upward decrease in grain size.

The fragments do not show any preferred orientation. Moreover the groundmass reveals no sign of flowage direction. Some individual grains, particularly alkali feldspars contain

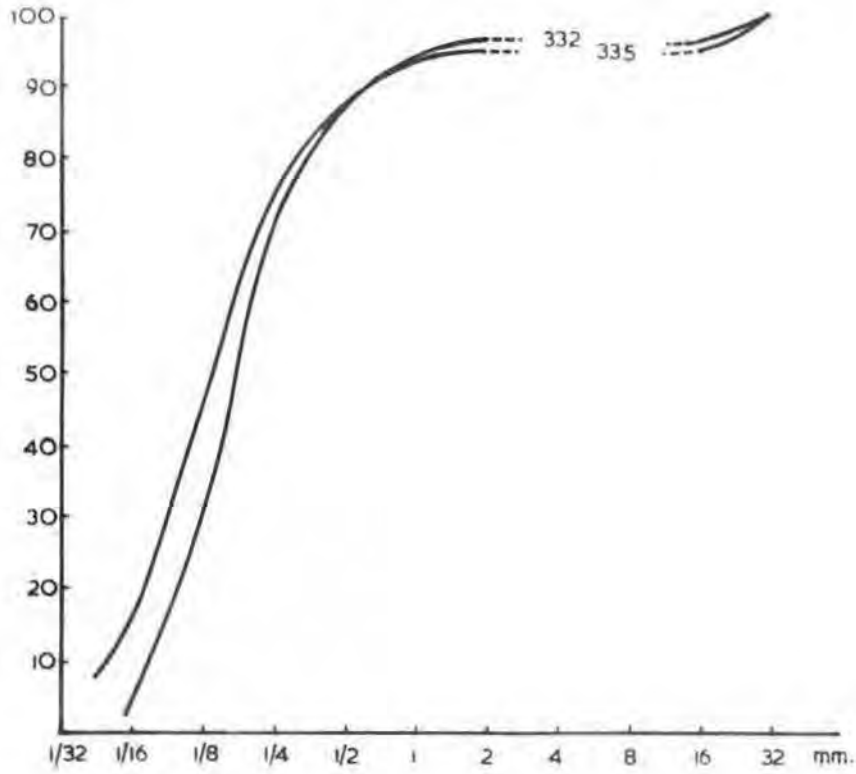

Fig. 31 Cumulative percentage curve for the minor axes of grains in the two volcanic breccias

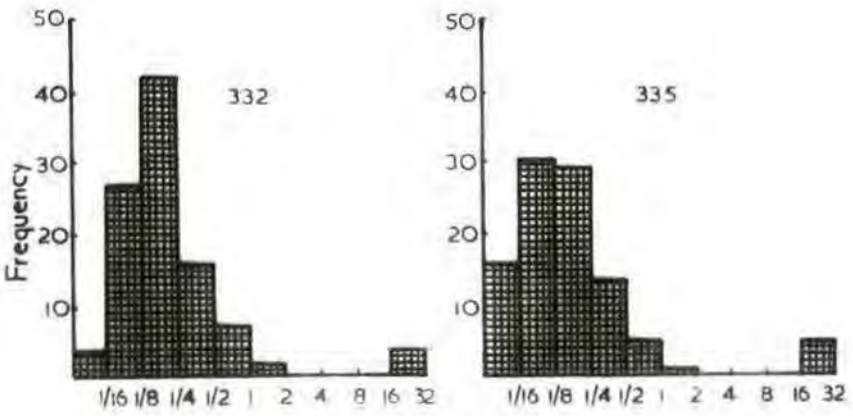

Fig 32 Histogram of minor axes of grains in the two volcanic breccias

S-like streaks (Plate 26). Individual grains having the same patterns exhibit no directional relationship to each other. This must have been a result of cooling in a relatively cool medium in which fragments keep a rotational movement whilst they are thrown upwards. The presence of druses which are mainly filled up by calcite, suggests comparison with the rising bubble phase of the fluidized bed of industry, within which the solid particles have a turbulent motion (Walton & O'Sullivan, 1950). A few individual fragments very similar to the main breccia in composition and texture, except that they are made from fine-grained materials, are set in the same matrix. This would suggest that the formation of the breccia took place in more than one stage.

Under the combined thermal metamorphism and metasomatism, actinolite is restricted to the magnesia-lime fragments together with chloritoid and scapolite. It is striking that these minerals developed mainly in the upper level. Skeletal and acicular specular hematite is commonly seen to occur in calcite, and it replaces calcite. Of additional importance is that calcification later than the specular hematite mantles the early calcite charged with specular hematite. Relatively large calcite aggregates having no actinolite or other neo-formation minerals also formed by calcification.

The probable temperature at which the volcanic breccia formed, may be established in the light of present temperature indicator minerals and the other indications. The presence of graphite in the phyllite and calc-schist fragments eliminates the possibility of temperatures above 550°C (Pitcher, 1950), and then absence of wollastonite reduces the temperature to under 400°C. Assuming the case that wollastonite does not form in the presence of plagioclase; then the diopside should have formed instead. As no diopside in the rock has been located, the maximum temperature decreases to 390°C. It is likely that the maximum temperature must have been below this value.

Petrogenesis of the metamorphic rocks

The metamorphic rocks in the Keban massif are undoubted examples of metasediments. So far there has been found no evidence in the massif of metamorphic rocks originally of non-sedimentary origin. The well-banded schists with alternate flaky minerals, quartz-feldspathic and calcite-feldspathic layers indicate a relict fabric from the original sediments (Turner & Verhoogen, 1960). Although only found in small proportions the frequent presence of rounded zircon and to a lesser extent, apatite provides further evidence for a sedimantary origin. The relative abundance of graphite, which is regarded as representing carbonaceous impurities in the originally pelitic rock also indicates primary depositional

layering. The striking fine scale banding seen in the schistose rocks is considered to be controlled by the original sedimentary bedding. Also the presence of helisitic structure in plagioclase metacrysts in which the direction of the original layering is traceable in streaks of inclusions resting parallel to the original rock structure, is evidence for a sedimentary origin. (Barth, 1951). Finally the high lime content together with features mentioned undoubtedly suggest derivation from a sedimentary source rather than an igneous origin.

The chlorite-epidote calc-schist, the marble schist and sericite-calc schist are clearly metamorphosed argillaceous limestones. The chlorite-epidote calc-schist contains green streaks of calc-silicate minerals that are interpreted as metamorphosed impure limestone. The dolomite marble certainly represents metamorphosed impure limestone (=dolomitized limestone). Almost pure marble undoubtedly is a derivative of pure calcite limestone. The calcareous graphite phyllite and the calcareous quartz phyllite indicate a metasediment originated from a calcareous shale. The overall evidence suggests that the bulk of the metamorphic rocks represent a series of argillaceous limestone, dolomitized limestone, pure limestone and calcareous shale.

In the light of field and laboratory evidence it is likely that the dolomitization of limestone took place prior to the regional metamorphism. The mottled, irregular development of nests of

dolomitized material in a groundmass of fine-grained marble, which sometimes have a pseudo-brecciated appearance is taken as positive evidence for an early stage dolomitization (Beales, 1953). The poor overall porosity gives proof supporting this. Late-stage diagenetic dolomites may be regarded as more likely to be porous than dolomites formed penecontemporaneously. (Fairbridge, 1957). Another characteristic of the early dolomites is the widespread presence of iron oxide, generally as limonitic grains. This form of the iron is thought to be due to the sulphate-reducing bacterial activity in the newly buried sediments, and thus can only be early diagenetic (Udluft, 1929). In fact, all the dolomite marbles particularly in the W to the Sifillitepe appear deeply stained by iron oxide. Even more emphatic perhaps is the smell given by the freshly hammered rock, which is attributed to an early-stage dolomite. Preliminary studies by Lucas (1952) show that the smell is caused by the ammoniacal salt of a volatile acid containing phosphorus. The salt tends to be lodged as inclusions in the dolomite crystals. The alternation of dolomitized marble with the marble layers particularly in the western prolongation of the field is noticeable support for an early stage dolomitization. The dispersion pattern of MgO as revealed by the chemical analysis of the samples gives no indication of a connection with the igneous body, which in the event has only very small amounts of MgO. (See Chapter V).

Petrogenesis of the quartz-syenite porphyry:

There is no doubt about the magmatic origin of these rocks; so far, no evidence to the contrary has been found. However it is worth mentioning some evidence in favour of a magmatic origin: a) Discordant relationships and disruption of the regional trend, b) The rock bodies have sharp contacts bordered in many cases by varied aureoles of thermally metamorphosed rocks, c) Cross-cutting dykes containing diversely oriented inclusions of the adjacent rock etc. d) There is uniformity of the over-all mineral composition, e) Consistancy in plagioclase content in the igneous body having the same mineralogical composition, f) Certain minerals, particularly alkali feldspar and plagioclase have a uniform composition within the same body, g) Steady increase in potassium content of the alkali feldspars at the expense of Ab towards margins.

It is more likely that isolated quartz-syenite porphyry bodies may result from the injection and consolidation of a magma desilicated by reaction with calcic rocks such as marble at depth. That the quartz-syenite porphyry consolidated at a shallow depth under a reduced volatile content is suggested by the presence of abundant sanidine, absence and small amounts of perthite, variability of the rock in texture, and to a lesser extent, mineral composition. The occurrence of trachytic and the other textures belonging to extrusive igneous rocks and hematitic dust-like

inclusions are regarded as having formed under near-surface conditions where free oxygen is available. (Hutchinson, 1956).

CHAPTER V

CHEMISTRY

Introduction

Analyses for major and trace components were carried out using the Philips XRF automatic spectrograph. Full details of the procedure are given in the Appendix. The FeO, H_2O were analysed by wet chemical methods. The normalized XRF analyses were adjusted to take into account the wet chemical deformations. CO_2 values were determined for a number of critical samples. The graphite content was analysed by the wet combustion method (see appendix) and as a check four samples with high graphite content were counted by the point counter 1000 points per sample. The effect of heating on the FeO content was considered and a simple correction was made in order to get a realistic value for graphite taking into account Fe_2O_3 also formed. The results are satisfactory, as there is fairly good agreement between the two methods (table 11). The remaining samples were analysed by the wet combustion method. The results are tabulated below.

Table 11

Sample No.	Wet Combustion %C	Point Counter %C
UP-1	4.80	4.04
UP-3	2.00	2.00
LP-1	2.60	3.00
LP-2	2.16	2.80

Ten quartz syenite porphyry samples collected from different localities throughout the area have been analysed by the wet chemical procedure based on the Shapiro method (Shapiro, cf., 1962). In addition, K_2O and CaO determinations were made by flame-photometer and wet chemical methods respectively on eight samples, for use in geochemical interpretation together with rubidium and strontium respectively.

Discussion of the chemical analysis

The chemistry of calc-schist: The three subdivisions of the calc-schist exhibit some notable differences in terms of chemical variation. The lower division is characterised by its high content of SiO_2, K_2O and Al_2O_3, relatively low CaO and nearly constant MgO (up to 40.25%, 7.31%, 12.27%, 19.36% and 1.89% respectively). The TiO_2 content reaches its maximum value among the analysed samples (Table 12). The ratio Fe_2O_3 to FeO is more than 4, marking comparatively intense oxidation. Another oxidation indicator H_2O is higher than in any other sample.

By contrast to the chlorite-epidote calc-schist, the middle subdivision (marble schist) contains comparatively low SiO_2, Al_2O_3 with the exception of MgO. The other elements

Table 12 Chemical analyses of the Calc-Schist

Sample No.	310	313	42	248	256	261	63	78
SiO_2	40.25	37.17	12.73	11.33	7.27	11.70	13.96	14.09
Al_2O_3	11.57	12.27	6.92	5.47	4.26	6.39	6.38	6.64
Fe_2O_3	3.65	4.78	2.19	2.22	2.29	2.42	3.48	3.50
FeO	0.42	1.06	0.54	0.41	0.44	0.61	1.15	1.11
MgO	1.89	1.88	4.61	2.79	1.90	1.78	1.26	0.58
CaO	18.66	19.36	39.88	42.51	45.90	42.09	39.95	40.08
Na_2O	0.02	0.32	0.20	0.21	0.20	0.13	0.35	0.47
K_2O	7.31	6.97	1.13	1.23	0.75	1.29	1.52	1.42
H_2O^-	0.49	0.23	0.05	0.07	0.07	0.10	0.06	0.05
TiO_2	0.83	0.61	0.38	0.31	0.36	0.39	0.37	0.47
MnO	0.26	0.14	0.05	0.06	0.06	0.06	0.12	0.10
CO_2	14.67	15.21	31.34	33.42	36.08	33.08	31.40	31.50
C	n.d	n.d	n.d	n.d	n.d	n.d	n.d	n.d

Lower subdivision: 310,313

Middle " : 42,248,256,261

Upper " : 63,78

particularly CaO show a sharp increase to as much as twice the amounts in the chlorite-epidote calc-schist.

The upper subdivision (sericite-calc schist) shows a slight increase in SiO_2, total iron and K_2O in comparison with the marble-schist. (Table 12).

The chemistry of dolomite marble: The MgO content of the dolomite marble is remarkably uniform along its strike, except for two samples, one of which has been taken from the southern extremity, which may indicate that the MgO content decreases outside the area mapped (Table 13). The overall MgO content varies between 20.73% and 28.89%, mainly being about 27.50%. By contrast, the variation along the dip appears to be erratic. Considering the four analysed samples along the Zereyandere traverse, the lower part has a MgO content of 13.65%, with an upward increase the content reaches 25.94% MgO, this increase becomes 27.62% at the 270 observation point. (See fig.16 in pocket). The upper levels are much richer in MgO, thus having 28.04% MgO in sample ZD-1. This steady increase is at variance with the results obtained from three samples collected at 50 m intervals in the main adit through the dolomite marble. Here the specimens start with 28.89% MgO, and decrease to 20.73%, and again increase to 26.47% at the top. From table 13 it is seen that there is no marked correlation between

the variation in CaO content and the MgO content. Along the Zereyandere traverse Cao/MgO ratio starting from the bottom is 2.97, 1.04, 1.06 and 1.09 respectively. As a whole this ratio stays between 1.03 and 2.92 giving an arithmetic mean of 1.23. The SiO_2 content remains uniform although exceptions occur where mineralization is present e.g. in one case the amount of SiO_2 exceptionally increases to 15.15%. The Al_2O_3 amount appears to be tied to SiO_2 content. In general the Al_2O_3 content stays below 1% or is below detection limits. The majority of samples have a Fe_2O_3/FeO ratio more than 1, suggesting effect of oxidation and mineralization.

The chemistry of phyllite: Table 14 shows the results of twenty-three phyllite analyses. In general, the phyllite is characterized by a high content of CaO varying greatly with respect to SiO_2 content. On the other hand a similar relation is present between CaO and Al_2O_3 contents in which CaO appears to be dependent reversly on the Al_2O_3 content, the highest Al_2O_3 value correspondes with the lowest CaO value, in other terms samples with high phyllosilicate composition are relatively poor in CaO content, which is also valid for MgO and K_2O against the CaO content in the same rock. CaO stays as low as 0.07% and as much as 31.42%. A marked increase in Al_2O_3 is also noted near the ore mineralization, e.g. G.507/B

Table 14 Chemical analyses of the Phyllite

Lower subdivision

	Sample No.	UP-3	LP-1	LP-2	UP-1	G-110	G-55	G-118	G-175/2	302	308	G-507/B	G-515	G-516
	SiO_2	47.70	33.12	44.75	38.95	42.65	38.93	42.50	37.62	43.25	37.23	57.01	42.74	58.79
	Al_2O_3	4.64	3.60	4.60	10.79	8.84	16.46	10.08	15.70	16.14	10.16	24.00	14.76	25.96
	Fe_2O_3	1.95	1.85	1.53	2.12	1.63	4.19	1.26	3.06	4.64	4.18	5.54	3.38	2.14
	FeO	0.64	0.22	0.62	1.12	1.00	3.10	1.22	2.44	3.29	1.88	1.22	0.84	1.67
Wt %	MgO	2.53	0.50	1.79	1.56	1.00	3.78	0.95	2.57	3.96	2.83	1.39	2.23	2.46
	CaO	20.65	31.42	24.23	18.37	23.85	16.05	23.30	18.39	13.22	21.86	1.80	17.09	0.07
	Na_2O	0.52	0.05	0.28	0.94	0.35	0.35	0.27	1.64	0.62	1.18	0.26	0.10	0.14
	K_2O	2.27	1.55	0.60	6.55	1.13	3.17	1.35	2.90	2.86	1.35	4.65	4.06	6.12
	H_2O^-	0.41	0.27	0.09	0.28	0.06	0.07	0.05	0.06	0.01	0.06	1.35	0.39	0.42
	TiO_2	0.35	0.10	0.28	0.77	0.39	0.80	0.40	0.76	1.00	0.63	1.04	0.67	1.17
	MnO	0.13	0.14	0.11	0.12	0.19	0.13	0.17	0.12	0.08	0.11	0.10	0.31	0.06
	CO_2	16.24	24.69	19.04	14.55	18.74	12.62	18.32	14.46	10.40	17.19	0.79	13.44	n.d.
	C	2.00	2.60	2.16	4.04	0.20	0.36	0.16	0.27	0.57	1.35	0.88	0.08	1.02

Upper subdivision

	Sample No.	26	34	26/1	81	84/2	86	126	148	182	246
	SiO_2	34.42	30.02	27.96	44.91	42.39	64.32	37.05	46.51	36.51	28.50
	Al_2O_3	4.96	3.17	5.47	5.59	18.65	8.15	6.37	6.65	5.80	11.25
	Fe_2O_3	2.21	9.14	2.46	3.05	4.40	1.58	2.25	2.03	2.94	3.75
	FeO	0.25	0.21	0.30	0.30	2.29	0.66	0.51	0.34	0.44	1.42
Wt %	MgO	0.42	1.37	0.51	0.68	3.09	1.26	1.18	0.73	1.77	2.11
	CaO	30.55	28.50	33.55	23.84	12.50	10.67	27.34	19.94	27.55	27.55
	Na_2O	0.08	0.07	0.06	0.13	0.49	1.18	0.40	0.19	0.45	0.37
	K_2O	0.74	2.05	0.79	0.82	3.46	1.15	0.90	5.06	1.22	2.36
	H_2O^-	0.18	0.20	0.22	0.12	0.05	0.07	0.11	0.15	0.08	0.08
	TiO_2	0.31	0.27	0.32	0.33	0.72	0.25	0.43	0.48	0.34	0.66
	MnO	0.09	0.16	0.09	0.09	0.11	0.05	0.09	0.12	0.09	0.07
	CO_2	24.01	22.42	26.37	18.74	9.82	8.39	21.49	15.68	21.66	21.66
	C	1.78	2.42	1.90	1.40	2.04	2.27	1.89	2.12	1.15	0.23

taken near the mineralization in the 726 m level shows characteristic enrichment in the Al_2O_3 up to 24.00%. K_2O dependent of Al_2O_3 becomes as high as 6.55% as in the UP-1. The TiO_2 is found in a close association with the total iron content. The graphite content seems to be independent of the other constituents. The ratio Fe_2O_3 to FeO is always more than 1, indicating relatively advanced stage oxidation and the effect of mineralization; furthermore the H_2O content increases with increase in the Fe_2O_3/FeO ratio.

The chemistry of marble: Table 15 illustrates the results of nineteen marble analyses. The marble is uniformly pure and the CaO content is variable within a small range, from 49.60% to 55.68%, but the majority shows a variation around 55% CaO. The impurity is usually less than 2% and never exceeds 8%. 9 analysed samples from the eastern marble have very constant CaO contents, giving a difference within a range of less than 1% CaO. From the comparison of chemical analysis, the eastern marble is relatively purer than the central marble in which CaO value decreases to 52.89%. Nevertheless, the CaO content tends to increase towards the southern part of the central marble. A reverse downward increase in CaO content is found through the succession. Exception occurs near the ore-shoots where the marble seems to have suffered a decrease in CaO content. This

Table 15 Chemical analyses of the Marble

	Sample No.	G-188	G-100	G-116	G-96	G-212/1	G-177	G-102	G-147	S-21	G-109	G-77	107/1	S-29	G-45	G-122	Im-1	153/2	165/1	G-109/1
	SiO_2	2.00	0.43	0.93	0.68	0.57	0.38	0.18	0.16	0.23	0.08	0.32	0.28	0.06	3.69	0.16	0.26	0.18	0.21	0.17
	Al_2O_3	0.64	0.14	0.68	0.40	0.26	0.27	0.16	0.15	0.17	0.13	0.30	0.33	0.18	1.71	0.25	0.30	0.28	0.34	0.09
	Fe_2O_3	0.44	0.09	0.81	0.09	0.27	0.46	0.01	0.12	0.17	0.06	0.07	0.42	n.d.	0.36	0.22	0.07	0.10	0.12	0.05
	FeO	0.28	0.16	0.21	0.15	0.93	0.22	0.16	0.28	0.10	0.13	0.17	0.19	n.d.	0.24	0.19	0.13	0.49	0.19	0.15
	MgO	0.77	0.81	1.15	0.09	n.d.	n.d.	0.12	0.31	0.05	n.d.	2.68	0.31	n.d.	2.80	0.86	0.40	0.31	0.22	n.d.
Wt %	CaO	52.82	54.70	53.26	54.72	53.50	55.08	55.50	55.10	55.36	55.48	52.89	54.87	55.82	49.60	54.54	55.09	54.78	54.97	55.68
	Na_2O	0.21	0.01	0.18	0.58	0.85	0.06	0.07	0.01	0.23	0.31	0.20	0.01	0.14	0.15	0.03	0.15	0.04	0.39	0.01
	K_2O	0.18	0.07	0.11	0.10	0.12	0.08	0.04	0.03	0.03	0.03	0.06	0.07	0.03	0.42	0.04	0.05	0.05	0.05	0.04
	H_2O^-	0.22	0.05	0.05	0.05	0.37	0.06	0.03	0.12	0.07	0.08	0.06	0.08	0.07	0.11	0.12	0.01	0.15	0.10	0.04
	TiO_2	0.04	0.02	0.05	0.03	0.02	0.03	0.02	0.02	0.02	0.02	0.03	0.02	0.02	0.07	0.02	0.02	0.02	0.02	0.02
	CO_2	41.61	43.40	42.48	43.00	41.28	43.19	43.64	43.31	43.50	43.52	43.09	43.20	43.77	40.44	43.21	43.51	42.94	43.27	43.74
	SO_4	0.79	0.14	0.09	0.11	1.83	0.17	0.09	0.39	0.06	0.16	0.12	0.22	0.08	0.41	0.37	0.01	0.67	0.14	0.01

depletion amounts relatively to 1.82%. Similar depletion also took place in the fault zones, e.g. the specimen 45/G comes from breccia in a fault zone at the 745 m level, whose CaO value shows a depletion, and a gain of SiO_2 and MgO respectively. MgO content appears to be variable without any relation to its field occurrence. Although several samples are devoid of MgO, the majority have an MgO composition varying from 0.05% to 2.80%. It is striking that specimens near ore-shoots give minimum values for MgO. By contrast an enrichment in SiO_2 and S content (expressed as SO_4) are evident from the table. The S enrichment is up to 1.83% SO_4.

The metasediments of the Keban massif are represented on the ACF and AFK diagrams of the quartz-albite-muscovite-chlorite subfacies of the greenschist facies (fig. 33).

The chemistry of quartz-syenite porphyry: Table 16 shows the results of ten quartz-syenite porphyry analyses. From the table it is seen that the most obvious feature of these analyses is their remarkable uniformity in certain elements. The Keban igneous rock is an intermediate rock mainly characterised by high silica content which shows only slight difference from specimen to specimen. By contrast to the silica content Al_2O_3 content varies between 16.29% and 18.50%. Another feature of the igneous rock is that of excess Al_2O_3, which is expressed in corundum forming between 0.51% and 4.38% in the normative

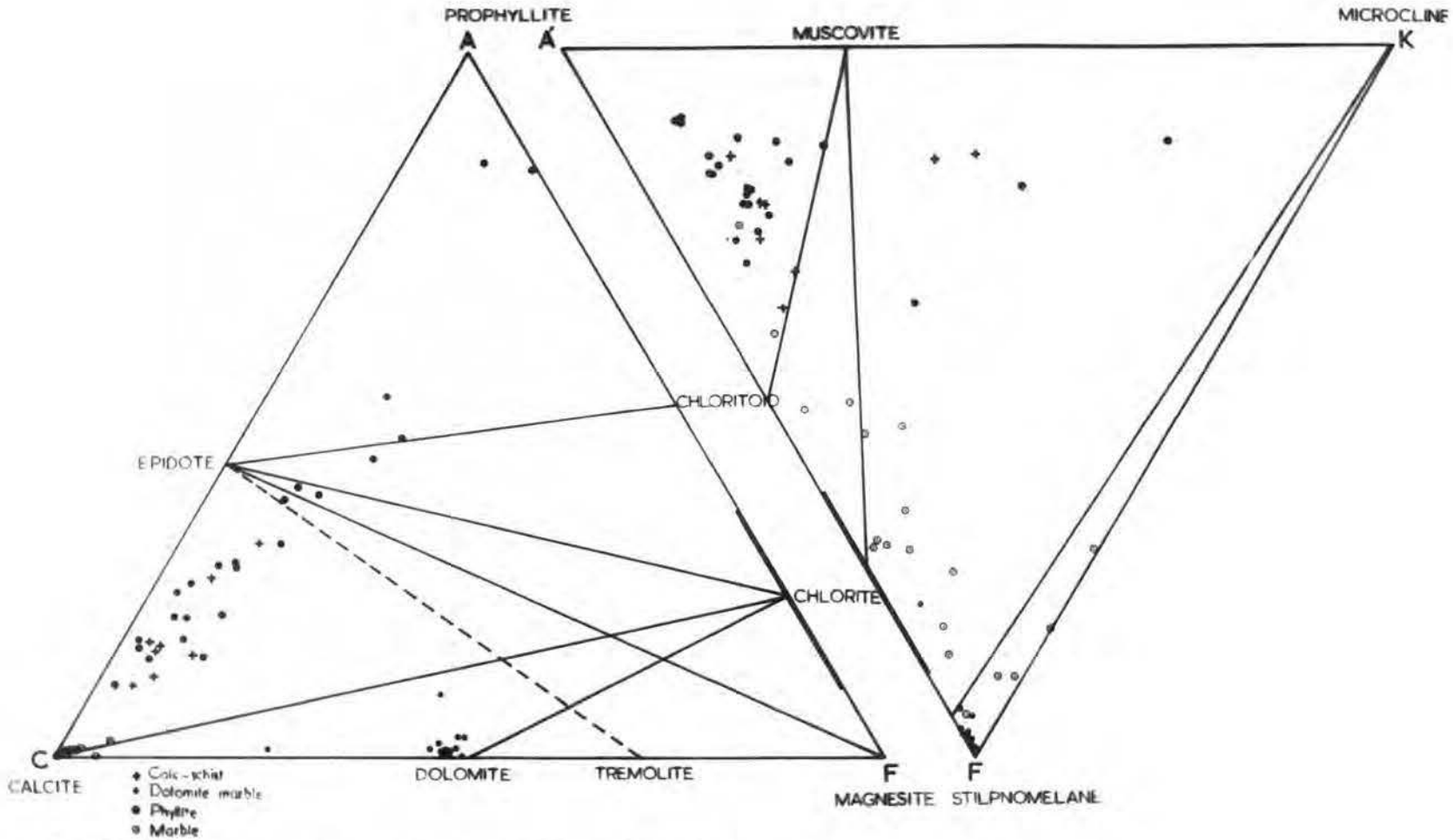

Fig. 33 The chemical compositions of the Keban metasediments plotted on ACF and ÁFK diagrams

composition. The variation in the K_2O content appears to be closely associated with the proportion of Na_2O except for the specimens TK-113 and 262 in which K_2O amounts to 9.98% whereas the proportion of Na_2O decreases to 1.65%. The quartz-syenite porphyry has an overall lower Na_2O/K_2O ratio between 0.16 and 1.20 and a low FeO/MgO ratio from 3.40 to 8.50 (see table 22). The arithmetic mean of ten specimens of quartz syenite porphyry is chemically comparable in a broad way to the moderately leucocratic quartz syenites in the Kungnat Fjeld (Upton, 1960 & Watts, 1966, table 17). In comparison with the Kungnat Fjeld rock, the Keban igneous rock contains more Al_2O_3, CO_2 and less total iron. Plots of ten total iron, alk and Mg on a ternary diagram shows close relation to the mean curve for the Gardar rocks (Fig.35). But their location towards the alk end of the curve suggests that the Keban rocks are much more differentiated than the Gardar rocks. This is also evident from the relatively low content of P_2O_5, TiO_2, total iron and MgO. On the other hand K, Na and Ca relation on a similar diagram gives a negative slope, and all ten points are located above the mean curve of 125 analyses for the Gardar rocks near the K end (fig.34). The relative abundance of Fe_2O_3 to FeO and high CO_2 content together with combined water are thought to result from some degree of

Table 16 Chemical analyses and C.I.P.W. norms of the Quartz Syenite Porphyry

	Sample No.	82	TK-150	TK-113	263	291	TK-151	262	274	G-125	TK-141
Wt %	SiO_2	63.62	63.80	61.46	60.96	62.65	63.65	62.04	63.02	63.52	62.70
	Al_2O_3	17.31	18.48	17.89	16.55	16.96	18.50	17.63	16.35	16.29	18.22
	Fe_2O_3	1.95	1.60	1.22	2.21	2.12	1.75	1.27	1.95	1.91	1.22
	FeO	1.25	1.28	0.86	1.82	1.12	1.34	0.97	1.34	1.28	1.02
	MgO	0.16	0.26	0.12	0.40	0.35	0.21	0.18	0.30	0.28	0.12
	CaO	3.40	2.20	3.45	2.56	2.14	1.93	3.41	2.72	2.38	2.48
	Na_2O	4.85	5.60	1.65	4.73	4.86	5.06	1.75	4.15	4.82	4.13
	K_2O	4.68	4.65	9.80	5.36	5.48	5.62	9.98	6.46	5.60	7.50
	ΣH_2O	1.12	1.10	0.53	2.42	2.42	1.18	0.34	1.70	1.80	1.05
	TiO_2	0.37	0.48	0.43	0.42	0.40	0.50	0.49	0.30	0.32	0.34
	P_2O_5	0.04	0.04	0.05	0.05	0.06	0.05	0.04	0.03	0.04	0.05
	MnO	0.16	0.17	0.20	0.19	0.15	0.07	0.05	0.10	0.12	0.15
	CO_2	0.98	0.30	2.27	2.03	1.27	0.33	2.32	1.78	1.34	0.83
	Q	12.36	9.18	13.32	10.86	12.42	18.84	16.14	12.66	12.24	6.84
	Or	27.80	27.80	57.82	31.69	32.25	33.36	58.94	38.36	33.36	44.48
	Ab	41.92	47.16	14.15	39.82	40.87	28.82	9.96	35.11	40.87	35.11
	An	9.73	8.34	1.67	3.09	1.67	6.95	2.78	1.67	2.50	6.12
	Cor	0.51	1.12	3.88	1.84	2.45	4.18	4.38	1.84	1.33	1.02
	Hy En	0.40	0.70	0.30	1.00	0.90	0.50	0.50	-	0.70	0.30
	Hy Fs	-	0.26	-	0.66	-	0.26	-	-	0.26	0.26
	Mt	2.78	2.32	1.62	3.25	2.55	2.55	1.62	2.78	2.78	1.86
	He	-	-	0.16	-	-	-	-	-	-	-
	Ilm	0.76	0.91	0.76	0.91	0.76	0.91	0.91	0.61	0.61	0.61
	Ap	0.34	0.34	0.34	0.34	0.34	0.34	0.34	0.34	0.34	0.34
	Calc	2.20	0.70	5.20	3.50	2.90	0.60	5.30	4.00	3.00	1.90

oxidation. A slight increase in Fe_2O_3 proportions towards the margins also provides evidence for increasing oxidation. In general, a marked enrichment in K_2O is present among the samples near the ore mineralization. e.g. G-125.

The specimens TK-150 and TK-151 represent relatively less altered rocks of the central body. A comparison between these and the other specimens analysed gives an indication of the changes during the general alteration. The alteration not only was effected by the simple addition of CO_2, H_2O, O, MnO, CaO and in most places K_2O but Na_2O, Al_2O_3, MgO appear to have migrated outwards from the igneous rock.

The Niggli values were calculated of the ten chemical analyses of the igneous rock samples for the eight parameters, the results of table 18 are plotted on fig.36.

The chemical formula of the quartz syenite porphyry samples analysed were obtained on the basis of cations in cell standard of Barth. Table 19 illustrates the rock formula for each specimen.

The composition of sanidine phenocrysts

Two sanidine crystals of samples TK-150 and TK-151 taken from the central part of the quartz syenite porphyry were separated for chemical analysis. The analysis was carried out by XRF using the international and the secondary standards,

Table 17 Comparison of analyses of quartz syenites

Sample No.	1	2	3	4	5	6	
SiO_2	62.74	62.24	60.64	63.54	62.80	Q	11.58
Al_2O_3	17.42	15.82	15.37	15.30	16.80	Or	38.36
Fe_2O_3	1.72	1.94	1.36	1.34	0.97	Ab	35.11
FeO	1.23	4.69	5.49	4.44	3.80	An	3.89
MgO	0.24	0.07	0.42	0.72	0.19	Cor	2.14
CaO	2.67	2.65	3.05	2.34	2.50	En	0.80
Na_2O	4.16	4.80	5.15	5.12	5.80	Hy Fs	0.13
K_2O	6.51	6.26	5.35	5.12	5.80	Mt	2.55
ΣH_2O	1.37	0.63	0.83	0.88	0.73	He	-
TiO_2	0.41	0.87	0.99	0.52	0.43	Ilm	0.76
P_2O_5	0.05	0.14	0.20	0.24	0.09	Ap	0.34
MnO	0.14	0.24	0.15	-	0.10	Calc	3.10
CO_2	1.35	-	0.36	0.15	-		

1. Average of 10 Quartz Syenite Porphyry specimens from the Keban area.
2. Quartz Syenite. North Conway Quadrangle, New Hants, U.S.A. (Chapman & Williams 1935)
3. Quartz Syenite, from Assorutit Intrusion, Tugtutog, Greenland. (Watt, 1966)
4. Syenite, Zaranda, Nigeria (Jacobson et al., 1958).
5. Moderately leucocratic Quartz Syenite, Kungnat Fjeld, Greenland. (Upton, 1960)
6. Average norm of 10 Quartz Syenite Porphyry analyses.

Quartz Syenite Porphyry

Table 18 - Niggli values

Sample No.	al	fm	c	alk	Si	mg	k	p
TK-151	48	11	9	31	284	0.10	0.52	0.03
262	44	9	16	32	263	0.13	0.85	0.03
274	40	14	12	34	263	0.19	0.49	0.02
G-125	41	13	11	35	271	0.18	0.43	0.03
TK-141	44	9	11	36	258	0.13	0.54	0.03
TK-82	42	12	15	32	260	0.10	0.38	0.03
TK-150	44	12	10	34	261	0.20	0.36	0.03
TK-113	44	8	15	33	255	0.13	0.80	0.02
263	40	16	11	33	250	0.24	0.43	0.03
291	42	13	10	35	266	0.23	0.57	0.06

Iron and magnesium were not detected; using the standard wet chemical methods neither combined water nor FeO could be detected (Table 20). Among other ions in solid solution TiO_2 amounts to 0.38%. The specimen TK-150 includes P_2O_5 and S in small amounts 0.05% and 0.02% respectively. The values calculated for the Z group (Si, Al, Ti) and X group (K, Na, Ca) on the basis of 32 oxygens are fairly close to the theoretical general formula $(K, Na, Ca)_4(Si,Al)_{17}O_{32}$. The general tendency is for a slight excess in the Z group, with a value of 16.17 and 16.10, while the X group shows a slight deficiency in comparison with the theoretical value of 4. This may be due to slight alteration of crystals, as proved by higher Al content than those reported by Spencer (1937), Hamilton et al (1956), Kozu et al. (1921) and Zsivny (1923). They give the following Z group values against the Al content analysed; 16.02, 18.92%; 16.00, 19.50%; 16.00, 18.63%; 15.97, 18.89%.

The analysed sanidine crystals may be inferred as "potash-anorthoclase" on the basis of chemistry. (Kimizuka, 1932).

Geochemistry of the quartz syenite porphyry:

The alkali elements

18 quartz-syenite porphyry samples including 10 samples for major element analysis have been analysed by the standard XRF method for their trace element content (Table 21). Lithium was not determinated by the XRF procedure for analysis; nevertheless it is worth mentioning the Li-bearing mica occurs as a skarn mineral in close association with magnetite at the Zereyandere section.

Quartz Syenite Porphyry:

Table 19 Rock compositions in terms of cations in the Standard Cell (Barth, 1952)

Sample No.													
TK-151	K 3.72	Na 3.42	Ca 2.11	Mg 0.31	Fe^{+3} 0.67	Fe^{+2} 1.17	Mn 0.07	Al 11.20	Ti 0.38	Si 65.71	O 160.00	CO_2 0.38	H_2O 4.10
262	K 6.50	Na 1.18	Ca 3.74	Mg 0.30	Fe^{+3} 0.50	Fe^{+2} 0.80	Mn 0.12	Al 10.26	Ti 0.37	Si 63.42	O 160.00	CO_2 2.25	H_2O 1.18
274	K 4.18	Na 4.06	Ca 2.97	Mg 0.49	Fe^{+3} 0.73	Fe^{+2} 1.16	Mn 0.24	Al 9.70	Ti 0.24	Si 63.62	O 160.00	CO_2 2.43	H_2O 5.70
G-125	K 3.68	Na 4.80	Ca 2.58	Mg 0.43	Fe^{+3} 0.75	Fe^{+2} 1.11	Mn 0.12	Al 9.28	Ti 0.24	Si 65.08	O 160.00	CO_2 1.85	H_2O 2.70
TK-141	K 4.96	Na 4.16	Ca 2.72	Mg 0.19	Fe^{+3} 0.50	Fe^{+2} 0.87	Mn 0.12	Al 11.10	Ti 0.25	Si 64.77	O 160.00	CO_2 1.18	H_2O 3.60
TK-82	K 2.94	Na 4.70	Ca 3.54	Mg 0.24	Fe^{+3} 0.71	Fe^{+2} 1.00	Mn 0.12	Al 10.02	Ti 0.29	Si 62.41	O 160.00	CO_2 1.29	H_2O 3.66
TK-150	K 3.08	Na 5.54	Ca 2.49	Mg 0.43	Fe^{+3} 0.62	Fe^{+2} 1.11	Mn 0.12	Al 11.11	Ti 0.37	Si 65.28	O 160.00	CO_2 0.44	H_2O 3.70
TK-113	K 6.42	Na 1.66	Ca 3.76	Mg 0.19	Fe^{+3} 0.50	Fe^{+2} 0.74	Mn 0.19	Al 10.80	Ti 0.31	Si 63.16	O 160.00	CO_2 3.21	H_2O 1.80
263	K 3.54	Na 4.30	Ca 2.83	Mg 0.61	Fe^{+3} 0.86	Fe^{+2} 1.54	Mn 0.19	Al 10.00	Ti 0.37	Si 62.50	O 160.00	CO_2 2.17	H_2O 8.26
291	K 3.54	Na 4.76	Ca 2.32	Mg 0.55	Fe^{+3} 0.80	Fe^{+2} 0.99	Mn 0.13	Al 10.13	Ti 0.30	Si 63.61	O 160.00	CO_2 1.77	H_2O 8.16

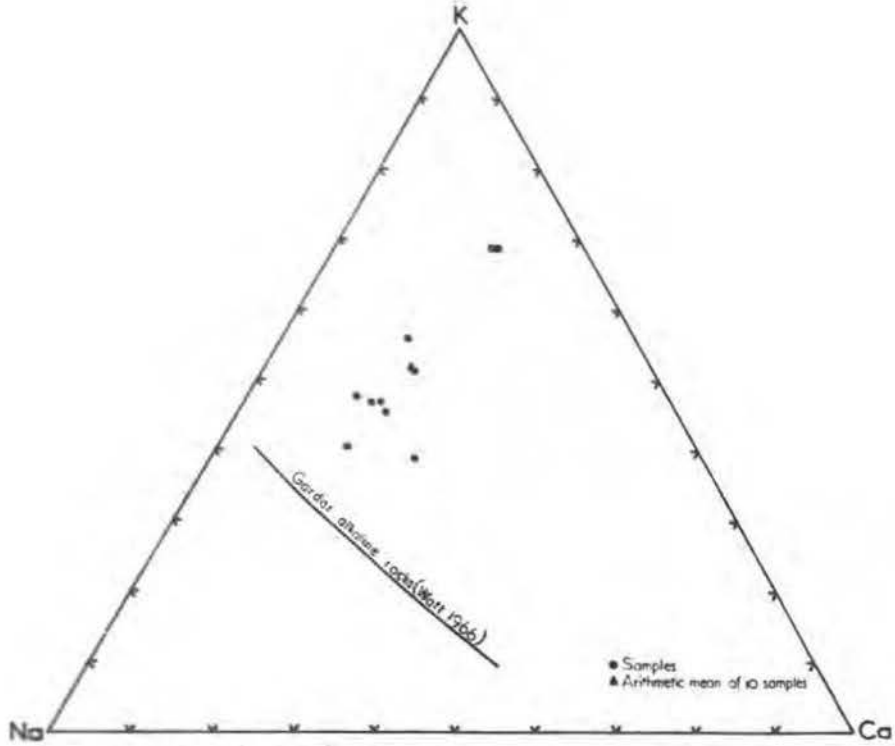

Fig 34 Na - K - Ca Variation in the Quartz Syenite Porphyry

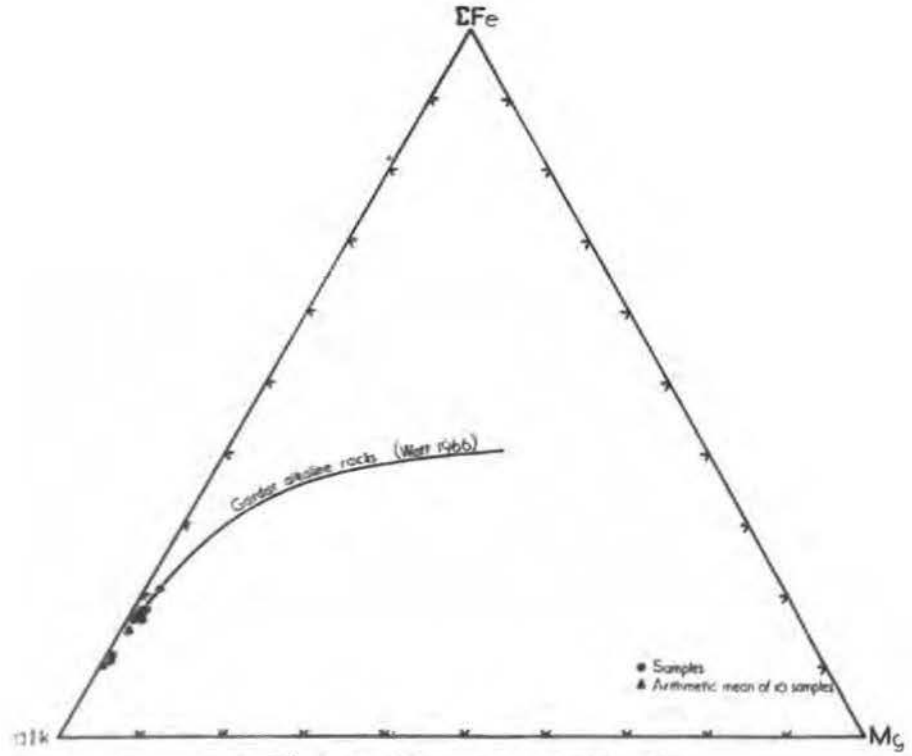

Fig 35 alk - ΣFe - Mg Variation in the Quartz Syenite Porphyry

Sodium and potassium: The Na_2O/K_2O ratio varying within a wide range, with a few exceptions, the general tendency is that the ratio exerts a decrease towards the margins, in other terms $Na_2O \times 100/Na_2O + K_2O$ ratio varies within the limit of 14 and 55. The results are tabulated in table 22.

The close association of potassium and rubidium in igneous rocks have been widely recognised and proved that anomalously high K/Rb ratios are common in highly differentiated rocks. By using the international standards G-1 and W-1, eighteen specimens were analysed for their K and Rb content. The standards gave 220 and 22 ppm rubidium respectively which are in good agreement with the recommended value for Rb in the former between 215 and 240 ppm, and 25 to 30 ppm in the latter (Taylor, cf. 1956). The results were plotted on a diagram based on Ahren's (1954) original diagram after Taylor (opt.cita). Fig.37 shows the close association of potassium and rubidium, except that of one sample and those beyond the limits of scatter, the majority of results fall within the limits of scatter. Those off-scatter samples display relative enrichment in both K and Rb content of the igneous rock. The Rb in the rock attains as much as 457 ppm, and the ratio of K to Rb remains from 180 to 405, giving an average of 268 (Table 22). It is found that the rocks low in Na e.g. TK-113 and 262 tend to have the highest

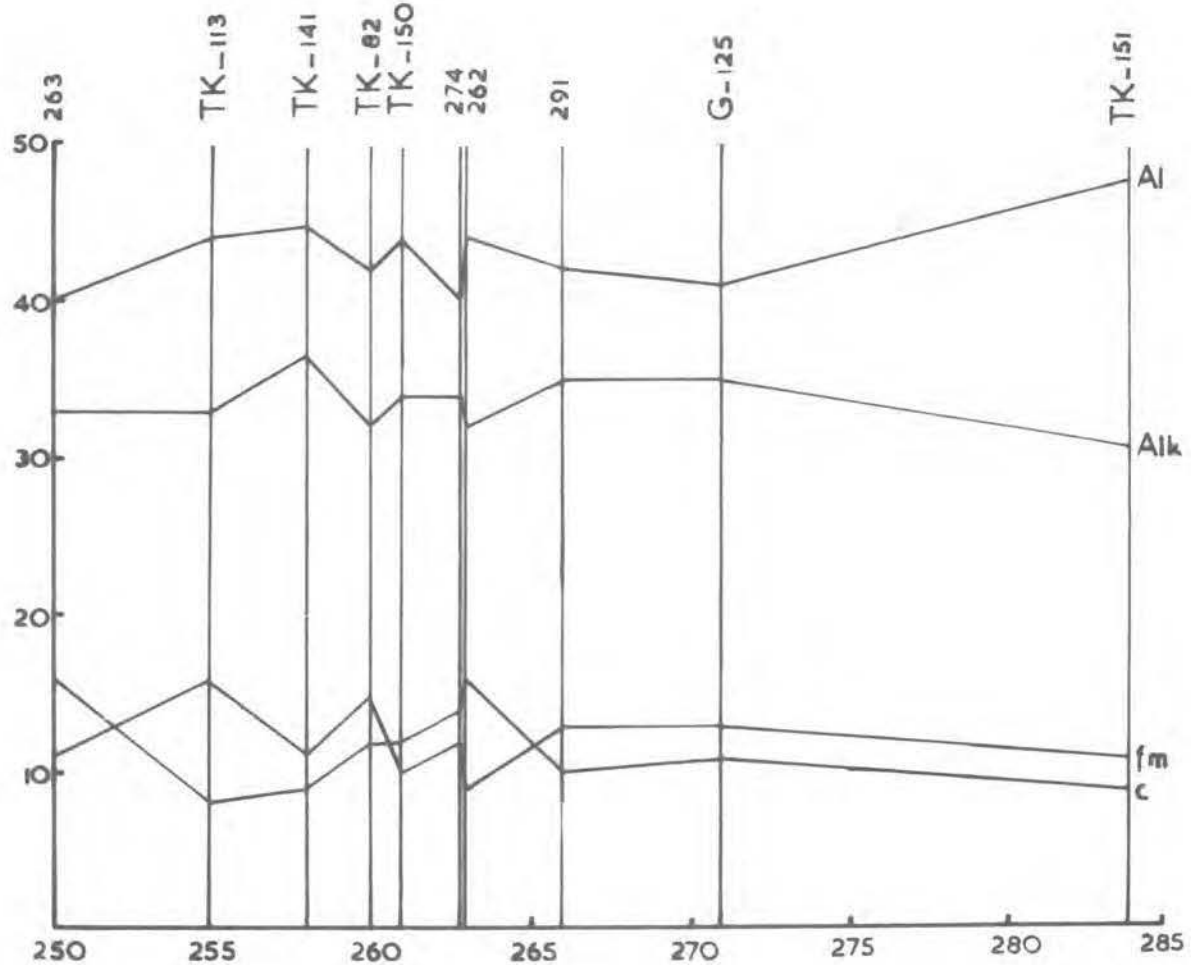

Fig. 36 Variation diagram of the Niggli values for the Keban quartz syenite porphyry

Rb values. Table 23 gives comparison of the arithmetical mean of 42 determinations of Ba, Sr, Zr and Rb in the North American granites, the mean of end product Mourne granites and the mean of 18 Keban quartz syenite porphyries.

Table 23

Sample Source	Ba	Sr	Zr	Rb		Reference Source
Mourne Granites	230	45	310	385	ppm	Taylor cf. 1956 Emeleus 1956
N. American Granites	1300	180	170	-	ppm	Taylor cf. 1956
Keban Q-syenites	2801	848	353	237	ppm	Present study

From the table relatively high values are in good agreement in order of differentiation and figures indicate that comparatively less differentiated magma was a source in forming the quartz-syenite porphyry in the Keban area.

The alkaline earth elements:

Calcium: Although the calcium content of the rock varies within limits of just over 1% there is a rough increase towards the margins e.g. the 82 samples representing the southernmost quartz-syenite porphyry has 2.43% Ca, while the central body contains as much as 1.54% Ca. However, this crude relation, it is believed, is not related with the differentiation, it may be a resultant of mutual reaction of

the rock together with the calcic host rock in the border zones.

Strontium and Barium: These two elements are found in a close relation to each other and their behaviour has long been significant from the point of differentiation. Sr shows a remarkable enrichment throughout the igneous rock, its content remains in a wide range from 497 ppm up to 1890 ppm giving an arithmetic average of 848 ppm which is about three times the average for syenites reported by Butler (1962). The liberated Sr from marble next to or through which the quartz-syenite porphyry passed in any depth may be in part responsible for the enrichment in addition to the relatively high differentiation. The plot of Ca against Sr has a positive slope as shown in fig.38. But the proportion of Sr against Ca is significantly higher than the figures given by Heier (1960).

The crustal abundance of Ba is about 670 ppm (Rankama and Sahama, 1950), and is concentrated in K minerals in which it replaces K. The Keban rock is characterised by its high Ba content giving an arithmetic mean of 2801 ppm. By contrast Turekian et al. (1961) reports an average of 1600 ppm for a similar type of rock. Ba/K relations give a positive slope, since the plots are found within a scatter zone except two plots

Table 20 Chemical analyses of sanidine crystals

Sample No.		TK-150	TK-151
Wt%	SiO_2	65.53	65.97
	Al_2O_3	19.71	20.15
	Fe_2O_3	n.d.	n.d.
	FeO	n.d.	n.d.
	MgO	n.d.	n.d.
	CaO	0.59	0.90
	Na_2O	3.21	2.96
	K_2O	10.64	9.58
	H_2O^+	n.d.	n.d.
	H_2O^-	n.d.	n.d.
	TiO_2	0.34	0.38
	P_2O_5	0.05	n.d.
	S	0.02	n.d.
	MnO	n.d.	n.d.
Number of ions on the basis of 32 (O)			
	Si	11.862	11.860
	Al_{+3}	4.193	4.269
	Fe_{+3}	-	-
	Ti	0.043	0.043
	Mg_{+2}	-	-
	Fe_{+2}	-	-
	Na	1.130	1.035
	Ca	0.109	0.172
	K	2.455	2.199
	Z	16.10	16.17
	X	3.69	3.41
Formula			
		$K_{2.45}Na_{1.13}Al_{4.19}Si_{11.86}O_{32}$	$K_{2.2}Na_{1.03}Al_{4.27}Si_{11.86}O_{32}$
Molecular percent			
	Or	66.5	64.6
	Ab	30.6	30.4
	An	2.9	5.0

having relatively high barium content. (Fig.39).

The other elements:

Aluminium: The Keban igneous rock is defined by high Al content varying between 9.72 and 8.62%, hence they are mainly acceptable as uniform in Al content. The average Al content is 9.22%, which is more than those of quartz-syenite tabulated in table 17, found elsewhere.

A close relation between Al and Ga in igneous rocks has been accepted since the early days of Goldschmidth and co-workers working in the 1930s. In igneous rocks the Ga/Al ratio increases in the later differentiates (Goldschmidth and Peters, 1931). As a completion Shaw (1957), points out that since Ga^{+3} (o.62Å) is of slightly larger ionic radius than Al^{+3} (o.51A°), Goldschmidth's camouflage principal would suggest that the Ga content of aluminous minerals might increase during the differentiation, and moreover that an increase in the Ga^{+3}/Fe^{+3} ratio also was to be expected.

Gallium: The crustal abundance of gallium is 19 ppm (Shaw, 1952). Ga can proxy for Al in silicates or for Fe^{+3} in magnetite, therefore the chief silicates concerned in the quartz-syenite porphyry are feldspars, in which it varies between 9 and 37 ppm. The Ga x 10,000/Al ratio in the igneous rock ranges from 1.23 to 4.28, giving an arithmetic mean of 2.60.

Titanium: Titanium shows a rather uniform content, which has slight change within a small margin. The average value is very near to that in the moderately leucocratic quartz syenite from the Kungnat Fjeld, but is less than those of quartz syenites quoted in table 17. The early stage sphene found in accessory proportions is regarded as the possible Ti source in the rock, along with the biotite and some opaque minerals.

Zirconium: The zirconium content of the igneous rock is less than that of the value found by Turekian in similar rocks. The average zirconium is 353 ppm in the Keban igneous rock in comparison with 500 ppm of Turekian and 550 ppm of Butler. On the other hand the mean is twice the mean of 42 North American granites. It may be that albitization caused this enrichment, since the relatively high content of Zr along with Nb is linked with the albitization (Sheinmann, 1961). In addition to albitization processes which may be in part responsible for Zr, the presence of zircon is an obvious source for the Zr of the Keban rocks.

Lead: As lead is the main contaminant in the area, it is likely that at least five out of the eighteen samples received contamination from the lead. In his investigation of the geochemistry of lead, Wedepohl (1956) found the maximum concentration of Pb in acidic rocks to be 20 ppm while

Table 21 Trace element analyses of the Quartz Syenite Porphyry

	Sample No.	82	TK-150	TK-113	263	291	TK-151	262	274	G-125	TK-141	112	163	171	175	276	303/A	KT	188
	Nb	5	42	40	52	42	30	30	48	41	44	42	37	42	38	10	17	43	39
	Zr	365	330	345	605	350	330	330	355	325	315	335	334	320	350	375	380	325	376
	Ga	31	22	35	30	18	12	20	37	15	18	10	25	22	9	36	24	10	32
	Ni	18	25	20	40	22	43	34	15	26	31	17	22	7	26	11	20	33	21
ppm	Cu	10	5	10	17	5	23	20	19	12	12	20	10	61	8	15	15	10	12
	Zn	54	1057	119	53	65	491	21	12	29	44	406	29	58	50	58	55	38	47
	Pb	76	26	22	36	30	101	11	2	10	31	11	76	410	284	20	75	38	15
	Mn	1240	1318	1550	1473	1163	543	388	775	930	1163	363	355	185	1570	318	440	900	650
	Sr	1005	618	618	593	795	497	1591	689	613	552	593	912	730	552	1675	1890	927	695
	Ba	2600	2400	4060	2400	2200	2130	3200	2460	2320	2680	2320	2230	4280	3030	2760	3660	3170	2865
	Rb	160	155	232	225	165	153	350	298	275	285	105	222	320	457	132	163	355	222

Table 22 Geochemical data for the Quartz Syenite Porphyry

Sample No.	K%	Rb ppm	K/Rb	Na_2O/K_2O	$\frac{Na_2O \times 100}{Na_2O + K_2O}$	FeO/MgO	MnO/FeO	Ga^{10^4}/Al
82	3.88	160	318	1.04	51	7.81	0.13	3.38
TK-150	3.86	155	235	1.20	55	4.92	0.13	2.25
TK-113	8.13	232	315	0.17	14	7.17	0.23	3.70
263	4.45	225	198	0.88	47	4.55	0.10	3.43
291	4.55	165	273	0.89	47	3.39	0.13	2.00
TK-151	4.66	153	198	0.90	47	6.38	0.05	1.23
262	8.28	350	358	0.18	15	5.39	0.05	2.14
274	5.36	298	223	0.64	39	4.47	0.07	4.28
G-125	4.65	275	182	0.86	46	4.57	0.09	1.74
TK-141	6.23	285	405	0.55	36	8.50	0.15	1.87
112	4.25	105	305	-	-	-	-	-
163	7.00	222	219	-	-	-	-	-
171	7.12	320	350	-	-	-	-	-
175	8.32	457	180	-	-	-	-	-
276	4.72	132	237	-	-	-	-	-
303	4.45	163	276	-	-	-	-	-
KT	8.35	355	249	-	-	-	-	-
188	7.05	222	243	-	-	-	-	-

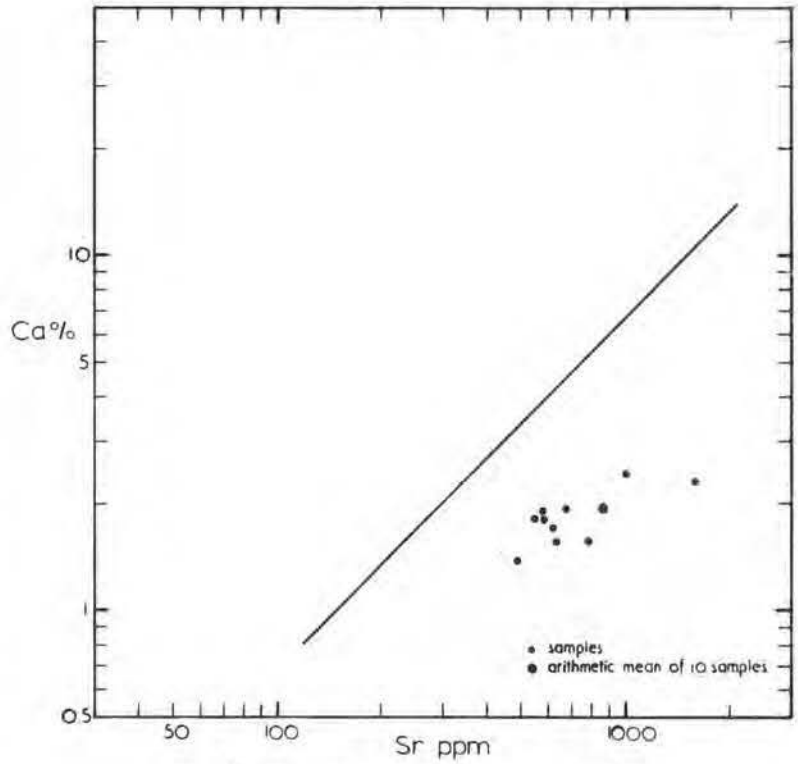

Fig. 38 Ca/Sr ratios in the quartz syenite porphyry

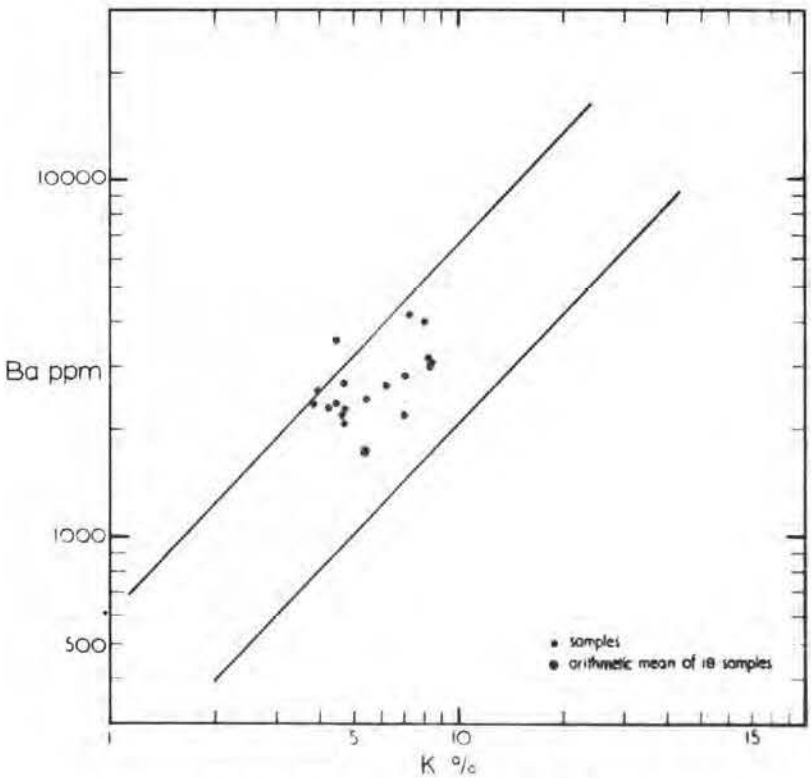

Fig. 39 Ba/K ratios in the quartz syenite porphyry

of FeO/MgO ratio whose mean is 5.13 also gives no clue on the relation. However, this ratio is accepted as a poor indication of increasing differentiation in the intermediate rocks.

Nickel: As a whole the amount of Ni is much more than the Cu content in the rock, and its content shows erratic variations regardless of Fe^{+2} and Mg^{+2}. It has been claimed Ni enters crystal lattices at the expense of Fe^{+2} rather than of Mg^{+2} (Ringwood, 1955). The Ni amount ranges between 7 and 43 ppm in the Keban igneous rock, while its value reaches as much as 100 ppm in the upper lithosphere (Goldschmidt, 1954).

Copper: Although Cu is geochemically mainly chalcophile, it is probable that in some instances, it also enters into the structures of the rock forming silicates (Rankama and Sahama, 1950), and the reported Cu content for intermediate igneous rocks is 38 ppm, compared with the crustal abundance of Cu being about 60 to 70 ppm. As a whole the Cu proportion in the quartz-syenite porphyry ranges from 5 to 23 ppm except for the sample 171 which carries strong evidence of contamination by hydrothermal influence.

Phosphorus: This element shows little variation as being a characteristic for intermediate rocks, and its presence in very small amounts is a resultant of differentiation. Ever-present apatite makes a source for phosphorus. Its reported

crustal abundance stays around 1050 ppm. (Taylor, 1964).

Distribution of Fluorine and Strontium in the marble

In order to establish dispersion pattern of certain elements in a marble next to an ore-shoot exposed in underground workings, a special group of analyses was made. Fluorine and strontium were studied since they show characteristic dispersion patterns in vein aureols. As the ore-shoot emplaced in a marble in the 668 m level was best for this purpose, the marble samples were taken as channel samples on a line heading off the ore-shoot at intervals of 50 cm (fig.11). Thus 21 samples collected were crushed into recommended size of about 20μ by a procedure described in the Appendix. The standard was prepared by the addition method (Ahrens and Taylor, 1961) and then diluted to obtain nine different concentrations of each element. Sr analyses were done on a Philips (PW1540) XRF with an electronic timer.

A slightly modified analytical technique after Ineson (1967) for the fluorine analyses was applied on a Hilger and Watts automatic large spectrograph (E.742) with glass optical system (E.744) by using the samples involving 0.15 gr of $CaCO_3$, 0.025 gr of CuO and 0.225 gr graphite as buffer to 0.2 gr sample. CuO is used to improve the reproducibility and the remaining elements to minimise the effects due to the fluctuation

of matrix. In order to reduce the background in a region where the CaF_2 bandhead occurs, a mixture of Argon 80% and Oxygen 20% through a home-made Stallwood type gas jet assembly at a rate of 5 lt/min was used.

The accuracy of the results only depends on that of standards used, and therefore they should be treated as comparable with them. For the accuracy of the method applied, the results obtained from the different techniques are tabulated in table 24 after Ineson (op.cita).

Table 24

Sample No.	Optical Spec(D)	Neutron Activation(W.S)	Pyro-hydrolsis (W.S.)
L/OE/3	3.70%	5.50%	5.21%
L/HW/4	0.72%	0.70%	0.44%

D - Durham University by Ineson, W.S. - Warren Springs Labs.

The optical spectrograph is much more accurate for certain elements when present in low concentrations. This may be evidenced from the L/HW/4 sample, where the comparatively low fluorine content gives a result which is in good agreement with the result from neutron activation.

Fig.40 illustrates the dispersion pattern of the fluorine. The F and Sr values with their corresponding distance from the ore-shoot are given in table 25. Although there are a few

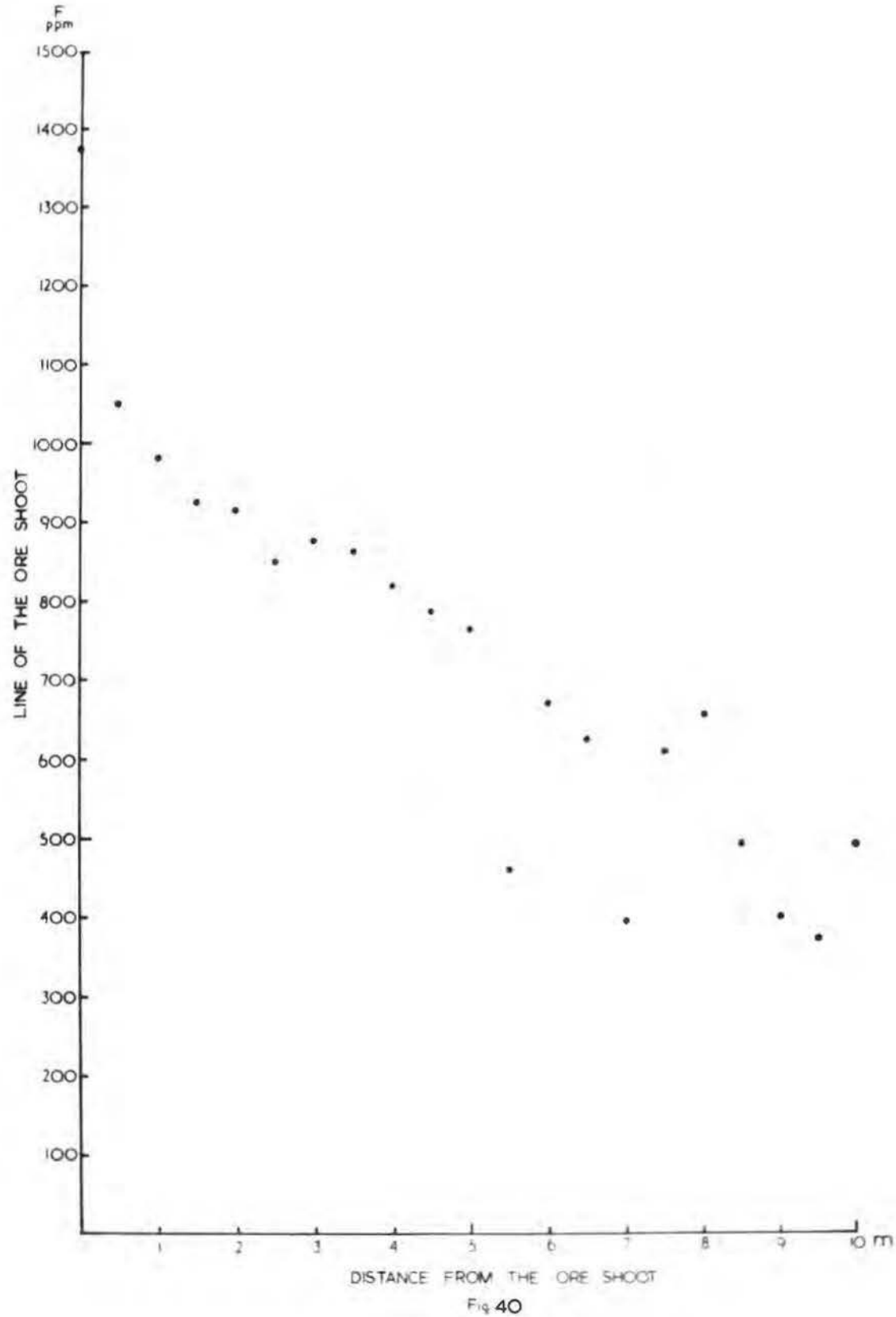
F
ppm
1500
1400
1300
1200
1100
1000
900
800
700
600
500
400
300
200
100
LINE OF THE ORE SHOOT
1
2
3
4
5
6
7
8
9
10 m
DISTANCE FROM THE ORE SHOOT

Fig 40

anomalous values, as a whole the F content displays a steady decrease outward from the ore-shoot. This dispersion pattern reveals the migration of the F brought by ore-forming fluids, and this type of dispersion pattern is referred to the type A of Reitan (1959).

In contrast, Sr exerts depletion in the immediate vicinity of the ore-shoot (fig.41). Excluding a few off range samples, the great majority of samples analysed shows a steady depletion away from the mineralization. Considering the average 205 ppm Sr content for five mineralization-free marbles, it is evidently clear that a depletion caused by ore fluids took place in the areas near the ore-shoots. This is related to the crystallization of the calcite which has liberated Sr from the crystal lattice. In fact Sr in a similar way to F is defined along the fractures, boundaries and cleavage traces of calcite and aragonite in which Sr is much more abundant.

It is believed that liberated Sr concentrated within the igneous rock rather than in the marble beyond the influenced area. The absence of any strontianite dyke at the surface or levels above mineralization areas and the quartz syenite porphyry indicates that they did not form any marked concentration. The abnormal richness of Sr in the igneous rock may be primary

Table 25 Fluorine and Strontium analyses of the Marble

Sample No.	Distance from the ore-shoot m	F ppm	Sr ppm
FS-1	0.00	1373	13
FS-2	0.50	1050	127
FS-3	1.00	982	62
FS-4	1.50	925	120
FS-5	2.00	917	139
FS-6	2.50	850	108
FS-7	3.00	878	127
FS-8	3.50	867	131
FS-9	4.00	818	139
FS-10	4.50	788	122
FS-11	5.00	765	170
FS-12	5.50	460	174
FS-13	6.00	672	181
FS-14	6.50	627	181
FS-15	7.00	395	183
FS-16	7.50	610	202
FS-17	8.00	658	166
FS-18	8.50	485	206
FS-19	9.00	402	214
FS-20	9.50	375	198
FS-21	10.00	483	210

although crustal contamination is likely. This possibility is further supported with the presence of the B type wall-rock dispersion pattern of Reitan (op.cita) which implies a process by which the element suffering depletion moves into veins or areas where it is found in lesser amounts.

From a study of the dispersion patterns of F and Sr there is seen to be an increase in F content together with a depletion in Sr. These may be useful as an indicator to locate ore-shoots or the quartz syenite porphyry which is found in close association with the ore mineralization in the Keban region.

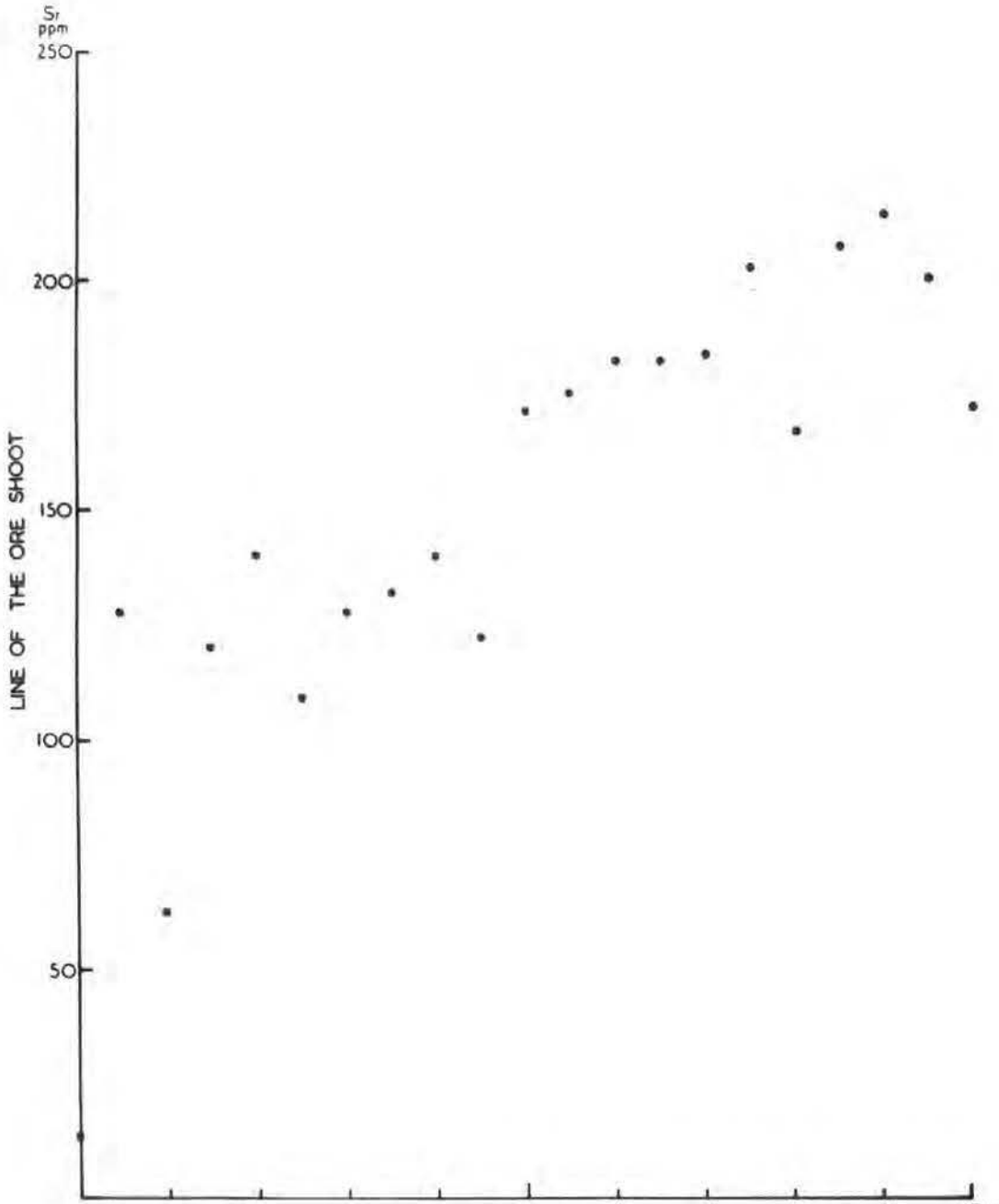
Sr
ppm
250
200
150
100
50
LINE OF THE ORE SHOOT
1
2
3
4
5
6
7
8
9
10 m
DISTANCE FROM THE ORE SHOOT

Fig 41

CHAPTER VI

METALLIC MINERALIZATION

A. General Introduction

In the Keban area there are several mineral occurrences all of which have been formed directly or indirectly from the quartz syenite porphyry intrusion. They are the main sulphide ore deposit, the magnetite-scheelite deposit, the manganese ore bodies and the secondary deposit of vanadinite-descloizite. The main sulphide ore deposit producing galena and sphalerite as well as by-product silver and a little gold from the concentrate is the only deposit of economic importance. The magnetite-scheelite deposit is accepted as being non-economic to run at present. In the following account each of the deposits will be considered individually.

B. The main sulphide deposit

During the field season in 1965 the Agamagara and the Derebaca together with some parts of the Firat deposit were completely inaccessable or blocked. Compilation had to be done from the available information provided by the company where the author was not able to enter and examine the orebodies.

Apart from the near surface mineralization around the Zeytindağ section where old working pits are still recognisable, the lead-zinc mineralization forms three major

E-W trending ore deposits; from S to N they are the Agamagara, the Derebaca and the Firat deposits (see figs 8 and 11 in pocket). What is known about the Agamagara deposit is that it is located between the surface and 800 m level. According to Schumacher (1957) the Agamagara and part of the Derebaca deposit, with a high grade of lead and zinc (25-30% Pb and 15% Zn respectively) were mined down to the 800 m level before 1880. The Derebaca deposit is made of several sizeable ore shoots, some connected some unconnected. In general this deposit has a variable thickness and widens along its strike and with depth down to the 800 m level where it branches into two individual ore shoots with similar trend and dip and runs keeping the same course down to the 775 m level. The more northerly of these two branches pinches out in the 745 m level - the main adit of the Firat deposit. A large NE-SW striking fault cuts through the southern branch whose continuation below the fault has been discovered further along the 745 m level to the S.

The present production is concentrated over the Firat deposit which essentially includes two separate ore bodies; for purposes of explanation these will be referred to as ore body I in the S and ore body II in the N. These are separated by a major NE-SW running fault zone. Each ore body is composed

of several individual ore-shoots which usually show fair continuation along their pinches with depth. By contrast the extension along their strike displays frequent interruption either due to tectonic causes or because they pinch out. Their thickness, size and mode of occurrence are in no way unusual for hydrothermal deposits of this type. In general both ore bodies appear to thin out upwards, as is shown by the lack of any sizeable occurrence on the 745 m level.

The main part of ore body I is emplaced within a gently dipping breccia zone between the footwall marble and the hanging wall phyllite at the level between 745 m and 705 m. The thickness of breccia zone attains 35 m at most. Beneath the zone quartz-syenite porphyry intruded the marble. Because of its emplacement and subsequent uplifting it produced a gently dipping breccia zone which provides suitable channelways for access of the metal bearing fluids, whilst the hanging wall phyllite has low permeability and so acts as a trap for the fluids. The ore body starts just above the 745 m level either in disseminated or fault filling mineralization within marble before the breccia zone is reached. With an increase in thickness the ore body proceeds down to the 712 m level, where it is locally called the "Dilimli" and reaches its maximum thickness of 18 m. Below this the ore body sharply thins, but it can still be followed for as much

as 40 m at the 705 m level. Beyond this depth its course is unknown. Since the ore body becomes thinner and thinner, and contains increasing amounts of iron sulphides it was not expected to continue as a workable deposit at depth. At this point the main breccia zone lies below the level and the author believes that this could well contain an ore body which has not so far been discovered. The contact between the marble and phyllite next to the igneous rock on the 709 m level includes ore mineralization in streaks near X = 9500 , Y =10000 . Ore body I is affected mainly by NW-SE trending gravity faulting.

The ore body II consisting of several more separate ore shoots covers a larger area than ore body I. Its maximum horizontal dimensions are 200 x 90 m and its thickness varies from 0.30 to 20.00 m. As a whole this ore body shows a steady continuation with depth. The northern extremity of the ore body is along a line where all the major ore shoots appear to die out without apparent tectonic cause. Despite its thickness at depth there is an enormous increase in the content of iron sulphide and this could be the reason why no further working has been carried out. Local concentrations of sphalerite within the ore body in the shallower levels between 688 and 705 m have undergone secondary alteration to smithsonite.

The Firat deposit involves several levels in order to

facilitate running and transport, the main adit driven through the barren rocks is at 745 m level which is linked with 705 m level by the F-16 winze. Another link is provided by a winze through ore body I. The second level being 727 m has its connection with 705 m via small winzes. The 705 m level is connected to 668 m level by the F-18 winze which also gives access to the 688 m level.

Controls of Mineralization

The major production at the main sulphide deposit has come from the numerous ore shoots that occur in the marble or along its mechanical contact with the phyllite close to the igneous rock. Therefore the major factor controlling the mineralization in the case of the Derebaca and Firat deposits is the association of these rock types with the addition of shearing and brecciation, which was provided chiefly by the uplifting movements. The general attitude of the ore shoots shows a close similarity to the main structural trend in the area, suggesting that the previous structure had also some influence in locating the mineralization. The ore minerals have replaced the triple rock association in varying degree, but there is a good evidence from underground workings and microscopic study that replacement favours the marble rather than the others. This is particularly evident from the fact that little marble as such

can be found within the deposit. Especially galena rich ones are invariably located within or near the marble. Since the phyllite has relatively low permeability, it provides a screen for trapping the ore carrying fluids, hence mainly high-grade commercial size ore shoots develop inside the marble covered by phyllite. In general the great majority of mechanical contacts between the triple rock association carry signs of mineralization from trace amounts to sizeable ore shoots. The iron sulphide rich ore bodies appear to tend to occur between phyllite and igneous rock. Folding caused by the uprising igneous body made ore location easy. The faults prior to or contemporaneous with the intrusion appear as another factor in locating the ores. The faults relating to ores are mainly divided into two major groups; those trending NW-SE generally dip to the NE with an angle from 25 to nearly vertical, which seem to include more ores than in the others. The faults striking NE-SW dip sharply to the NW and are of minor importance for ore location. Finally foliation planes both of phyllite and marble, and some vugs created by preceding fluids in the marble may act as favourable sites for minor mineralization.

In short, the ~~fracture~~ feature consistently linked with the ore bodies and the associated non-commercial metallic ores in the

main sulphide deposit is the mechanical contacts of marble and phyllite near to igneous rock, source rock, together with folding and faulting in order of importance.

Mineralogy

The main sulphide deposit has a complex mineralogy which is dominated by sphalerite and galena, but numerous other opaque minerals occur at the mine. Among these are pyrite, arsenopyrite, pyrrhotite, marcasite, löllingite, tennantite, chalcopyrite, neodigenite, covellite, wittichenite, bornite and the others. The copper minerals increase in amount with depth but they are not recovered and go into the tailings. The gangue mineral is chiefly calcite, but quartz and fluorite are present in subordinate amounts.

Table 26 gives details of assay values and production for 1964.

Table 26

	Pbs	Zns
Ore tons	19,400	17,768
Concentration	1.626	1.858
Grade %	3.14	3.40

Sphalerite Zns: Sphalerite is the most important sulphide in the mine, more abundant than galena and increasing in amount with depth. Most of the sphalerite in the ore bodies is

massive; free standing sphalerite crystals lining vugs in marble account for only a very small amount of the sphalerite present. The mineral is chiefly found together with galena, pyrite and arsenopyrite. Some sphalerite grains along with galena occur in a matrix of gangue minerals. The ore mineral forms discrete, irregular and anhedral grains up to 2.5 mm in diameter. In general the size lies within a wide range from 0.01 to 2.5 mm at most. Infrequent euhedral grains never exceed 0.3 mm in diameter. In polished section the grey colour sometimes with a brownish tint, internal reflection and isotropism are very distinctive. It takes a moderate polish, and small grains without gangue inclusions appear to be well polished. Sphalerite is interstitial to arsenopyrite, pyrite and marcasite, and fractures in these minerals are partly filled by sphalerite which occasionally replaces pseudomorphically marcasite and pyrite. Marcasite is replaced by sphalerite on a large scale so that a multi-lamellar appearance is produced. Cataclastic, crustified banding, caries and reticulate textures are found as subordinate textures next to a universal polyhedral texture.

In polished specimens two kinds of sphalerite according to their internal reflection are recognisable; the great majority of sphalerite shows distinct internal reflections of

reddish brown while the other variety gives a dull internal reflection of yellowish brown. Particularly sphalerite replacing marcasite falls into the latter group. This variation in properties clearly indicates that the iron concentration in solid solution varies from one type to another. From the microscopic standpoint samples with distinct internal reflection sometimes contain exsolved pyrrhotite while the other appears to be devoid of exsolved pyrrhotite. Internal texture in the sphalerite becomes visible after etching the mineral with a solution of $KMnO_4$ + H_2SO_4 1:1 (Short, 1964) for one minute and reveals common lamellar polysynthetic twinning and less common complex twinning. Sometimes the lamellar twins appear to be bent. A few grains of sphalerite exhibit zoning even visible without etching.

Inclusions of either chalcopyrite or pyrrhotite are characteristic features of the sphalerite even where these minerals do not form externally to the ore mineral. In many instances they are seen together within sphalerite but all sphalerite does not necessarily include chalcopyrite blebs and these show no proportional relation to external chalcopyrite. The specimens containing chalcopyrite and pyrrhotite are mainly located at lower levels and the several examples indicate that the amount of pyrrhotite exceeds

chalcopyrite at depth. Chalcopyrite commonly occurs in inequidimensional, angular to rounded, drop-like blebs varying in size from 50 to 750 micron, or in rods mainly having a random distribution throughout the sphalerite. By contrast some blebs up to 500 micron in diameter may form a triangular lattice texture and sometimes concentric rings of blebs are found (Plate 27). These textures are indicative of an origin by exsolution. Pyrrhotite occurs in rounded, irregular blebs or in subhedral to euhedral grains. Some discrete pyrrhotite blebs appear to be oriented along the crystallographic directions of sphalerite. In a few specimens pyrrhotite is found in oriented lamellae which look to be disconnected. They probably resulted from exsolution due to minor sulphur addition with consequent coalesing (Barton et al. 1966). The average cell size of sphalerite for 5 measurements is 5.418 Å.

Galena PbS: Galena is next to sphalerite in importance but has a far more restricted occurrence, and is mainly associated with sphalerite and pyrite as well as gangue calcite. Galena shows a wide range in size and crystallinity; it has every transition from fine-grained to coarse grained (75 mm) but coarser grains tend to show a greater preference for occurring within calcite in which they are usually found in discrete,

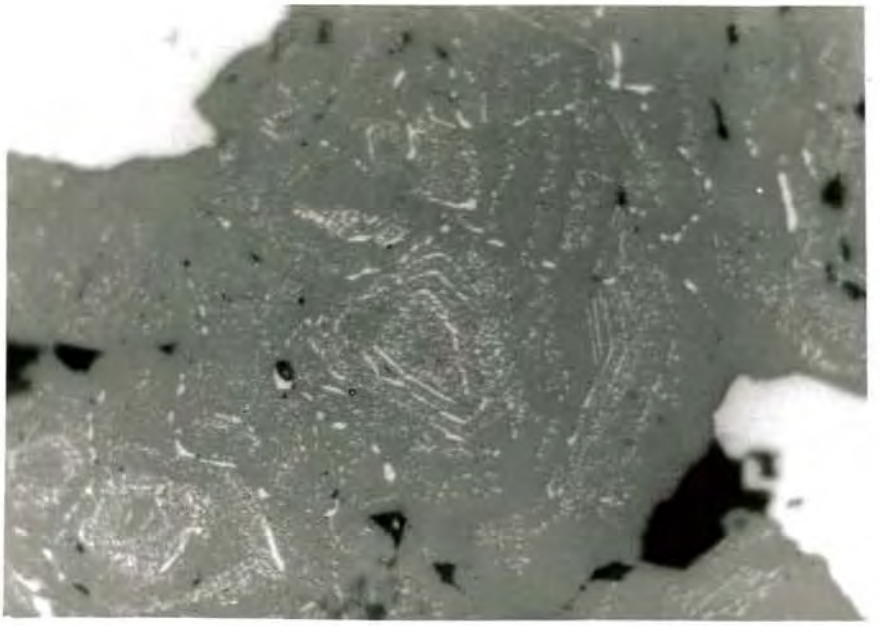

Plate 27 Concentric and linear alignment of chalcopyrite blebs in sphalerite. Reflected light, x200.

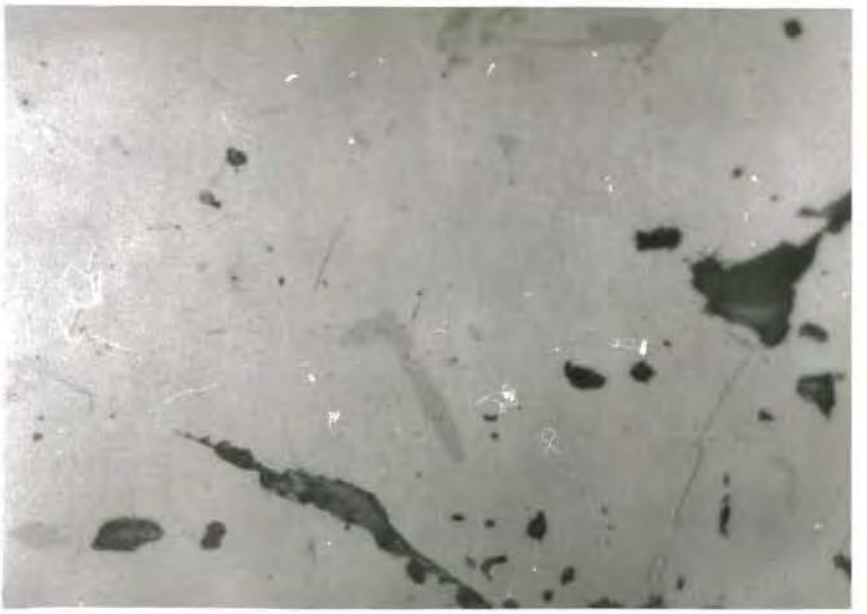

Plate 28 Directional alignment of polybasite inclusions in galena. Reflected light, x200.

euhedral crystals. However, the great majority of grains belong to the anhedral fine-grained group. Galena involves several forms; of them massive, discrete crystals and vein-like patterns are most abundant. The vein-like galena always fills fractures particularly pyrite and arsenopyrite grains. A limited number of specimens show galena, sphalerite and pyrite forming a crustification along a foliation plane within marble. In this crustification galena mixed with calcite occupies the central position. Vug filling galena is found in the marble, producing well-formed euhedral crystals up to a maximum of 1 cm in diameter, which are sometimes coated with calcite. The presence of galena alone in such a vug may suggest that it was formed by solutions depleted of other sulphide forming elements. Galena chiefly replaces pyrite, arsenopyrite, sphalerite and chalcopyrite. Beside the gangue inclusions, inclusions of pyrite and arsenopyrite in galena tend to be euhedral in galena, but chalcopyrite, sphalerite and the others form irregular clots or patches. When associated with pyrite in fault fillings, galena does not show the cataclastic texture of the brittle pyrite, but has undergone plastic deformation and by remobilization may cement the pyrite fragments. Distinct cleavage traces and accompanying triangular pits are found to be bent and broken in extreme cases.

The average cell-size of galena for 4 measurements is 5.935 A°.

The Keban mine has long been known as a silver producer. The silver is present both in lead and zinc concentrates in various proportions. The present investigation shows that the silver content of the galena arises in three different ways. Firstly, an electron microprobe scan of homogeneous galena shows a small amount of silver regularly distributed throughout the grains. Thus the galena contains some silver in solid solution. Secondly, galena sometimes contains small blebs or laths up to about 10 microns in size along the (111) planes of a mineral believed to be polybasite $8(Ag,Cu)_2S.(Sb,As)_2S_3$ (Plate 28). The mineral is grey with a greenish tint, slightly pleochroic and distinctly anistropic with greyish polarization colours. The apparent reflectivity is somewhat less than that of galena and the hardness about the same as galena. Qualitative examination with the microprobe showed the presence of Ag, Cu, Sb and a trace of As. Finally tennantite, $5\ Cu_2.2(Cu,Fe)S.2As_2S_3$ is commonly found as inclusions in galena and sometimes appears to be replacing it. Microprobe examinations of several of these inclusions failed to detect any silver. However, tennantite also occurs outside the galena, and this did show the presence of silver by microprobe examination. Although this external

tennantile is often separate from galena, it may also grow on and partly replace galena. Thus, due to incomplete separation during concentration, it may contribute to the silver content. It is interesting that these microprobe results suggest two separate types of tennantite, although no optical difference between the two was noticed.

In sphalerite, silver-bearing tennantile inclusions were the only source of silver found by microprobe examination.

Pyrite FeS_2: Pyrite is an ever-present iron sulphide and its abundance becomes much more with depth e.g. the northern part of ore body II turns into an all-pyrite ore shoot at the 668 m level. The mineral is found in a close association with the other iron sulphides as well as both galena and sphalerite. Pyrite found in the gangue however is usually without any other sulphide mineral. The crystal form shows variations from euhedral to anhedral with a grain size between 0.05 mm and 5 mm. Despite its originally euhedral nature, most pyrite crystals are classified as being anhedral due to post mineralization events. In shattered zones the pyrite has broken into irregular fragments as well as into well developed rectangular fragments displaying a good 100 cleavage. Therefore there is every transition from pyrite grains with slightly fractured outlines to mylonitic pyrite.

It is usually in massive concentrations, discrete grains or more commonly in association with one or more other sulphide minerals.

Two kinds of pyrite on the basis of mode of occurrence can be recognised in addition to normal crystalline pyrite; a few specimens include rounded balls up to 2.5 mm diameter consisting of intergrowths of small anhedral pyrite grains. These balls with a minimum size of 0.1 mm are embedded in a matrix containing the other sulphides. Several of these pyrite assemblages were checked semi-quantitatively for their Co, Ni and Cu trace element content by microanalysis in comparison with the normal pyrite (Table 27).

Table 27

Mineral	Co	Ni	Cu	ppm
Ball pyrite	400-450	50-100	10-50	
Normal pyrite	300-350	50-100	10-50	

According to Bjørlykke (1945), and Bjørlykke et al. (1950) the higher Co content of the ball pyrite probably indicates that it is of earlier and higher temperature formation than the normal pyrite. Thus it is possible that the balls are fragments of early formed pyrite, broken off and carried in suspension away from their place of origin, rounded during transportation, and later deposited where they are now found, to be cemented

by later mineralization. This mechanism would require that the transporting fluid should have a high velocity to be able to carry pyrite fragments of this size. Such high velocities have not normally been envisaged for ore forming fluids.

As an alternative hypothesis, these balls might be produced by mechanical abrasion during movement along a fault plane after early mineralization, again followed by a second phase of mineralization. However, other evidence seen in the polished specimens suggests that such movement tends rather to produce angular fragments.

Pyrite occasionally shows abundant inclusions of gangue minerals, or of chalcopyrite and other copper sulphides, even in cases where the copper minerals are not found in the surrounding ore. Coarse grained pyrite from the lower levels locally contains appreciable amounts of ilmenite in rounded or elongate grains. The ilmenite is identified from its colour estimated reflectivity and strong anisotrophy (Plate 29). Pyrite grains in thin plates within galena may have resulted from the movement of the soft mineral, because these plates are arranged en echelon. Replacement of pyrite by the other ore minerals is a common feature. No twinning or zoning was seen during the microscopic examination. Crustified banding, caries,

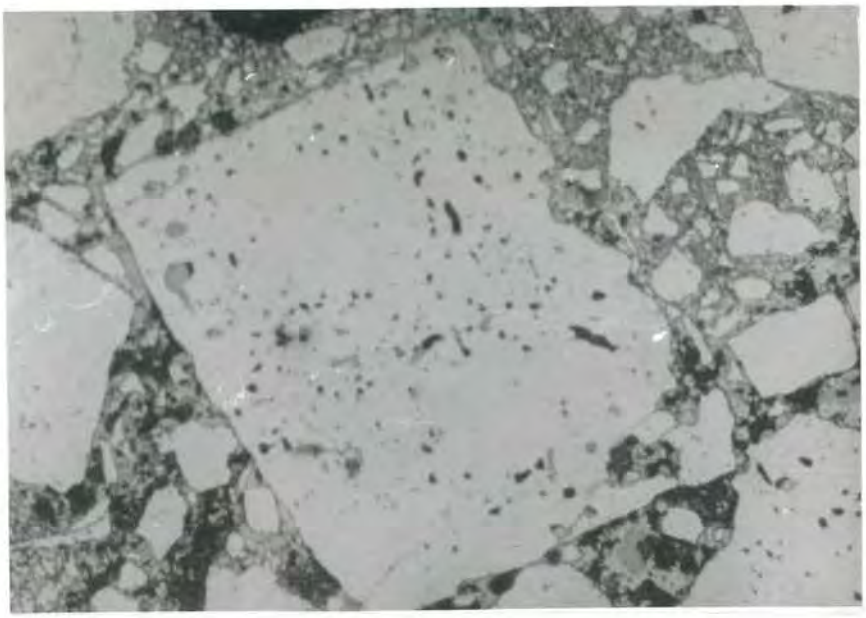

Plate 29 Pyrite grains consisting of numerous ilmenite inclusions of different size and form. Reflected light, x200.

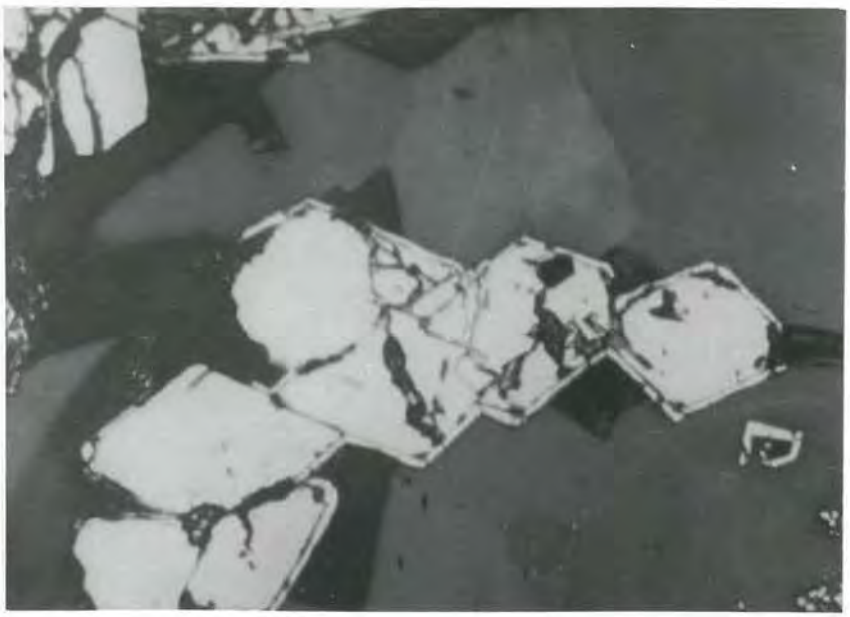

Plate 30 Marcasite coating well-developed, rhomb-shaped arsenopyrite crystals. Reflected light, x80.

cataclastic and polyhedral textures are among those found in the specimens examined. The average cell-size of pyrite for 3 measurements is 5.417 A° .

Arsenopyrite FeAs: Arsenopyrite is next to pyrite in importance among the iron sulphides, and is always found in close association with pyrite and leollingite. It occasionally makes local concentration which has a general tendency of increasing with depth. Arsenopyrite mainly occurs in aggregates, comprising several tens of euhedral and subhedral grains of fine grain size. When it makes association with the other sulphides, arsenopyrite tends to be in separate grains. Grains enclosed in gangue are usually euhedral in shape. The characteristic rhomb-shaped cross-sections and prismatic crystals are universally common. In general arsenopyrite appears to be much more euhedral in comparison with pyrite. Grain size shows frequent variation from place to place within a range lying between 0.01 and 3 mm in long dimension. Lamellar arsenopyrite crystals are not uncommon, and they seem to lie in random orientation. Some grains occurring in calcite show exceptional growth with a grain size attaining up to 1 mm in long dimension. In addition to these, subhedral arsenopyrite crystals are also present in subordinate amounts. Locally some arsenopyrite grains appear to be zoned; this is particularly

pronounced in rhomb-shaped crystals. The thickness of zones varies greatly from grain to grain, the zone boundaries are sharp but no relation to the crystal size has been established. The zoning probably indicates fluctuation in arsenic supply as the mineral formed. Another feature with respect to arsenic is that locally arsenopyrite pseudomorphically replaced by marcasite, suggestive of simple arsenic exchange. Moreover many arsenopyrite grains by preference rhomb-shaped cross sections are coated by marcasite in regular films as much as 0.01 mm thick in accordance with the crystal boundaries. The contact between arsenopyrite and marcasite films is apparently sharp which may suggest no mutual reaction took place (Plate 30). A space between closely spaced arsenopyrite crystals is filled by marcasite in this way giving rise to a poikitic appearance. Simple twinning is very common with an occasional appearance of contact twins. Arsenopyrite fills the space between pyrite and less commonly sphalerite. In return some sphalerite occupy part fractures in arsenopyrite. Replacement of arsenopyrite by galena, sphalerite, leollingite and the copper bearing minerals has a widespread distribution. Some individual crystals are preferentially replaced by fringes of galena causing the crystals to be ragged-edged. The majority of arsenopyrite grains are free from any inclusion, particularly

those occurring in the galena, but sometimes various sulphides, particularly chalcopyrite, are locally found as inclusions in arsenopyrite, where multi-phase mineralization is present. Arsenopyrite includes small amounts of gold, as is proved by electronprobe microanalysis which shows rather evenly distributed traces of gold together with tiny micron size patches of much greater gold concentration, in the X-ray image. Four arsenopyrite samples taken from the different levels were run for their d_{131} values to estimate their sulphur and arsenic content using the method described by Morimoto et al. (1961). The results are tabulated in table 28 (Figs 42, 43).

Table 28

Sample No.	Level m	d_{131} A	S Atomic %	As Atomic %	Fe Atomic %
154	705	1.6332	33.70	33.50	32.80
146	705	1.6332	33.70	33.50	32.80
122	732	1.6334	33.50	33.70	32.80
106	745	1.6330	34.00	33.40	32.60

From the table arsenic and sulphur content show negligible variation with respect to depth.

Arsenopyrite is as cataclastic as pyrite in places of shearing thus producing irregulal fragments of differing size. The fragments without matching walls suggest continued pressure with the additional mobilization of the soft minerals.

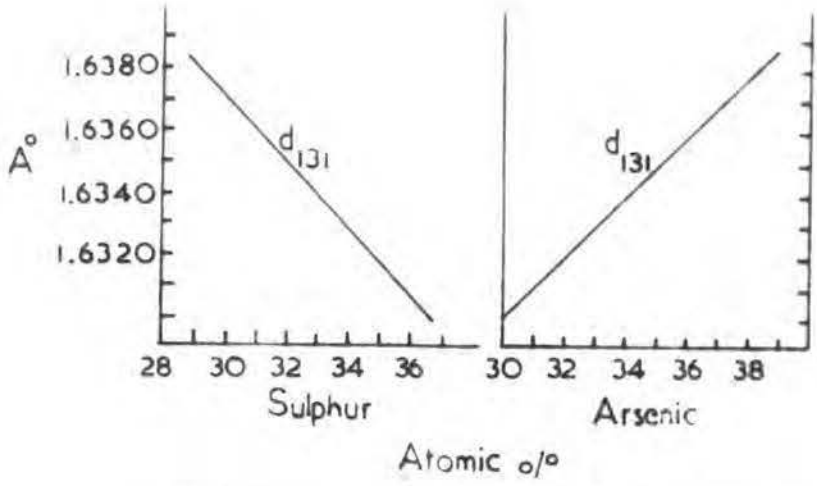

Fig.42 d_{131} reflection against S & As in arsenopyrite

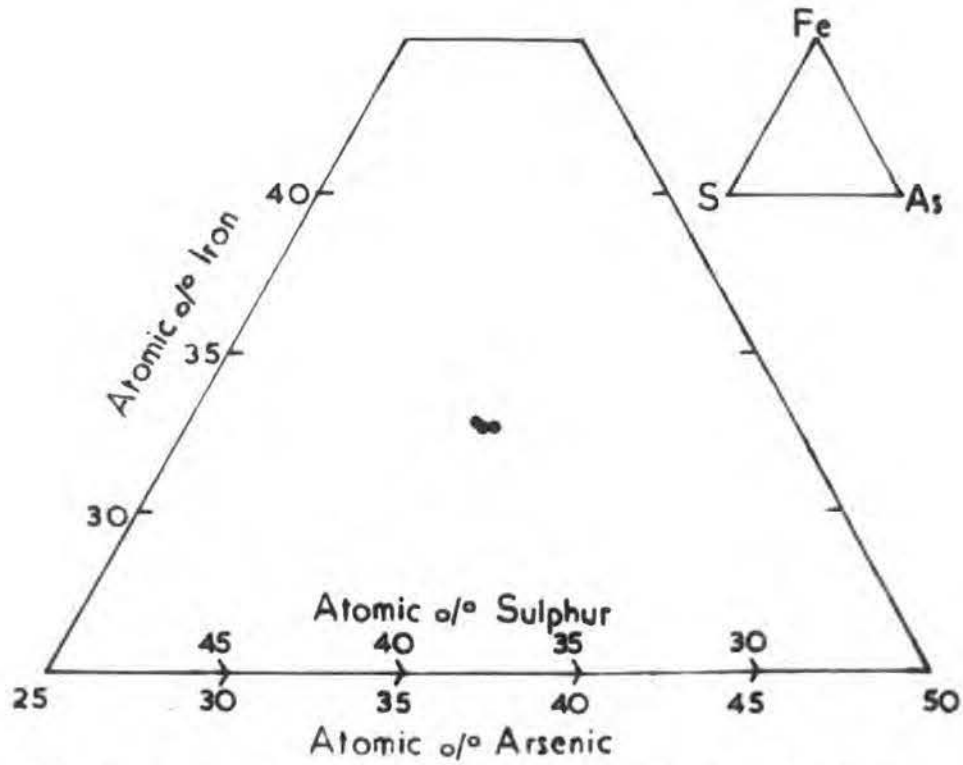

Fig.43 Compositional variation of arsenopyrite from the main sulphide ore deposit.

(After Morimoto, 1961)

Marcasite FeS_2: Marcasite is mainly associated with pyrite, arsenopyrite and sphalerite in order of importance, and in the gangue as minute discrete grains. Both euhedral and anhedral grains are distributed evenly. Marcasite crystals take a moderate polish and show distinct reflection pleochroism. The polarization colours of emerald green and purple are quite distinctive. Grain size is always restricted into the fine-grained group. In many examples crystalline marcasite tends to coalesce so that very fine-grained aggregates produce circular zones with a distinct boundary throughout the matrix. Similar grains with euhedral outlines inward fill the fractures within sphalerite thus producing crustification. Euhedral marcasite being first stage in generation is mainly included in sphalerite which in return is interstitial to lamellar marcasite in certain localities (Plate 31). Coarse and lamellar twinning occur in marcasite crystals. Cataclastic, crustified banding, polyhedral and colloform texture develop in marcasite. Several polished specimens contain colloform marcasite alternating with blue covellite and neodigenite, most likely derivatives from chalcopyrite. This may suggest that the supergene process could create this kind of marcasite since the marcasite continues to form after the supergene production of both minerals. Beside the primary marcasite, very small

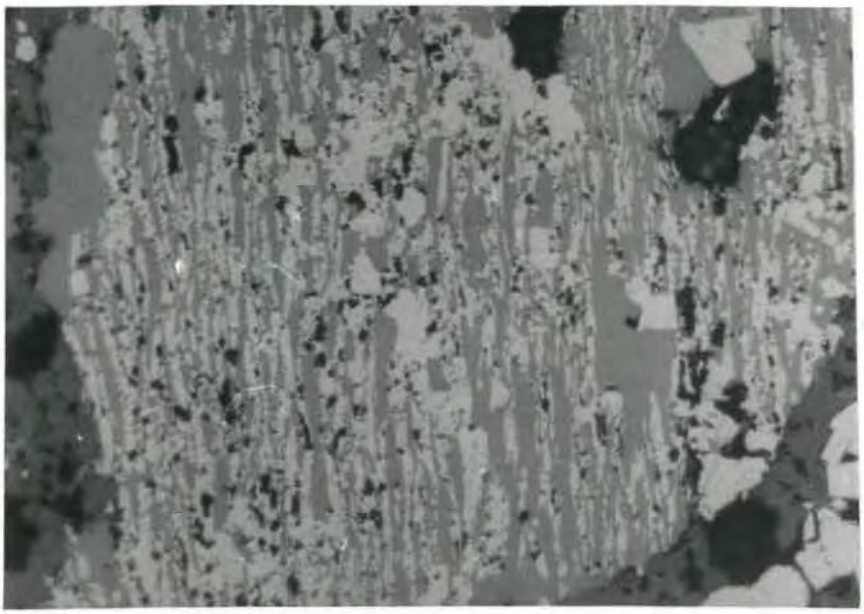

Plate 31 Lamellar marcasite interstitial to sphalerite.
Reflected light, x200.

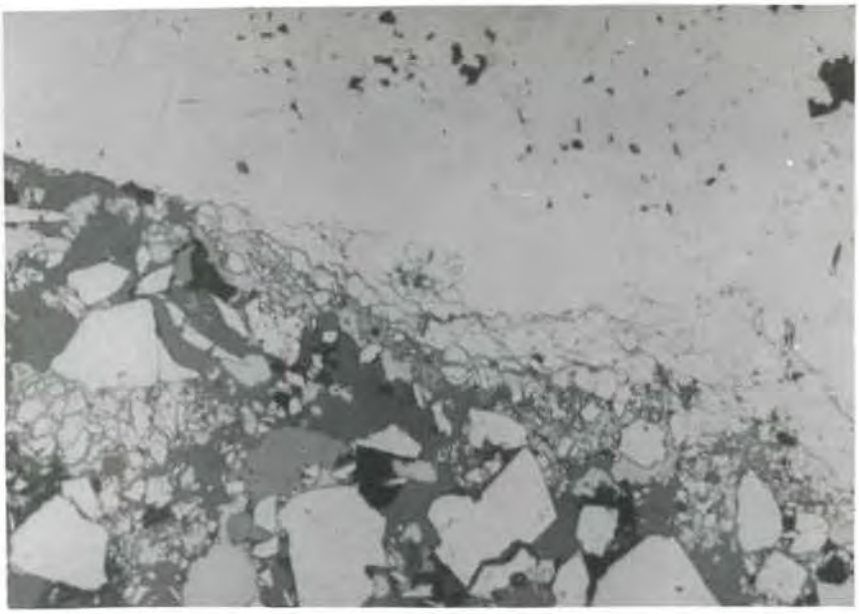

Plate 32 Loellingite replacing pyrite and arsenopyrite.
Reflected light, x200.

amount of secondary marcasite forms from the alteration of pyrrhotite.

Loellingite $(Fe,Co,Ni)As_2$: Loellingite is one of the constituents of the pyrite-arsenopyrite assemblage. Although limited in occurrence, the mineral becomes locally important. Grains mainly being anhedral display variations within the fine-grain size. White colour with slightly yellowish tint and strong anistropism in shades of greenish blue distinguish it from both minerals. This identification has been confirmed by qualitative microprobe analysis. Loellingite is mainly interstitial to euhedral arsenopyrite crystals, and replaces it to some extent, by contrast to that some loellingite also coats fractured pyrite crystals in varying thickness, and produces an irregular contact, apparently replacing pyrite (Plate 32). Replacement of sphalerite and arsenopyrite by loellingite is locally seen. Loellingite coating cataclastic pyrite is also fractured, but the fractures in the loellingite do not match with those in the pyrite which indicates the tectonic influence over the pyrite prior to loellingite formation, and these fractures have been widened outward by the invasion of soft minerals. Individual loellingite grains particularly suffer fracturing, and they always produce roughly square fragments, between which covellite and less

commonly galena occur in specimens from the 668 m level, Firat deposit.

Pyrrhotite $Fe_{1-x}S$: Pyrrhotite is a common accessory constituent to the sulphide mineralization but is not as widely distributed as the other accessory iron sulphides. It occurs in granular aggregates as well as in small grains associated with chalcopyrite and sphalerite. In contrast to many other sulphides the pyrrhotite is generally in discrete grains disseminated throughout the gangue mineral and sulphide mineralization. The individual euhedral grains measure up to 0.1 mm in diameter, but irregular and anhedral grains are somewhat smaller up to 0.05 mm across. The pyrrhotite is generally associated with pyrite. Sphalerite is the most important host mineral to accommodate pyrrhotite which is mainly found in euhedral grains without apparent connection to chalcopyrite blebs in sphalerite. Pyrrhotite appears to follow crystallographic directions in sphalerite. Along the peripheries and fractures of the pyrrhotite grains most commonly occurred outside sphalerite grains, it shows slight alteration to pyrite and marcasite.

Chalcopyrite $CuFeS_2$: Chalcopyrite is widespread but less abundant than the major sulphides, it does not exceed accessory proportions. In general the relative abundance of chalcopyrite

appears to increase with depth, and locally the copper content of the ore attains as much as 2%. It is generally associated with the other sulphides, chiefly sphalerite, galena, pyrite and tennantite in order of importance, and it also occurs alone within the gangue. Chalcopyrite forms irregular patches or clots with a dimension varying from 0.01 to 0.53 mm long. The twinning is not uncommon. Apart from the chalcopyrite replacing pyrite, it is usually surrounding by zones of alteration products such as covellite, bornite and neodigenite. Chalcopyrite is also locally within fractures cutting pyrite, arsenopyrite and sphalerite. It is a common feature downward that the chalcopyrite is interstitial to euhedral pyrite and arsenopyrite, and this kind of chalcopyrite is invariably free from alteration. Some chalcopyrite grains have lamellar valeriite as disconnected crystals forming a triangular lattice texture, in others bornite occurs in this form (Plate 33). Chalcopyrite replaces pyrite, arsenopyrite, marcasite and sphalerite in varied proportions. In some examples chalcopyrite replaces arsenopyrite in lamellar way.

Covellite CuS. This copper mineral displays variation in amount with respect to chalcopyrite and the other copper minerals. The covellite is distributed as pseudomorphs after chalcopyrite in the gangue as well as forming alteration rims.

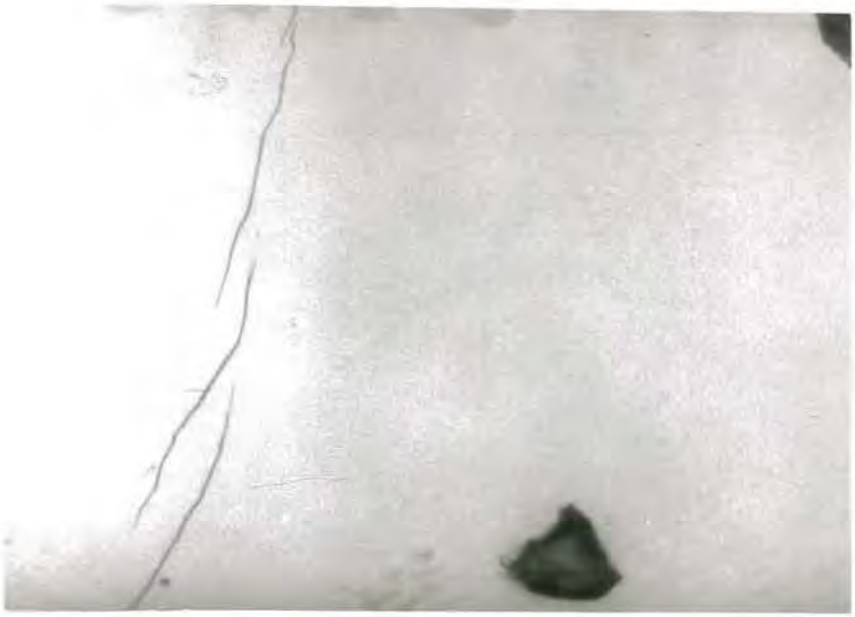

Plate 33 Valeriite inclusions in chalcopyrite.
Reflected light, x500.

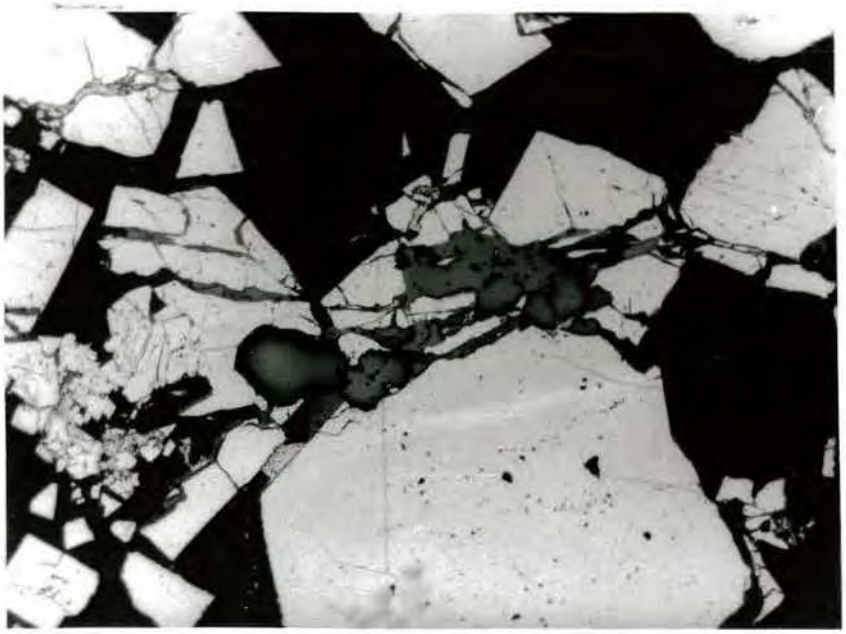

Plate 34 Blaubleibender covelline and fromboidal neodigenite replacing and filling fractures in cataclastic pyrite. Reflected light, x200.

Both primary and secondary covellite are present. The former occurs almost always in lamellae along with neodigenite and less commonly alone. In contrast, the secondary covellite is a supergene product from the other copper minerals, and it is found as clots or coating made of numerous inequigranular grains around the primary copper minerals. Although not common, another covellite variety has been identified in a few specimens, which is slightly darker blue in colour than for usual covellite and gives no characteristic orange reddish-brown colour under the crossed nicols, and has very weak anistropism. These optical features are in favour of a covellite variety that Ramdohr calls the "blaubleibender covellin" Cu_9S_5. The blaubleibender covellin always appears to be associated with pyrite (Plate 34)Moh (1964).studied the stability field of this mineral in the presence of vapour under which condition blaubleibender covellin can exist only 157° ± 3°C. Blaubleibender covellin and covellite can coexist stably as independent phases below 157°C. Zies et al. (1916) have produced experimentally blaubleibender covellin by treating copper-iron sulphides with $CuSO_4$ dissolved in water under the conditions present in oxidation, leaching or enrichment zones. The coexistance of blaubleibender covellin and covellite indicates a step in the reactions towards equilibrium (Moh,1964).

Neodigenite $4Cu_2S.CuS$: Neodigenite, although of minor amounts, appears to be widely distributed through the ore bodies at depth. The mineral is a common constituent of the pyrite, chalcocite and sphalerite assemblage. Two kinds of neodigenite are distinctly present; the granular neodigenite usually with covellite, and the colloform neodigenite which is identical apart from its slightly darker blue colour. The colloform neodigenite is mainly interstitial to the early formed sulphides. The granular neodigenite replaces tennantite and chalcopyrite which in turn may have neodigenite inclusions indicating at least contemporaneity in formation. The granular neodigenite commonly involves lamellar covellite as exsolution hence it is probably that neodigenite contains increasing amounts of Cu_2S or CuS in solid solution. (Krieger, 1932 and Palache et al. 1944) (Plate 35).

Bornite $5Cu_2S.Fe_2S_3$: The bornite is proportional to chalcopyrite, and its amount increases with depth. The mineral occurs in close relation with chalcopyrite, neodigenite and covellite as well as in gangue minerals. Typical fine-grained aggregates with clear irregular boundaries coating chalcopyrite in various thickness are very characteristic. Since the great majority of the bornite forms aggregates this suggests a slow cooling. (Edwards, 1939).

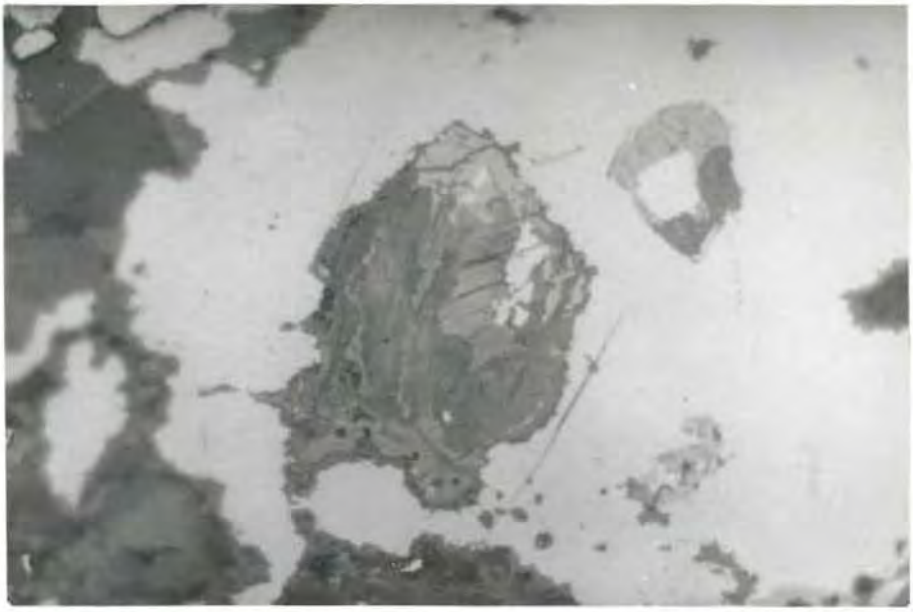

Plate 35 Neodigenite with lamellar covellite. Reflected light, x200.

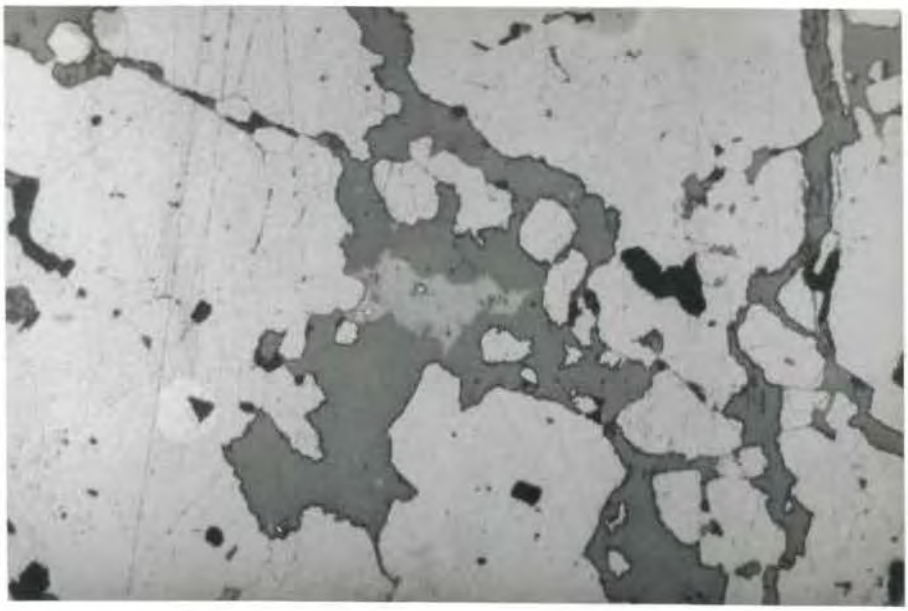

Plate 36 Wittichenite. Reflected light, x200.

Chalcophanite $(Mn.Zn)O.2MnO_2.2H_2O$: Chalcophanite was observed in one specimen in which it occurs along with chalcopyrite, covellite and galena. Angular grains with moderately sharp edges appear to have a reflectivity about the sphalerite region. Reflection pleochroism and anistropism are strong and characteristic. It differs from hetaerolite by its higher reflectivity.

Sulfo-salts:

Five sulfo-salts have been identified in the main sulphide deposit; tennantite, wittichenite, chalcocite, bournonite and boulangerite. Of them tennantite is distributed widely.

Tennantite $5Cu_2S.2(Cu.Fe)S.2As_2S_3$: This sulfo-salt was identified by its optical properties and confirmed by use of the electron microanalyser which showed abundant trace Sb in addition to the major constituent elements. The tennantite is not present in all specimens but where found it is usually closely associated with galena, chalcopyrite and sphalerite in order of decreasing importance. Occasionally its presence with pyrite and arsenopyrite is also seen, where sometimes it is a fracture filling material. Mainly chalcopyrite and less commonly arsenopyrite and pyrite are found in tennantite as inclusions. The mineral seems to replace sphalerite, chalcopyrite and partly galena which in turn accommodates the bulk of the tennantite present. Tennantite with bluish-green grey colour,

medium reflectivity and weak anistropism forms irregular patches in general less than 1 mm in size.

Wittichenite $3Cu_2S\ Bi_2S_3$: Wittichenite was qualitatively identified by the electron microanalysis technique which recorded the presence of Cu and Bi in essential amounts,and Sb and As in abundant trace amounts in order of abundance. The mineral is creamy white with a brownish tint, and has a reflectivity moderately high, greater than for chalcocite. Reflection pleochroism and anistropism are distinctly weak. There is no visible internal reflection. The wittichenite is always found together with chalcopyrite and less frequently with sphalerite. Its proportion seems to be related to the chalcopyrite present in a section. When they are adjacent, wittichenite rims chalcopyrite. Locally both of them are interstitial to arsenopyrite and pyrite whose fractures are infrequently filled by wittichenite. In sphalerite the mineral is involved as rounded or angular blebs in differing size. This mineral offers a fruitfull area for further quantitative study on both electron microprobe and microscope along with subsidiary techniques. (Plate 36).

Chalcocite Cu_2S: Chalcocite appears to be a supergene product, since it is fine-grained inequigranular and always associated with the other supergene copper minerals

(Uytenbogaardt, 1951). Chalcocite is mainly found together with chalcopyrite and wittichenite. It also occurs intergrown with neodigenite, the boundary between the two being irregular and suggesting that chalcocite is replacing neodigenite.

Bournonite $2PbS.Cu_2S.Sb_2S_3$ and Boulangerite $5PbS.2Sb_2S$: These are the sulfo-salts found in very small amounts in galena, and only in a few of the specimens examined. Wherever seen, both of the minerals occur together, following crystallographic directions in the galena. Bournonite is usually in irregular elongated blebs with fibrous ends. Its reflectivity is apparently less than for galena from which the bournonite is distinguished by reflection pleochroism in shades of greenish grey and distinct anistropism in light grey. In contrast to bournonite, boulangerite occurs in lamellar blades with sharp ends which are not connected with the ends of other lamellae. It is slightly greenish in colour compared with galena, but less green than bournonite. High reflectivity (as much as galena) small rotation angle 2^{o} and strong anistropsim in light grey are characteristic.

Alteration and secondary minerals

Alteration and related process are widespread in the Keban mining area where gossans are mostly present, and oxidized zones are generally important at contacts including

the triple rock association. The primary sulphide ores have undergone fairly complete and spotty oxidation down to about the 668 m level. The oxidized zones are composed essentially of smithsonite, hydrous iron oxide of various types and gypsum. Associated with them are hemimorphite, hydrozincite, cerussite, anglesite, malachite and azurite found in subordinate amounts in order of abundance. Iron stained gossans show the boxwork texture characteristic of leached sulphide ores. The original sphalerite is represented both by dark brown coarse cellular and brown fine cellular boxworks. The original galena is traceable by yellowish cleavage boxwork of powdery sulphur. Some of the voids have been completely filled by soft, earthy brick-red coloured limonite.

Among the secondary minerals, smithsonite, malachite and azurite merit brief explanation.

Smithsonite $ZnCO_3$: The smithsonite covers large areas between the 705 m and 688 m levels in the underground workings. Lenticular masses of smithsonite having a thickness between 0.50 and 11.00 m usually display a core of unoxidized primary ore. Smithsonite in cavernous masses is brownish coloured, but in vugs it forms botryoidal reniform masses of pale green colour. The identity of both types has been checked by XRD. Some of the botryoidal surfaces are covered very thinly by hydrous iron oxide. In a few cases, cavities up to 0.5 m in

size contain stalachtes with a maximum diameter of 5 cm. These have a core of concentrically banded smithsonite surrounded by a rim of calcite.

Malachite $CuCO_3.Cu(OH)_2$ and azurite $2CuCO_3.Cu(OH)_2$: These two supergene products occupy fractures in chalcopyrite as well as its peripheries. Although they are in subordinate amounts, their local enrichment may occur in places where chalcopyrite has a relatively high concentration. Both minerals form irregular patches or clots.

The primary ore minerals and their secondary derivatives found in the main sulphide deposit are summarized in table 29.

Table 29

Primary ore minerals	Secondary minerals
Sphalerite	Smithsonite, hydrozincite, hemimorphite
Galena	Anglesite, cerussite
Pyrite	Limonite
Pyrrhotite	Marcasite, pyrite
Chalcopyrite	Covellite, chalcocite, malachite, azurite, brochantite and iron oxides.

Paragenesis

The relative ages of some minerals have already been explained in the foregoing pages. Here more detail with respect to their relative formation is discussed; (Table 30).

In the main sulphide deposit the pyrite (with a little

ilmenite) was first to form, and after a break was still being deposited during the later stages of mineralization in association with the chalcopyrite. Marcasite crystals are included in the sphalerite and in return irregular aggregates of marcasite replace sphalerite grains peripherally. Marcasite also replaces pseudo-morphically, and coats arzenopyrite, therefore it is concluded that this mineral formed at two different times. The pyrrhotite appears to have crystallized contemporaneously with the earlier sphalerite. The well-formed arsenopyrite crystals are present as inclusions in euhedral forms within sphalerite and chalcopyrite, but arsenopyrite also includes and replaces sphalerite, and therefore the arsenopyrite must have had two steps of formation whose last step apparently was much longer than the previous step. All available evidence is in favour of a single continuous step in which the sphalerite formed, but the presence of relatively iron-rich and poor varieties may suggest a long period of formation. The chalcopyrite represents two steps of formation. The first step being less abundant is characterised as exsolution within sphalerite, while the second step is pronounced by abundant chalcopyrite which later fills fractures in sphalerite, and replaces or coats it. Galena occurs late in the sequence, but this has also been shown to be the case in many similar deposits. The relative ages of the major

metallic minerals together with a few of their subordinate minerals are well established. The remaining metallic minerals are far less abundant; therefore the determination of their relative ages is based on fewer observations and their position in the paragenetic table must be regarded as an approximation. Nevertheless, it is apparent that the sulfo-salts except bournanite and boulongerite, are slightly earlier than galena. As a whole they are attributed to later cooler fluids than those that deposited pyrite, sphalerite and chalcopyrite.

Table 30

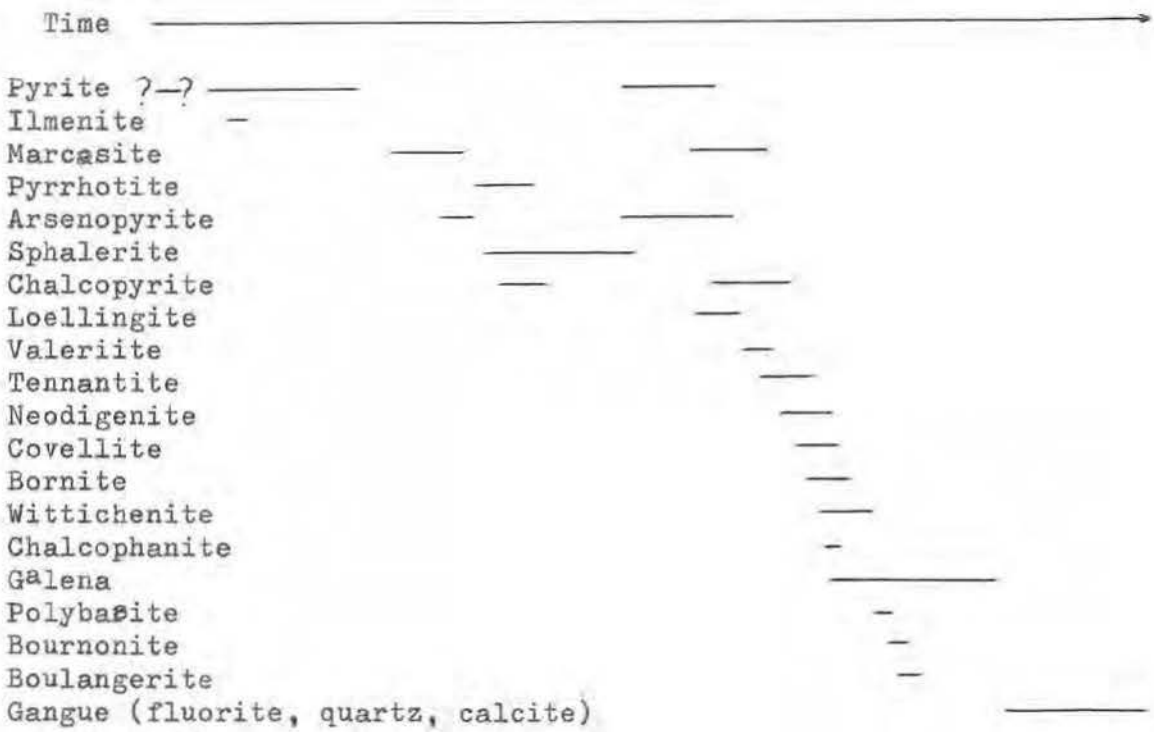

Origin and classification

The main sulphide deposit shows much evidence favouring epigenetic deposition. The main line of evidence for the hydrothermal origin are as follows: a) The presence of igneous rock, b) Evidence of replacement, c) Alteration of wall-rock, d) Paragenetic sequence, e) Presence of gangue minerals, f) Mode of occurrence of ore-shoots and dykes, g) Evidence of temperature of deposition, h) Zoning etc.

The presence of the quartz syenite porphyry: The igneous rock and its close association to the ores no doubt indicates the igneous rock as a source for the mineral bearing solutions. As clearly pointed out before ore locations are related to the igneous rock and all mineralization wherever present in the area is connected to it. The quartz syenite porphyry itself includes some sizeable ore mineralization. The nature of the igneous rock, namely intermediate rock approaching to acidic variety accords with the contact metasomatic phenomena which requires an igneous rock with high water content to transport and deposit included metal ions into the carbonate host rocks.

Evidence of replacement: Replacement is a common feature all along the ore bodies, and it is pronounced where the ore occurs within marble. Many galena rich ore bodies include remnants of non-assimilated phyllite xenoliths and less

commonly marble fragments. Although examples are limited, a couple of quartz syenite porphyries have suffered replacement by lead and zinc which by preference replaced their matrix. Banded sulphide minerals in marble or phyllite which were replaced along S foliation planes and fractures have residuals of the host rock in thin irregular layers. In the course of ore-fluid movements, sizeable vugs were mainly formed within marble, and in turn, were filled or lined by the sulphide minerals. This process of formation of solution cavities and later filling of these cavities independently under altered conditions has been discussed by Garrels and Dreyer (1952). Both thin section and ore microscopy studies show many replacement features proving the operation of metasomatic processes.

In short preservation of rock structure, mineral pseudomorphs, transection, embayment and absorbtion.....are the features in favour of replacement phenomena.

Alteration of wall-rock: It is expected that a replacement ore body will be accompanied by extensive metasomatic alteration of the country rocks. In the Keban area distinct wall-rock alteration has occurred and this has been discussed in detail earlier in Chapter II.

Paragenetic sequence: The generally accepted order of

deposition for metallic minerals in similar epigenetic deposits (Lindgren, 1933 and Bateman, 1956) is pyrite, arsenopyrite, pyrrhotite, tennantite, sphalerite, chalcopyrite, bornite, galena and sulfo-salts. There are, of course, overlapping and minor reversals of the order of the minerals. The paragenetic sequence given in the foregoing pages is in good agreement with the generally accepted order of deposition except for a few sulfo-salts. Although it is extremely difficult to estimate how much differentiation occurs from hydrothermal solutions, differentiation in a given ore body is tracebale in qualitative terms, which is a characteristic feature of a hydrothermal deposit.

Presence of gangue minerals: The gangue minerals accompanying ores are conspicously present in the area. Of them calcite, quartz, fluorite and gypsum are found with local enrichment in occurrence.

Mode of occurrence of ore-shoots and dykes: Alignment of the ore-shoots broadly makes a sheet-like pattern which accords well with the general trend and dip of the area. Therefore it appears to lie concordant with the host rock. Despite its general appearance it is virtually discordant to the host rock. The structural control was the cause for its appearance. A close-up check shows presence of many cross-cut ore-shoots,

dykes, fault and breccia filling along with fracture ore mineral associations. The contact relationships, such as discordant contacts, rapid lateral termination of ore zones, sharp contacts and remnant of wall-rocks all negate the remote possibility for a syngenetic deposit.

Evidence of temperature of deposition: A maximum temperature obtained from the table by Jaeger (1957) (see page 212) may be suggested at 690° C. On the other hand temperature studies on the different ore minerals were able to establish a temperature range from 225° C to 620° C at which most of the ore minerals of the main sulphide ore body formed. This temperature agrees with those usually thought to occur in mesothermal deposits.

Zoning: Ore deposits of hydrothermal origin commonly show evidence of zoning with respect to the known magmatic source. This zoning could be either in the ore body or in the total arrangement of the ore bodies of a district. In addition, particularly in the main sulphide deposit, there is zoning in individual ore bodies. At Firat the sequence found with increasing depth is silver, lead-zinc and copper.

The temperature estimations and the other evidence listed above suggest a mesothermal origin for the main sulphide deposit, on the basis of Lindgren's classification. The recent

investigation and suggestion by Hanuš (1960) regarding the nature of metasomatising fluids shed more light on the metasomatic deposit. In fact in the presence of unfilled solution cavities, it is regarded as incomplete metasomatism therefore the deposit may be better classified as being a mesothermal semi-metasomatic deposit.

To explain the phenomena let us see the definition of metasomatism by Lindgren: "The word metasomatism is now applied to the process of practically simultaneous capillary solution and deposition by which a new mineral of partly or wholly differing chemical composition may grow in the body of an old mineral aggregate" (1933). According to definition this process takes place in the environment of a solid rock in such a way that in the place of soluble rock soon after a minute open space is formed, and the formation or existance of open spaces of supercapillary size is excluded in the process. On the other hand according to Garrels and Dreyer metasomatism can be acceptable as a special case of simultaneous solution and deposition which are two independent processes that can act independently under altered conditions. Hanuš (1960) defines the metasomatism as a process of continuous formation of subcapillary open spaces and of their very little retarded filling by a new mineral. This definition also accepts that

metasomatism may result from two independent processes acting, between which there is an interval of time. This definition covers the formation of solution cavities, and subcapillary spaces beside the supercapillary open spaces of Lindgren, and filling of pre-existing cavities.

For a soluble rock mineralization it is essential that the penetrating hydrothermal solutions must be undersaturated by some of the components in the host rock with a simultaneous oversaturation by certain components, and the metasomatism can proceed only when the degree of undersaturation of the solution by components taken from the host rock. With respect to oversaturated and undersaturated of the thermal solution Hanuš claims two more processes (Metasomatism + capillary filling, solvate apposition) in addition to three known processes included in the metasomatism (Capillary filling, metasomatism, solvation). The presence of solution cavities, cavities filled by a metallic mineral and cavities having no metallic mineral in the main sulphide deposit include all metasomatic processes proposed before. But they all exclude or omit the partially filled solution cavities. This kind of pattern is formed by a process of what Hanuš (1959) terms "solvate apposition" which is defined as a process of formation of solution cavities of supercapillary size and of their simultaneous but only partial

filling with new minerals. This kind of metasomatism is formed by thermal solutions capable of forming more free space than it can simultaneously fill with newly formed minerals.

Generally the solvate apposition shows local enrichment at higher levels which could be the result of impoverishment in the metal ion content of the solution. Exceptions occur at lower-level locations such as the Dilimli ore-shoot whose foot wall marble is full of undoubted solutions cavities. As a whole beside the other metasomatic processes, solvate apposition took part in forming the main sulphide ore deposit, but it is hard to estimate its participation into the volume at the present stage.

Since the metasomatic process and its products are dependent on the thermal solutions in which variations caused the above-mentioned formations, it is safe enough to conclude that the thermal solutions showed considerable variation during the metasomatism. Indeed late calcification in the paragenetic sequence indicates that after early sulphides had been deposited the hydrothermal solution probably became alkaline, since calcite is precipitated probably in alkaline or at least in neutral environment at any pressure (Scherbina, 1956). However, it has been experimentally proved that a considerable amount of calcite

can be dissolved in an acid environment. (Malinin, 1962).

C. The Zereyandere and Kebandere contact metasomatic deposits

Around the igenous body at the Zereyandere and Kebandere sections metallic mineralization of iron oxides and sulphides occur together with the skarn minerals. The former section is characterised by a magnetite occurrence which forms lenses and dykes either in the contact between the igneous rock and the dolomite marble or in the roof part of the igneous rock. Additional separate formations are located in large dolomite marble xenoliths within the quartz-syenite porphyry which also contains cross-cutting magnetite dykes. Beside the several low-grade occurrences, mixed with skarn and the host rock, there are a few massive deposits and almost pure magnetite makes up a small high-grade occurrence parallel to the igneous contact. Within the magnetite mass there are skarn minerals lying in thin streaks of a few cm thick in a good parallelism to the primary bedding in the dolomite marble, the inference being that the dolomite marble was directly replaced.

In the river bed of Zereyandere, the seven major magnetite occurrences making up the bulk of the deposit, appear to keep a similar attitude to the general trend. The eastern most magnetite dykes in the contact dip sharply to the SE with a thickness of maximum 2.00 m, and include contamination from

the skarn minerals as well as a network of late-stage clear calcite. Further W the second magnetite dipping with an angle of 30 to the SE replaces the completely recrystallized dolomite-marble within the igneous rock and its thickness amounts up to 3.00 m. Further away another magnetite occurrence of 3.00 m thick is found within the quartz- syenite porphyry, and dips gently to the SE. A dolomite marble block inlier measuring 150 m across has several magnetite lenses with an apparent thickness of barely 1.50 m thick. In the extreme W a large igneous body passes several disseminated magnetite formations. Some distance S to the Zereyandere a number of small size magnetite bodies with or without manganese minerals in substantial proportions are present on slopes facing the river. A group of closely spaced magnetite lenses barely 0.50 m thick is located roughly parallel to foliation planes of dolomite marble, 250 m N of the Nimri Yazligi on the W bank of the Firat river. Magnetite also occurs subordinate to scheelite and other minerals in the Kebandere section. A number of other small (up to 1 m length) magnetite bodies form, but these are scarcely worth further description. No estimation of the ore reserves or the depth of the magnetite bodies has yet been made.

The mineralization in the Kebandere section is of interest mainly because of the occurrence of scheelite. The outermost

1 m thickness of the quartz-syenite porphyry may contain up to 3% of schoelite, and rarely small veinlets of scheelite occur on fracture surfaces within the igneous rock at somewhat greater distances from the contact. A sizeable concentration of this type occurs about 1 km SE of Keban town, on which some exploration workings were carried out. The mineralization also spreads into a 12 m wide skarn aureole between the igneous rock and marble blocks within the calcareous quartz phyllite but the amount of scheelite decreases away from the contact. Another deposit next in importance to this one occurs 350 m due S of it. No visible igneous rock outcrops are found here, but intense alteration on the surface indicates close proximity of the igneous rock at a shallow depth. Lenses of pyrite, chalcopyrite mineralization contain very small amounts of scheelite, whose presence can be revealed by UV lamp. The sulphide lenses are found in narrow zones lying approximately parallel to the river, along its two sides as far as the 161 observation point in the west. (Fig.16). Finally a sharp bend in the road cuts through the eastern end of the Nalli Ziyaret body and exposes some discrete uneconomic scheelite mineralization on fracture surfaces. No other scheelite has been reported or found elsewhere.

Both the Zereyandere and Kebandere sections are dissimilar

in several aspects, such as mineral assemblage of opaque and non-opaque minerals involved, their distribution, relative proportions and finally the conditions under which the minerals originated. However, they are essentially similar deposits on the basis of origin, and are therefore treated together.

Controls of mineralization

The contact metasomatic deposits of magnetite are mainly within or near the dolomite marble which because of its solubility and plasticity gives suitable conditions for interactions with iron-rich solutions. When the magnetite is within dolomite marble xenolith it tends to follow the primary foliation planes, but in dolomite marble in contact with igneous rock, mineralization apparently follows the general trend of the contact. Otherwise magnetite forms dykes and lenses near the roof of the igneous rock. The calc-silicate minerals associated with magnetite are described elsewhere and seem to have been formed earlier than the magnetite. They are interbanded with it and their earlier formation may have selectively localized the ore.

In the Kebandere, scheelite and the other ore minerals mainly occupy fractures, joints fissures and foliation planes of the host rock as well as occurring in the matrix. The sintectonic fractures, each a few centimeters or meters long, are commonly mineralized. But none of them are large enough to

create a commercial deposit and nowhere do fracture filling form a pronounced consistent pattern. The host rock and Ca-silicate skarn minerals appear to have acted selectively in location of minerals, for scheelite is mainly found in calcium rich areas, and the other sulphides occupy by preference Ca-silicate rich areas.

Mineralogy

The mineralogy of the skarn zones is relatively simple, consisting mainly of magnetite, scheelite, specular hematite, pyrite, chalcopyrite, marcasite and traces of gold in order of decreasing importance.

Magnetite Fe_3O_4: Magnetite is the only mineral ore found in major amounts, and it occurs principally in the Zereyandere section. In polished section, polyhedral textures and banded textures are seen. The massive and disseminated magnetite grains show erratic variations in grain size. Nevertheless the majority of the grains lie between 0.02 mm and 0.13 mm in diameter. Aggregates of uniform size of 0.02 mm are very common throughout the ore body. Loosely spaced magnetite crystals have a local tendency towards banding of maximum 0.5 mm thick, interlayered commonly with gangue minerals and less commonly chalcopyrite. Relatively large magnetite grains barely 0.10 mm in diameter occur next to gangue minerals making a resemblance of vug filling

material. Despite its euhedral nature, anhedral magnetite is also present in equal proportions to euhedral ones; it would be likely the case that post mineralization solutions were partly responsible for obliterating their original form. Particularly discrete crystals next to aggregates carry witness to that kind of influence by producing corroded and obliterated crystals. Moreover it is a frequent case to find both euhedral and anhedral grains of different size together within a small distance which may infer selective effect of fluids and difference in grain growth. However, when they are in aggregates they are almost made from euhedral grains of uniform size. Beside the clear magnetite grains, the majority are mainly full of non-opaque and, to a smaller extent, opaque inclusions.

Under reflected light two kinds of magnetite are distinctly observed; those mainly occurring in the central parts of the deposit have a slightly brownish-yellowish tint, whilst those found in the border zones next to the igneous rock show a bluish tint. Cell-size measurements are 8.391A and 8.380A respectively.

Magnetite shows alteration to geothite and less commonly lepidocrocite (both minerals confirmed by XRD). Acicular and tiny discrete geothite grains usually occur in between individual magnetite grains, and also near the border of banded magnetite, which may be due to the effect of fluids on its formation. In places euhedral magnetite develops very thin rims of geothite. The rim geothite tends to penetrate along cleavage traces and

fractures so that an irregular contact between the two minerals is produced. Goethite locally forms eutectic-like intergrowths. The presence of lepidocrocite seems to be restricted to the ore bodies near to the contact of dolomite marble and igneous rock, where it develops intensively between loosely spaced magnetite grains leaving irregular relics of primary magnetite. Although not widespread, hematite forms along the cleavage traces and cracks within magnetite. There are also some euhedral magnetite grains embedded in a skarn mineral that shows complete alteration to martite. Since the occurrence of hematite is largely near fractures in or near grain boundaries of magnetite, it is obvious that it results from oxidation. The absence of primary hematite throughout the ore bodies at the Zereyandere section also proves this claim.

Goethite also occurs as thin concentric zones within calcite crystals occurring within the magnetite ore. The exact mode of formation of this goethite is obscure, but its presence suggests some variation in conditions during formation of the ore. From the mutual relation between magnetite and skarn minerals, magnetite postdates the silicate minerals. Exceptions do occur, particularly at the Zereyandere section where some micaceous minerals and garnet are found to embed and replace magnetite whose projection is euhedral towards the skarn minerals, suggesting that

it predates the late-stage micaceous skarn minerals. Intensive corrosion of some magnetite grains also proves the presence of later fluids, from which the late skarn minerals were derived.

Maghemite γFe_2O_3: A few examples of the metastable form of Fe_2O_3, known as γFe_2O_3 or maghemite were observed in magnetite grains at the Zereyandere section. Maghemite showing apparent greyish blue colour with a high reflectivity (Ramdohr, 1950) forms a regular grid pattern which appears to develop independently of the crystallographic form of the host mineral, and it can only be observed under high magnification. According to Högg (1935) maghemite is a defect structure derived from that of magnetite by removal of some of the iron. The maghemite from the Zereyandere section, it is believed, results from the supergene alteration of magnetite.

Specular hematite Fe_2O_3: Specular hematite occurs exclusively at the Kebandere section where beautiful fibrous and radiating platy crystals with a strong micaceous parting may grow up to 1 cm in size. Some of them are grouped in rosette-like clusters. The majority of the mineral is euhedral in form. The common lamellar twinning forms on $(01\bar{1}2)$. The specular hematite is full of early-stage skarn inclusions, and is replaced by chalcopyrite. These relations indicate that the ore mineral is closely associated with skarn minerals and chalcopyrite. Because of tectonic distrubances a movement taken place along

0001 translation plane is revealed by the distorted twinning planes. The ore mineral suffers little alteration around borders and partings.

Scheelite $CaWO_4$: Scheelite seems to have occurred mainly in a quartz-syenite porphyry whose alkali feldspars clearly did equilibrate during formation. This mineral forms entirely as discretely disseminated subhedral or euhedral grains of acute rhombs. (Plate 37). The highly fractured mineral exhibits low birefringence of the first order with a high relief. Grains are ranged between 1 mm and 0.25 mm in size. Its distinct cleavage in two directions and symmetric extinction are characteristic. Under the microscope they appear in the matrix and on the euhedral alkali feldspar crystals as overgrowths. Some of them are found as euhedral casts of feldspars which have been completely altered and removed during the formation of the scheelite. In marble, scheelite is interstitial to or overgrown on calcite grains. In hand specimens the crystals are an undistinctive pale-yellowish white or icy white colour. Under ultraviolet radiation they fluoresce in colours ranging from greenish or bluish-white to greenish-yellow. Such yellowish fluorescence indicates the presence of Mo and possible Mn (Greenwood, 1943), but no molybdenite has been located throughout the skarn zones.

The shceelite appears to be very stable, it is everywhere unaltered and has not reacted with any of the coexisting minerals.

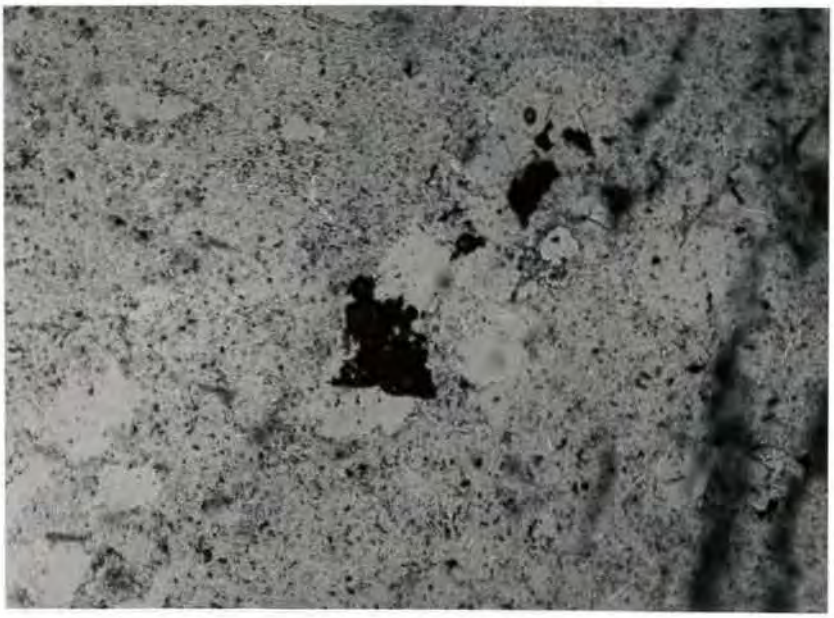

Plate 37 Rhomb-shaped crystal of scheelite resting on an alkali feldspar. x80.

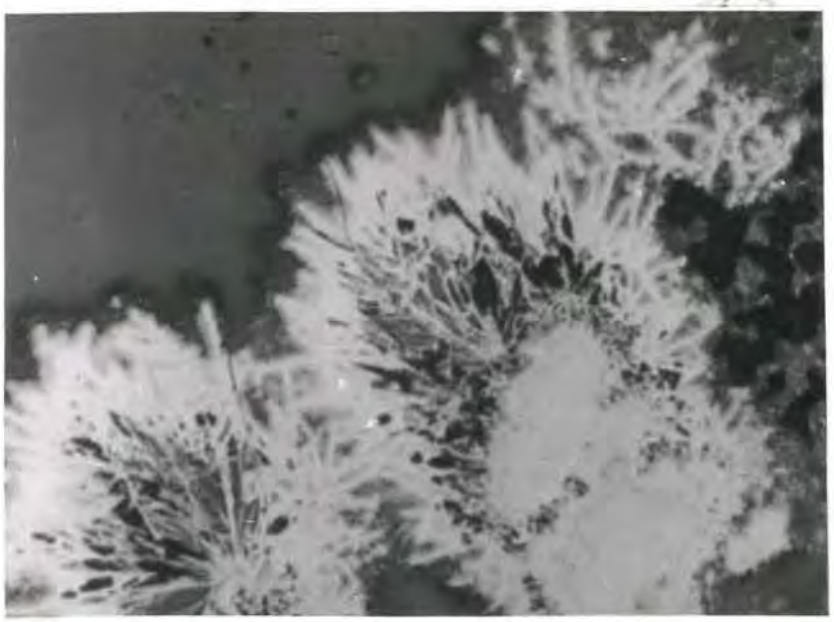

Plate 38 Colloform psilomelane and hair-like pyrolusite formed in a carbonate matrix. Reflected light, x80.

It is not particularly associated with the other ore minerals, and was observed only in contact with most of the skarn minerals present. The scheelite is much more commonly in contact with the Ca-silicates than with the other ore minerals. In this connection it displays no pronounced preference except in local favouring of grossularite; but this could be a coincidence because grossularite is much more abundant among the skarn minerals. It was probably deposited later than these silicates in the section.

Pyrite FeS_2: Pyrite being a subordinate mineral present in very small amounts at the Zereyandere ore deposit, becomes a major constituent in the Kebandere ore deposit where in extreme cases, it is found in masses of lenses up to 1.00 m long. Pyrite mainly in euhedral grains, has a wide size ranging from 0.01 mm to 1.5 cm in diameter. As revealed by polished samples from different localities there must have been at least three generations of pyrite formation. The first pyrite to crystallize is found as blebs along parting planes of magnetite. The second one is usually euhedral and relatively bigger than the previous pyrite in size, and appears to be in close relation with chalcopyrite in which euhedral grains of pyrite as inclusions are present. This pyrite is euhedral to magnetite and to the late-stage skarn minerals. Finally vein filling pyrite along with calcite

cuts the magnetite ore bodies.

Marcasite FeS_2: This accessory mineral in very small amounts was only located within the skarn zone of Kebandere section. Euhedral fine-grained marcasite invariably develops as inclusions in chalcopyrite and magnetite, beside a few crystals encountered within the gangue minerals.

Chalcopyrite $Cu_2S.Fe_2S_3$: Chalcopyrite is found in proportions varying greatly from place to place. It occurs as an accessory mineral to the magnetite in the Zereyandere section while the mineral comes after the specular hematite in abundance elsewhere. Chalcopyrite is always in anhedral grains measuring 0.01 by 0.5 mm at most or in prolonged irregular patches. Despite its descrete nature, some chalcopyrite grains tend to go together so that they make irregular bands within a gangue layer, interbanded with magnetite. The chalcopyrite together with the other sulphides displays a strong tendency to associate with the gangue minerals rather than magnetite. Exceptions occur where chalcopyrite rims and replaces magnetite. The majority of chalcopyrite with rugged outlines, presumably due to corrosive effect of fluids are enclosed by gangue materials rich in hydrous iron oxides of colloform texture. It is an infrequent case that interstitial chalcopyrite to skarn minerals show lamellar twinning on a 111 translation plane.

The chalcopyrite suffers intense alteration to covellite which usually forms fibrous grains more or less vertical to its outlines, thus producing a pattern something like corona texture. Another common alteration product is goethite which forms tiny grains, sometimes associated with covellite. Needle-like, individually oriented valeriite crystals as exsolution within a few chalcopyrite grains are only visible under high magnification.

Gold Au: Although native gold has been reported (Kumbasar, 1964) to be present in very small accessory amounts in connection with chalcopyrite particularly at the Kebandere section, the present author failed to locate any of them even after careful study especially concentrated on chalcopyrite. But considering the mineral association of similar deposits gold is presumably present in the area.

Alteration and secondary minerals

Alteration of ore minerals in the contact aureole seems to be directly proportional to the size of the ore bodies present. Some aspect of alteration along with their derivatives have already been explained with respect to their primary minerals from which they derive. In general hydrous iron oxides together with some secondary copper minerals are formed. Of them bornite and brochantite merit brief explanation.

Bornite $5Cu_2S.Fe_2S_3$: The bornite occurs invariably along with chalcopyrite. Anhedral and lath-like bornite always appears to replace chalcopyrite along its border, crystallographic directions and cross-cutting fractures. No evidence for the primary formation of bornite has been found.

Brochantite $Cu_4SO_4(OH)_6$: Only the Kebandere section involves this secondary copper mineral at surface where the water circulation and humidity are a minimum. The brochantite develops around chalcopyrite grains and along its cracks. Some chalcopyrite grains become isolated at times within a matrix of brochantite and hydrous iron oxides. The identity of this mineral was confirmed by XRD.

Paragenesis

The relative ages of some minerals have already been explained previously with respect to their invariable mutual relations. In this section it is discussed in more detail; the results are given in table 31.

The earliest metallic mineral to form throughout the skarn zones was pyrite, nowhere were the sulphur bearing minerals observed to predate pyrite, which was deposited in three stages during the mineralization. As some magnetite crystals include euhedral pyrite inclusions, this becomes evidence for early pyrite, but it is believed that the period was very short. During the magnetite mineralization pyrite

also occurred in considerable amounts, finally the fracture filling pyrite incorporated with the calcification produced in the last stage. The magnetite appears to have formed continuously until the second stage skarnification took place, this was the stage at which dominantly phyllosilicates were generated. After a relatively long period the second stage magnetite associating and coating the previous ones formed during a short period of time. From the mutual relations primary marcasite occurred together with the magnetite, most probably being in its early period. There is much evidence that the chalcopyrite is later than magnetite, from encrustation and replacement textures, whilst the chalcopyrite crystallized partly simultaneously with the specular hematite which is less commonly replaced by chalcopyrite whose inclusions in return are mainly specular hematite. Some goethite grains in thin rims after chalcopyrite are found to occur within well-formed carbonate rhombs of late-stage generation, inferring another generation of chalcopyrite for a relatively short time. As stated before scheelite is associated with the skarn minerals rather than the metallic ores, and because of this, it is concluded that the scheelite formed towards the end of the skarn formation. Finally calcification with clear calcite cutting all the ore bodies completed the sequence. The secondary minerals are excluded in the

paragenetic table.

Table 31

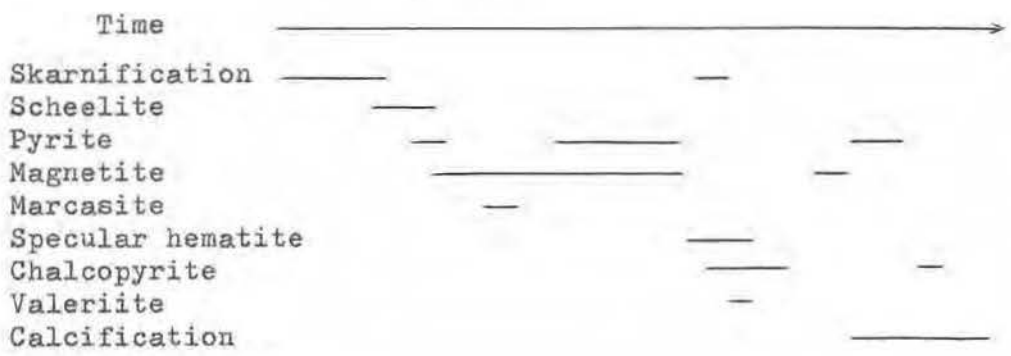

Origin and classification

The spatial relationship of the ore bodies to the intrusive rock strongly suggests that ore deposition and intrusion of the igneous rock in the area are related phenomena. Mutual reaction between fluids from the igneous rock and the dolomite marble host rock caused silicate deposition, and solution of the carbonate, $CaCO_3$, which in turn helped to increase permeability. The high temperature during the replacement made easy the reactions to form the metasomatic minerals. The stresses generated in the course of replacement and subsequent cooling resulted in further local fracturing in the adjacent rock, which supplied further access to the fluids. The contacts and nearby the host rocks are full structures of this kind confirming that the above phenomena existed during emplacement.

The mutual relation between the igneous rock and the ores suggests that the crystallizing igneous rock was the source for the fluids forming the ores, as well as the skarn minerals, and the paragenetic relationship indicates that the fluid supply continued for a relatively long time with probable fluctuations. The formation of sulphide and oxide minerals of iron in different amounts at different times suggests variations in the oxygen and sulphur fugacities in the system.

No evidence has been found in favour of descending fluids. On the contrary all the evidence present proves that the metasomatising fluids were ascendant. Alteration of the quartz syenite porphyry supplies further evidence for the fluids which passed through the igneous rock.

Among the metallic minerals, the formation of magnetite merits a brief explanation in the light of both field and laboratory observations. Many magnetite deposits have been ascribed to residual solutions rich in iron (Bateman, 1951), but the author himself left several major open questions needing to be explained. These questions are related to its solubility and precipitation. On the other hand Shand (1947) believes that many such residual solutions are alkaline and do not contain dissolved iron. Such solutions from crystallizing magmas are postulated to be relatively enriched in Na and

and K ions, and thus they have an alkaline reaction. The recent analytical data for fluid inclusions in hydrothermal minerals invariably indicate the presence of Na^{+}, Ca^{+2}, K^{+} and Mg^{+2} as dominant cations, and Cl^{-}, HCO_3^{-} and SO_4^{-2} as the dominant anions (Smith, 1953; Roedder, et al. 1963). Among these ions Na^{+} and Cl^{-} are normally the most abundant. Therefore it may be postulated that most of the ore bearing fluids are alkaline in nature. From the chemical analysis of the igneous rock, an enrichment of alkalies is found, and albitization is common near to the ore bodies. A local proof is provided by a quartz syenite porphyry sample (No. 276) taken from the locality next to a magnetite ore body in which majority of the plagioclase apparently was turned into alkali feldspars. Shand believes the solutions include a hydrosol of ferrous hydroxide, kept in suspension by the alkalies. This claim is supported by the fact that ferrous hydroxide is insoluble in alkaline solutions. By the removal of alkalies in the solution, the hydrosol suffers self-oxidation, forming magnetite, water and free hydrogen according to the equation:

$$3Fe(OH)_2 \longrightarrow Fe_3O_4 + 2H_2O + H_2\uparrow$$

The close association with the igneous contact of the ore

mineralization the ore mineralogy and abundance of skarn minerals place the deposits at Kebandere and Zereyandere into the contact metamorphic class of deposits as defined by Lindgren (1933).

D. The Manganese occurrence

Although in minor amounts some manganese ores occur in the Keban area. The distribution of manganese outcrops appear to be exclusively concentrated on the slopes facing the Firat river. Among them apparently separate lenses of ore with a distance of 50 m to each other make relatively sizeable occurrence. These outcrops measuring barely 10x1 m each lie along a contact of the hanging-wall marble to the foot-wall dolomite marble, 200 m S of the abandoned Derebaca main entrance. As it was revealed by XRD analysis, manganese tends to have emplaced in the foot-wall dolomite marble rather than the marble. Another manganese occurrence associating with magnetite in subsidiary proportions occurs within the sericite calc-schist, and locates 500 m S of the Zereyandere magnetite deposit. In addition to these, there are several individual spot occurrences of manganese around the upper part of the Karamagaradere in the N.

Controls of Mineralization

As a whole, the position and alignment of small-scale manganese outcrops give an inference that they may well be members of what may be called a sheet-like manganese ore body which seems to concordant with the general trend and dip of the major folding. Fissure and fracture fillings may also play a minor part in localising the ore. All sizeable outcrops are found comparatively remote from the igneous rock.

Mineralogy

In the area three manganese minerals were identified by using different techniques involving microscope, XRD, electron probe and reflectivity. The minerals are psilomelane, cryptomelane and pyrolusite. Of them psilomelane is the commonest and most widespread.

Psilomelane $BaMn^{+2}Mn_6^{+4}O_{16}(OH)_4$ (Ramdohr, 1956): Psilomelane most frequently occurs as botryoidal and colloform masses and less frequently in concentric layers which alternate with very thin silvery-grey concordant pyrolusite layers. Botryoidal and colloform psilomelane turns into randomly oriented hair-like pyrolusite along its grain boundaries, which sometimes are aligned so that eye-shaped outlines are produced. (Plate 38). In many instances psilomelane appears to have mixed with the other manganese minerals. In colloform occurrence some psilomelane layers are separated by concordant calcite layers

attaining up to 0.01 mm. thickness, that indicate a break at the time of deposition. Colloform texture is generally traversed by lateral shrinkage cracks. Vein-filling manganese ore also includes all three manganese minerals. They make isolated patches and botryoidal areas through the clear calcite veins cutting the dolomite marble. Minor hematite, goethite and lepidocrocite occur with the manganese minerals in that order of importance.

Reflectivity measurements of several large grains were carried out against the international standards of the glass, sica and silicon for reflectivity at four wavelengths by a reflectivity assemblage fitted with a digital electronic stabilizer suggested by Nichol and Phillips (1964). The results are given in table 32.

Table 32

Standard	480	520	580	640
Glass	26.22	25.50	24.31	23.30
Sica	28.89	27.90	26.25	24.96
Silicon	29.38	28.09	26.50	25.41

These values are in good agreement with those given for psilomelane (op.cit.).

For conformation of the identification of the minerals, drilled out powder of the mineral by a dentist drill under the

microscope was subjected to X-ray powder analyses by the procedure (see Appendix) modified after Nichol (1962). Table 33 illustrates the XRD data for psilomelane.

Table 33

Fleischer & Richmond 1943	Ramdohr 1956	Ian Nichol 1962	Present 1968
dA	dA	dA	dA
4.21			4.22
3.83			3.82
3.48		3.45	
3.32			
3.22			
2.97			2.97
2.84			
2.61			
2.40		2.41	
2.36	2.38		
2.25		2.25	2.26
2.19		2.19	2.18
2.14	2.16	2.15	2.16
1.82	1.81	1.82	
1.73		1.73	
1.71	1.71		
1.64		1.64	1.61
1.56	1.55	1.56	
1.52			
1.42	1.42	1.42	
1.40	1.39	1.39	
		1.30	

Pyrolusite MnO_2: Pyrolusite appears to the eyes, to be higher in reflectivity than psilomelane. The mineral with very fine felted ice flower-like texture occurs both in colloform bands frequently alternating with psilomelane and in randomly oriented needles. Pyrolusite as fracture filling

makes crustification which includes commonly psilomelane next to the host rock wall with sharp boundaries. In places where pyrolusite replaces the carbonate host rock, it becomes a matrix to euhedral crystals of carbonate materials thus producing a texture very similar to diabasic texture. The colour under the reflected light is greyish with a distinct silvery tint and in oil it is pleochroic in slightly bluish shade. Anistropism is strongly pronounced even in hair-like grains in shades of blue grey with slightly greenish tint. Since the hair-like mineral is too small for the reflectivity purpose, and its aggregates are not big enough to cover a suitable area under the microscope, no reflectivity measurement could be possible.

Cryptomelane $MnK.Mn_6O_{14}$: Cryptomelane appears always associated with psilomelane. Under the microscope some relatively large areas seem to have been from very thin layers of both minerals. A microprobe traverse across a suitable area having different banding proved qualitatively the presence of Ba and K in major amounts. The K gives the peak positions at frequent intervals between the two non-peak areas which undoubtly coincide with the psilomelane layers, on the probe chart. It is concluded that the two minerals are very intimately mixed with psilomelane predominating over cryptomelane.

Paragenesis

Since no direct relationship of the manganese minerals to the main sulphide deposit was observed, and no certain age relationships could be established. The absence of any evidence for high temperature manganese minerals such as jacobsite and braunite is in favour of low temperature formation. Replacement of the dolomite marble also suggests that it did not suffer very much heat. Finally the position of the manganese ore bodies in the zonal arrangement negates a high temperature formation. Therefore it is possible that the manganese minerals indicate a late-stage in the paragenetic sequence.

Origin

The ore minerals exhibit typical colloform texture in which psilomelane, pyrolusite and cryptomelane show spheroidal or banded appearance. In many cases alternate concentric bands of psilomelane, pyrolusite and calcite are found. Regular colloform banding of a different generation of psilomelane with slight variation in colour and reflectivity is quite common. Pyrolusite is commonly present as needles either lining the vugs in crudely oriented or spheroidal base of psilomelane is scattered in irregular directions, generally indicating deposition in open space, shrinkage cracks, mainly

traversing laterally the concentric rings of psilomelane which were evidently formed by surface tension within the original colloidal gel suggest shrinkaging during the consolidation and deposition. Moreover, characteristic spherical nodules of the three minerals in close contact with one another deformed each other mutually without breaking, which indicates that at the time of deposition they were non-rigid ore gels rather than solid. Their close association with clear calcite veinlets in the dolomite marble in which both minerals have smooth and sharp contacts towards the host rock indicates that they only filled the interstitial spaces between carbonate grains rather than replacing them, suggesting their limited replacement ability due to mainly low temperature (Plate 39). Finally no other manganese minerals replaced by psilomelane, cryptomelane or pyrolusite were observed. This is also negative evidence for a supergene origin. As a whole all evidence tends to be in favour of colloidal deposition for the manganese ores in the Keban area.

E. Secondary deposits

Among the secondary minerals, vanadinite and descloizite merit a brief explanation as they have been assumed to provide a guide for further lead-zinc prospecting in the area, but the present author does not support this view. Both of them are

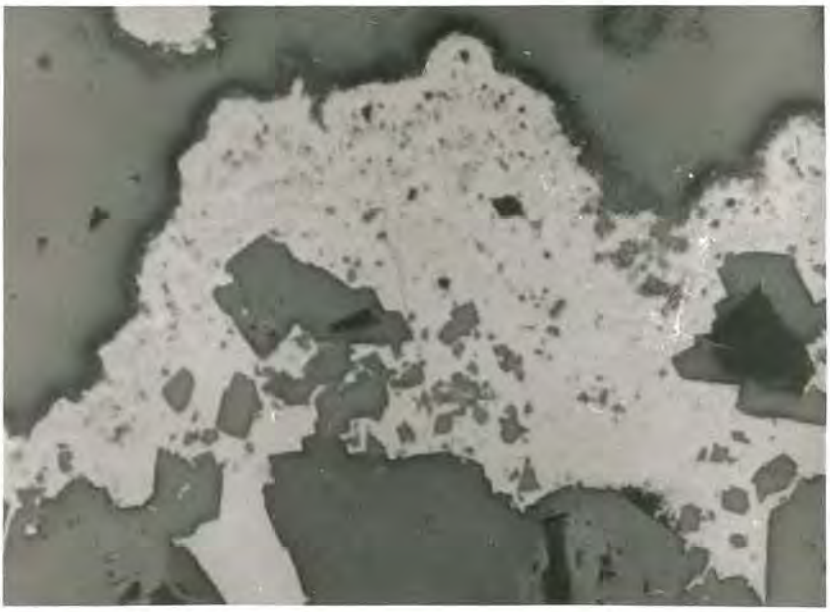

Plate 39 Mixture of psilomelane and pyrolusite replacing carbonate grains give rise to form diabasic texture. Reflected light, x80.

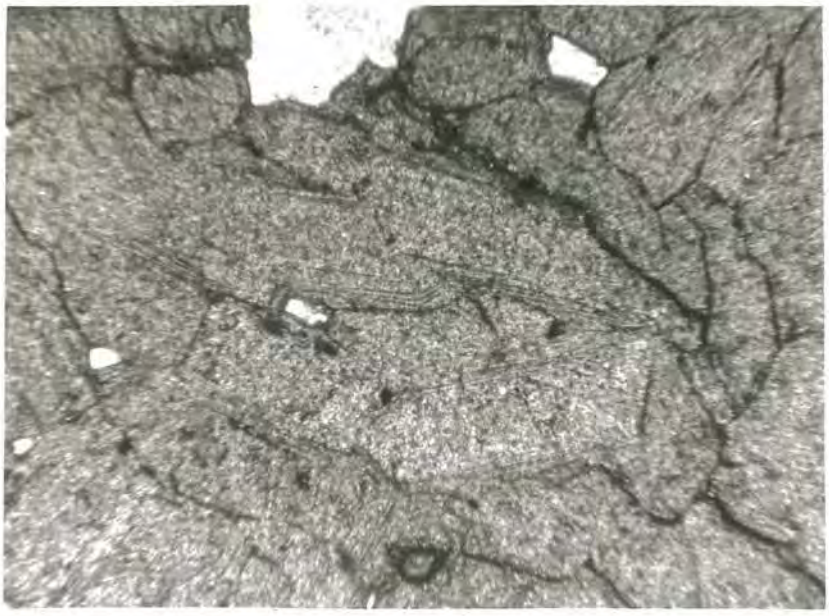

Plate 40 Euhedral vanadinite crystals showing zoning. Ordinary light, x50.

only found in a cave between the overlying dolomite marble and the sericite calc-schist at the bottom, 250 m due N of the Nimriyazligi summer camping site on the W bank of the Firat river. They line the cave wall all around in a sheet of several cms thick. Vanadinite and its accompanying descloizite occur in a separate body with some hydrous iron minerals.

The presence of severely sheared zones where secondary lead minerals are growing marks their depositional control.

Mineralogy

Vanadinite $Pb_5(VO_4)_3Cl$: The typical Keban vanadinite consists of transparent yellowish-brown, short hexagonal prisms terminated at both ends by basal pinacoid faces. The largest crystal observed measures 0.5 by 0.1 cm and the smallest crystals are of microscopic dimensions. These prisms are often merged together at one end to form somewhat radiating bunches. Vanadinite is slightly pleochroic with O = brownish yellow, E = Brownish orange-yellow. The pleochroism is particularly pronounced in cores of large grains which may indicate a change in the composition. Zoning is a common feature, thus producing terraced-prism faces with frequent intervals due to parallel growth. (Plate 40). These faces, which are not due to fracturing, are clearly interpreted as

the result of crystal growth and this is marked in different coloured bands which are repeated many times in a single crystal of vanadinite. The changing in colour shows that changes in composition took place during the formation of individual crystals. The colour and uniaxial figure of the vanadinite may be an indication of the presence of arsenic. The cell-size measurement on a XRD chart under the conditions cited in the Appendix gives: a = 10.31 A° , c = 7.34 A°, and c/a = 0.712 A°.

Descloizite $Pb(Zn,Cu)OHVO_4$: Descloizite occurs in a variety of forms with varying crystallinity. They are found as interlayers barely 1 mm thick, between calcite/dolomite and vanadinite which suffers replacement by descloizite (Plate 41). The vugs lined by euhedral vanadinite crystals include fine-grained, stained descloizite sheets in the middle portions, lying over the vanadinite basement. In many vugs where loosely spaced free-standing euhedral vanadinite crystals grow a rim of descloizite with a thickness ranging from 0.01 to 0.5 mm encrusts the underlying crystals. The mineral, with an ever-present earthy looking staining shows a pleochroism stronger than for the vanadinite. The pleochroic scheme is as follows: α = greenish yellow, β = orange brown. The twinning is very common as it is in the vanadinite. The striking colour variations in a single grain or grains next to each other may

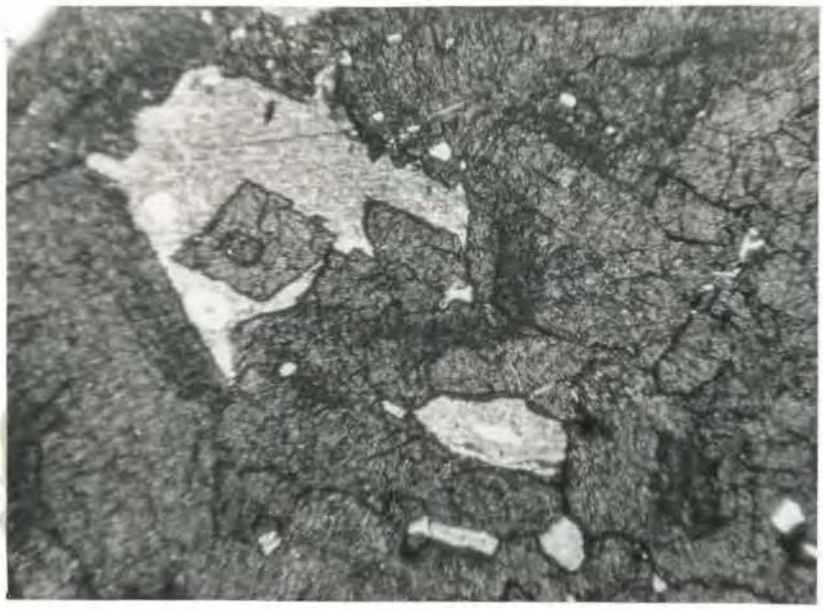

Plate 41 Deslcoizite grains replacing and coating vanadinite grains. Ordinary light, x32.

Plate 42 Flotation process.

by caused by small differences in composition. Descloizite pseudomorphs after vanadinite and apparent replacement features suggest it is relatively younger than the vanadinite.

Origin and classification

These supergene products of the lead-zinc deposit are believed to take their lead, zinc and copper content from the primary sulphides. V is the tenth in abundance among the metals in the earth's crust, and is markedly enriched in certain sedimentary rocks. However, it is a well known fact that shales in general show the highest, and dolomite and limestone the lowest vanadium contents amongst sedimentary rocks (Wasserstein, 1945). Therefore the shale horizons are accepted as the most likely source in many similar occurrences. In the Keban area the phyllite metamorphic equivalent of shales is regarded as the most probable source for the V and this assumption is also based on the analytical data of Maucher (1937) who reported 0.003% V_2O_5 in the sphalerite + galena, 0.01% V_2O_5 in the quartz syenite porphyry and 0.02% V_2O_5 in the phyllite. As stated before the minerals obviously occur in a close association with the dolomite marble rather than the phyllite. This may be explainable by its relatively great solubility which attracts V. Notestein (1918) has long before established the mutual relations of both V and calcite which precipitates V from vanadyl sulphate solution which is

soluble in solutions of alkali carbonates and bicarbonates. In this way V may be leached by sulphate bearing ground waters and precipitated by calcite. Moreover zoning of both minerals indicates a prolonged period of deposition, subjected to repeated variations in the composition of the depositing solutions. This deduction is also in full agreement with a supergene theory of formation.

Crustal abundance of V and its enrichment in certain rocks creat a better case in favour of lateral secretion of the element than in the case of geochemically rare elements like Pb and Cu. The lateral secretion implies a process of mobilization of elements from a solid rock and their precipitation in openings nearby. Lovering (1963) has recently introduced the term of lithogene to describe the process more accurately and emphasize source evnironment. According to the author a lithogene deposit is one where rocks or mineral deposits have been modified by the selective mobilization and recrystallization of some of their chemical constituents to form a later generation of minerals more than a cm away from the place where the elements were mobilized. The agent mobilizing the elements might be any kind of water such as porosity water in the rock except one that did not contribute magmatic elements to the final mineral deposit.

This definition and further explanation about the

environment and process from which vanadinite and descloizite form, appear to accord with those present in the Keban area therefore the vanadinite-descloizite occurrence is well-classified as being lithogene.

It is most unlikely that these occurrences indicate that additional lead-zinc ore bodies can be found further away from the known ore bodies, as has been suggested by other workers in the area.

F. Zoning

The Keban area gives a good example of zoning. The ore bodies are immediately adjacent to the intrusive rocks. In a broad way zoning appears to be present outwards from the two centres, the Zereyandere section in the S, and the Kebandere section in the N respectively. There, as well as in the linliers within the quartz syenite porphyry bodies; magnetite, scheelite, pyrite and chalcopyrite are most abundant and they create the two separate inner zones around the centres, between them the main sulphide ore deposit forming the intermediate zone lies about in the middle of the area. This intermediate zone is followed with a zone mainly dominated by the manganese minerals. Finally the outermost zone is composed of vanadinite and descloizite formed by migration of certain minerals from the main sulphide ore deposit.

Peripherally outward from the igneous bodies, from areas of high temperature to those of lower temperature, there is clearly a gradual change in mineralization from scheelite and iron oxides to copper sulphides then iron sulphides. There are however local interruptions of this general pattern.

Vertical zoning, one of the most striking features of hydrothermally formed deposits, is seen through the main sulphide ore deposits. From the assays and microscopic study, it is found that an orderly sequence is lacking at the higher levels, because the silver and zinc appear to occur abundantly above the lead. (300 qr/t silver, 1 gr/t gold, 12% zinc at the Derebaca deposit were recorded). The Dilimli ore-shoot is another case where lead formed below a zone generally dominated by zinc. This recycling and lack of orderly sequence at higher levels have been regarded by some authors, as caused by mineralizing solutions of complex chemical composition. In general the lower levels e.g. 668 m level (in 1965) have dominantly massive pyrite occurrences and a relative enrichment in copper content appears to start to enter into the deposit at about the 705 m level. The zinc content decreased down to about 3% at the 668 m level in 1965, along with the silver content which becomes 140 gr/t compared with 300 gr/t at higher levels. As stated before the silver content according to early reports was about 980 gr/t at surface. The Zn/Pb ratio

was 1,3 at the higher levels including the upper part of the Derebaca deposit, and general increases up to 2 were reported at the levels between the 745 m and 688 m levels after which the ratio falls down to about 1 at the lower levels (1965). Although only present in minor amounts, gold maintains a steady content throughout the workings.

G. Flotation process

This well-known ore dressing process was applied to some ore samples on a laboratory scale, in order to obtain galena and sphalerite concentrates free from associated minerals. The tailings and middlings, although they are important for commercial applications were not considered to be of importance on the laboratory scale, because sufficient purified ore could be obtained from the concentrate. To check the accuracy of the process, 8 recovered loose samples were counted on a basis of 300 points each under a binocular microscope. The results read off on the chart after Barringer, (1954) show the analytical error between 1.10% and 2.50% or in other words percent of maximum probable undesirable compounds ranges from 1 to 4.7. Table 34 gives further explanation on accuracy. The purified sulphides have been subjected to trace element analysis and cell-size measurement.

At the early stage of grinding the samples were cut into

Table 34 Grain counts of purified samples (loose)

Sample No.	Ore	Points Counted	Undesirable Points	Desirable Points	Max Probable amt.of desired Ore %	Max Probable amt.of undesired Ore %	Analytical Error %
520/1	Galena	300	8	292	97.30	2.70	1.80
507	"	300	5	295	98.30	1.70	1.20
B/N-1	"	300	11	289	96.30	3.70	2.25
800	"	300	3	297	99.00	1.10	1.00
B/N-1	Sphalerite	300	14	286	95.30	4.70	2.50
800	"	300	13	287	95.70	4.30	2.30
120/2	"	300	10	290	96.70	3.30	2.05
159/1	"	300	6	294	98.00	2.00	1.55

two or more pieces by a hydraulic jack, after which cuttings were turned into chips in a vibrating crusher. Though Taggart and others recommend a grain size between +48 and -60 mesh, the mesh size +60, -90 was found to be most satisfactory for the purpose, and the right size was obtained on a ball mill containing holder with three tungsten carbide balls in three-minute operation time. The holder was never loaded more than one-half of the full capacity. For each flotation process 100 gr ground ore with a pulp dilution of 20% was used.

A 1 litre buchner separation funnel with the porosity 4 is the main cell-tank but instead used bubble-columnar cell, which has so large lip (home-made) slightly dipped that to allow bubbles loaded with ore particles pouring into the smaller separation funnel connected with the vacuum. The bubble column funnel was connected into the pressure air tap supplied. In the case of over froth manually operated glass plate was in use in order to skim. The concentration of desired ore which gathers in the small funnel is removed after drying out by aceton. The tailing/middling in the bubble column funnel have been allowed attacking by aquia-regia to remove. After several attacking by aquia-regia the funnel is washed out by tap water. Now the funnel is ready for another run. Each concentration was run three times in order to make

sure that the sample is purified (plate 42).

The flotation reagents and methods for galena separation suggested by Pryor and by Sutherland were applied separately. The method based on Sutherland's research with a slight modification to meet the features of the ores were used with satisfying results. Sodium-di-ethyl dithiocarbonate 30 mgr per litre as collector, and sodium hydroxide N to bring up to 12,6 pH the pulp alkalinity which also acts as depressant over sphalerite and pyrite (critical pH value for sphalerite 6.2, for pyrite 10.5, for galena >13 below which values the mineral particles float) were used, 2-3 drops of creozote help to produce abundant bubbles in the cell. The pulp alkalinity was checked by a Pye pH meter.

Taggart's method was applied to samples having relatively coarse galena scattered within marble, which requires simple separation of a metal sulphide from its gangue mineral. 0.0068 gr. per 100 gr of ore of KEX (Potassium Ethyl-Xanthate) as collector, 0.0068 gr per 100 gr of ore of cresol and 2 drops of pine oil were employed. The alkalinity of pulp was maintained at 8.5 pH with addition of sufficient Na_2CO_3.

The method after Rey was found to be most satisfactory in the case of slight abundance of pyrite over sphalerite which is easily separated from the former. 0.00453 gr per 100 gr of ore of KEX as collector, 0.15 gr per 100 gr of ore of CaO to

bring the pulp alkalinity between 8-9 pH, 0.045 gr per 100 gr of ore of $CuSO_4$ as depressant and 1-2 drops of creozote to produce more froth when bubbles are not good enough, were used. Tap water was in use for all processes.

H. Trace element analysis of the sulphides

The sulphides purified by the flotation technique have been subjected to trace element analysis on the XRF automatic spectrograph. First a chart was run for each base sample of sulphide in order to detect the trace elements present. Then the standards were prepared so as to include detected elements on the basis of the addition method. In addition to minor elements shown in table 35 for galena; gold, radium and probably uranium are present, but in the absence of spec pure standards it was impossible to calculate their proportions, therefore they have been omitted from the table. Arsenic and iron, in galena and sphalerite respectively have been found far above the trace amounts. Table 35 and 36 illustrate the elements examined and their amounts in galena and sphalerite.

Trace elements in galena

The substitution of other elements for lead in galena has long been in doubt because many of them may be present in associated minerals. Among the trace elements, As, Sb, Bi and Ag have all been reported (Fleischer, 1955). As stated

Table 35 Trace element analyses of the purified galenas

	Sample No.	800	507	520/1	122	159/1	229	146	138/2	159	126	B-N/1	120/1	B-12	154	109	Ave.of 15
	Ag	747	735	818	875	1493	905	962	1032	903	875	880	623	1231	614	905	1046
	Bi	358	418	405	376	415	398	397	387	346	393	407	362	410	390	415	392
	Mo	55	55	52	47	60	60	58	47	46	50	73	56	48	53	49	54
	Sb	1015	956	1087	1265	1797	965	1260	1168	1183	1158	1130	950	1527	812	1370	1176
ppm	Ni	62	97	62	75	76	80	73	78	65	73	72	77	76	133	77	78
	Sr	37	33	37	48	40	62	43	35	31	35	47	45	34	37	36	40
	Ba	152	48	75	253	90	275	85	72	125	240	150	247	250	160	80	153
	Te	205	159	138	185	162	185	162	190	207	163	177	181	160	165	187	175
	Ga	39	41	40	38	40	13	35	40	32	41	39	32	38	37	40	36
%	As	1.45	1.41	1.39	1.42	1.41	1.38	1.41	1.41	1.33	1.42	1.39	1.44	1.40	1.40	1.40	1.40
	Sb/Ag	1.36	1.30	1.33	1.45	1.20	1.06	1.30	1.13	1.31	1.32	1.28	1.52	1.24	1.32	1.51	1.12
	Bi/Ag	0.48	0.57	0.50	0.43	0.28	0.44	0.41	0.38	0.38	0.45	0.46	0.58	0.33	0.64	0.46	0.37

before galena itself includes evenly distributed Ag in the lattice, in addition to the silver ex-solution. 12 samples out of 15 have trace Ag less than 1000 ppm. Only one sample shows exceptional richness in silver as much as 1493 ppm. As pointed out by Fleischer (op.cit.) there is a close connection between Ag and Sb values, the table becomes a repetition of the suggestion, in which the Ag value is a function of the Sb value obtained. Whenever the Ag content increases, so does the Sb content or vice-versa. The Sb/Ag ratios vary from 1.06 to 1.52. The Sb always dominates over the Ag content in the corresponding galena specimen. The variation in Sb content is most likely an effect of its solubility in galena. The relative concentration of Sb varies with the galena crystal habit, and the lowest concentrations occur in octahedral crystals. (Marshall, 1961).

Trace elements in sphalerite

The trace elements in the sphalerite samples studies are: Mn, Cd, Cr, Cu, Ga, Co, Ge, Sb and In. Of these elements the last three were most probably below the detection limit of the machine, while Co is an intermittent element usually below the detection limit too. A possibility for the intermittent presence of Co on the chart is that it may be a contaminant from pyrite. The amount of Mn is variable in the range from 700 ppm to 4425 ppm, but the majority of the samples appear to

Table 36 Trace element analyses of the purified sphalerites

	Sample No.	800	106	103	140/2	126	13	159/1	120/1	194	122	B-N/1	229	165	154	121/2	AVE of 15
	Mn	1297	3160	4425	3275	1300	1245	700	2250	3600	2035	1435	1242	1005	1033	2006	2000
	Cd	905	913	515	680	785	935	887	973	352	395	1092	918	970	958	810	805
ppm	Cu	125	90	85	105	130	85	90	95	120	88	92	183	177	195	120	119
	Cr	90	102	115	115	110	78	95	88	82	122	92	74	80	94	95	96
	Ga	72	85	75	60	56	91	76	87	80	62	60	51	75	62	55	70
%	Fe	10.81	13.10	13.85	12.71	10.33	10.20	9.09	9.80	11.55	10.50	10.35	12.65	8.90	13.05	10.90	11.19

have Mn between 1000 ppm and 2000 ppm Cd ranges from 352 to 1092 ppm. With a few exceptions the Mn and Cd content of a sample are apparently independent of each other. On the other hand the total iron composition of sphalerites analysed by the spectrometer accounts for a major constituent rather than trace. According to results obtained total iron content of sample is broadly a function of the Mn content. The highest total iron content found is 13.85% compared with a highest reported iron content for sphalerites of 26%. Cd being mainly substituted for zinc has a close relation to sphalerite, which may be explained by the relative ionic radii (Zn = 1.86A° , Cd = 1.89 A°). The Cd content shows great variation between 515 ppm and 1092 ppm giving an arithmetic mean of 805 ppm for 15 samples. In all specimens Cr has been found to be present. Its content is variable within a small range with an average of 96 ppm for 15 samples. Cu and Ga are ever-present trace elements in the specimens giving an arithmetic averate of 119 and 70 ppm for 15 samples respectively.

The presence of Cr in the Keban sphalerite is significant, and it is attributed to the orogenic belt which is characterized by ultrabasic rocks along with other acidic rocks, and the Cr is believed to be derived from this kind of ultrabasic rock, which is present around the Keban massif.

Trace elements in sphalerite may indicate the magma type

from which the sphalerite formed (Evrard, 1945) and may also indicate the metallogenetic province to which the magmatic source belongs. The metallogenetic province from which the Keban sphalerite is derived, is characterized by relatively high concentrations of Mn, Ga and Cr, with low concentration of Cd and Cu. These values are comparable with those found in the ore deposit of the Central Alps in Italy (Gabor, 1968) where Mn, Ga, Cd and Cu give an arithmetic average of 449, 215, 3375 and 17 ppm for 16 samples respectively.

No systematic variation of trace element content was detected in any of these minerals. This conclusion differs from those of other investigators most of whom have suggested a clear relationship of trace element content with temperature of formation.

CHAPTER VII

GEOTHERMOMETRY

Introduction

The temperatures of formation of minerals and ore deposits have long been paid attention, as this data can be helpful in the solution of abstract geological problems and in answering practical problems in economic geology. A series of temperature determinations in an ore deposit could establish the original temperature gradient from which the direction of motion of the ore carrying fluids could be inferred and findings of this kind with the aid of other local factors could lead to new prospects.

In the Keban area there have been found several materials suitable for different kinds of method suggested by others, but their application and reliability have long been in argument. Since the majority of them are of limited reliability, the combined results for the area will give only an approximate temperature range within which most of the minerals are believed to have formed. Among the methods applied are the iron content of sphalerite, the iron deficiency in pyrrhotite and d_{102} spacing of arsenopyrite. The indirect results obtained from microscopic studies will also be given in addition to the direct results. The contact metasomatic deposits at the Zereyandere and Kebandere section

unlike the main sulphide deposit, have no minerals from which temperatures may easily be estimated. Although approximate, a heat flow estimate provides a general idea for the maximum temperatures which were present within the contact zone. Some microscopic evidence appears also to be helpful in connection with the heat flow estimation.

Temperature of the main sulphide deposit

Sphalerite as a geothermometer

Although controversial, this method has been used widely, Kullerud (1953) has shown experimentally that the amount of iron present in solid solution in sphalerite is a function of the temperature of formation, provided that excess iron is available at the time of formation. In the presence of excess sulphur, iron will form pyrite rather than enter into sphalerite. As it is known now, the Keban sphalerites are characterised by high content of iron which indicates sulphur deficiency excess sulphur would have formed pyrite instead of iron in sphalerite. In many places, however, sphalerite is found in what appears to have been in equilibrium with pyrrhotite and chalcopyrite at the time of formation. Since neither pyrrhotite nor chalcopyrite are sulphur saturated minerals their presence indicates that sulphur was not in excess during the deposition of associated minerals.

Sphalerite samples purified by means of flotation

techniques were used for the cell-size measurements from which the temperature estimations have been done. The cell-size values were determined using a wide-angle focusing XRD and a Philips powder camera (114.59 mm in diameter) loaded with Industrial-G fast X-ray film. The estimated temperatures of crystallization of these sphalerites uncorrected for confining pressure are summarized in table 37.

Table 37

Sample No.	Cell-size A°	Mol.% FeS	Temp.C
109	5.4185	20.00	620°
120/1	5.4169	16.25	540°
229	5.4172	16.90	550°
B-N/1	5.4184	20.00	620°
165	5.4168	16.25	540°

The trace element analysis for sphalerite shows a maximum individual concentration of 4425 ppm Mn, 1092 ppm Cd and a maximum combined concentration of 5215 ppm of trace elements in sphalerite. Studies of Kullerud (1953) and Skinner (1959) on the effect of Mn, of Kullerud (1953) on the effect of Cd, and of Toulmin (1960) on the effect of Cu on the sphalerite-pyrrhotite equilibrium relations prove that no correction is required to the temperature estimates owing to the low concentration of these elements.

Iron deficiency in pyrrhotite

Arnold (1962) has recently determined experimentally the

solvus relationship between hexagonal pyrrhotite and pyrite. According to him the percentage of iron in pyrrhotite was temperature dependent, but insensitive to pressure. The temperature values obtained from the pyrrhotite geothermometer from the Highland-Surprise Mine where sphalerite occurs along with the pyrrhotite geothermometer were found to agree well with values obtained from the sphalerite. Subsequently Buseck (1962) and Kullerud et al. (1963) have attempted to apply the method to monoclinic pyrrhotite-pyrite assemblages. Following the suggestions some arguments mainly regarding the minor elements in pyrrhotite have been raised by some others. Among them Sawkins et al. (1964) with the aid of fluid inclusions study of fluorite and quartz, and sphalerite as a geological thermometer have proved that the pyrrhotite is not safe enough to use as a thermometer. He found a maximum temperature far below 250°C, below which no pyrrhotite is known to form. On the other hand pyrrhotite itself indicates a temperature between 450°C and 530°C.

Despite the above arguments, an attempt was done on two natural pyrrhotites, associating with pyrite from the main sulphide ore deposit. The d_{102} values after correction for shrinkage give d=2.081 and d=2.090 A° corresponding to 48.68 atomic percent iron and 49.62 atomic percent iron respectively. But on the diagram of the equilibrium relations in the system

FeS-S prepared by Arnold, there is a gap for iron content over 47.50 atomic percent. Therefore the pyrrhotite from the main sulphide deposit of the Keban area was found not applicable as a geological thermometer.

Arsenopyrite-Pyrite-Loellingite relation

Clark (1960) has experimentally shown that d_{131} spacing of arsenopyrite is a function of variation of the arsenopyrite composition, namely d_{131} spacing is related to the temperature at which the arsenopyrite with known composition forms. Therefore measurement of d_{131} spacing makes possible an estimation of its temperature of formation. Arsenopyrite, pyrite and loellingite coexist in many polished specimens taken from the different localities through the underground workings, and four of them were determined by the method described by Clark on a Philips XRD. The temperature results are tabulated in table 38.

Table 38

Sample No.	d_{131} A°	Temp. C
106	1.6330	450°
122	1.6334	472°
146	1.6332	465°
154	1.6332	465°

Four analysed samples give an arithmetic mean of 461 °C for a temperature of formation. This value is lower than the

critical value of 491°C above which pyrrhotite forms instead of pyrite. These results are all obtained from arsenopyrite shown by microscopic study to be of later formation than associated sphalerite. As stated earlier, arsenopyrite of earlier formation than sphalerite has also been found. However, such arsenopyrite exists alone and so could have formed at any temperature between 300° and 702°C.

Microscopic evidence

The ore microscopy study provides some evidence for formation temperatures of certain mineral assemblages. Of them unmixing temperatures given by exsolution patterns are of primary importance. Temperatures deduced from this type of evidence range from 78° to 550°C at most.

The presence of covellite lamellae as an exsolution within neodigenite indicates a temperature above 78°C (Palache et al., 1944) Coexistance of blaubleibender covellin with covellite marks a temperature below 157°C (Moh, 1964). Valeriite exsolution in the chalcopyrite is attributed to the temperature of 225°C by Borchert (1934) who also establishes a temperature of formation of 500°C for bornite exsolution in chalcopyrite. Despite lack of agreement on the figures for sphalerite-chalcopyrite assemblage provided by Buerger (1934), Borchert (1934), and Schwartz (1931); 350-400°C, 550°C and 650°C respectively, the average temperature of sphalerite found

by its iron content is in good agreement with what is suggested by Borchert. In short, the microscopic evidence suggests a progressive decrease in temperature at which the metallic mineral assemblage of the main sulphide deposit formed.

Temperature of the contact metasomatic deposit

Microscopic evidence

The contact metasomatic deposits provide comparatively limited evidence for estimating the temperature of formation. Although it is very rare chalcopyrite grains include valeriite exsolution indicating a minimum temperature of 225 C. The widespread presence of pyrite and of zoned anistropic grossularite correspond to a temperature of formation below 743 C (Kullerud, 1953). The formation of wollastonite indicates a temperature range from 660 to 800 C.

Heat flow estimation

Although approximate a heat flow estimate gives a general idea of the upper temperature that existed within the ore-bearing contact zones around the igneous rock. According to Jones (1934) and Lovering (1934), the temperature gradient away from the contact into the country rock is sharp at the beginning but it rapidly becomes less as the country rocks are heated. The temperature at the contact, stays fairly invariable for a long period in the course of cooling of the

igneous rock and the country rock is warmed. It is explainable by a "heat wave" running outward from the corresponding igneous rock (Jones, 1934). This heat wave moves slowly, and warms the country rock rapidly; after the rocks are warmed up, the cooling is slow. From this in a relative distance within the contact zone, temperatures are similar to those in the contact between the host and igneous rock. Moreover the temperature in contact is relatively higher than any spots in the country rock. If a temperature in the contact is known, this provides an upper temperature at which the minerals formed.

By using the table developed by Jaeger (1957) the contact temperature for an igneous rock with a melting range between 1200 -700 °C is 691° C. This value considers the latent heat of solidification and heat loss by volatiles. Although the figure appears to be much higher for an igneous rock having short melting range, this may be accepted as being the maximum temperature for hottest part of the rock. This maximum temperature is in broad agreement with the 743°C suggested by Kullerud for the association pyrite/garnet.

Lovering (1955) suggests that a temperature of approximately between 850° to 900° C is about suitable for quartz monzonite or granite magmas in the hotter parts of the intrusive body, this suggestion appears to cover syenite magmas

as it lies between the two magmas in the classification. According to Lovering, the leading edge of a sill, dyke or other intrusions, may be as low as 700° C.

In short in the light of different suggestions a maximum approximate temperature of 700° C for the contact metasomatic deposits is suggested as the most suitable temperature below which the metallic minerals form in order of decreasing temperature.

REFERENCES

Ahrens, L.H. & Taylor, S.R. 1961 Spectrochemical Analysis: Addison-Wesley, Massachusetts, U.S.A. p.454.

Arni, P. 1937 Keban madeni hakkinda: Private report on the Keban mine, M.T.A.

Arnold, R.G., Coleman, R.G.& Fryklund, V.C. 1962 Temperature of crystallization of pyrrhotite and sphalerite from the Highland-Surprise Mine, Coeur D'Alene District, Idaho: Econ. Geol., vol.57, pp.1163-1174.

Badgley, P.C. 1965 Structural and Tectonic Principles: A Harper Int. Student reprint.

Barringer, A.R. 1954 The preparation of polished sections of ores and mill products using diamond abrasives and their quantitative study by point counting methods: Trans. Inst. Min. Met., vol 63, pp.21-41.

Barth, T.F.W. 1951 Theoretical Petrology: John Wiley & Sons, Inc.

Barth, T.F.W. 1955 Representation of rock analysis: Jour. Geol., vol 63, pp.348-363.

Barton, P.B.Jr., & Toulmin, P. 1966 Phase relations involving sphalerite in the Fe-Zn-S system: Econ. Geol., vol 61, pp.815-849.

Bastin, E.S. 1960 Interpretation of Ore Textures: Geol. Soc. Amer. Mem. 45 (Reprinted).

Bateman, M.A. 1951 Formation of late magmatic oxide ores: Econ. Geol. vol 46, pp.404-426.

Bateman, M.A. 1956 Economic Mineral Deposits: John Wiley and Sons, Inc.

Baykal, F. 1966 Türkiye Jeoloji Haritasi 1/500,000 ölçekli Sivas sheet: M.T.A. publication.

Beales, F.W. 1953 Dolomite mottling in Pallisser (Devonian) limestone, Banff and Jasper National Parks, Alberta: Bull. Amer. Assoc. Petr. Geol., vol 37, pp.2281-2293.

Bill, H.,Sierro,J. & Lacroix, R. 1967 Origin of colouration in some fluorites: Amer. Min., vol 52, pp.1003-1008.

Bjørlykke, H. 1945 Innholdet av Kobolt: svavelkis fra norske nikkelmalmer: Norsk Geol. Tids., vol 25, pp.11-15.

Bjørlykke, H. & Jarp, S. 1950 The content of cobalt in some Norwegian sulphide deposits: Norsk Geol. Tids, vol 28, pp.151-156.

Borchert, H. 1934 Über Entmischungen im System Cu-Fe-S und ihre Bedeutung als geologische Thermometer: Chem. der Erde, vol 9, pp.145-172.

Borchert, H. 1952 Keban ceuher yataklarinda yapilan tetkikata dair rapor: Private report,M.T.A.

Bowen, N.L. 1940 Progressive metamorphism of siliceous limestone and dolomite: Jour. Geol., vol 48, p.225.

Bowen, N.L. 1956 The Evolution of the Igneous Rocks: Dover Publ. Inc., New York.

Buerger, N.W. 1934 The unmixing of chalcopyrite from sphalerite: Amer. Min., vol 19, pp.525-530.

Burnham, W.C. 1962 Facies and types of hydrothermal alteration: Econ. Geol. vol 57, pp.768-784.

Burri, C. 1964 Petrochemical Calculations Based on Equivalents, Methods of P. Niggli. Oldbourne Press.

Buseck, P.R. 1962 Ann. Rep. of Director Geophys. Lab., Carnegie Inst., Washington, Year Book 61, p.161.

Butler, J.R., & Smith, A.Z. 1962 Zirconium, niobium and certain other trace elements in some alkali igneous rocks: Geochim. et Cosmochim Acta; vol 26, pp. 945-953.

Chapman, R.W. 1935 The Percy ring-complex: Amer. Jour. Sci. 5th ser., vol 30, pp.401-431.

Clark, L.A. 1960 The Fe-As-S system: Phase relations and applications - Part II: Econ. Geol. vol 55, pp.1631-1652.

Coe, K. 1959 Boudinage structure in West Cork, Ireland: Geol. Mag., vol 96, No.3. pp.191-200.

Deer, W.A., Howie, R. & Zussman, J. 1962 Rock Forming Minerals: Vol 1,4,5. Longmans.

Dickson, J.A.D. 1965 A modified technique for carbonates in thin section: Nature, vol 205, No. 4971, p.587.

Dunham, K.C. 1937 The paragenesis and colour of fluorite in the English Pennines: Amer. Min. vol 22, p.468.

Dunham, K.C. 1952 Fluorspar: Mem. Geol. Surv. Gt. Britain. Special Rep. Mon. Resources Gt. Britain, vol 4.

Edwards, A.B. 1939 Some observations on the mineral composition of the Mount Lyell copper ores, Tasmania and their modes of occurrence: Austr. Inst. Min. Met. Proc., N.S. 124.

Edwards, A.B. 1960 Texture of Ore Minerals and Their Significance: Aust. Inst. Min. Met. (Reprinted).

Emeleus, C.H. 1956 Studies of the granophyres and related rocks of the Slieve Gullion Tertiary Igneous complex, Ireland: Unpbl. Ph.D. thesis, Uni. of Oxford.

Erentöz, C. 1966 Contribution a la stratigraphie de la Turquie: Bull. M.T.A., No.66.

Evamy, B.D. 1963 The application of a chemical staining technique to a study of dedolomitization: Sedimentology, vol 2, pp.164-170.

Evrard, P. 1945 Minor elements in sphalerites from Belgium: Econ. Geol. vol 40, pp.568-574.

Fairbridge, W.R. 1957 The dolomite question: Amer. Assc. Petr. Geol., pp.125-178.

Feofilov, P.P. 1956 On the nature of green colour of fluorite: Mem. Soc. Russe Min., vol 85, p.569.

Fischbach, 1900 Keban madeni hakkinda: Private report on the Keban mine, M.T.A.

Fleischer, M. 1955 Minor elements in some sulphide minerals: Econ. Geol. Fiftieth Ann. Vol. pp.970-1024.

Fleischer, M. & Richmond, W.E. 1943 The oxides of manganese: Econ. Geol. vol 38, p.269.

Freud, H. 1966 Applied Ore Microscopy Theory and Technique: The McMillan Co.

Gabor, D. & Perna, G. 1968 Le mineralizzazioni a galena e blenda del Trentino-Alto Adige e loro contenuto in elementi accessori: Sym. Int. Sui Giacimenti Minerari Delle Alpi. Sept.1966.

Garrels, R.M. & Dreyer, R.M. 1952 Mechanism of limestone replacement at low temperatures and pressures: Bull. Geol. Soc. Amer. vol 63, pp.325-380.

Geoffrey, D.J. 1961 Keban kursun ve çinko madeni, Elazig vilayeti: Private report, M.T.A.

Goldschmidth, V.M. 1931 Nachr. Ges. Wiss: Math.Phys. Kl.184, Göttingen.

Goldschmidth, V.M. 1954 Geochemistry: Oxford Press.

Goldschmidth, V.M. & Peters, C.L. 1931 Zur Geochemie des Ga: Nachr. Ges. Wiss. Göttingen, Math.Phys. Kl.1, pp.165-183.

Greenwood, R. 1943 Effect of chemical impurities on scheelite fluorescence: Econ. Geol. vol 38, pp.56-64.

Groves, A.W. 1951 Silicate Analysis: George Allen & Unwin Ltd.

Grubenmann, U. 1910 Die Kristallinen Schifer: Verlag von Gebrüder Borntraeger, Berlin.

Hägg, G. 1935 Die Kristallstructur des magnetischen Ferriozyds. Gamma-Fe_2O_3: Zeits. Phys. Chemie, vol 29/B, pp.95-103.

Hamilton, W.B. & Neuerburg, G.J. 1956 Olivine-sanidine trachybasalt from the Sierra Nevada, California: Amer. Min. vol 41, p.851.

Hanus, V. 1959 Zum problem der erzlagerstättenbildenden Metasomatose: Vestnik Ustredniho ústavv geologickeho, roc XXXIV.

Hanus, V. 1960 Hydrothermal metasomatism and its relationship to other ore forming process: Int. Geol. Congr. Report of the twenty-first session. Norden, pp.67-78.

Harker, A. 1964 Metamorphism: Methuen & Co. Ltd. (Reprinted)

Heier, K.S. 1960 Petrology and geochemistry of high-grade metamorphic and igneous rocks on Langøy, Northern Norway: Norg. Geol. Undsök. Nr.207, pp.1-246.

Hoeppener, R. 1955 Tectonik im Schiefergebirge: Geol. Rdsch., vol 44, pp.26-59.

Holland, J.G. & Brindle, D.W. 1966 A self consistent mass absorbtion correction for silicate analysis by X-ray fluorescence: Spectrochim Acta., vol 22, pp.2083-2093.

Hutchinson, R.M. 1956 Structure and petrology of Enchanted Rock Batholite, Llano and Gillespie counties, Texas: Geol. Soc. Amer. Bull., vol 67, pp.763-805.

Ineson, P.R. 1967 Trace element geochemistry of wall-rock alteration in the Pennine orefield and Cumberland ironfield: Unpbl. Ph.D. thesis, Univ. of Durham.

Jacobson, R.R.E., Macleod, W.N.& Black, K.R. 1958 Ring-complexes in the younger granite province of Northern Nigeria: Geol. Soc. London, Mem.1, pp.1-66.

Jaeger, J.G. 1957 Neighbourhood of a cooling intrusive sheet: Amer. Jour. Sci., vol 255, p.305.

Jones, R.B. 1934 Temperature relations to ore deposition: Econ. Geol. vol 29, pp.711-724.

Ketin, I. 1966 Tectonic units of Anatolia (Asia Minor): Bull. M.T.A., No.66.

Kimizuka, K. 1932 A study of potash-anorthoclase from Taiji, Kii province, Japan: Jap. Jour. Geol. Geogr., vol 9, p.213.

Kovenke, V. 1937 Rapport sur le gite de magnetite de la concession de Divrik: Private report, M.T.A.

Kozu, S. & Seto, K. 1921 Sanidine from the Eifel: Sci. Rep. Tohoku Imp. Univ., vol 1, p.25.

Krieger, P. 1932 An association of gold and uraninite from Chihuahua, Mexico: Econ. Geol., vol 27, pp.651-660.

Kullerud, G. 1953 The FeS-ZnS system. A geological thermometer: Norsk Geol. Tids., vol 32. pp.61-147.

Kullerud, G., Doe, B.R., Buseck, P.R. & Tröflen, P.F. 1963 Ann. Rep. Director Geophys. Lab., Carnegie Inst., Washington Year Book 62, p.210.

Kumbasar, I. 1964 Keban bölgesindeki cevherlesmelerin petrografik we metallojenik etüdü: Doktora tezi, Ist. Tek. Uni.

Lemish, J. 1959 Measurement of pore size distribution in some hydrothermally altered wall-rocks: Econ. Geol. vol 54, p.1360.

Lindgren, W. 1925 Metasomatism: Bull. Geol. Soc. Amer. vol 36.

Lindgren, W. 1933 Mineral Deposits: New York.

Lovering, T.S. 1935 Theory of heat conduction applied to geological problems: Bull. Geol. Soc. Amer., vol 46, pp. 69-94.

Lovering, T.S. 1949 Rock alteration as a guide to ore, East Tintic district, Utah: Econ. Geol., Mono 1.

Lovering, T.S. 1955 Temperatures in and near intrusions: Econ. Geol. Fiftieth Ann. Vol., pp.249-281.

Lovering, T.S. 1963 Epigenetic, diplogenetic, syngenetic and lithogene deposits: Econ. Geol., vol 58, pp.315-331.

Lucas, G. 1952 Premiers resultats d'une etude sur le produits odorants des calcaires fetides: C.R. Acad. Sci., Paris, vol 234, pp.121-123.

Lundgardh, P.H. 1948 Ann. Roy. Agric. Coll. Sweden, vol 15, p.1.

Malinin, C.A. 1962 Quoted in the Int. Geol. Congr. Report of the twenty-third session Czechoslovakia, 1968. Endogenous ore deposits, p.303.

Marshall, R.R. & Joensuu, O. 1961 Crystal habit and trace element content of some galenas: Econ. Geol., vol 56, pp.758-771.

Mason, B. 1958 Principles of Geochemistry: John Wiley & Sons, Inc., New York.

Maucher, A. 1937 Keban madeni zuhurati hakkunda mineralojik rapor: Private report, M.T.A.

Moh, G.H. 1964 Blaubleibender covellite: Ann. Rep. Director Geophys. Lab. Carnegie Inst., Washington, Year Book 63, p.208.

Moorhouse, W.W. 1964 The Study of Rocks in Thin Section: A Harper Int. Student reprint.

Morimoto, N. & Clark, L.A. 1961 Arsenopyrite crystal-chemical relations: Amer. Min. vol 46, pp.1448-1469.

Nichol, I. 1962 A study of some opaque manganese minerals: Unpubl. Ph.D. thesis, Univ. of Durham.

Nichol, I. & Phillips, R. 1964 Measurements of spectral reflectivity of manganese oxides: Miner. Mag., vol 35, pp.200-213.

Niggli, P. 1936 Über Molekülarnormen zur Gesteinsberechnung Schweiz: Min. Petr. Mitt., vol 16, pp.295-317.

Niggli, P.	1954	Rocks and Mineral Deposits: Freeman & Co., San Fransisco.
Noble, J.	1955	The classification of ore deposits: Econ. Geol. Fiftieth Ann. vol. Part I, pp.155-169.
Notestein, F.B.	1918	Some chemical experiments bearing on the origin of certain U-V ores: Econ. Geol., vol 13, p.50.
Oelsner,	1938	Keban madeni hakkinda rapor: Private report, M.T.A.
Palache, C., Berman, H. & Frondel, C.	1944	The System of Mineralogy of J.D. Dana and E.S. Dana: John Wiley & Sons, Inc., vol 1, (7th Ed.)
Pitcher, W.S.	1950	Calc-silicate skarn veins in the limestone of Lough Anure, Co. Donegal: Miner. Mag., vol 29, pp. 126-141.
Pitcher, W.S. & Read, H.H.	1952	An appinitic intrusion-breccia at Kilkenny, Maas, Co. Donegal: Geol. Mag., vol 89, pp. 328-336.
Pryor, E.J.	1965	Mineral Porcessing: Elsevier Publishing Co., (3rd Ed.)
Ramdohr, P.	1950	Die Erzmineralien und ihre Verwachsungen: Akad. Verlag, Berlin.
Ramdohr, P.	1956	The manganese ores. Symposium del Manganeso XX Congreso Geologico Internacional, vol 1, pp. 19-73.
Rankama, K. & Sahama, Th.G.	1950	Geochemistry: The Uni. of Chicago Press.
Reitan, P.	1959	Pegmatite veins and the surrounding rocks: Norsk. Geol. Tids., vol 39, pp.197-229.
Rey, M., Merre,P., Mancuso, R. & Formanek, V.	1961	Fiftieth Ann. Froth Flotation: Colo. Sch. Min. Qly., July.

Reynolds, D.L. 1954 Fluidization as a geological process, and its bearing on the problem of intrusive granites: Amer. Jour. Sci., vol 252, pp.577-614.

Rickard, M.J. 1961 A note on cleavages in crenulated rocks: Geol. Mag., vol 98, pp.324-332.

Riley, J.P. 1958 Rapid analysis of silicate rocks and minerals: Anal. Chim. Acta., vol 19, pp.413-428.

Ringwood, A.E. 1955 The principles governing trace element distribution during magmatic crystallization: Geochim. et Cosmochim. Acta, vol 7, pp.189-202.

Robertson, F. 1951 Sphalerite-dolomite orientation relations at the Renfrew zinc prospect, Ontario. Amer. Min., vol 36, p.116.

Roedder, E., Ingram, B. & Hall, W.E. 1963 Studies of fluid inclusions. III. Extraction and quantitative analysis of inclusions in the miligram range: Econ. Geol. vol 58, pp.353-374.

Rosenblum, S. 1956 Improved techniques for staining potash feldspars: Amer. Min. vol 41, pp.662-664.

Sağiroğlu, G. 1952 Keban volfram zuhurati hakkinda rapor: Private report, M.T.A.

Sawkins, F.J., Dunham, A.C. & Hirst, D.M. 1964 Iron-deficient low temperature pyrrhotite: Nature, vol 204, No.4954, pp.175-176.

Scherbina, B.B. 1956 Quoted in the Int. Geol. Congr. Report of the twenty-third session, Czechoslovakia, 1968, Endogenous ore deposits, p.303.

Schneiderhöhn, H. 1952 Erzmikroskoposches Praktikum: E. Schweizerbart'sche, Verlagsbuchhandlung.

Schouten, C. 1962 Determination Tables for Ore Microscopy: Elsevier Publishing Co.

Schulman, J.H., Evans, L.W., Ginter, R.J. & Murata, K.J. 1947 The sensitized luminescence of Mn activated calcite: Jour. Appl. Phys., vol 18, pp.732-739.

Schumacher, F. 1957 Maden Yataklari Bilgisinin Esaslari: Ist. Tek. Uni. publ. No. 532, p.190.

Schwartz, G.M. 1931 Intergrowths of bornite and chalcopyrite: Econ. Geol., vol 2c, pp.186-201.

Schwartz, G.M. 1951 Classification and definitions of textures and mineral structures in ores: Econ. Geol., vol 46, pp. 578-591.

Shand, S.J. 1947 The genesis of intrusive magnetite ad related ores: Econ. Geol., vol 42, pp. 634-636.

Shapiro, L. & Brannock, W.W. 1955 Rapid determination of CO_2 in silicate rocks: Anal. Chem. vol 27, pp.1796-1797.

Shapiro, L. & Brannock, W.W. 1962 Rapid analysis of silicate, carbonate and phosphate rocks: U.S. Geol. Surv. Bull. No. 1144-A.

Shaw, D.M. 1952 The geochemistry of thallium: Geochim. et Cosmochim Acta, vol 2, pp. 118-154.

Shaw, D.M. 1957 The geochemistry of gallium, indium, thallium - a review: Progress in Physics and Chemistry of the Earth, vol 2, pp. 164-211.

Sheinmann, Yu.M., Apel'tsui, F.R. & Nechaeva, E.A. 1961 Ore mineralization of alkaline complexes: Geol. Mestorozhd Redkikh Elementov, Vses. Nauchn. Issled. Inst. Mineral'n Syr'ya, No. 12-13, p.127.

Short, M.N. 1964 Microscopic Determination of the Ore Minerals: U.S. Geol. Surv. Bull. No.914. (2nd Ed.).

Skinner, B.J. 1959 Effect of manganese on the sphalerite geothermometer (Abstr.): Geol. Soc. Amer. Bull., vol 70, p.1676.

Skinner, B.J., Barton, P.B. Jr. & Kullerud, G. 1959 Effect of FeS on the unit-cell edge of sphalerite: Econ. Geol., vol 54, pp. 1040-1046.

Smith, F.G. 1953 Historical Development of inclusion Thermometry, Toronto: Univ. of Toronto Press.

Smith, J.V. & Gay, P. 1958 The powder patterns and lattice parameters of plagioclase feldspars II: Miner. Mag. vol 31, pp.744-762.

Spencer, E. 1937 The potash-soda feldspars. I. Thermal stability: Miner. Mag., vol 24, p.453.

Sriramadas, A. 1957 Diagrams for the correlation of unit cell-edges and refractive indices with the chemical composition of garnets: Amer. Min., vol 42, p.294.

Stanton, R.L. 1958 Abundance of copper, zinc and lead in some sulphide deposits: Jour. Geol., vol 66, pp.484-502.

Steyn, J.G.D. 1954 Spectrographic and X-ray data on some fluorites from the Transvaal, South Africa: Miner. Mag., vol 30, p.327.

Stillwell, F.L. & Edwards, A.B. 1945 The mineral composition of the Black Star copper orebody, Mt. Isa, Queensland Proc. Austr. Inst. Min. Met., No.139, pp.149-159.

Streckeisen, A. 1967 Classification and nomenclature of igneous rocks: N. Jb. Miner. Abh. 107, 2 und 3, pp. 144-240.

Sutherland, K.L. & Wark, I.W. 1955 Principles of Flotation: Austr. Inst. Min. Met., p.118.

Taggart, A.F. 1951 Elements of Ore Dressing: John Wiley & Sons Inc., New York.

Taylor, S.R. 1964 Abundance of chemical elements in the continental crust: a new table: Geochim. et Cosmochim. Acta. vol 28, pp.1273-1285.

Taylor, S.R., Emeleus, C.H. & Exley, C.S. 1956 Some anomalous K/Rb ratios in igneous rocks and their petrological significance: Geochim. et Cosmochim. Acta, vol 10, pp. 224-229.

Tolun, N. 1950 Keban jeolojik etüdü: Private report, M.T.A.

Toulmin, P. 1960 Effect of copper on sphalerite phase equilibria - a preliminary report (Abstr.) Geol. Soc. Amer. Bull., vol 71, p.1993.

Tröger, W.E. 1959 Optische Bestimmung der gesteinsbildenden Minerale: E. Schweizerbart'sche, Verlagsbuchhandlung, Stuttgart.

Turekian, K.K. & Kulp, J.L. 1956 The geochemistry of strontium: Geochim. Cosmochim. Acta, vol 10, pp. 245-296.

Turekian, K.K. & Wedepohl, K.H. 1961 Distribution of the elements in some major units of the earth's crust: Geol. Soc. Amer. Bull. vol 72, pp.175-192.

Turner, F.J. 1948 Mineralogical and structural evolution of the metamorphic rocks: Geol. Soc. Amer. Mem. 30.

Turner, F.J. & Verhoogen, J. 1960 Igneous and Metamorphic Petrology: McGraw-Hill, New York (2nd Ed.).

Turner, F.J. & Weiss, L.E. 1963 Structural Analysis of Metamorphic Tectonites: McGraw-Hill, New York.

Tuttle, O.F. 1952 Optical studies on alkali feldspar: Amer. Jour. Sci., vol 2, pp. 553-567.

Udluft, H. 1929 Die genesis der Hächenhaft verbreiteten Dolomite des mitteldevonischen Massenkalkes: Jahrb. Preus, Geol. Landesants, vol 50, pp. 396-436.

Upton, B.G.J. 1960 The alkaline igneous complex of Kungnat Fjeld, South Greenland: Medd. om Grønland, vol 123, No.4, pp. 5-145.

Uytenbogaardt, W. 1951 Tables for microscopic identification of Ore Minerals: Princeton Uni. Press.

Voll, G. 1960 New work on petrofabrics: Liverpool and Manchester Geol. Jour., vol 2, pp.503-567.

Wager, L.R. & Michell, L.R. 1951 The distribution of trace elements during strong fractionation of basic magma - a further study of the Skaergaard intrusion, East Greenland: Geochim. et Cosmochim. Acta vol 1, pp. 129-208.

Wahlstrom, E.E. 1950 Introduction to Theoretical Igneous Petrology: John Wiley & Sons, Inc., New York.

Walton, M.S. Jr.,& O'Sullivan, R.B. 1950 The intrusive mechanics of a clastic dyke: Amer. Jour. Sci., vol 248, pp. 1-21.

Wasserstein, B. 1945 Discussion on paper by C.M. Schwellnus: Proc. Geol. Soc. South Africa, vol XC, p.48.

Watt, W.S. 1966 Chemical analyses from the Gardar Igneous Province, South Greenland: Grønlands Geologiske Undersøgelse, Rapport No.6., pp. 1-92.

Wayne, M.B. 1962 Wall-rock alteration in the Cochiti Mining District, New Mexico: Bull. Sta. Bur. Min. & Mine. Resources. No. 59, New Mexico Inst. Min. Tech.

Wedepohl, K.H. 1956 Untersuchungen zur Geochemie des Bleis: Geochim. et Cosmochim. Acta, vol 10, pp. 69-148.

White, W.S. 1949 Cleavage in East-Central Vermont: Trans. Amer. Geophys. Union, vol 30, pp.587-594.

Williams, H., Turner, F.J. & Gilbert, C.M. 1965 Petrography, An Introduction to the Study of Rocks in Thin Sections: Vakils, Feffer & Simons, Pvt. Ltd., Bombay.

Winkler, H.G.F. 1965 Petrogenesis of Metamorphic Rocks: Springer-Verlag, Berlin.

Wright, T.L. 1968 X-ray and optical study of alkali feldspar, II. An X-ray method for determining the composition and structural state from measurement of 2θ values for three reflections: Amer. Min. vol 53. pp.88-104.

Yener, H. 1935 Keban madeni hakkinda: Private Report, M.T.A.

Zeis, E.G. & Allen, E.T. 1916 Some reactions involved in secondary copper sulphide enrichment. Econ. Geol., vol 11, pp. 407-503.

Zsivny, V. 1923 The chemical composition of sanidine from Vegardo: Math. Termeszett. Ertesitö, Budapest, vol 40, p. 114.

APPENDIX

STAINING TECHNIQUE

Staining technique for dolomite and calcite (Dickson, 1965)

Procedure	Time	Carbonate	Result
Etching 1.5% HCl	10-15 secs	Calcite Ferroan calcite	Considerable etch
		Dolomite Ferroan dolomite	Negligible etch
Staining 0.2 gr ARS*per 100cc. 1.5% HCl 2.0 gr PF*per 100cc. 1.5%HCl Mixed in ratio ARS:PF = 3:2	30-45 secs	Calcite	Very pale pink-red depending on optical orientation
		Ferroan calcite	Very pale pink-red, pale blue-dark blue, two superimposed give mauve-purple-royal blue
		Dolomite	No colour
		Ferroan dolomite	Pale-deep turquoise, depending on ferrous content
Staining 0.2 gr ARS per 100cc. 1.5% HCl	10-15 secs	Calcite Ferroan calcite	Very pale pink-red
		Dolomite Ferroan dolomite	

*ARS: $CO.C_6H_4.CO.C_6H(OH)_2.SO_3\ Na+H_2O$, *PF: $K_3Fe(CN)_6$

Staining technique for dolomite and calcite (Evamy, 1963)

Staining reagents	Calcite			Dolomite		
Compositions are given in weight %	Fe^{+2} free	Fe^{+2} poor	Fe^{+2} rich	Fe^{+2} free	$\frac{Fe^{+2}}{Mg^{+2}} < 1$	$\frac{Fe^{+2}}{Mg^{+2}} > 1$
Critical solution strengths are underlined	Calcite	Ferroan calcite		Dolomite	Ferroan dolomite	Ankerite
Time min.	± 1	± 1		± 1	± 1	± 1
0.2% HCl 0.2% ARS	red	red	red	not stained	not stained	not stained
0.2%HCl 0.5-1.0%PF	not stained	light blue	dark blue	not stained	light blue	dark blue
0.2% HCl 0.2% ARS 0.5-1.0% PF	red	mauve	purple	not stained	light blue	dark blue

Staining technique for alkali feldspar (Rosenblum, 1956)

Procedure	Time	Result
Etching; by leaving a thin section uncovered face down over HF vapour	10-15 secs	Negligible etch
Staining; by cobaltinitrite (saturated)	15-20 secs	Yellow

WET COMBUSTION TECHNIQUE

Graphite analysis of the phyllite by the wet combustion method

In this method, graphite is simply converted into CO_2. The

loss after considering the other losses due to water and oxidation of iron, was calculated as being C. Watch glasses loaded with 0.5 gr of finely ground powder of rock samples containing graphite were stored in an electric oven under various time and temperature conditions. 18 hour operating time and 375°C have been found most satisfactory. The effect of oxidation on FeO in each sample was checked twice before and after heating. The differences with respect to water and FeO were subtracted from the total loss found after heat treatment.

PREPARATION TECHNIQUE

Sampling procedure:

All the samples used for different analysis purpose were crushed to the required size in the following succession:

a) Splitting by hydraulic jack reducing the size to one inch pieces.

b) Further reduction using a jaw rock crusher.

c) Cone quartering.

d) Final crushing on a Tema Disc Mill (Type T-100) for 2 to 6 minutes. This process provides a powder containing particles of about 20 micron.

e) Bricquetting by using boric acid powder on a press at a pressure of 7 tons for 5 minutes. (For only major element analysis).

Preparation of standards for trace element analysis:

Standards were prepared by the addition method (Ahrens and Taylor, 1961) using a sample which was believed to be representative of all trace elements possibly present in a similar sample as the base for "Master Mix". These were prepared to contain 2500 ppm of spec-pure compound of elements. Each master mix was placed in a screw topped plastic bottle with three plastic mixing balls and shaken for 4 hours on a Spex Mixer Mill, it was then diluted with its own base sample to obtain concentrations of 2500, 1000, 750, 500, 400, 300, 200, 100, 50 ppm of each element.

Contamination correction

To correct for small amounts of contamination from the W tube employed (only for P.W. 1540 XRF), the intensity of each element line was counted using spec-pure SiO_2 as a fraction of the WLI line intensity: for each sample the intensity of the WLI peak was measured and a simple correction for contamination done by this ratio. Only lead, nickel and copper have been found as contaminant and these were present in negligible amounts.

X-RAY TECHNIQUE

X-ray diffraction technique:

Apart from the identification purpose for some minerals, the following analyses have been done on the Philips high-angle XRD (P.W. 1051); the composition and structural state of alkali

feldspars, structural state of plagioclase, d-spacing of arsenopyrite and cell-size measurements of vanadinite. The cell-size measurements for garnets, fluoride, pyrite, magnetite, sphalerite and galena, and d-spacing of pyrrhotite were carried out by a large camera (114.59 mm in diameter), attached to the P.W. 1051 XRD. An exposure time of 6 and 15 hours for X-ray films has been found satisfactory for the above mentioned processes.

All materials to be analysed except for manganese minerals and pyrrhotite which were drilled out from polished specimens, were separated under a binocular microscope. Afterwards the sample was stuck on the end of pyrex glass hair using collodian as adhesive. Attention was paid to obtaining a uniform distribution of the material on the glass hair. The glass hair was subsequently mounted in the camera and centred using the centring device.

For the powder camera purpose Ilford Industrial G fast X-ray films were used and developed using standard processes. The films were measured on a standard Hilger and Watts film measuring scale, with a vernier capable reading to $\mp$0.05 mm. The shrinkage corrections were applied for every film. The operating conditions are given in the table below.

X-ray study of alkali feldspar

Radiation	:	CuKα Ni Filter, 40 kv, 20 mA
Slits	:	1°,0.1°,1°
Goniometer	:	1/2° /min.
Counter	:	Scintillation, 1730 v
Discriminator	:	Att. 8.40 Chan.8
Chart-speed	:	800 mm/hr
Counter	:	R.M.2 T.C.4 Mult.1
Operation	:	R.M.
Range scanned	:	2θ 19°-52°
Peaks	:	2θ Int. Std. 28.30, Analysis peaks 20.91, 27.72, 41.65, 50.95.
Mount type	:	Smear, Int. Std. CaF_2 (Analar) 1/4

X-ray study of plagioclase

Radiation	:	CuKα Ni Filter, 40 kv, 20 mA
Slits	:	1°, 0.1°, 1°
Goniometer	:	Ossillator, at least once, 1/8° /min
Counter	:	Scintillation, 1730 v
Chart-speed	:	400 mm/hr
Counter	:	R.M.4, T.C.8, Mult.1
Operation	:	R.M.
Range scanned	:	2θ 28°-32°
Peaks	:	No int. std. Analysis peaks, 2θ 30.15, 30.48, 31.23
Mount type	:	Cavity

X-ray study of arsenopyrite

Radiation	:	CuKα Ni Filter, 40 kv, 20 mA
Slits	:	1°, 0.1°, 1°
Goniometer	:	Normal
Counter	:	Prop. 1730 v
Discriminator	:	Prop. counter + discriminator Att.4, Ampl. 25.6 v Chan.4.
Chart-speed	:	200 mm/hr
Counter	:	R.M.2, T.C.8, Mult.1
Operation	:	R.M.
Range scanned	:	2θ 55.5°-56.5°
Peaks	:	2θ Int. Std. 55.79 Analysis peak, 56.28
Mount type	:	Smear, Int. Std. CaF_2 (Analar) 1/4

X-ray study of manganese mineral

Instrument	:	Norelco generator unit
Radiation	:	Cr Kα, V Filter 20 kv, 8 mA
Camera	:	57.3 mm with fine collimeters
Exposure time	:	13 to 15 hours
Film	:	Ilford Industrial G fast

X-ray fluorescent technique

The major element analysis of the metamorphic rocks has been run on the Philips (P.W.1210) automatic spectrograph against the four international standards of G-1, S-1, T-1, W-1 plus 28 secondary standards supplied by the department. The operating conditions are tabulated in table.

Element	Peak 2θ	Tube	Generator	kv	mA	Crystal	Path	Collimeter	Counter	Counts	Time
SiO_2	109.15	W	1575	60	32	LiF 110	V+G	Coarse	Flow	FC	-
Al_2O_3	145.13	W	1575	60	32	LiF 110	V+G	Coarse	Flow	FC	-
Fe	85.72	W	1575	60	8	LiF 110	V+G	Coarse	Flow	FC	-
MgO	79.05	W	1575	50	40	LiF 110	V+G	Coarse	Flow	FC	-
CaO	45.07	W	1575	60	8	LiF 110	V+G	Coarse	Flow	FC	-
Na_2O	105.05	W	1575	50	40	LiF 110	V+G	Coarse	Flow	FC	-
K_2O	50.58	W	1575	6	8	LiF 110	V+G	Coarse	Flow	FC	-
TiO_2	36.58	W	1575	6	8	LiF 110	V+G	Coarse	Flow	FC	-
P_2O_5	87.50	W	1575	50	40	LiF 110	V+G	Fine	Flow	FC	-
S	73.50	W	1575	50	40	LiF 110	V+G	Coarse	Flow	FC	-
MnO	62.89	Cr	1575	70	30	LiF 110	Air	Fine	Flow	FT	20

XRF Trace element analysis

Trace elements in galena

Element	Peak 2θ	Tube	Generator	kv	mA	Crystal	Path	Collimeter	Counter	Counts	Time
Te	18.26	W	1675	60	32	LiF	110	V+G	Fine	S	FT	40
Sb	19.08	W	1675	60	32	LiF	110	V+G	Fine	S	FT	40
Ag	22.68	W	1675	60	32	LiF	110	V+G	Fine	S	FT	40
Mo	28.93	W	1675	60	32	LiF	110	V+G	Fine	S	FT	100
Sr	35.85	W	1675	60	32	LiF	110	V+G	Fine	S	FT	100
Bi	39.11	W	1675	60	32	LiF	110	V+G	Fine	S	FT	100
As	48.78	W	1675	60	32	LiF	110	V+G	Fine	S	FT	100
Ba	15.60	W	1675	60	32	LiF	110	V+G	Fine	S	FT	40
Ga	56.20	W	1675	60	32	LiF	110	V+G	Fine	F+S	FT	100
Ni	71.24	W	1675	60	32	LiF	110	V+G	Fine	F+S	FT	100

Holder: Rotating circular holder with mylar window beneath aluminium cover top, locked by a plastic cover.

Operating conditions for trace elements in sphalerite

Element	Peak 2θ	Tube	Generator	kv	mA	Crystal	Path	Collimeter	Counter	Counts	Time
Cd	20.95	W	1670	60	32	LiF	110	V+G	Coarse	S	FT	40
Fe	85.65	W	1670	40	8	LiF	110	V+G	Coarse	F+S	FT	10
Mn	95.20	W	1670	60	32	LiF	110	V+G	Coarse	F+S	FT	40
Cr	107.12	W	1670	60	32	LiF	110	V+G	Coarse	F+S	FT	40
Cu	65.62	W	1670	60	32	LiF	110	V+G	Coarse	F+S	FT	40
Ga	56.20	W	1670	60	32	LiF	110	V+G	Coarse	F+S	FT	40

Operating conditions for trace elements in fluorite

Element	Peak 2θ	Tube	Generator	kv	mA	Crystal	Path	Collimeter	Counter	Counts	Time
Sr	35.83	W	1675	60	32	LiF 110	V+G	Coarse	S	FT	40
Ba	15.60	W	1675	60	32	LiF 110	V+G	Coarse	S	FT	40
Zr	32.12	W	1675	60	32	LiF 110	V+G	Coarse	S	FT	40
Rb	37.98	W	1675	60	32	LiF 110	V+G	Coarse	S	FT	40
Zn	60.63	W	1675	60	32	LiF 110	V+G	Coarse	S	FT	40
Cu	65.62	W	1675	60	32	LiF 110	V+G	Coarse	S	FT	40
Ni	71.32	W	1675	60	32	LiF 110	V+G	Coarse	S	FT	100

Operating conditions for trace elements in quartz syenite porphyry

Zr	28.31	W	1670	48	20	LiF 110	V	Fine	S	FT	64
Nb	30.20	W	1670	48	20	LiF 110	V	Fine	S	FT	64
Sr	35.64	W	1670	48	20	LiF 110	V	Fine	S	FT	64
Rb	37.78	W	1670	48	20	LiF 110	V	Fine	S	FT	64
Pb	40.70	W	1670	48	20	LiF 110	V	Fine	S	FT	64
Ba	15.60	W	1670	48	20	LiF 110	V	Fine	S	FT	64
Mn	101.70	W	1670	48	20	LiF 110	V	Fine	S	FT	64
Ni	75.39	W	1670	48	20	Lif 110	V	Fine	S	FT	64
Cu	69.23	W	1670	48	20	LiF 110	V	Fine	S	FT	64
Zn	63.89	W	1670	48	20	LiF 110	V	Fine	S	FT	64

Operating conditions for strontium in marble

Sr	35.64	W		48	20	LiF 110	V	Fine	S	FT	64

OPTICAL SPECTROGRAPH TECHNIQUE

Fluorine analysis by the optical spectrograph

Operating conditions for the determination of fluorine in marble

Instrument : A Hilger & Watts Automatic Large Spectrograph E 742

Charge preparation	: Johnson Matthey spec pure cupric oxide J.M. 40 (int.std.), National Carbon Co. graphite SP2, (buffer), Analar calcium Carbonate.
Charge ratio	: 0.2 gr sample, 0.15 gr $CaCO_3$, 0.025 gr CuO, 0.225 gr C mixed in a plastic vial using Spex Mixer Mill No.8000
Electrode type	
Anode	: National Carbon Co. carbon rods (Cat.No.L. 4306) 3/16"
Dimension of crater	: 1/8" x 2.5 mm
Cathode	: Johnson Matthey Carbon rods (Cat.No.J.M. 1205) 5 mm.
Optical system	
Wavelength range	: 4600-9600 A°
Lens system	: Hilger E958 focused on slit - 7 step sector using 4 steps (2:1) ratio
Slit	: Height 6 mm, width 0.07 μ
Camera diaphram	: 14 mm
Plate	: Ilford R40
Analytical gap	: 4.4 mm
Exposure	
Special conditions	: Arc in an atmosphere of argon: oxygen (ratio 80/20) at a flow rate of 5 H./min. through a modified Stallwood jet
Current	: 6.8 A d.c. short circuit
Burn	: 6 A d.c.
Timing	: Preburn: None, Exposure 30 secs.
Photographic	
Developer	: Ilford PO Universal for 4 mins. at 20°C.
Fixer	: Kodak AM33+H for 3 mins.
Washing	: 25 mins.
Finishing	: Plates rinsed in distilled water containing Kodak photo-flo solution to ensure drying free from spots.
Drying	: On an Applied Research Labs. Inc. dryer at mark 2 for 10 mins.
Lines	
Analysis	: CaF_2 5291.0 bandhead
Internal standard	: Cu 5105.541

KEY TO UNDERGROUND MAPS

MARBLE

PHYLLITE

DOLOMITE MARBLE

QUARTZ-SYENITE PORPHYRY

BRECCIA ZONE

FAULT

INFERRED FAULT

FOLIATION PLANES

LOCATION OF SAMPLES

ORE-SHOOT

ORE MINERALIZATION IN STREAKS

PROBABLE LIMIT OF ORE BODIES

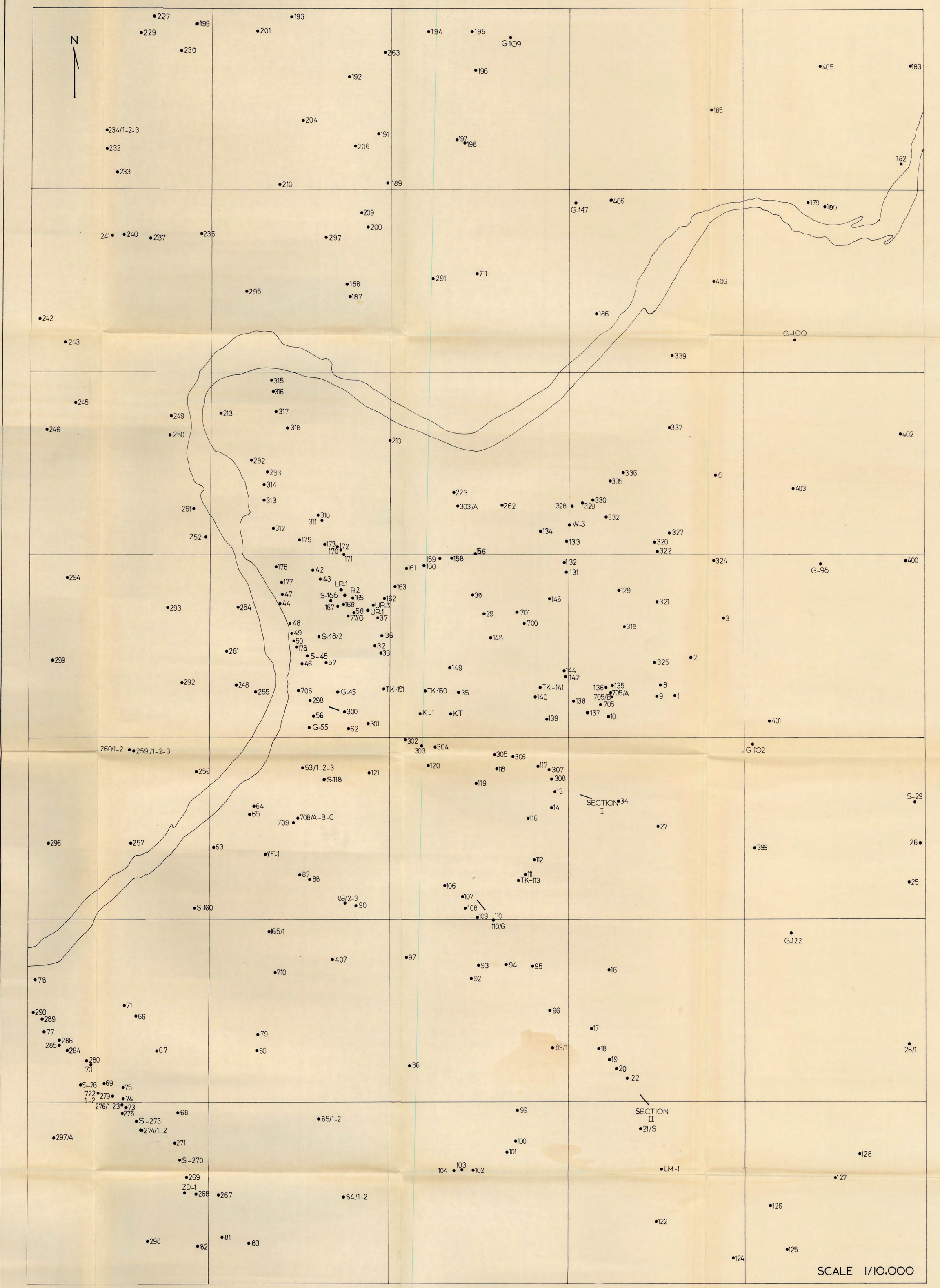

Fig. 16 Sampling map of the Keban area
(Surface samples only)

Fig. 45 CROSS SECTIONS OF THE MAIN SULPHIDE DEPOSIT

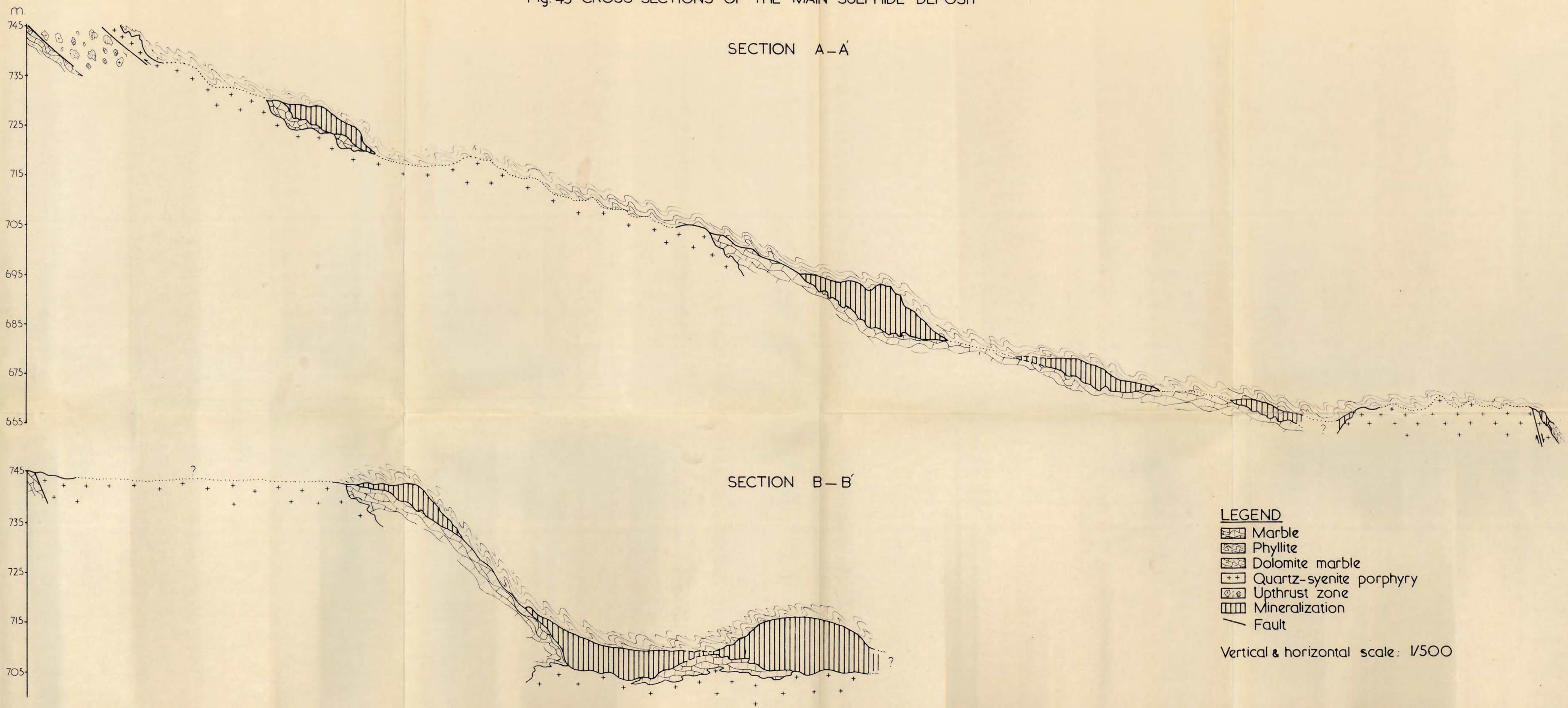

Fig. 44 CROSS SECTIONS OF THE GEOLOGICAL MAP OF THE KEBAN AREA

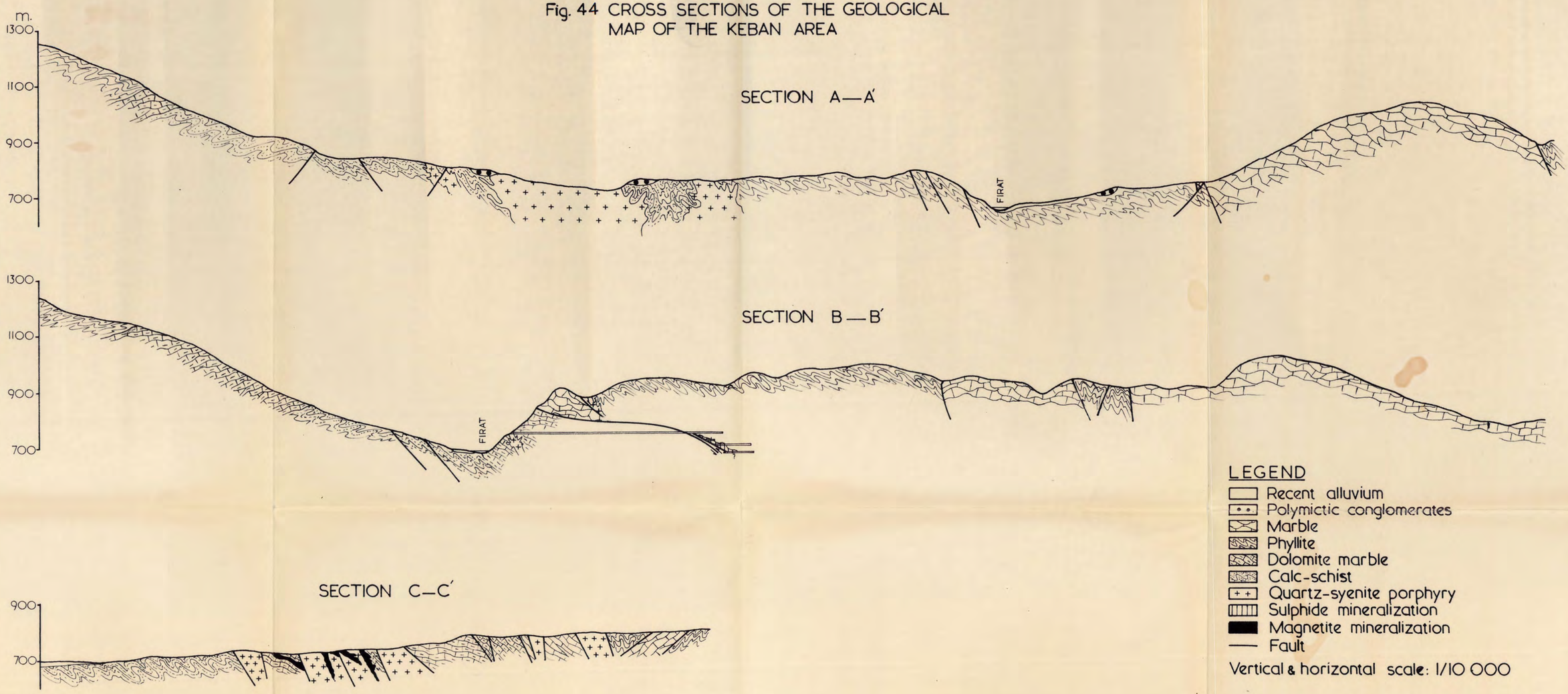

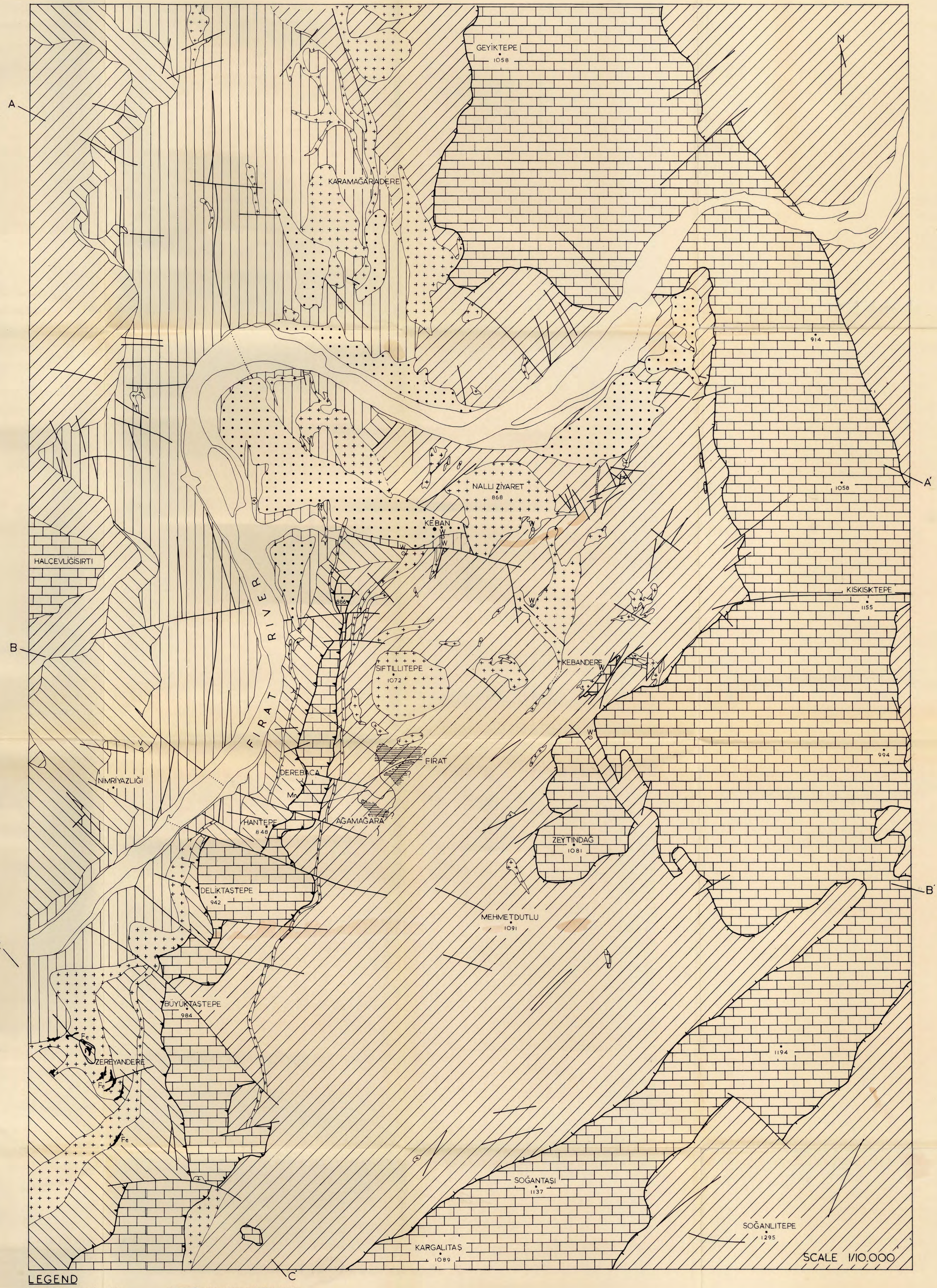

LEGEND

- Recent alluvium
- Polymictic conglomerates
- Marble
- Phyllite
- Dolomite marble
- Calc-schist
- Quartz-syenite porphyry
- Volcanic breccia
- Projection of the main sulphide deposit
- Fe — Magnetite deposit
- W — Scheelite deposit
- Mn — Manganese occurrence
- V — Vanadinite-descloizite occurrence
- A—A' Section line

Fig. 8 The geology of the Keban area

N

SCALE 1/10.000

LEGEND

- Inclined lineation
- Horizontal lineation
- Foliation
- Fold axis
- Fault
- Inferred fault
- Upthrust
- Mechanical contact
- Inclined joint
- Vertical joint

Fig. 12 Structural geology of the Keban area

N

ORE BODY II

ORE BODY I

LEVEL 745 m

LEVEL 727 m.

LEVEL 705 m.

LEVEL 688 m.

LEVEL 668 m

LEVEL 712 m.

UPTHRUST BRECCIA ZONE

MAJOR FAULT ZONE

Sampling traverse

DILIMLI ORE SHOOT

F-16

F-18

A — A'

B — B'

9700

9650

9600

9550

9500

9850

9900

9950

10000

10050

10100

Fig. 11 Underground map of Sheet C

Fig. 9

Fig. 9 Underground map of Sheet A
(Main adit 745 m level)
Scale 1/500

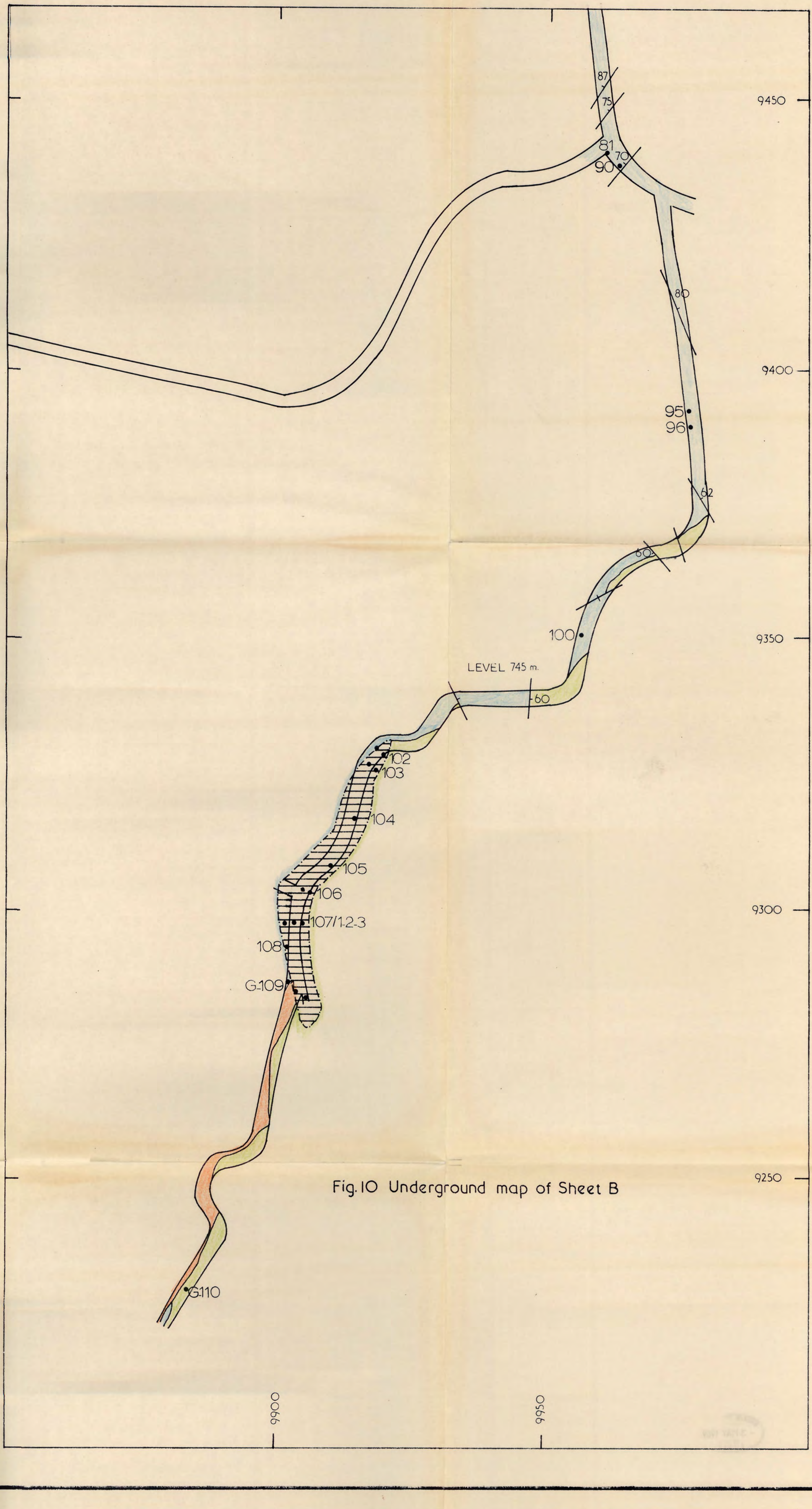

Fig. 10 Underground map of Sheet B